SEDIMENTOLOGY AND ORGANIC PETROLOGY OF THE CARBONATE RAMP AND REEF FORESLOPE SUCCESSIONS IN THE MIDDLE DEVONIAN KEG RIVER FORMATION, RAINBOW AND ZAMA SUB-BASINS, NORTHWESTERN ALBERTA, CANADA

BY

NAOMI S. WIEBE

A Thesis
Submitted to the Faculty of Graduate Studies
in Partial Fulfillment of the Requirements
of the Degree of

MASTER OF SCIENCE

Department of Geological Sciences
University of Manitoba
Winnipeg, Manitoba

THE UNIVERSITY OF MANITOBA

FACULTY OF GRADUATE STUDIES

*****

COPYRIGHT PERMISSION

SEDIMENTOLOGY AND ORGANIC PETROLOGY OF THE CARBONATE RAMP AND REEF FORESLOPE SUCCESSIONS IN THE MIDDLE DEVONIAN KEG RIVER FORMATION, RAINBOW AND ZAMA SUB-BASINS NORTHWESTERN ALBERTA, CANADA

BY

NAOMI S. WIEBE

A Thesis/Practicum submitted to the Faculty of Graduate Studies of The University of Manitoba in partial fulfillment of the requirement of the degree

Of

MASTER OF SCIENCE

ABSTRACT

Isolated reefs of the Middle Devonian Keg River Formation in the Rainbow and Zama sub-basins are important oil and gas reservoirs in northwestern Alberta. Oils in these reservoirs were sourced, in part, by organic-rich laminites in the formation. An integrated approach combines stratigraphy, sedimentology, organic petrology, and organic geochemistry in the study of organic-rich laminites in the Rainbow and Zama sub-basins. This method facilitates interpretation of the depositional history, regional stratigraphic correlation, paleoenvironment, and paleoecology of these organic-rich laminites. The primary control on organic matter (OM) accumulation and preservation in these laminites is evaluated in the context of the "productivity vs. preservation" controversy, which provides insight into the relationship between elevated nutrient levels, high phytoplanktonic productivity, and Devonian reef growth.

Three units of organic-rich laminites occur in the Keg River Formation of the Rainbow Sub-basin: (1) the lower Rainbow laminite (LRL) in the middle of the Lower Keg River Member carbonate ramp (at the base of cycle R2); (2) the middle Rainbow laminite (MRL) at the base of Upper Keg River Member reefs (at the base of cycle R3); and (3) the upper Rainbow laminite (URL) near the base of of the Upper Keg River Member (in cycle R3) in off-reef and foreslope positions. Two organic-rich laminites occur in the Keg River Formation of the Zama Sub-basin: (1) the lower Zama laminite (LZL) at the base of Upper Keg River Member reefs (at the base of cycle Z2); and (2) the upper Zama laminite (UZL) near the base of the Upper Keg River Member (in cycle Z2) in off-reef

and foreslope positions. Interpreted stratigraphic correlation between the Rainbow and Zama sub-basins demonstrates that shallowing upward cycles R1 and R2 in the Rainbow Sub-basin correlate to cycle Z1 in the Zama sub-basin and that cycles R3 and Z2 are also correlative. This suggests a correlation between the MRL and the LZL as well as between the URL and the UZL.

Representative samples of organic-rich laminites were analyzed using white and ultra-violet incident light microscopy. These techniques facilitated identification of macerals and determination of organic facies (OF) based on the distribution and characteristics of these macerals. In both the Rainbow and Zama sub-basins the LRL, MRL, and LZL are all interpreted as primarily OF B, characterized by small, thin-walled alginites and acanthomorphic acritarchs. This evidence is indicative of accumulation and preservation of organic matter (OM) due to depth related anoxia. The URL and UZL in off-reef positions are interpreted as primarily OF B with secondary OF A signatures, characterized by dominant large, thick-walled alginites. These OF are indicative of OM accumulation and preservation due depth related anoxia and episodic, elevated phytoplanktonic productivity (algal blooms). In contrast, the URL and UZL in reef foreslope positions are interpreted as primarily OF A, characterized by dominant large, thick-walled alginites which indicate accumulation and preservation of OM due to algal blooms. This interpretation suggests that foreslope environments were not sufficiently deep for depth-related anoxia to be the primary control. The URL and UZL in foreslope positions were deposited coevally with reef growth in the Upper Keg River Member

which may suggest that Middle Devonian reefs could tolerate or at least recover from episodic eutrophication which triggered algal blooms.

ACKNOWLEDGEMENTS

I would like to thank all the people who made this thesis possible by generously sharing their knowledge, expertise, and resources. First and foremost, I would like to express my deepest gratitude to Dr. Nancy Chow, my thesis advisor. Nancy was always supportive and generous with her time and knowledge. I would also like to thank Dr. Jack Wendte, without whom this project would have been impossible. Jack took me under his wing at the Geological Survey of Canada in Calgary in the summer of 2000 and met with me during his lunch hour, after hours, and on weekends to offer assistance while I logged core, constructed cross-sections and interpreted facies. Dr. Wendte's experience working in the Devonian of Alberta and his vast mental catalogue of knowledge was the greatest resource a graduate student could hope to access during their studies. Dr. Lavern Stasiuk, also at the Geological Survey of Canada in Calgary, introduced me to all aspects of organic petrology including sample preparation, microscopy, and interpretation. Dr. Stasiuk opened my eyes to the potential uses of organic petrology and its importance to my particular study. I would also like to thank all of the staff at the Geological Survey of Canada in Calgary for their assistance.

Financial support provided for my thesis from Anderson Exploration Ltd. (formerly Ulster Petroleum) was crucial to the success of my project. I would like to thank Mr. Graeme Bloy very much for sharing his expertise and resources. Logistical support was offered Talisman Energy Inc., and the staff of the information resource center at Talisman Energy Inc. was extremely helpful.

Last but definitely not least, emotional support from my better half, Doug Goda, was crucial to the success (and completion) of this project. Without his support, encouragement, and assistance this would have never been possible.

TABLE OF CONTENTS

page

page

LIST OF APPENDICES

LIST OF FIGURES

page

page

LIST OF TABLES

page

LIST OF OVERSIZE ENCLOSURES

CHAPTER 1: INTRODUCTION

1.1 Prologue

Devonian strata in the Western Canada Sedimentary Basin (WCSB) are of significant economic importance because of the abundance of carbonate reservoir rocks in the succession. Over 55% of recoverable oil reserves and approximately 27% of recoverable gas reserves in Western Canada are contained within Devonian carbonate rocks (Podruski *et al.*, 1987; Reinson *et al.*, 1993). Although the WCSB is in the mature stages of development, there are still reserves to be found; over a decade ago it was estimated that 23% of Devonian conventional oil and 56% of Devonian gas were yet to be discovered (Podruski *et al.*, 1987; Reinson *et al.*, 1993). Both the realized and unrealized potential of Devonian strata in the WCSB have stimulated extensive research interest.

The Middle Devonian Keg River Formation in the Rainbow and Zama sub-basins in northwestern Alberta contains important reservoirs and source rocks (Campbell, 1992). Previous studies of the Keg River Formation have focused primarily on the oil-producing reef facies of the Upper Keg River Member (e.g., Hriskevich, 1966; Langton and Chin, 1968). The carbonate ramp succession of the Lower Keg River Member, as well as off-reef and reef foreslope strata of the Upper Keg River Member, has been largely neglected. However, organic-rich facies in the Lower Keg River Member are source rocks for the Upper Keg River Member reefs (Fowler *et al.*, 2001). In addition, correlations between the Rainbow and Zama sub-basins remain tenuous, despite apparent

genetic link between these sub-basins, the abundance of hydrocarbons within both sub-basins, and the potential value of ascertaining inter-basinal relationships.

The integration of sedimentology and organic petrology offers valuable insights for deciphering paleoenvironmental conditions in the Rainbow and Zama sub-basins. Carbonate sedimentology, utilizing detailed core descriptions and petrophysical well logs, aids identification of genetic sequences in the Keg River Formation based on the description of different lithofacies and the recognition of small-scale shallowing-upward cycles. Organic petrology is used to characterize organic facies that provide key information for paleoenvironmental interpretation and offers insight into the more global problem of primary controls on organic matter accumulation, and the relationship of organic matter (OM) accumulation to reef growth and demise.

Many questions remain unanswered about the Lower Keg River Member and organic-rich facies within the Rainbow and Zama sub-basins. This comprehensive study addresses some of the gaps in our understanding of this succession by focusing on the Lower Keg River Member and the reef foreslope strata of the Upper Keg River Member. It includes a detailed description and interpretation of the sedimentology and organic petrology in the Rainbow and Zama sub-basins, stratigraphic correlations between these two sub-basins, and identification of the primary controls on accumulation and preservation of OM in organic-rich laminites of the Keg River Formation.

1.2 Previous Studies

A number of comprehensive overviews of the Devonian System in the WCSB have been published including those by Williams (1984), Burrowes and Krause (1987), Moore (1988), Wendte (1992a), and Meijer Drees (1994). Isolated, hydrocarbon-bearing reefs of the Rainbow Sub-basin have been studied since the early 1960's (e.g., Hriskevich, 1966; Langton and Chin, 1968; Barss *et al.*, 1970; Schmidt *et al.*, 1985; Campbell, 1987). Very few studies of similar reefs in the Zama Sub-basin have been published (e.g., McCamis and Griffith, 1967; Walsh, 1986). There are few recently published papers that directly address sedimentology and/or source rocks within the Keg River Formation in the Rainbow and Zama sub-basins (e.g., Fowler *et al.*, 2001). The most recently published papers are engineering studies concerned primarily with horizontal drilling practices and enhanced recovery techniques. Chernyk (1994), Nikakhtar *et al.*, (1996), McIntyre *et al.*, (1996), Fong *et al.*, (1996), and Wong and Fong (1997) focused on reservoir engineering within the Rainbow Sub-basin. Davison *et al.*, (1999) described tertiary recovery within the Zama Sub-basin. Statistical studies used fractal geometry to estimate exploration success within the Rainbow Sub-basin (Cheng *et al.*, 2000) and integrated data sets including exploration history, geological play characteristics, and seismic prospecting activity to construct favorability maps of the Rainbow Sub-basin (Chen *et al.*, 2000).

1.3 Geologic Setting

The Keg River Formation forms the lower portion of the Upper Elk Point Subgroup in northern Alberta, the location of this study (Figs. 1.1 and 1.2). Carbonate, evaporite, and

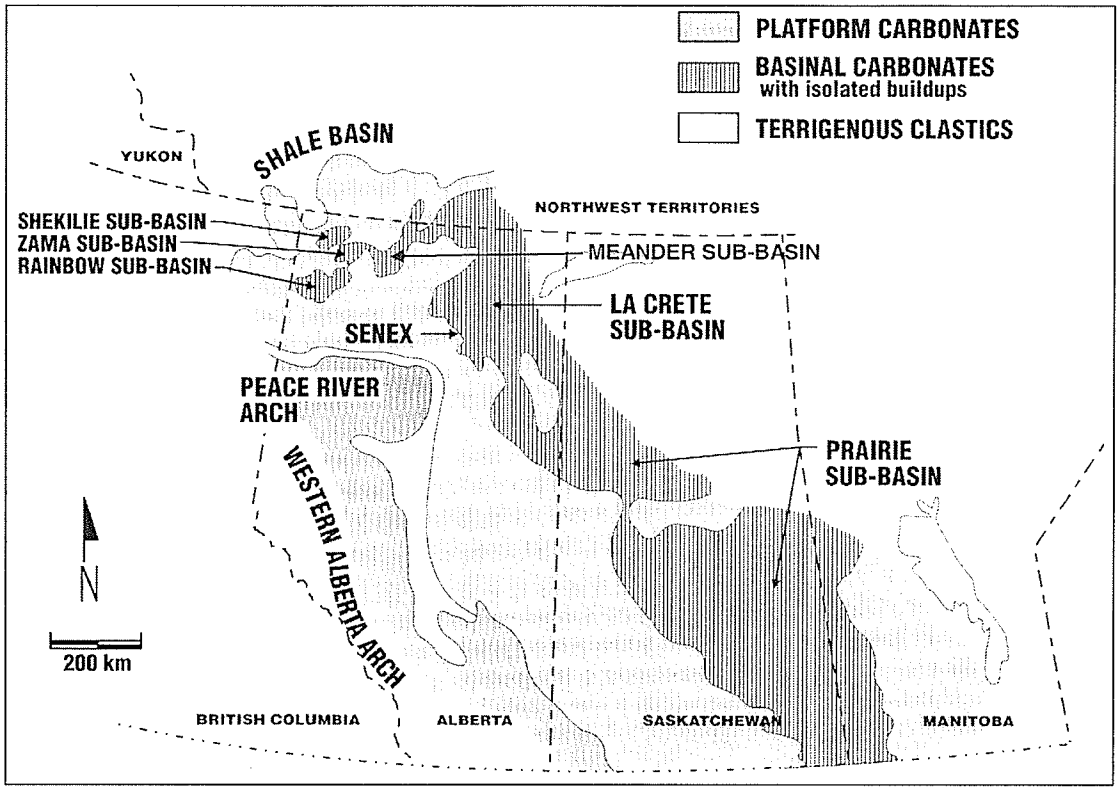

Figure 1.1 Map showing the distribution of the major environmental facies of the Keg River Formation in Alberta, Saskatchewan, and Manitoba deposited in the Elk Point Embayment. Lower Keg River bituminous laminites have widespread distribution in the Rainbow, Zama, and La Crete sub-basins (modified from Chow *et al.*, 1995a).

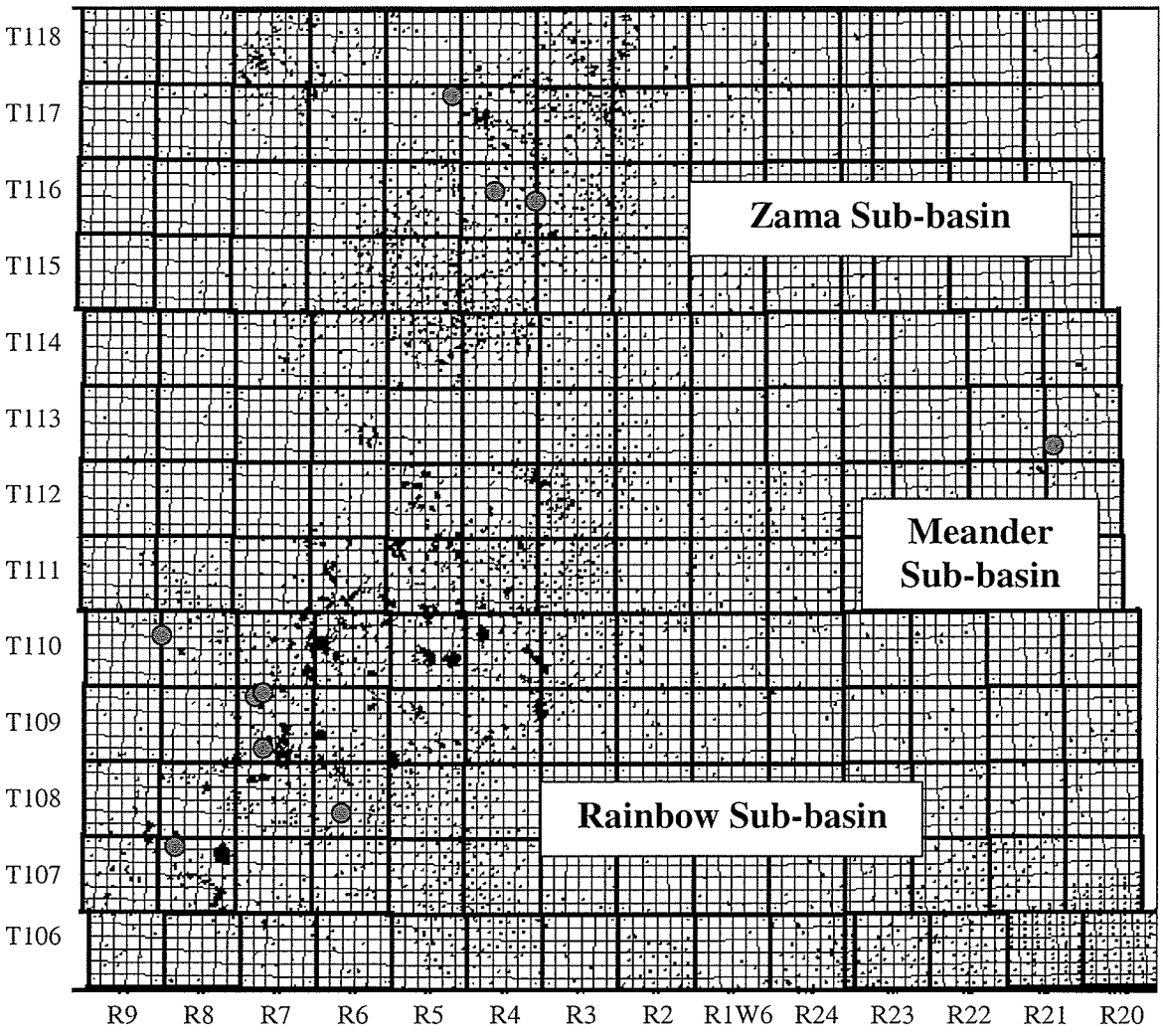

Figure 1.2 Map of study area highlighting the Rainbow and Zama sub-basins and indicating the location of wells (black dots) and the distribution of cores examined (red dots). Refer to Figure 1.1 for general location of the study area with respect to provincial borders.

minor siliciclastic rocks of this subgroup were deposited in the widespread Elk Point Embayment that stretched from northeastern British Columbia and the District of Mackenzie southeastward into the Williston Basin of southern Saskatchewan, Manitoba, North Dakota, and Montana (Fig. 1.1) (Meijer Drees, 1994).

The Western Alberta Arch in southwestern Alberta formed a barrier between the Elk Point Embayment and a smaller, time-equivalent embayment in southwestern British Columbia, called the Golden Embayment (Meijer Drees, 1994).

During the Eifelian, open-marine waters invaded the Elk Point Embayment depositing evaporitic and carbonate sediments of the Chinchaga Formation in the Rainbow and Zama region (Meijer Drees, 1994). At this time, the Rainbow and Zama region was expressed as a broad topographic low separated from the rest of the Elk Point Embayment by regional highlands. The Peace River Highland formed an emergent boundary to the south of the Rainbow and Zama area, and the Tathlina Highland formed an emergent boundary to the north. During the later, regressive phase of this open-marine incursion, the fossiliferous, shallow-marine ramp succession of the Lower Keg River Member was deposited in the Rainbow and Zama region (Campbell, 1992; Meijer Drees, 1994). The lower part of the Winnipegosis, upper Lonely Bay, Dunedin, and Nahanni formations represent the lateral equivalents of the Lower Keg River Member (Fig. 1.3) (Meijer Drees, 1994). The regressive phase is also represented in southeastern British Columbia by the Harrogate and Mount Forster formations (Fig. 1.3).

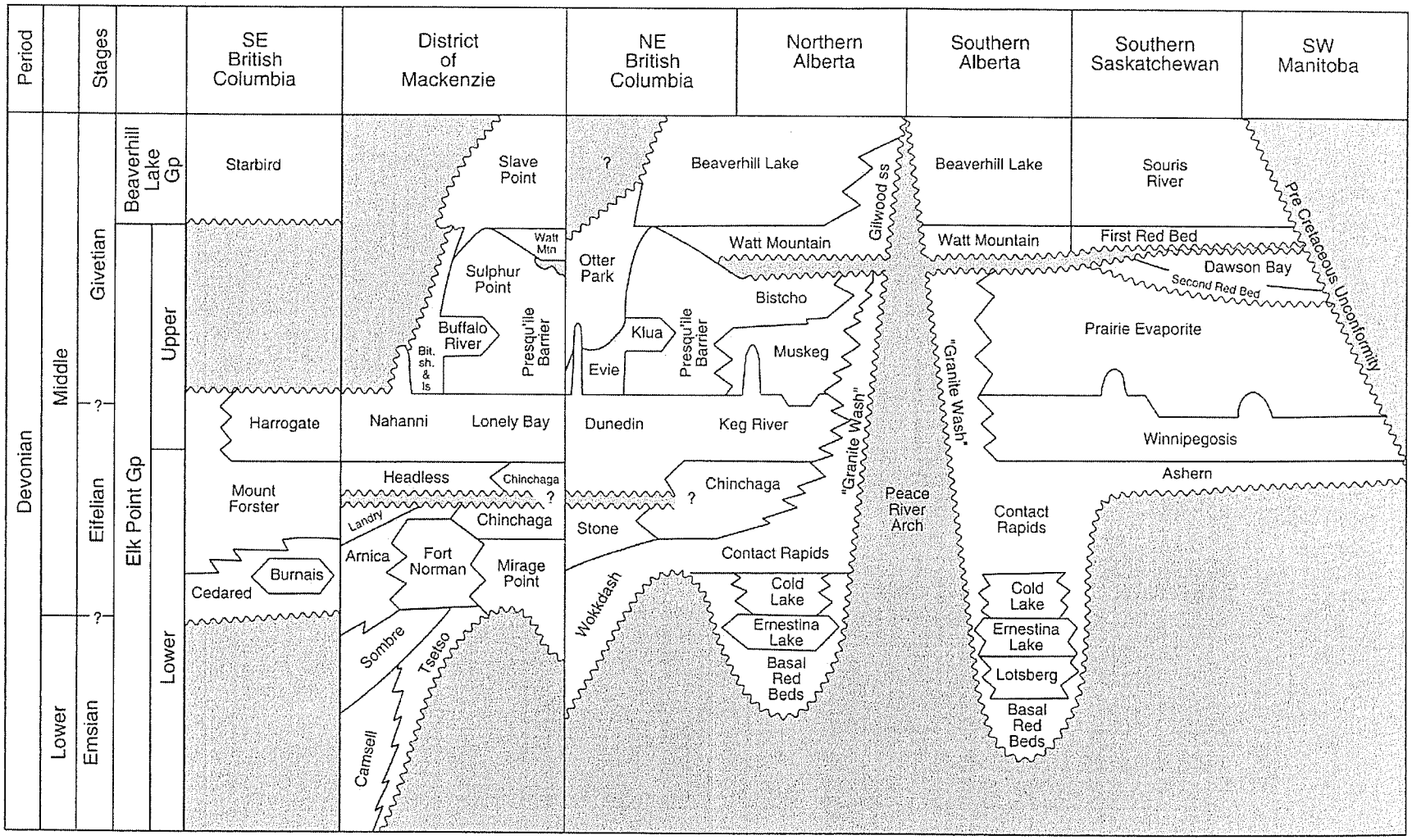

Figure 1.3 Correlation chart for the Lower and Middle Devonian strata of the Elk Point Group (from Meijer Drees, 1994).

Deposition of the Keg River Formation and its lateral equivalents continued during a subsequent late Middle Devonian transgressive phase caused by increased subsidence or a rise in relative sea level (Meijer Drees, 1994). This transgressive phase resulted in basin differentiation and facilitated vertical reef growth in the Upper Keg River Member in the Rainbow and Zama sub-basins in northern Alberta, as well as in stratigraphically equivalent units elsewhere in the WCSB (Meijer Drees, 1994). Langton and Chin (1968) recognized small pinnacle reefs (~1.6 km diameter at the circular base, up to a maximum of ~250 m thick) and large pinnacle reefs (~2.4 km diameter at the base which is circular to elongate in plan view, up to a maximum of ~250 m thick), as well as atoll reefs, within the Rainbow Sub-basin. Large atolls have oval bases approximately 6.4 km long and 4 km wide, and are characterized by lagoonal facies enclosed by an organic-reef rim. Small atolls (also called crescent-atolls) are approximately 3.2 km long and 1.6 km wide at the base with the long axis oriented in a north-northwest direction. A crescent-shaped organic reef rim developed preferentially on the northeast side of each atoll and lagoon facies developed behind this rim. Reef foreslope and off-reef facies of isolated reefs remain relatively consistent throughout the Rainbow and Zama sub-basins despite the variations in reef morphology (McCamis and Griffith, 1967; Langon and Chin, 1968). In both sub-basins, the reef foreslope is a depositional margin characterized by an accreting slope of reef talus that extends from the reef core and merges gradually with the basin floor (cf. Enos and Moore, 1983). Dipmeter evidence from the Rainbow Sub-basin indicates a reef foreslope angle of 20-25° with considerably lower slope angle in distal foreslope positions (Langton and Chin, 1968). This concave foreslope morphology probably developed as sediment bypass occurred along the steeper slopes of the proximal

foreslope and mass wasting products settled in the distal foreslope (cf. Coniglio and Dix, 1992). off-reef deposits in the Rainbow Sub-basin consist of a basal crinoid-rich unit overlain by sparsely fossiliferous shale and limestone which exhibit decreasing grain size, organic matter, and intraclasts progressively higher in the section (Langton and Chin, 1968). These changes indicate decreasing energy upwards due to relative sea level rise. McCamis and Griffith (1967) also observed fine, reef-derived material in inter-reef positions in the Zama Sub-basin.

As vertical reef accretion progressed in the Rainbow and Zama sub-basins, other parts of the Elk Point Embayment experienced deposition of widespread bank carbonates during the late Middle Devonian transgression (Meijer Drees, 1994). At this time, the Presqu'ile Barrier was formed by the amalgamation of vertically accreting reefs at the entrance of the Elk Point Embayment and the Hay River Bank accreted vertically to form a barrier between the Rainbow Sub-basin to the south and the Zama Sub-basin to the north

Conditions in the Elk Point Embayment became restricted due to the effects of the Presqu'ile Barrier which limited influx of sea water into the embayment (Campbell, 1992; Meijer Drees, 1994). Shallow water carbonate growth was terminated by a relative sea level drop attributed to either to a regional sea level fall or to evaporitic drawdown (Campbell, 1992). This sea level drop led to exposure of reefs and carbonate banks in the Rainbow and Zama sub-basins and development of hypersaline conditions. Precipitation of anhydrite and halite of the Muskeg Formation filled the sub-basins and were deposited throughout the Elk Point Embayment in northern Alberta. Laterally equivalent Prairie

Evaporite salts were deposited in southern Alberta, southern Saskatchewan, and parts of southwestern Manitoba in supratidal flats, coastal lagoons, and ephemeral lakes remaining behind the Presqu'ile Barrier in the restricted Elk Point Embayment (Meijer Drees, 1994).

1.4 Economic History of the Rainbow and Zama Sub-basins

Exploration within the Rainbow Sub-basin began in 1954 (Cheng *et al.*, 2000) and by March 1965, Banff Oil Ltd. and Aquitaine Company of Canada Ltd. had discovered oil in a Middle Devonian reef within the sub-basin (Hriskevich, 1966). Following the discovery well (Banff Aquitaine Rainbow West 7-32-109-9 W6M), exploration in the area intensified resulting in the discovery of 56 Middle Devonian reefs by 1967, 38 of which held commercial quantities of hydrocarbons (Langton and Chin, 1968). Petroleum exploration continues in the Rainbow Sub-basin and as of 1993, a total of 375 wells had been drilled resulting in 66 oil discoveries, 11 gas discoveries, 79 oil and gas discoveries, and 219 unsuccessful wildcats (Cheng *et al.*, 2000). The Rainbow Field and the Rainbow South Field have been established in the Rainbow Sub-basin. In the Rainbow Field, the in-place volume of oil is ~219.7 10^6m^3 (~1,318.2 MMBbls) and the in-place volume of gas is ~32,118 10^6m^3 (~1,124.1 Bcf) (Meijer Drees, 1994). In the Rainbow South Field, the estimated in-place volume of oil is ~45.7 10^6m^3 (~274.2 MMBbls) and the estimated in-place volume of gas is ~9,316 10^6m^3 (~326.1 Bcf).

The petroleum potential of the Zama Sub-basin was realized in 1966 when a wildcat well, British American-Hudson's Bay Zama North 16-19-116-4 W6M, encountered

hydrocarbons within a Middle Devonian reef (McCamis and Griffith, 1968). Following this discovery well, hundreds of wells have been drilled in the Zama sub-basin. The Zama Field has estimated in-place oil reserves of ~85.1 10^6m^3 (~510.6 MMBbls) and in-place gas reserves of ~8,205 10^6m^3 (~287.3 Bcf) (Meijer Drees, 1994).

1.5 The Study

1.5.1 Objectives of Study

The carbonate ramp and forereef successions of the Keg River Formation in the Rainbow and Zama sub-basins were studied using an integrated approach that combined stratigraphy, sedimentology, organic petrology, and organic geochemistry in order to:

1) develop a stratigraphic framework and depositional model for the Lower Keg River Member and reef foreslope facies of the Upper Keg River Member in these sub-basins;
2) establish stratigraphic correlations of the Lower Keg River Member between the two sub-basins;
3) determine the primary controls on OM accumulation and preservation within organic-rich, laminated units in the Keg River Formation; and
4) evaluate the effects of OM accumulation on the growth of Devonian stromatoporoid reefs.

Reef facies of the Upper Keg River Member were not examined.

1.5.2 Study Location

The study area extends from Township 106 to 117 and from Range 21 W5M to Range 9 W6M and is situated approximately 600 km northwest of Edmonton, Alberta. The area encompasses the Rainbow Sub-basin (Township 106 to 111 and Ranges 2 to 10 W6M), the Zama Sub-basin (Township 114 to 119 and Ranges 3 to 8 W6M), and the western part of the Meander Sub-basin (Fig. 1.2).

1.6 Methodology

1.6.1 Selection of Wells

Ten wells within the study area were selected for examination and description based on the following criteria: a) penetration of the Chinchaga Formation, Lower Keg River Member, and Upper Keg River Member in foreslope or off-reef positions, b) presence of core and/or cuttings for the intervals of interest, and c) cored intervals containing organic-rich, laminated units. Six of the selected wells are within the Rainbow Sub-basin, three wells are in the Zama Sub-basin, and one well is in the Meander Sub-basin (Appendix A).

Only one well from the Meander Sub-basin was chosen because this sub-basin was a secondary part of the study. Stratigraphic correlation between the Meander Sub-basin and the Rainbow and Zama sub-basins was attempted (Encl. 1 and 2), and preliminary sedimentology and organic petrology were completed, but a lack of data precluded further work.

1.6.2 Cross Section Construction

Petrophysical logs (gamma ray, sonic, and bulk density) for all wells from which core or cuttings had been examined were incorporated into a stratigraphic cross section in order to illustrate stratal geometry and stratigraphic correlations within the study area (Encl. 1 and 2). Correlations of lithostratigraphic units between wells were based on integration of petrophysical log signatures (mainly gamma ray, sonic, and density), and observations from detailed core and cuttings examination (Appendix B, Encl. 1 and 2). The top of the Chinchaga Formation was used as the datum because of the nearly flat-lying depositional nature of this contact (cf. McCamis and Griffith, 1967; Langton and Chin, 1968; Barss *et al.*, 1970; Schmidt *et al.*, 1985; Walsh, 1986).

1.6.3 Core Examination and Description

Over 50 m of core from 9 drill cores were examined in detail, photographed, and sampled for sedimentological, organic petrological, and geochemical analysis (Appendix B). This work was undertaken from June to August, 2000 at the Core Research Center of the Alberta Energy and Utilities Board (A.E.U.B.) in Calgary, Alberta. Core descriptions recorded lithology, skeletal and non-skeletal allochemical constituents, structures, porosity types, and color variations (Appendix B). Core depth was corrected to log depth by matching lithological changes observed in drill cores to corresponding log signatures. For example, the obvious lithological change from the Chinchaga Formation anhydrite to the overlying Lower Keg River Member carbonate was readily recognizable in both core and bulk density logs. A total of 160 m of cuttings samples from 3 wells was also examined at the Core Research Center in July 2000.

Several lithologic classification schemes were used in this study. Dunham's (1962) classification of limestones as modified by Embry and Klovan (1971), was used as a classification scheme for all carbonate rocks observed (Fig. 1.4A). Dolostones had sufficient fabric preservation to allow classification using this scheme. Dunham's modified classification lends itself well to core studies in which detailed description of depositional textures are used for paleoenvironmental interpretations. The classification of Choquette and Pray (1970) was utilized in the description of porosity (Fig. 1.4B) and the classification of Maiklem *et al.* (1969) for anhydrite was used to describe the Chinchaga and Muskeg Formations.

Core was examined wet using a hand lens and binocular microscope. Limestone and partially dolomitized limestone core were etched using dilute (10%) hydrochloric acid to better observe small-scale features such as biotic constituents, porosity, sedimentary structures and other characteristics which can be concealed by dust, saw marks, and damage to the core. Dolostone core was sanded with coarse then fine grit sandpaper in order to facilitate observation of primary textures obscured by dolomitization. Alizarin Red-S solution was utilized on selected core segments in order to determine the amount of dolomite present (Appendix C.1).

Cuttings samples were examined wet and dry using a binocular microscope in order to determine lithology, and skeletal and non-skeletal allochemical constituents. These samples provided information about depositional environments not represented in core (i.e., distal foreslope and off-reef positions).

A

ALLOCHTHONOUS LIMESTONES (ORIGINAL COMPONENTS NOT ORGANICALLY BOUND DURING DEPOSITION)						AUTOCHTHONOUS LIMESTONES (ORIGINAL COMPONENTS ORGANICALLY BOUND DURING DEPOSITION)		
LESS THAN 10% >2 mm COMPONENTS				GREATER THAN 10% >2 mm COMPONENTS		BY ORGANISMS WHICH ACT AS BAFFLES	BY ORGANISMS WHICH ENCRUST AND BIND	BY ORGANISMS WHICH BUILD A RIGID FRAMEWORK
CONTAINS LIME MUD (<0.03 MM)		NO LIME MUD		MATRIX SUPPORTED	>2 mm COMPONENT SUPPORTED			
MUD SUPPORTED		GRAIN SUPPORTED						
<10% GRAINS	>10% GRAINS							
MUDSTONE	**WACKESTONE**	**PACKSTONE**	**GRAINSTONE**	**FLOATSTONE**	**RUDSTONE**	**BAFFLESTONE**	**BINDSTONE**	**FRAMESTONE**

B

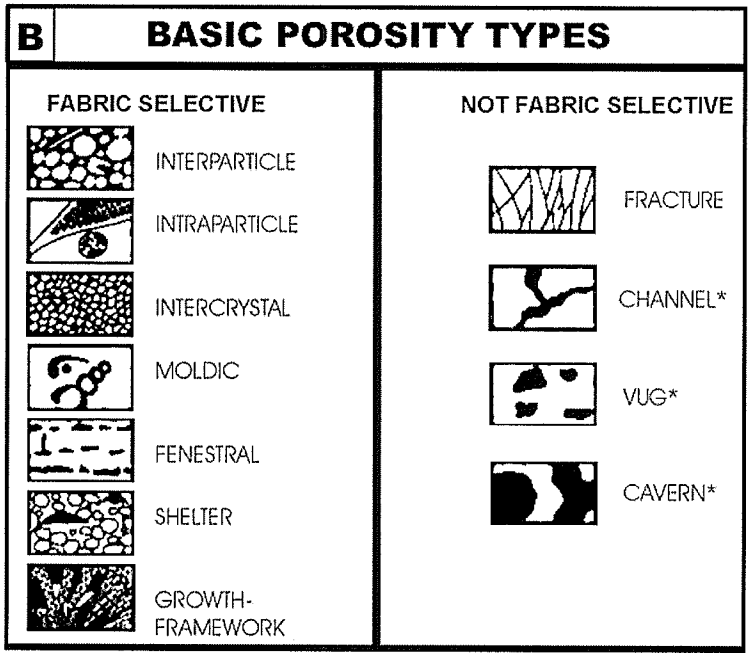

Figure 1.4 A) Dunham's (1962) classification of limestones as modified by Embry and Klovan (1971) (modified from Reijers and Hsu, 1986). B) Geological classification of porosity in carbonate rocks (modified from Choquette and Pray, 1970).

1.6.4 Carbonate Petrography

A number of representative samples was taken from each lithofacies described. A total of 111 standard (5 cm x 7.5 cm) thin-section were prepared and subsequently stained using a 50:50 mixture of Alizarin Red-S and potassium ferricyanide in order to determine the degree/distribution of dolomitization and to identify ferroan carbonate (Appendix C.1). All thin-sections were examined and described for allochems, matrix, cement, and fine-scale sedimentary structures to complement core descriptions (Appendix D). Thin-sections were examined using a conventional Nikon OPTIPHOT-POL petrographic microscope. Photomicrographs were taken using a MICROFLEX UFX-IIA photomicrographic attachment. Percentage estimates were based on visual assessment in conjunction with comparison charts for estimating percentages of constituents by volume in thin sections (Terry *et al.*, 1955). The crystal size classification of Folk (1957) was used to describe authigenic constituents (Table 1.1) and the Udden-Wentworth size class scale was used for grain size (Wentworth, 1922). The dolomite texture classifications of Gregg and Sibley (1984) and Sibley and Gregg (1987) were utilized for description of all dolomite observed (Fig. 1.5).

Table 1.1 Size scale for authigenic constituents of carbonate rocks (modified from Folk, 1957).

CLASSIFICATION	SIZE
Extremely coarsely crystalline	>4 mm
Very coarsely crystalline	1 – 4 mm
Coarsely crystalline	0.25 - 1 mm
Medium crystalline	0.062 - 0.25 mm
Finely crystalline	0.016 – 0.062 mm
Very finely crystalline	0.004 - 0.016 mm
Aphanocrystalline	<0.004 mm

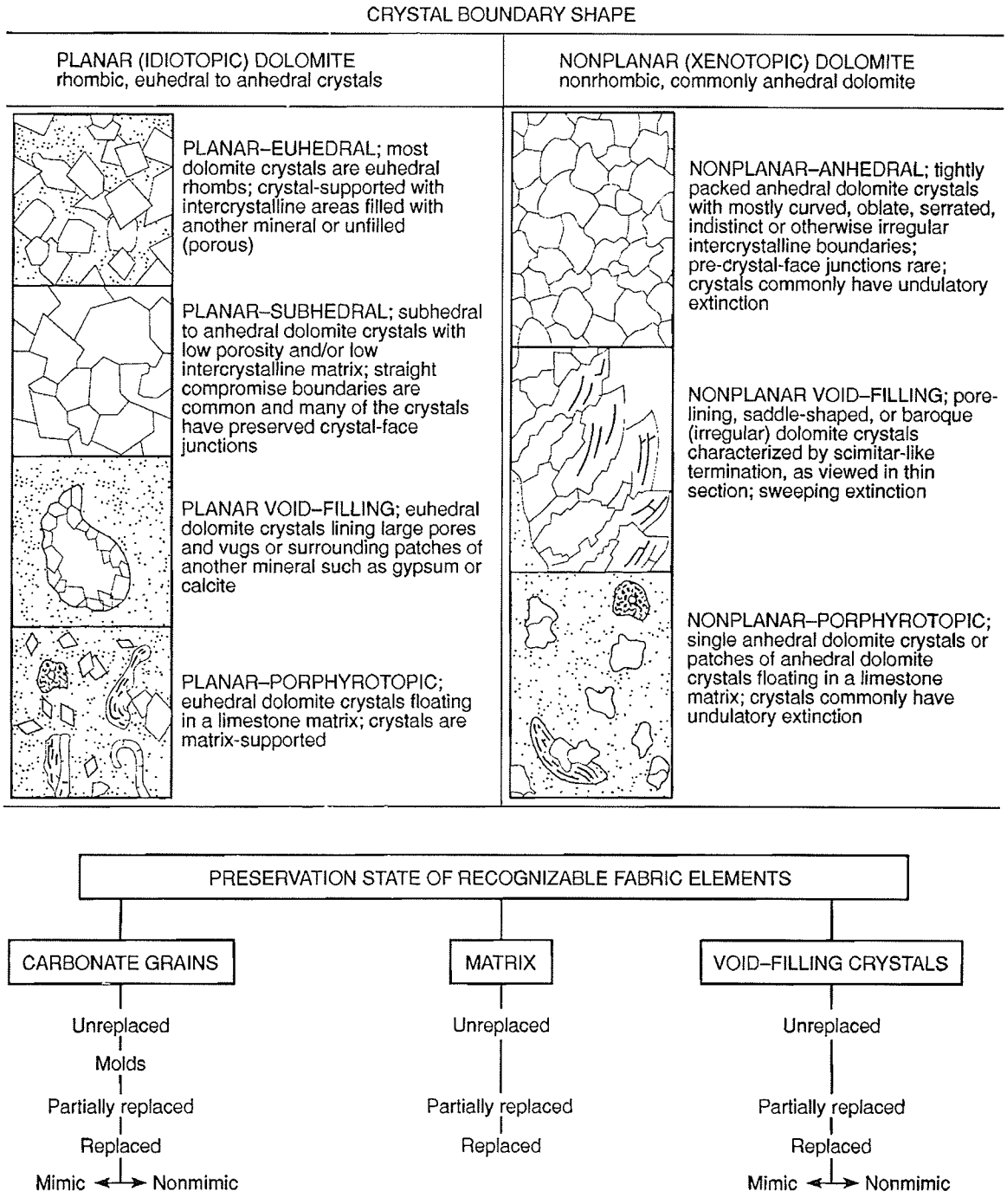

Figure 1.5 Classification of dolomite textures (from Gregg and Sibley, 1984; Sibley and Gregg, 1987).

Diffused plane-polarized light microscopy (Appendix C.2) was used to facilitate observation of relict grains and textures in partially and completely dolomitized carbonates. Such grains and textures can be rendered "invisible" to conventional petrographic methods. In fact, dolostones viewed under plane-polarized light and crossed nicols can be recrystallized to the point that they display only a crystalline texture and provide little additional information on depositional origin.

1.6.5 Organic Petrology and Rock-Eval Pyrolysis

A total of 81 samples was selected from the nine drill cores examined for the purpose of organic petrology (Appendix F). An effort was made to sample the most organic-rich intervals present in each core. These samples were selected based on a number of criteria including: a) relatively dark color ranging from dark brown to grey or black, b) laminated appearance, c) fissile nature indicating the presence of argillaceous material, and d) presence of oil-staining in the sample interval. After collection, this sample set was "high-graded" based on total organic carbon (TOC) and other geochemical parameters determined by Rock-Eval 6 (the most recently developed Rock Eval apparatus) pyrolysis done on 74 organic-rich samples in the Organic Geochemistry Laboratory at the Geological Survey of Canada in Calgary (Appendix G) (refer to Behar *et al.*, 2001 for a full discussion of Rock Eval 6 technology). During Rock-Eval pyrolysis, powdered samples are gradually heated in the absence of oxygen to yield organic compounds (Peters, 1986). This method provided rapid determination of kerogen type, kerogen evolution, and hydrocarbon source potential of samples (Tissot, 1984) (Appendices E.2 and E.3). Geochemical data collected by Rock-Eval pyrolysis were also used to create

hydrogen index vs. oxygen index plots (HI vs. OI plots) which facilitate determination of kerogen types and thermal maturity as well as hydrogen index vs. maximum temperature plots (HI vs. T_{max} plots) indicating kerogen quality.

Sixteen samples were eliminated from the data set due to sampling density and/or low TOC values. The remaining 65 samples (55 from the Rainbow Sub-basin, 7 from the Zama Sub-basin, and 3 from the Meander Sub-basin) were analyzed using organic petrology. Lack of appropriate core in the Zama and Meander sub-basins combined with time constraints on this study prevented more evenly distributed sampling.

1.6.6 Organic Petrology

Samples selected for organic petrology (incident light microscopy) were prepared in the form of polished pellet mounts, 2.5 cm diameter (Appendix E.1). Care was taken to orient the larger sample fragments (up to 1 cm^3) in order to display views both perpendicular to bedding and parallel to bedding within each pellet mount. Representative particulate sample matter was packed around these oriented sample blocks to maximize the sample surface area available for microscopic analysis within each pellet mount.

All samples selected for organic petrology were analyzed in the Organic Petrology Laboratory at the Geological Survey of Canada in Calgary following the procedure in Stasiuk (1999) (Appendix F). Optical data were collected using a Zeiss Axioplan II Universal incident and transmitted light microscope equipped with an ultra-violet (UV)

(HBO 100W mercury) light source and white (halogen 12v, 100w) light source. A Zeiss high-precision scanning stage was utilized for semi-automated petrographic analysis. Zeiss blue-violet 400-440 nm (460 nm beam splitter; 470 nm barrier filter) and green 510-560 nm (580 nm beam splitter; 590 nm barrier filter) excitation filters were used for qualitative and observational aspects of fluorescence microscopy. Samples were leveled on a standard petrographic glass slide, and then scanned using a variety of objectives (X25 water, X40 water, X60 water, and X100 air). Observed macerals were classified based on morphology and fluorescence. Digital images were captured using two different systems: (1) a Diagnostic Instruments ccd system (3 CHIPHRPOGO-CMT) combined with Kontron image analysis software (KS400 version 2.7) and (2) a SPOT high resolution digital camera and software.

CHAPTER 2: STRATIGRAPHY

2.1 Elk Point Group

The Elk Point Group of Early to Middle Devonian age was given group status by Belyea (1952) and subsequently formal and informal units of the Elk Point Group (Fig. 1.3) were introduced by a number of authors including Baillie (1953), Law (1955), Sherwin (1962), Belyea and Norris (1962), Gray and Kassube (1963), Hriskevich (1966), and McCamis and Griffith (1967). The base of the Elk Point Group is defined by the pre-Devonian erosional unconformity and the top is defined at the top of the Watt Mountain Formation, a shale unit that overlies an unconformity, or by the stratigraphically equivalent unconformity where the Watt Mountain Formation is absent (Meijer Drees, 1994). The Elk Point Group is divided into two subgroups. The Lower Elk Point Subgroup comprises, in ascending order, the Basal Red Beds, Ernestina Lake, Cold Lake, and Chinchaga formations. The Upper Elk Point Subgroup comprises, in ascending order, the Keg River, Muskeg, Sulphur Point and Watt Mountain formations. A Devonian first-order depositional cycle, the Upper Elk Point Megacycle, as defined by Wendte (1992b), consists of the succession from the base of the Cold Lake Formation to the top of the Sulphur Point Formation (Campbell, 1992) (Fig. 2.1). For the purposes of this study, discussion of stratigraphy will be limited to the Chinchaga, Keg River, and Muskeg formations.

Devonian depositional cycles are identified by transitional to sharp contacts that occur between packages of deep-water facies that overlie shallow-water facies or more

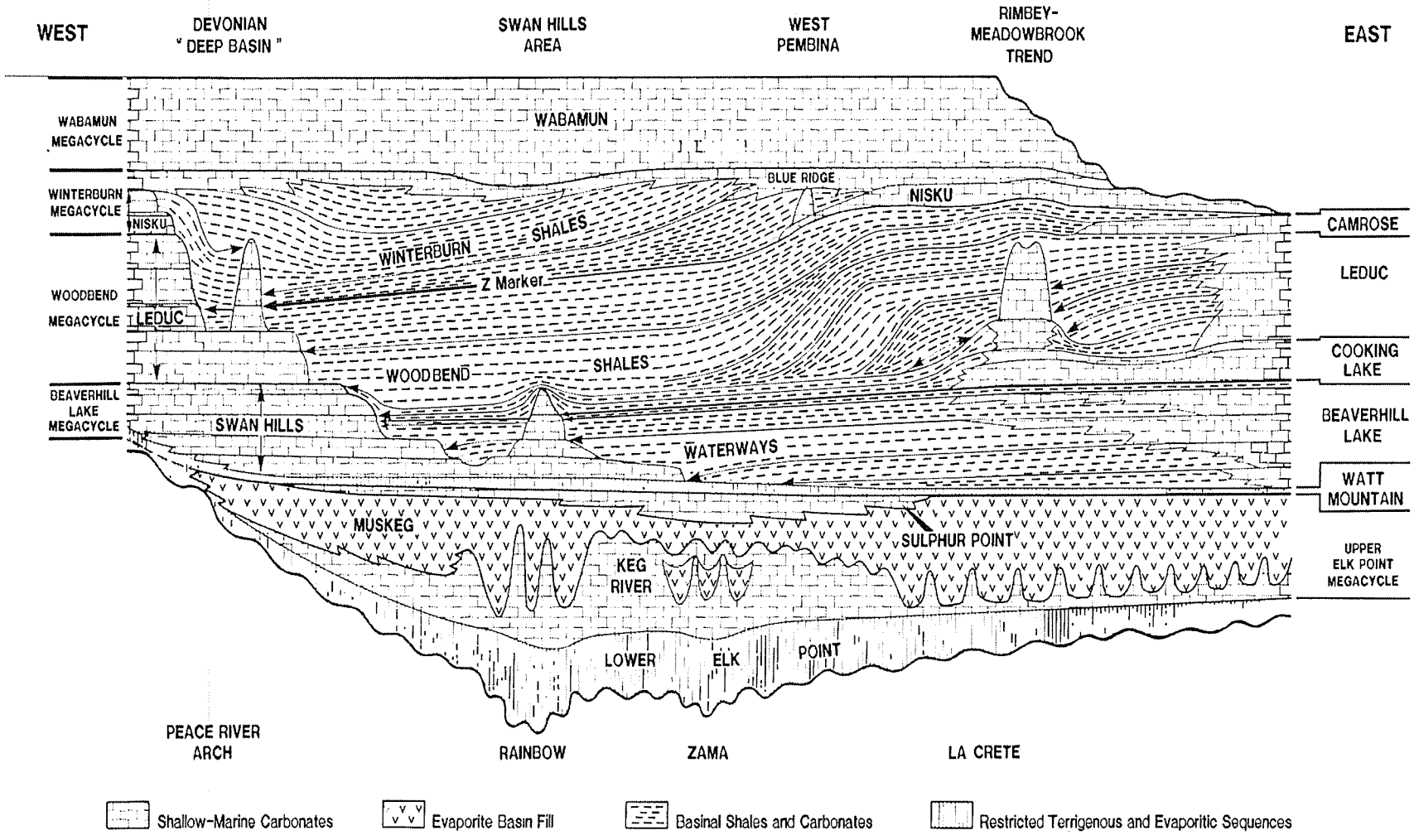

Figure 2.1 Composite schematic cross section illustrating cyclicity of Devonian sequences and the distribution of their major facies. First and second order cycles are shown (from Wendte, 1992b).

basinward facies that overlie more bankward facies (Wendte, 1992b). Such facies transitions can be attributed to a number of allocyclic (externally controlled) factors, including eustatic sea-level rise and subsidence, and autocyclic (internally controlled) factors, such as decrease in sedimentation rates, all of which can initiate new cycles of sedimentation (Galloway, 1989). Individual depositional cycles, as well as stacking patterns of these cycles, influence the distribution and effectiveness of potential source, reservoir, and seal facies (Wendte, 1992b).

2.2 Chinchaga Formation (Upper Chinchaga Formation)

The Chinchaga Formation, as proposed by Law (1955), is the uppermost stratigraphic unit in the Lower Elk Point Subgroup. This anhydrite and dolostone unit is 76 m thick at the Imperial Zama Lake 15-22-115-10 W6M well and thins to 0 m where it onlaps the margins of the Peace River and Tathlina arches. This formation overlies Precambrian basement and early Devonian basal, detrital red beds in the vicinity of these arches. The base of the Chinchaga Formation is abrupt and is defined as the upper limit of red coloration visible at the top of the underlying red bed (Law, 1955). The top of the Chinchaga Formation is gradational and is defined as the highest occurrence of more than trace anhydrite below the Keg River Formation carbonate rocks. This formation extends from the Fort Nelson area of northeastern British Columbia across northern Alberta and north into the southern District of Mackenzie. The type section of this formation is in the California Standard 2-22-117-5 W6M well between 1670 and 1732 m (5475 and 5680 ft) depth.

The Chinchaga Formation at the type locality is predominantly light grey to brown anhydrite with minor brown to brownish grey, aphanocrystalline dolostone (Glass, 1990). These units are underlain in some wells by a variety of lithologies including quartz sandstone with argillaceous and anhydritic cements, anhydrite and anhydrite-rich dolostone, and a dolomitic shale unit. In the vicinity of basement uplifts such as the Tathlina and Peace River arches, increasing proportions of quartz sand and shale occur in the Chinchaga Formation. This formation lacks fossils and represents deposition in a restricted, evaporitic setting.

2.3 Keg River Formation

The Keg River Formation, first proposed by Law (1955), is the basal formation in the Upper Elk Point Subgroup. This widespread carbonate unit disconformably overlies the Chinchaga Formation in both the Rainbow and Zama sub-basins. The Keg River Formation ranges from 10 m thick where it onlaps the Peace River Arch to 300 m thick in the Rainbow Sub-basin (Glass, 1990). The Keg River Formation extends eastward to the Saskatchewan border and is correlative with the Winnipegosis Formation in Saskatchewan and Manitoba (Glass, 1990). To the north of the Peace River Arch, the Keg River Formation extends east to the 4^{th} Meridian where it onlaps the Precambrian Shield and extends west to the Shekilie Barrier near the British Columbia/Northwest Territories border. The type section is in the California Steen River 2-22-117-5 W6M well at depths of 1588 to 1669 m (5210 to 5475 ft) (Law, 1955). The section is composed of brown, slightly argillaceous, skeletal limestone with ostracods, brachiopods, and

crinoids which is overlain by brown and brownish grey, slightly argillaceous, microcrystalline to aphanocrystalline dolostone.

The Lower Keg River Member and the correlative Lower Winnipegosis Member are composed of open-marine ramp carbonate rocks which are overlain by bank and/or isolated reef carbonate strata of the Upper Keg River and the correlative Upper Winnipegosis members (Campbell, 1992).

2.3.1 Rainbow Sub-basin

Hriskevich (1966) subdivided the Keg River Formation in the Rainbow Sub-basin into the Lower Keg River Member, the Upper Keg River Member, and the Rainbow Member (Fig. 2.2). The type section of the Lower Keg River Member, as defined by Hriskevich (1966), is the Banff Aquitaine Rainbow West 7-32-109-8 W6M well between 2018 and 2064 m (6622 and 6772 ft) depth. The Lower Keg River Member ranges from 20 to 30 m thick but is not always recognizable (Hriskevich, 1966). This member is subdivided into a lower carbonate unit and an upper argillaceous unit. The carbonate unit is composed of slightly argillaceous, fine-crystalline dolostone with abundant crinoid ossicles and local argillaceous calcisiltite laminae. The argillaceous unit is predominantly argillaceous calcisiltite containing scattered crinoid ossicles and brachiopod fragments, with minor interbedded calcareous shale.

The type section of the Upper Keg River Member of Hriskevich (1966) is the Imperial *et al.* Black Creek 10-27-109-9 W6M well from 2018 to 2064 m (6622 to 6772 ft) depth.

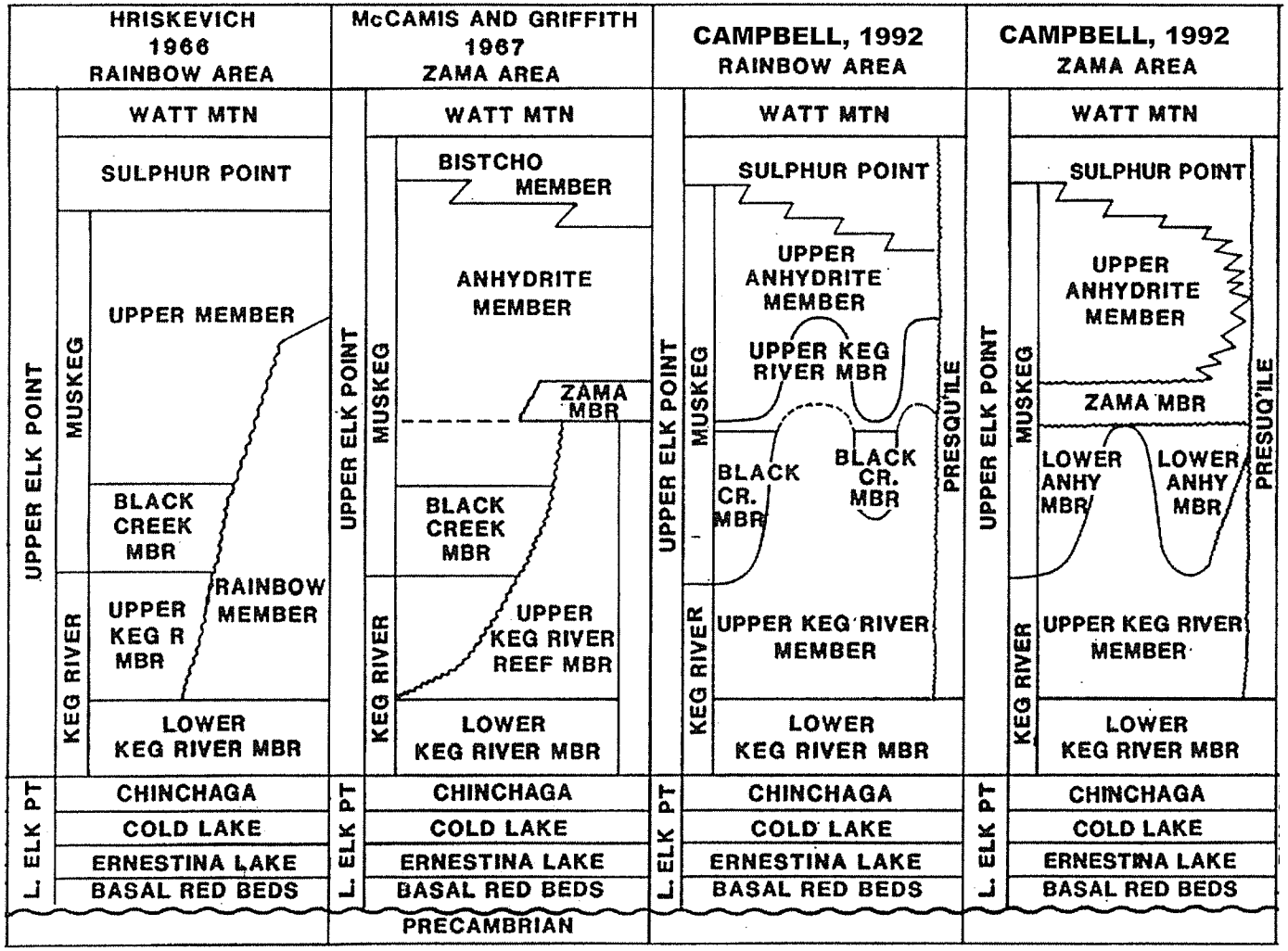

Figure 2.2 Stratigraphic nomenclature of the Elk Point Group (from Campbell, 1992).

Three subdivisions of this member within the Rainbow Sub-basin were proposed by Hriskevich (1966): a lower carbonate unit, a middle argillaceous unit, and an upper carbonate unit. In the type section, the lower unit is 11 m thick and composed of fine to very fine crystalline dolostone with abundant crinoid ossicles and minor coral fragments. The middle unit is 21 m thick and consists of interbedded calcareous shales and bituminous limestones with abundant tentaculids. The upper unit is 14 m thick and is made up of calcilutite with rare fossils such as amphiporids.

The Rainbow Member of the Keg River Formation ranges from 60 to 260 m thick and is a name used only within the Rainbow Sub-basin (Hriskevich, 1966). This member has its type section in the 2-32-109-8 W6M well between 1788 and 2018 m (5866 and 6622 ft) depth. The Rainbow Member is a mostly dolomitized reef unit and ranges from boundstones to packstones and grainstones which have been extremely altered by cementation, leaching, late-stage dolomitization, fracturing, anhydrite replacement, and deposition of bitumen in pore spaces (Glass, 1990). Hriskevich (1966) recognized three stages of reef growth within the Rainbow Member. The lower stage is typically composed of mottled light and dark grey to brown, fine to coarse-crystalline dolostone with well developed intercrystalline and vuggy porosity. The intermediate stage is calcisiltite to calcirudite, 39 m thick, with abundant stromatoporoids, corals, bryozoans, algae, crinoids, gastropods, pelecypods, brachiopods, and ostracods. Dolomitization created secondary porosity including leached organic vugs (biomoldic porosity), organic porosity developed in stromatoporoids (intraskeletal porosity), and intergranular porosity. The uppermost stage, 16 m thick, is completely dolomitized and ranges from light to dark

brown, laminated dolopackstones to dolograinstones with vague remnants of stromatoporoids.

2.3.2 Zama Sub-basin

McCamis and Griffith (1967) subdivided the Keg River Formation in the Zama Sub-basin into the Lower Keg River Member and the Upper Keg River Reef Member (Fig. 2.2). The Lower Keg River Member is the same as that of Hriskevich (1966). The Upper Keg River Reef Member ranges from 50 to 105 m thick and its type section is in the Zama North 16-19-116-4 W6M well between 1500 and 1560 m (4922 and 5117 ft) depth. It is composed of reef limestones and dolostones that are stratigraphically equivalent and very similar sedimentologically to the lower two stages of reef growth in the Rainbow Member of Hriskevich (1966). It is important to note that McCamis and Griffith (1967) did not identify, in the Zama Sub-basin, a stratigraphic equivalent to the Upper Keg River Member of Hriskevich (1966).

2.3.3 Stratigraphic Nomenclature Used in This Study

Campbell (1992) simplified the stratigraphic nomenclature for the Rainbow and Zama sub-basins by developing terminology appropriate for utilization in both these sub-basins (Fig. 2.2). Campbell (1992) adopted the definition of the Lower Keg River Member as presented by previous authors (Hriskevich, 1966; McCamis and Griffith 1967). However, Campbell (1992) defined an Upper Keg River Member in both the Rainbow and Zama sub-basins that encompasses the Upper Keg River Member and Rainbow Member of Hriskevich (1966) as well as to the Upper Keg River Reef Member of

McCamis and Griffith (1967). Due to its simplicity and utility, the stratigraphic nomenclature of Campbell (1992) will be used as a basis for the this study (Fig. 2.2).

When defined in this manner, the Upper Keg River Member in the Rainbow Sub-basin reaches a maximum thickness of 230 m at the crest of the thickest reefs (Campbell, 1992) and has no expression (i.e., zero thickness) in true off-reef locations (pers. comm., J. Wendte, 2001). Maximum reef development in the Zama Sub-basin reached only 104 m thick (13-07-116-4 W6M), significantly less than the buildups in the Rainbow Sub-basin (McCamis and Griffith, 1967). Zama reefs may have experienced stunted growth relative to Rainbow reefs if elevated subsidence rates occurring in the Rainbow Sub-basin provided more accommodation space in this basin than in the Zama Sub-basin (Campbell, 1992).

Reef demise (culmination of Upper Keg River Member deposition) is marked by deposition of the overlying Upper Anhydrite Member of the Muskeg Formation, which was deposited in response to increasing restriction and salinity (Campbell, 1992). Reefs in the Rainbow Sub-basin reflect an extended period of reef growth when compared to reefs in the Zama Sub-basin (Campbell, 1992). Rainbow reefs grew in a series of stages that can be correlated to the reef stage in Zama, as well as to the overlying Zama Member, and to part of the Upper Anhydrite Member. Therefore, because the Zama Sub-basin was shallower than the Rainbow Sub-basin, reefs in the Zama Sub-basin met their demise due to restriction and elevated salinity earlier than those in the Rainbow Sub-basin.

2.4 Muskeg Formation

The Muskeg Formation was described by Law (1955) and later subdivided into a number of units by Belyea and Norris (1962), Hriskevich (1966), McCamis and Griffith (1967) and Klingspor (1969). These units include the Black Creek and Upper Anhydrite members in the Rainbow Sub-basin and the Lower Anhydrite, Zama, and Upper Anhydrite members in the Zama Sub-basin (Fig. 2.2). The Muskeg Formation is a widespread evaporitic unit extending across much of the northern half of the Elk Point Embayment. This unit displays variable lithologic character ranging from carbonate-rich, evaporite-poor rocks in the northwest to carbonate-poor, evaporite-rich rocks in the southeast. The Muskeg Formation is composed of brownish grey to yellowish grey cryptocrystalline to microcrystalline dolostone, and cryptocrystalline to microfragmental limestone, interbedded with white, grey and brown anhydrite and halite (Law, 1955). The type section is in the California Standard Steen River well 2-22-117-5 W6M at depths between 1377 and 1589 m (4513-5210 ft). This is the thickest unit of the Elk Point Group in northern Alberta ranging from 270 m thick in Imperial Keg River well 1-17-102-2 W6M to 0 m thick near the Peace River Arch. The base of the Muskeg Formation is defined where a gradual change occurs from carbonate rocks of the underlying Keg River Formation to interbedded anhydrite and dolostone. The Watt Mountain Formation disconformably overlies the Muskeg Formation. The basal Watt Mountain Formation is typically terrigenous clastic rocks or limestone breccia (Law, 1955).

In the Rainbow and Zama sub-basins, the Muskeg Formation is divided into three units (Fig. 2.2.) (Campbell, 1992). The lower evaporite succession consists of the Black Creek

Salt in the Rainbow Sub-basin and the Lower Anhydrite Member in the Zama Sub-basin. The intermediate carbonate interval includes the Zama Member in the Zama Sub-basin and a poorly developed equivalent in the Rainbow Sub-basin. The upper evaporite succession consists of the Upper Anhydrite Member in both the Rainbow and Zama sub-basins.

CHAPTER 3: SEDIMENTOLOGY

3.1 Introduction

Detailed core descriptions (Appendix B), thin section examination (Appendix D), and petrophysical log examination have provided the basis for defining nine lithofacies in the carbonate ramp and reef foreslope to off-reef successions in the Keg River Formation in the Rainbow and Zama sub-basins (Table 3.1). Five of these lithofacies comprise the ramp deposits of the Lower Keg River Member: A) bituminous laminite, B) irregular-bedded lime mudstone, C) nodular crinoid-brachiopod wackestone, D) massive crinoid-brachiopod wackestone, and E) bioturbated crinoid-brachiopod floatstone (Fig. 3.1). Three lithofacies represent reef foreslope deposits of the Upper Keg River Member: F) bituminous peloidal laminite, G) massive peloidal-skeletal dolopackstone to dolograinstone, and H) stromatoporoid-coral dolofloatstone to dolorudstone (Fig. 3.2). Lithofacies I, non-fossiliferous dolomudstone, occurs at both the base of the Lower Keg River Member and the top of the Upper Keg River Member.

3.2 Lithofacies A: Bituminous Laminite

3.2.1 Description

This lithofacies ranges from 30 cm to 4.5 m thick and consists of very dark brown to black, argillaceous lime mudstone to styliolinid-tentaculitid wackestone interlaminated with black, bituminous laminae (Fig. 3.3). Carbonate laminae and beds are 0.1–2 cm thick and near-horizontal. This lithofacies is predominantly undolomitized, although locally the extent of dolomitization ranges from 10-90%. One pervasively dolomitized

Table 3.1 (Part A) Summary of characteristic features of lithofacies A to E.

	LITHOFACIES NAME	COLOR	LITHOLOGY	SEDIMENTARY STRUCTURES	ALLOCHEM ABUNDANCE (% OF VOLUME)	MAJOR CONSTITUENTS (size, % of lithofacies)	MINOR CONSTITUENTS	THICKNESS	LOWER CONTACT	UPPER CONTACT	DOLOMITIZATION	POROSITY	SUMMARY OF DEPOSITIONAL ENVIRONMENT	FACIES ASSOCIATION
A	Bituminous laminite	dark brown to black	argillaceous lime mudstone to styliolinid-tentaculitid wackestone	regular laminae, allochems aligned parallel	1-55%	Styliolinids (<2 mm, up to 55%)	Trace tentaculitids, crinoids, brachiopods, and ostracods	0.3 - 4.5 m	grad.	grad.	primarily undolomitized, locally 10-90% dolomitization	trace	Low-energy, deep-subtidal environment situated below storm wave-base, characterized by pervasive dysoxic to anoxic conditions.	OUTER RAMP
B	Irregular-bedded lime mudstone	light, medium, and dark brown	argillaceous lime mudstone to styliolinid-tentaculitid wackestone	irregular bedding, allochems aligned parallel	1-30%	Styliolinids (<2 mm, up to 30%)	Trace tentaculitids, crinoids, brachiopods, and ostracods	0.6 - 4.5 m	grad.	grad.	none	trace	Low-energy, deep-subtidal environment situated below storm wave-base, characterized by dysoxic conditions.	
C	Nodular crinoid-brachiopod wackestone	dark grey to medium brown	skeletal wackestone to floatstone	nodular, compressed microstylolites	10-75%	Crinoids(<1 mm, up to 25%), styliolinids (<2 mm, up to 25%), brachiopods (<5 mm long, up to 20%), and intraclasts (<10 mm long, up to 10%)	Ostracods (<1 mm, up to 10%), gastropods (<1 cm, up to 5%), trace tentaculitids, thamnoporids, *Coenites*, peloids, *Girvanella*, and *Renalcis*	1 - 8 m	grad.	grad.	none to 30%	trace vuggy, intercrystalline	Low-energy, deep-subtidal environment situated below storm wave-base, characterized by oxygenated conditions.	
D	Massive crinoid-brachiopod wackestone	dark grey to black	crinoid-brachiopod wackestone to floatstone	massive to vaguely laminated, minor tempestites	20-85%	Crinoids (1-5 mm, up to 30%), brachiopods (~5 mm long, up to 35%), ostracods (<1 mm, up to 20%), and styliolinids (<2 mm, up to 15%)	Bivalves, peloids (up to 60% locally), trace gastropods, tentaculitids, thin tabular stromatoporoids, thamnoporids, *Coenites*, *Alveolites*, tabular tabulate corals, and *Girvanella*	1 - 29 m	grad.	grad.	none to 100%	<5% fracture, intercrystalline	Low to moderate-energy, deep-subtidal environment situated near storm wave-base, characterized by fully oxygenated conditions.	MID-RAMP
E	Bioturbated crinoid-brachiopod floatstone	medium brown to grey	crinoid-brachiopod floatstone to rudstone, crinoid rudstone, brachiopod rudstone, oncoid floatstone	burrow mottled	35-75%	Crinoids (<10 mm diameter, up to 75%), brachiopods (<2 cm long, up to 35%), and styliolinids (<2 mm, up to 15%)	Trace ostracods, bivalves, gastropods, peloids, intraclasts, grapestones, *Girvanella*, and oncoids (up to 30% locally)	0.5 - 7 m	grad.	grad.	15-100%	1% intercrystalline, vuggy, biomoldic	Moderate-energy, intermediate to deep-subtidal environment situated between storm and fairweather wave-base, characterized by fully oxygenated conditions.	

Table 3.1 (Part B) Summary of characteristic features of lithofacies F to I.

	LITHOFACIES NAME	COLOR	LITHOLOGY	SEDIMENTARY STRUCTURES	ALLOCHEM ABUNDANCE (% OF VOLUME)	MAJOR CONSTITUENTS (size, % of lithofacies)	MINOR CONSTITUENTS	THICKNESS	LOWER CONTACT	UPPER CONTACT	DOLOMITIZATION	POROSITY	SUMMARY OF DEPOSITIONAL ENVIRONMENT	FACIES ASSOCIATION
F	Bituminous peloidal laminite	buff to very light grey with black laminae	peloidal-skeletal dolopackstone to dolograinstone	regular and irregular laminae	40-60%	Styliolinids (<2 mm, up to 30%), undifferentiated brachiopods and bivalves (up to 20%), peloids (up to 20%), and crinoids (up to 10%)	Trace gastropods, ostracods, stromatoporoid fragments, *Coenites*, and grapestones	0.5 - 4.5 m	mod. sharp	very grad.	25-100%	1% intercrystalline	Moderate-energy, intermediate to deep-subtidal environment situated between storm and fairweather wave-base, characterized by oxygenated conditions punctuated by episodes of dysoxia to anoxia.	REEF FORESLOPE
G	Massive peloidal-skeletal dolopackstone to dolograinstone	buff	peloidal-skeletal dolopackstone to dolograinstone	massive	up to 85%	Crinoids (up to 40%), undifferentiated brachiopods and bivalves (up to 35%), peloids (up to 25%), ostracods (up to 10%), and styliolinids (up to 10%).	Small bulbous stromatoporoid fragments (locally abundant)	0.5 - 14.5 m	very grad.	grad.	25-100%	up to 20% intercrystalline, minor intraparticle, moldic, vuggy, fracture	Moderate-energy, intermediate-subtidal environment situated between storm and fairweather wave-base in fully oxygenated conditions.	
H	Sromatoporoid-coral dolofloatstone to dolorudstone	buff to medium brown	stromatoporoid-coral dolofloatstone to dolorudstone with peloidal-skeletal dolopackstone to dolograinstone	massive to bioturbated	30-80%	Stromatoporoid fragments (>2 cm size) of the following forms: wafer (<1 cm thick), thin tabular (1-5 cm thick), thick tabular (>5 cm thick), small hemispherical (up to 5 cm thick), and small bulbous (1 cm diameter). Crinoids (up to 25%), peloids (up to 20%), thamnoporid fragments (~1.5 cm long, up to 25%), *Alveolites* (<7 cm size).	Trace undifferentiated brachiopods and bivalves, ostracods, gastropods, styliolinids, intraclasts, oncoids, *Coenites* (<5 mm diameter), and solitary rugose corals	0.1 - 26 m	grad.	sharp	20-100%	up to 25% intercrystalline, minor fracture, intraparticle, vuggy, biomoldic	Moderate-energy, intermediate-subtidal environment situated between storm and fairweather wave-base in fully oxygenated conditions.	
I	Non-fossiliferous dolomudstone	buff to light grey	dolomudstone	variable: massive, haloturbated, brecciated	up to 30%	none	Locally minor crinoids, undifferentiated brachiopods and bivalves, ostracods, and styliolinids	1 - 1.5 m	sharp	?	100%	<1% intercrystalline, vuggy, fracture	Low-energy, high salinity, restricted environment.	EVAPORITIC CONDITIONS

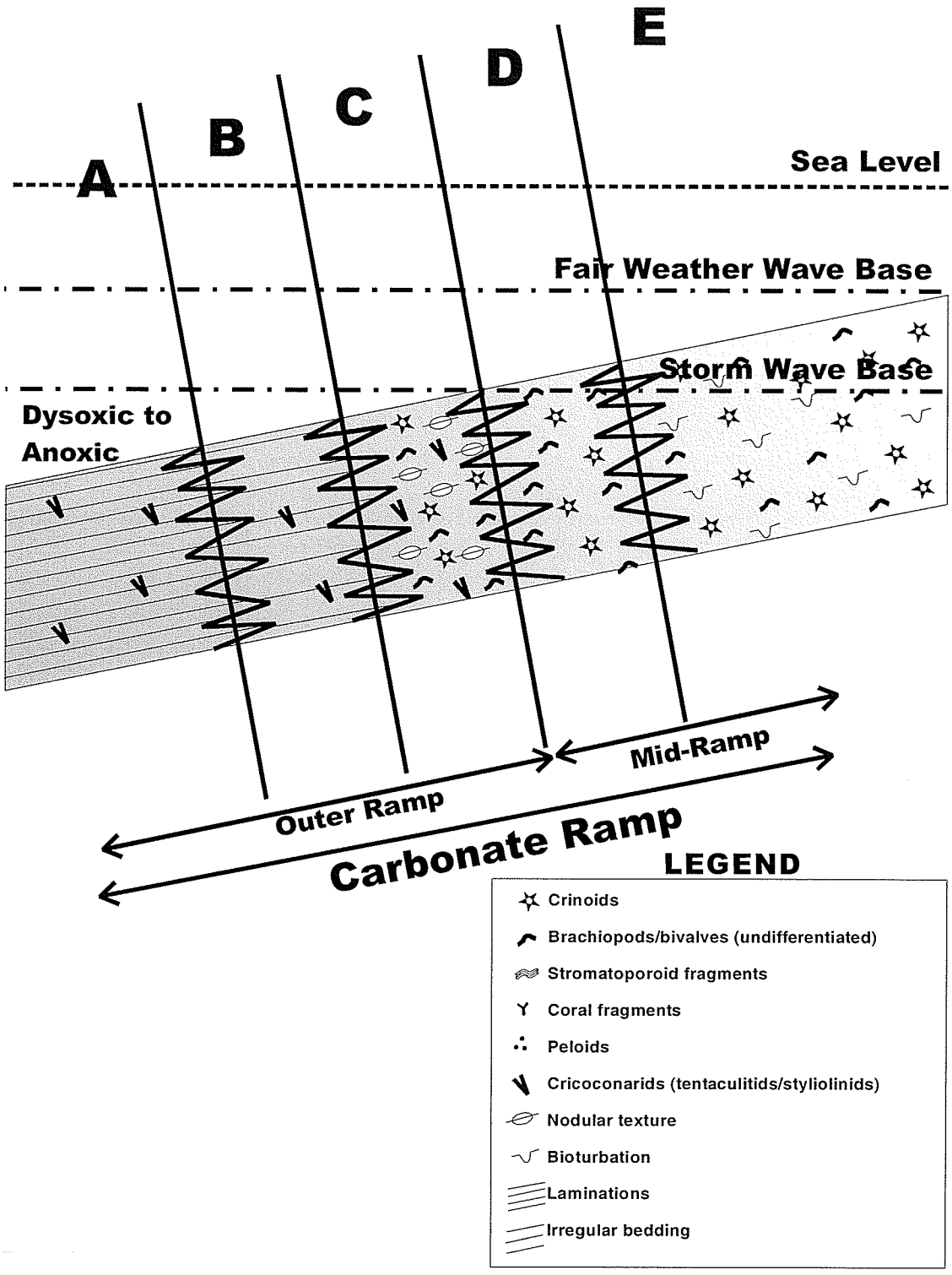

Figure 3.1 Schematic diagram for the Lower Keg River Member illustrating the interpreted depositional settings of lithofacies A to E, major constituents, structures, and the relative positions of the depositional environments of the outer ramp and mid-ramp lithofacies associations. No scale is implied.

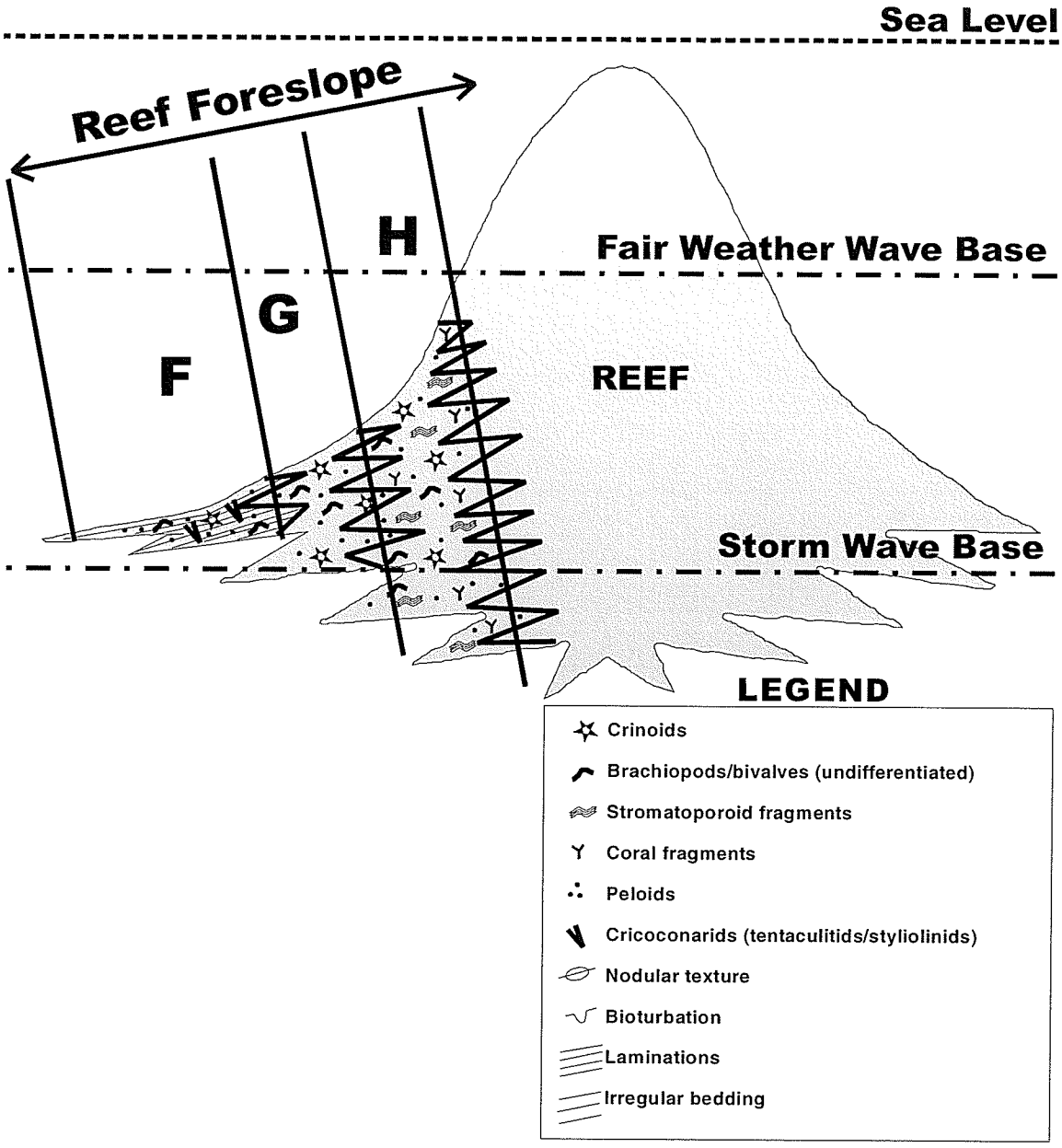

Figure 3.2 Schematic diagram for the Upper Keg River Member illustrating the interpreted depositional settings of lithofacies F to H, major constituents, structures, and the foreslope lithofacies association. No scale is implied. Note: lithofacies I is not illustrated in this diagram because it occurs at the base and top of the Keg River Formation associated with the Chinchaga Formation and the Muskeg Formation respectively.

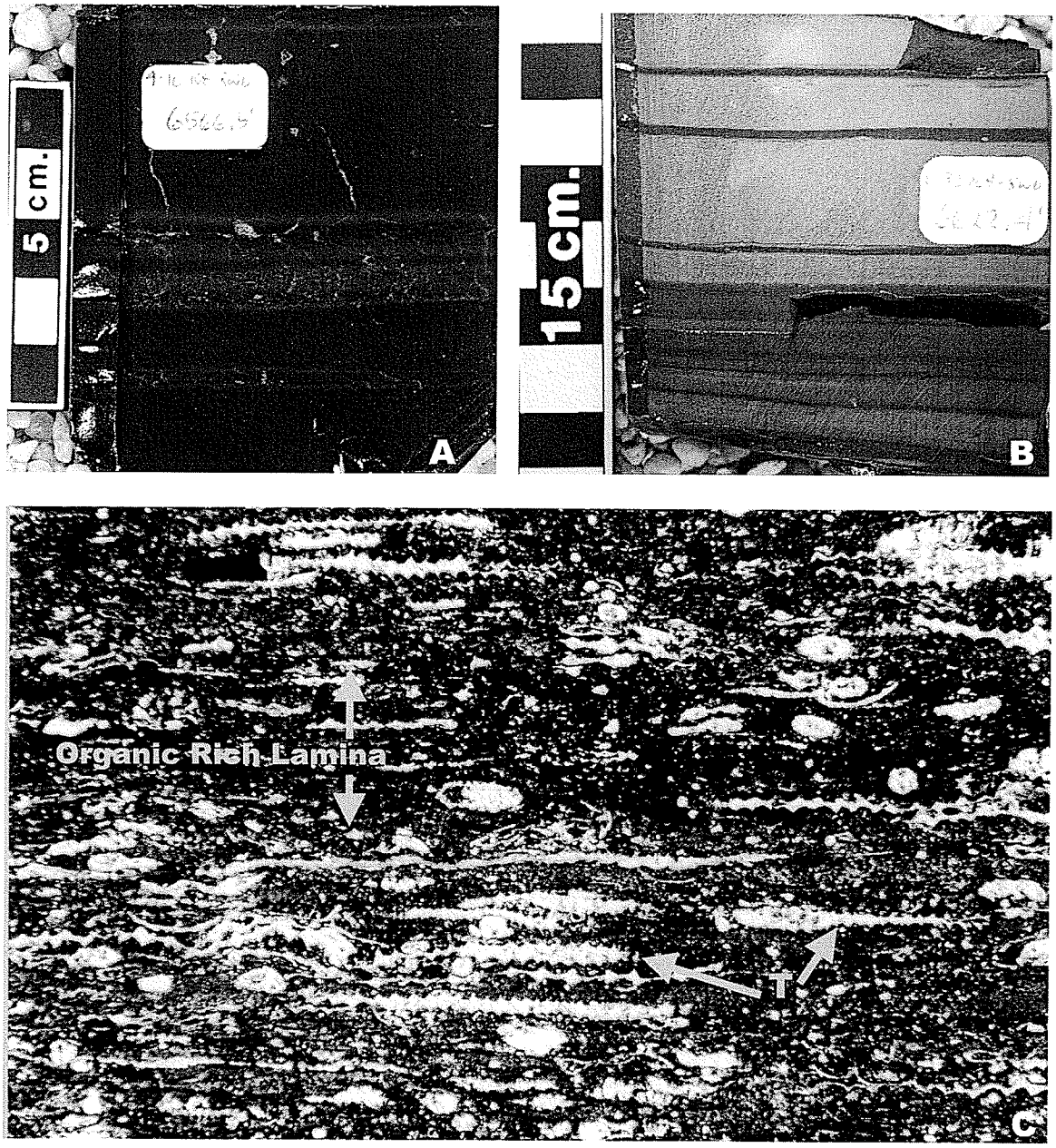

Figure 3.3 Lithofacies A: bituminous laminite. A) Core photo of laminated, bituminous, styliolinid wackestone. Bituminous beds appear black due to OM concentrations or light brown due to abundant terrigenous clay. Carbonate laminae and thin beds are medium grey but not visible in this photo. 4-16-108-8 W6M, 2001.5 m (6566.5 ft). B) Core photo of laminated, bituminous styliolinid dolowackestone. Dolomitized carbonate laminae to thin beds appear light grey and bituminous laminae to thin beds appear black to medium brown. 6-32-109-8 W6M, 2018.5 m (6622.4 ft). C) Thin-section photomicrograph of laminated, bituminous tentaculitid wackestone showing flattened tentaculitids (T) oriented parallel to bedding, and organic-rich lamina. Field of view is 2.5 mm wide. 4-19-116-4 W6M, 1575.5 m (5169 ft).

example of the lithofacies was observed in 6-32-109-8 W6M at 2018.5 m depth where the carbonate laminae are homogeneous, light grey dolomudstone to dolowackestone (Fig. 3.3B). Bituminous laminae are near-horizontal and <40 μm thick, although locally these laminae are grouped into 0.3-1 cm thick layers and stylolitized. Total organic carbon (TOC) content ranges from 0.1-13.8% with a median TOC content of 1%. This lithofacies has trace intercrystalline, intraparticle, fracture, and vuggy porosity.

Faunal constituents comprise 1-55% of lithofacies A and consist of predominantly styliolinids (a smooth-sided conical form of cricoconarid), as well as minor fragmented crinoids, complete and fragmented brachiopods, tentaculitids (a ribbed conical form of cricoconarid), bivalves, and ostracods, generally <2 mm in size. Allochems are oriented parallel to laminations and are concentrated in the carbonate laminae (Fig. 3.3C).

Nonplanar, aphanocrystalline dolomite is most abundant in bituminous laminae, but also occurs as lenses in carbonate laminae and filling intraparticle porosity. Radial-fibrous calcite cement commonly rims the internal and external surfaces of cricoconarid (styliolinid and tentaculitid) and brachiopod tests. Radial-prismatic calcite cement is ubiquitous on styliolinid tests, lining the external and internal surfaces.

Very finely crystalline, anhedral to euhedral pyrite is common (5-10%) in lithofacies A, occurring as framboids concentrated in bituminous laminae, as indistinct pyritic patches within the carbonate laminae, as pyritized allochems, and within intraparticle porosity of

allochems such as cricoconarids, brachiopods, and ostracods. Trace anhydrite, quartz, and bitumen are also present filling intraparticle porosity in allochems.

The bituminous laminite lithofacies can be identified on petrophysical logs by characteristic high gamma ray values and high interval transit times. The amplitude of the log response depends on the volume of clay and OM present in the bituminous laminae of this lithofacies.

3.2.2 Interpretation

The bituminous laminite lithofacies is interpreted to have been deposited in a low-energy, deep-subtidal environment below storm wave-base, characterized by pervasive dysoxic to anoxic conditions. Evidence for a low energy, deep-subtidal setting is the abundance of micrite, terrigenous mud, and OM. Micrite may have formed by inorganic precipitation, breakdown of calcareous green algae, and from disintegration of skeletal debris (cf. Stoakes, 1980; James and Kendall, 1992). Clay-sized terrigenous sediment is interpreted as hemipelagic sediment that entered the intracratonic basin by fluvial or aeolian transport, or by coastal erosion that may have been derived from the Peace River Arch (cf. Coniglio and Dix, 1992). Such fine-grained sediment can be transported great distances from shore by deep-water currents. Fine-grained OM was derived primarily from marine phytoplankton (refer to Chapter 6: Organic Petrology). Other evidence for deep-subtidal deposition is the paucity of shallow marine fauna and the predominance of cricoconarids, which are considered to have been planktonic. They are usually found parallel to bedding in deep-marine limestones suggesting post-mortem settling out from

surface waters into inhospitable bottom waters (cf. Stoakes, 1980; Stearn and Carroll, 1989).

Lithofacies A lacks typical indications of storm wave action, such as hummocky and swaley cross-stratification, grading, gutter casts, interference ripple caps, shell coquinas, fining-upwards sequences, and erosional surfaces, indicating that the deposition of lithofacies A occurred below storm wave-base (cf. Jones and Desrochers, 1992). Minor accumulations of small allochems (crinoids, brachiopods, bivalves, and ostracods) in laminae-parallel concentrations are suggestive of suspension settling from sediment-seawater plumes originating upslope (cf. Coniglio and Dix, 1992). These plumes may have been triggered by tidal flux, storms, ocean currents, or mass wasting. Laminae-parallel shell concentrations may also reflect natural variability in sediment supply and benthic organism mortality rates, or possibly reworking of sediments by deep-water currents.

Pervasive dysoxia or anoxia in the lithofacies A depositional setting is evidenced by the abundance and preservation of mm-scale laminations. Benthic scavenging and bioturbation in an oxygenated marine environment would have destroyed these features (Leggett, 1985). Lithofacies A is also characterized by low faunal diversity (ostracods and rare brachiopods) and a predominance of cricoconarids further supporting restricted conditions due to dysoxic or anoxic bottom waters (Wilson, 1969; cf. Stoakes, 1980). The presence of laminae-parallel concentrations of cricoconarids may be related to mass

mortalities of pelagic organisms resulting from expansion of the dysoxic/anoxic layer into the habitats of these fauna (cf. Chow *et al.*, 1995a).

3.3 Lithofacies B: Irregular-Bedded Lime Mudstone

3.3.1 Description

Lithofacies B, 0.6-4.5 m thick, is composed of dark brown lime mudstone to styliolinid wackestone (herein referred to as carbonate beds) interbedded with medium to light brown, argillaceous lime mudstone to argillaceous styliolinid wackestone (herein referred to as argillaceous beds) (Fig. 3.4A). Each bed type is ~1-4 cm thick and comprises approximately 50% of the lithofacies. Bed contacts are very irregular and commonly distinct, but are locally gradational. The extremely irregular, laterally discontinuous nature of the argillaceous beds imparts a nodular to mottled appearance to the lithofacies. Carbonate beds appear massive to faintly laminated, whereas the argillaceous beds exhibit more pronounced laminations defined by concentrations of disseminated particles of OM and allochem concentrations aligned parallel to bedding. This lithofacies has trace intercrystalline and fracture porosity.

Allochems comprise 1-30% of this lithofacies and are limited to very small skeletal grains (<2 mm size). Styliolinids are the most abundant allochems and only trace ostracods, gastropods, crinoids, and brachiopods are present. Allochems are aligned parallel to the laminations (Fig. 3.4B), and this alignment is more pronounced within the argillaceous beds than within the carbonate beds.

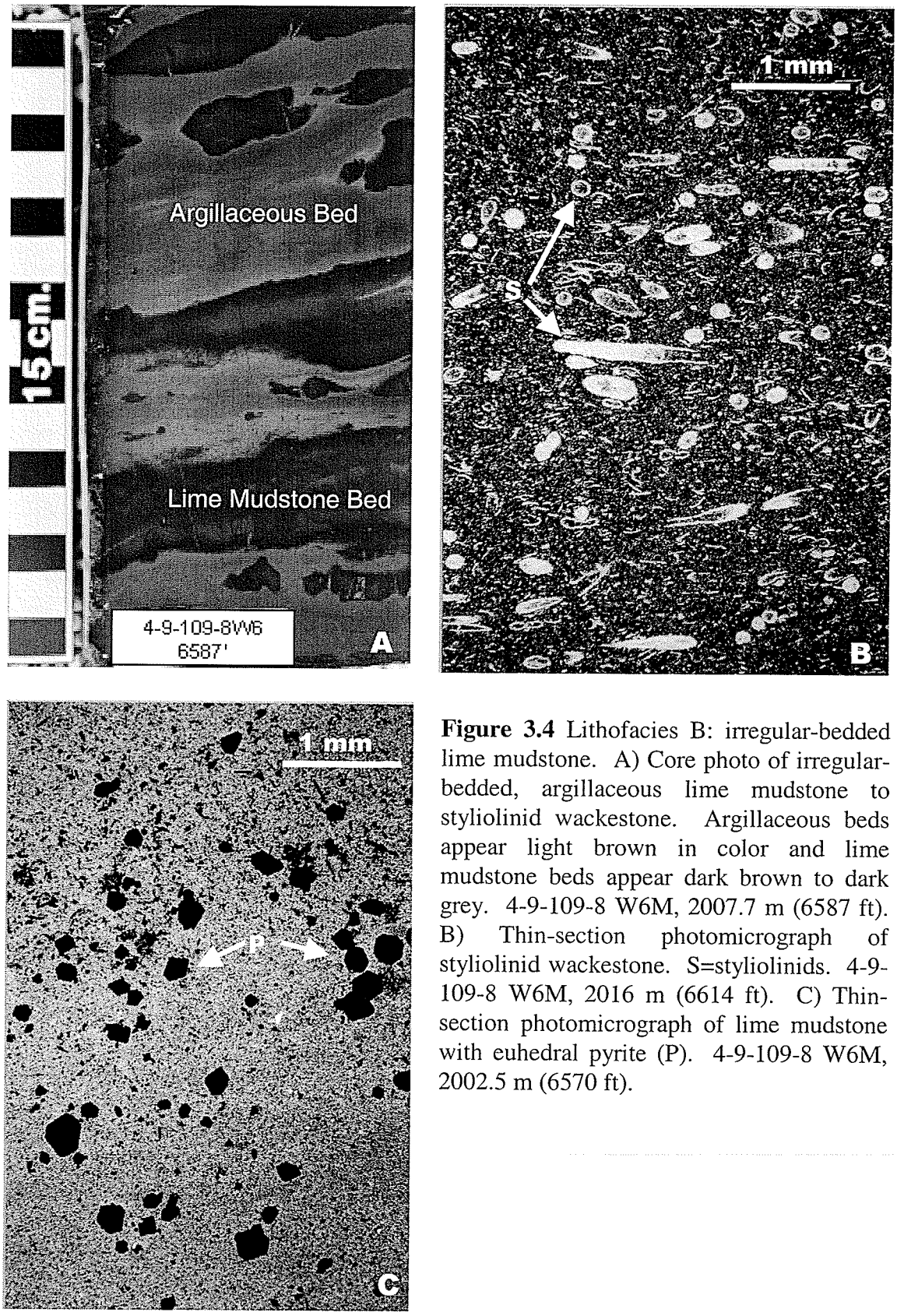

Figure 3.4 Lithofacies B: irregular-bedded lime mudstone. A) Core photo of irregular-bedded, argillaceous lime mudstone to styliolinid wackestone. Argillaceous beds appear light brown in color and lime mudstone beds appear dark brown to dark grey. 4-9-109-8 W6M, 2007.7 m (6587 ft). B) Thin-section photomicrograph of styliolinid wackestone. S=styliolinids. 4-9-109-8 W6M, 2016 m (6614 ft). C) Thin-section photomicrograph of lime mudstone with euhedral pyrite (P). 4-9-109-8 W6M, 2002.5 m (6570 ft).

Lithofacies B is predominantly undolomitized, however, minor (<5%) nonplanar, very fine crystalline dolomite occurs locally. This lithofacies also contains the other diagenetic fabrics observed in lithofacies A. In addition to all the pyrite forms recognized in lithofacies A, pyrite in lithofacies B (1-10%) also occurs as fine crystalline, subhedral equant crystals, and fine to medium crystalline, anhedral laths which are randomly oriented (Fig. 3.4C). Pyrite crystals are concentrated along laminae in the argillaceous beds, as well as disseminated throughout the carbonate beds.

3.3.2 Interpretation

Lithofacies B is interpreted to have been deposited in a low-energy, deep-subtidal environment below storm wave-base, similar to the depositional environment interpreted for lithofacies A (refer to Section 3.2.2 for the supporting evidence). In contrast to lithofacies A, however, lithofacies B may have been deposited in oxygen-reduced bottom waters rather than completely anoxic bottom waters. The irregular-bedded texture of lithofacies B is interpreted as the result of limited bioturbation by sparse infauna and/or by early diagenesis of the sediments (cf. Stoakes, 1980). Stoakes (1980) described an interbedded micritic limestone and calcareous shale lithofacies from the Ireton Formation (Upper Devonian) of central Alberta that is comparable to lithofacies B. He suggested that sediments probably accumulated at low rates from settling of material suspended in the water column. The low sedimentation rates allowed early diagenetic reorganization of calcite into layers, lenses, and nodules. Differential compaction of the argillaceous and carbonate beds probably accentuated the early cementation texture to create irregular-bedding (Wilson, 1969).

3.4 Lithofacies C: Nodular Crinoid-Brachiopod Wackestone

3.4.1 Description

Lithofacies C ranges from 1 to 8 m thick and consists of dark grey to medium brown, nodular skeletal wackestone to floatstone (Fig 3.5A). Nodules are typically 1-2 cm long but range from 0.5 to 4 cm long and they have rounded elliptical to irregular form. They locally coalesce to form irregular beds similar to those observed in lithofacies B. The nodules are somewhat lighter colored than the matrix and gradational contacts are common. The matrix tends to be more argillaceous, organic-rich, and locally less skeletal-rich. Dark colored, wavy laminae in the matrix (up to 5 mm thick) wrap around skeletal grains and nodules and feather out into the matrix where no nodules are present (Fig. 3.5C). These laminae are argillaceous, organic-rich, and commonly stylolitized. Stylolites commonly occur as bundles of many thin stylolites which diverge laterally (horsetail microstylolites).

Skeletal allochems, typically up to 5 mm in size, comprise from 10 to 75% of the lithofacies and are more diverse than in lithofacies B. They include small crinoids, styliolinids, small brachiopods, ostracods, gastropods, rare tentaculitids, thamnoporids, *Coenites*, and microbial structures including *Girvanella* and *Renalcis* (refer to Table 3.1 for more detail). Ovoid to irregular intraclasts (commonly <3 mm long and 2 mm wide, but ranging up to 10 mm long) comprise up to 10% of this lithofacies. These intraclasts are compositionally similar to the nodules, however, they contain more skeletal grains and have sharp, commonly pyritized contacts with the matrix. Peloids are also present.

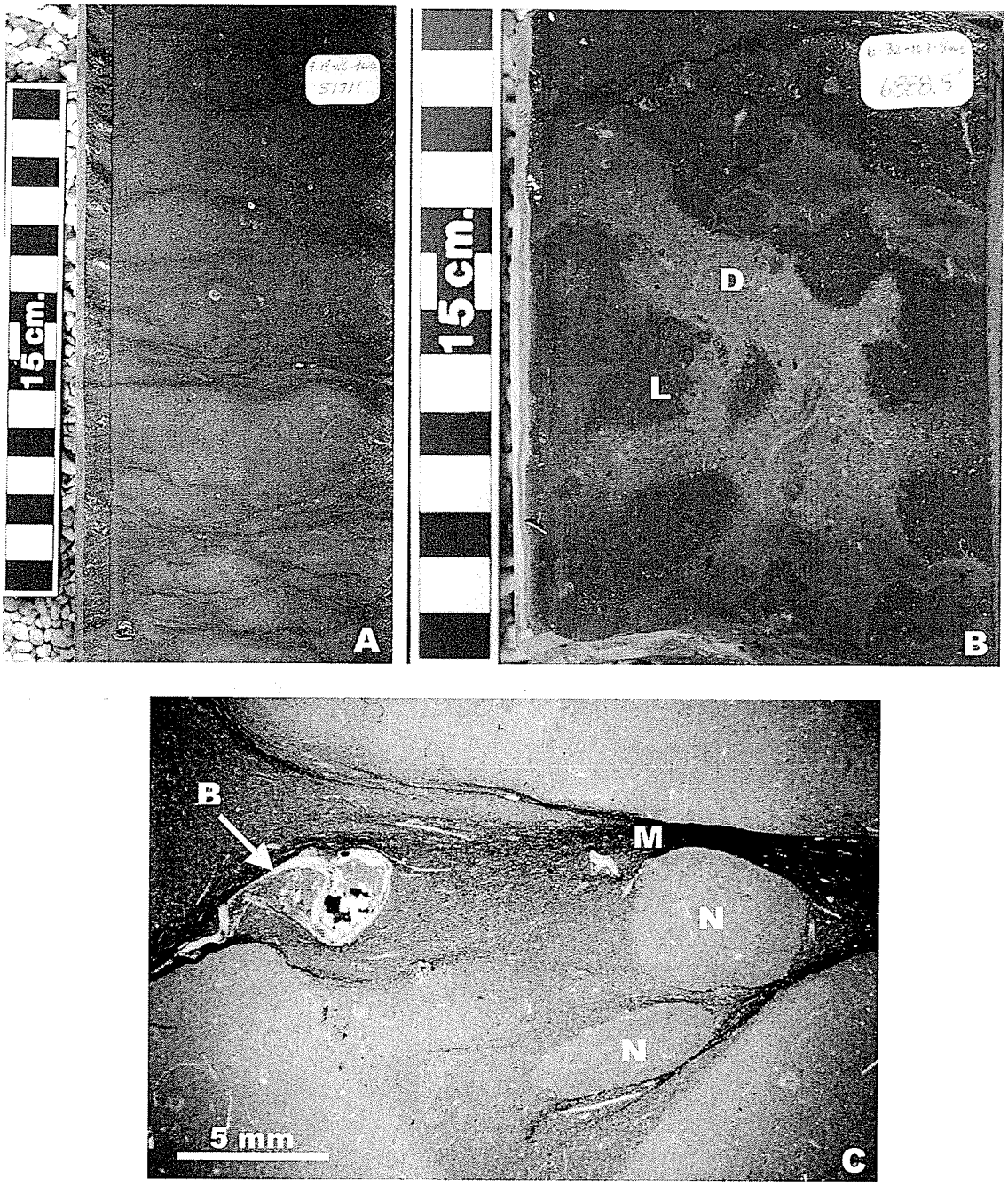

Figure 3.5 Lithofacies C: nodular crinoid-brachiopod wackestone. A) Core photo of nodular crinoid-brachiopod wackestone exhibiting organic-rich laminae wrapping around abundant nodules. 4-19-116-4 W6M, 1576.1 m (5171 ft). B) Core photo of partially dolomitized nodular crinoid-brachiopod wackestone exhibiting very irregular dolomitized mottles (D) in a limestone matrix (L). 6-32-107-9 W6M, 2099.6 m (6888.5 ft). C) Thin-section photomicrograph of nodular crinoid-brachiopod wackestone nodules (N) and horsetail microstylolites (M), as well as a brachiopod fragment (B). 4-9-09-8 W6M, 2011.7 m (6600 ft).

Partial dolomitization (up to 30%) of this lithofacies is rare but locally creates a texture consisting of light grey dolowackestone mottles (~1-5 cm wide) with very irregular shape and distribution (Fig. 3.5B). Dolomite is nonplanar and very finely crystalline. Dolomitized mottles have gradational contacts with the undolomitized skeletal wackestone to floatstone matrix and dolomitization does not appear to be fabric selective.

Vugs and fractures are present but porosity remains low (<5%) due to several stages of cementaction which include (from oldest to youngest): (1) coarsely crystalline, anhedral calcite cement which lines vugs and fractures; (2) extremely coarsely crystalline, anhedral ferroan calcite cement; (3) extremely coarsely crystalline, anhedral saddle dolomite; (4) coarsely crystalline euhedral anhydrite; and (5) coarsely crystalline pyrite which is found in the center of completely filled vugs. Trace intercrystalline porosity is also present. Pyrite (up to 10%) occurs as finely crystalline pyrite disseminated throughout the lithofacies, framboids, and silt-sized spheres associated with fractures and vugs. Trace chalcedonic quartz replaces some allochems and occurs within the matrix as botryoidal masses.

3.4.2 Interpretation

Lithofacies C is interpreted to have been deposited in a low-energy, deep-subtidal environment below storm wave-base, based on similar evidence as identified for the interpretation of lithofacies A (refer to Section 3.2.2). However, lithofacies C appears to have accumulated in a setting with more oxygenated conditions than those of lithofacies A or B. Evidence for oxygenated bottom waters is the presence of more diverse and

abundant open-marine fauna than that observed in either lithofacies A or B. Abundant crinoids and brachiopods, which are an open-marine assemblage (cf. Campbell, 1992; James and Bourque, 1992; Jones and Desrochers, 1992), dominate lithofacies C, whereas they are only minor constituents of lithofacies A and B, which are dominated by cricoconarids. The presence of corals (thamnoporids and *Coenites*), and microbial features are also suggestive of more open-marine conditions (e.g., James and Bourque, 1992), although corals could have been transported in from the shallow-subtidal during gravity flows induced by storm activity or other processes (cf. Coniglio and Dix, 1992). The bioturbated appearance of this lithofacies also suggests that bottom waters and sediments must have been oxygenated in order to support active bioturbating organisms. However, the persistent presence of small amounts of OM within this lithofacies suggests that oxygenation was not sufficient for thorough bioturbation, scavenging, and oxidation of OM.

Numerous authors have described nodular limestones of various ages from many regions worldwide and a variety of interpretations for the origin of nodules have been suggested (e.g., McCrossan, 1958; Hallam, 1964; Hopkins, 1972; Tucker and Kendall, 1973; Noble and Howells, 1974; Kennedy and Garrison, 1975; Wanless, 1979; Mullins *et al.*, 1980). Although more detailed petrography is required, nodules in lithofacies C are tentatively interpreted as the result of selective cementation prior to compaction. Organic-rich and argillaceous laminae (insoluble residues) were probably concentrated around these nodules as microstylolites during differential compaction (cf. Wilson, 1969; Scoffin, 1987). The matrix was cemented subsequently (cf. Noble and Howells, 1974). Selective

cementation is considered to have been influenced by subtle variations in permeability and porosity caused by bioturbation. The irregular-shaped dolomitic areas in lithofacies C are similarly interpreted to have been controlled by subtle porosity and permeability variations, possibly influenced by bioturbation.

3.5 Lithofacies D: Massive Crinoid-Brachiopod Wackestone

3.5.1 Description

Lithofacies D consists of dark grey to black, crinoid-brachiopod wackestone to floatstone, 1-29 m thick (Fig. 3.6). The argillaceous and organic-rich matrix includes micrite and dolomicrite. This lithofacies is predominantly massive, although vague laminations occur locally, defined by concentrations of organic and argillaceous material and by skeletal fragments and peloids (skeletal-peloidal packstone to grainstone, up to 10 cm thick) (Fig. 3.6B). This lithofacies may be partially dolomitized (10-40%) to pervasively dolomitized.

Allochems, ranging from 20% to 85%, are more abundant in lithofacies D than the previously described lithofacies. The most abundant allochems, which are up to 5 mm size, include crinoids, undifferentiated brachiopods and bivalves, brachiopods, ostracods, and styliolinids. Rare gastropods, tentaculitids, *Girvanella*, thin tabular stromatoporoids, and a variety of corals including thamnoporids, *Coenites*, *Alveolites*, and undifferentiated tabular tabulate corals are also present. Peloids are abundant locally and intraclasts compositionally similar to the matrix are rare.

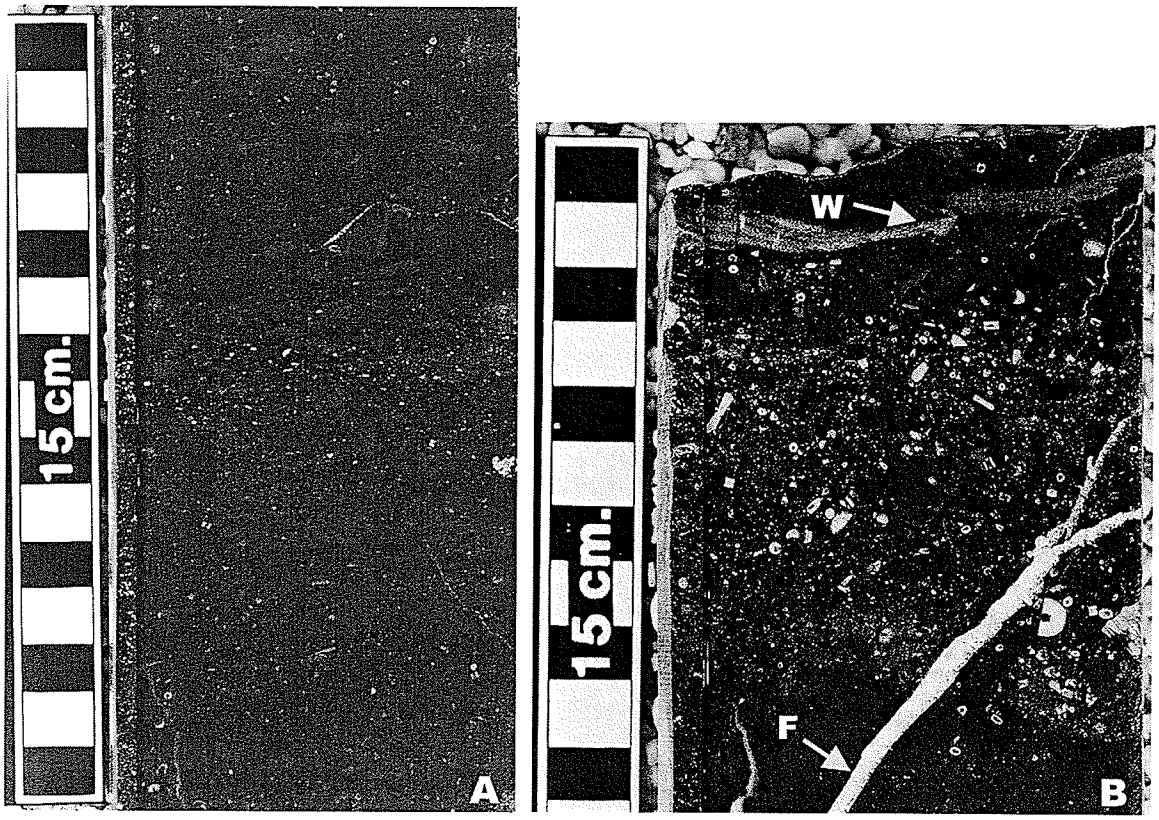

Figure 3.6 Core photos of lithofacies D: massive crinoid-brachiopod wackestone. A) Massive to vaguely laminated crinoid wackestone. White specks are crinoid ossicles. 4-9-109-8 W6M, 2030 m (6660 ft). B) Crinoid floatstone with skeletal-peloidal packstone matrix. Abundant white to buff colored crinoid ossicles, a thin tabular ("wafer") stromatoporoid (W) and an anhydrite-filled fracture (F) are visible in this photo.

Dolomite occurs preferentially with microstylolites and organic-rich laminae as nonplanar, medium to coarsely crystalline mosaics and as planar-euhedral, medium to coarsely crystalline dolomite scattered throughout the matrix. Isopachous radial-fibrous calcite cement occurs in peloidal grainstone. Anhedral megaquartz (up to 3 mm x 1 mm) locally replaces skeletal allochems, and pyrite occurs in the same form as observed in lithofacies A, B, and C. Minor fracture porosity and intercrystalline porosity in limestones are enhanced by dolomitization (up to 5% porosity). Locally, trace sphalerite occurs in pores.

3.5.2 Interpretation

The interpreted depositional environment for lithofacies D is a low to moderate energy, deep-subtidal environment near storm wave-base. Similar evidence as documented for lithofacies A, B, and C supports the interpretation of low energy, deep water conditions (refer to Section 3.2.2). However, the presence of horizontal beds of skeletal-peloidal packstone to grainstone in lithofacies D indicates higher-energy processes, suggesting that this lithofacies may have been deposited in an environment that was intermittently affected by storm events. Storm deposits (tempestites) have been well documented by various studies that have described features that are dependent on factors such as water depth, proximity to the sediment source, and the frequency and intensity of storm events (e.g., Aigner, 1985; Sami and Desrochers, 1992; Jones and Desrochers, 1992). The grainstone beds in lithofacies D lack the more unequivocal features of tempestites (as listed in Section 3.2.2) although grainstones comprised of bioclasts, ooids, and/or peloids ranging to interbedded grainstone-mudstone, such as those observed in this lithofacies,

commonly indicate tempestites (Jones and Desrochers, 1992). Alternatively, these beds could have been deposited below the storm wave-base by suspension settling from sediment/seawater plumes originating upslope (cf. Coniglio and Dix, 1992; refer to Section 3.2.2), or they could represent sediment reworking by deep-water currents.

The diverse fauna of lithofacies D is comparable to that observed in lithofacies C and therefore is also interpreted as indicative of oxygenated, open-marine conditions and/or sediments transported downslope from the shallow-subtidal zone (refer to Section 3.4.2). Lithofacies D lacks evidence of pervasive bioturbation, although the presence of locally abundant peloids may reflect the activity of burrowing and grazing organisms (cf. Jones and Desrochers, 1992). Intermittent dysoxic conditions may have prevented more extensive bioturbation and facilitated preservation of OM.

3.6 Lithofacies E: Bioturbated Crinoid-Brachiopod Floatstone

3.6.1 Description

Lithofacies E, ranging from 0.5 to 7 m thick, is highly variable and composed of medium brown to grey, crinoid-brachiopod floatstone to rudstone showing pervasive bioturbation. Pervasive bioturbation imparts a mottled light (dolomite) and dark (limestone) appearance to lithofacies E attributed to preferential dolomitization of burrows (Figure 3.7), and well- defined vertical burrows are present locally (Fig. 3.8C). Sharp-based beds, up to 50 cm thick, of crinoid rudstones, brachiopod rudstones, and oncoid floatstones occur locally (Fig. 3.8A). The matrix is skeletal wackestone which includes

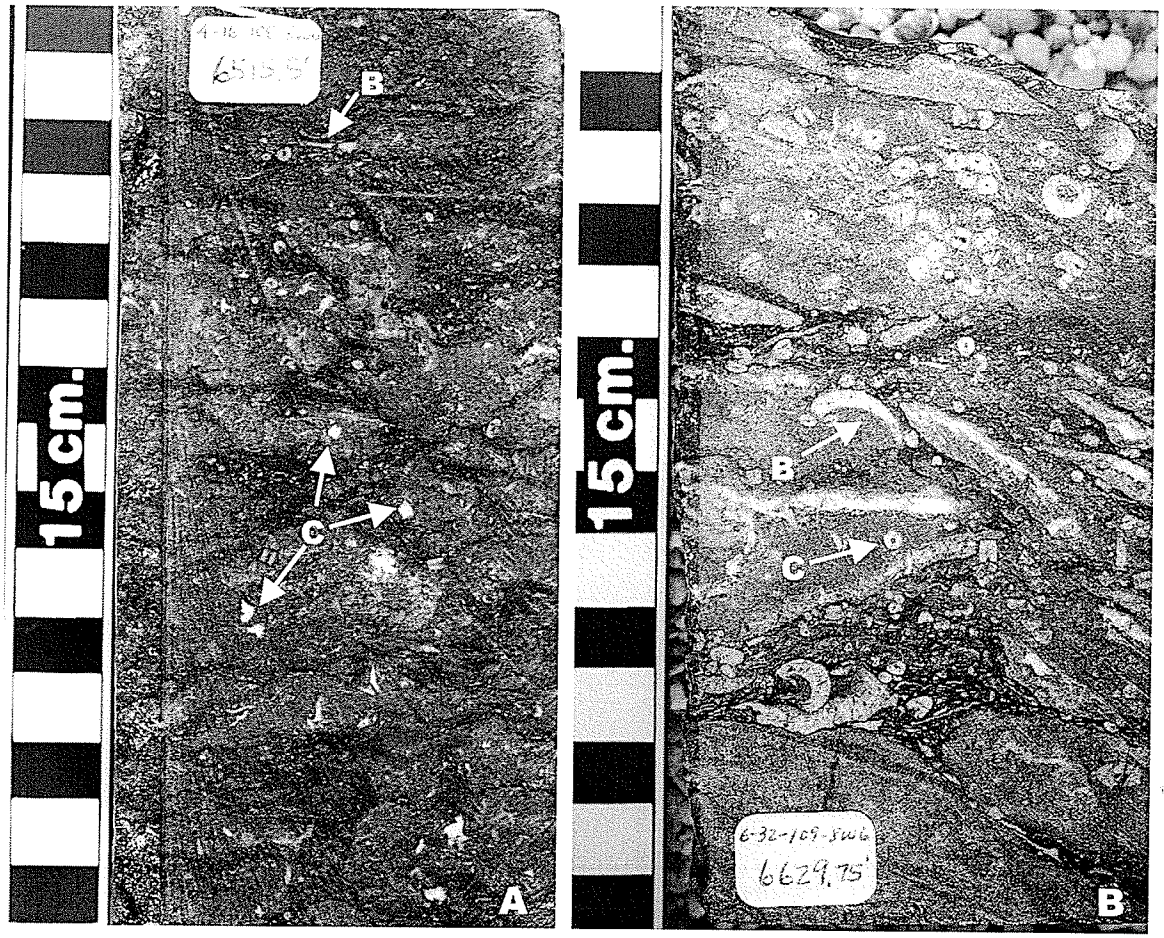

Figure 3.7 Core photographs of lithofacies E: bioturbated crinoid-brachiopod floatstone. A) Pervasively bioturbated crinoid-brachiopod floatstone. C=crinoids, B=brachiopods. 4-16-108-8 W6M 1985.9 m (6515.5 ft). B) Pervasively bioturbated crinoid-brachiopod dolofloatstone to dolorudstone. C=crinoids, B=brachiopods. 6-32-109-8 W6M, 2020.8 m (6629.75 ft).

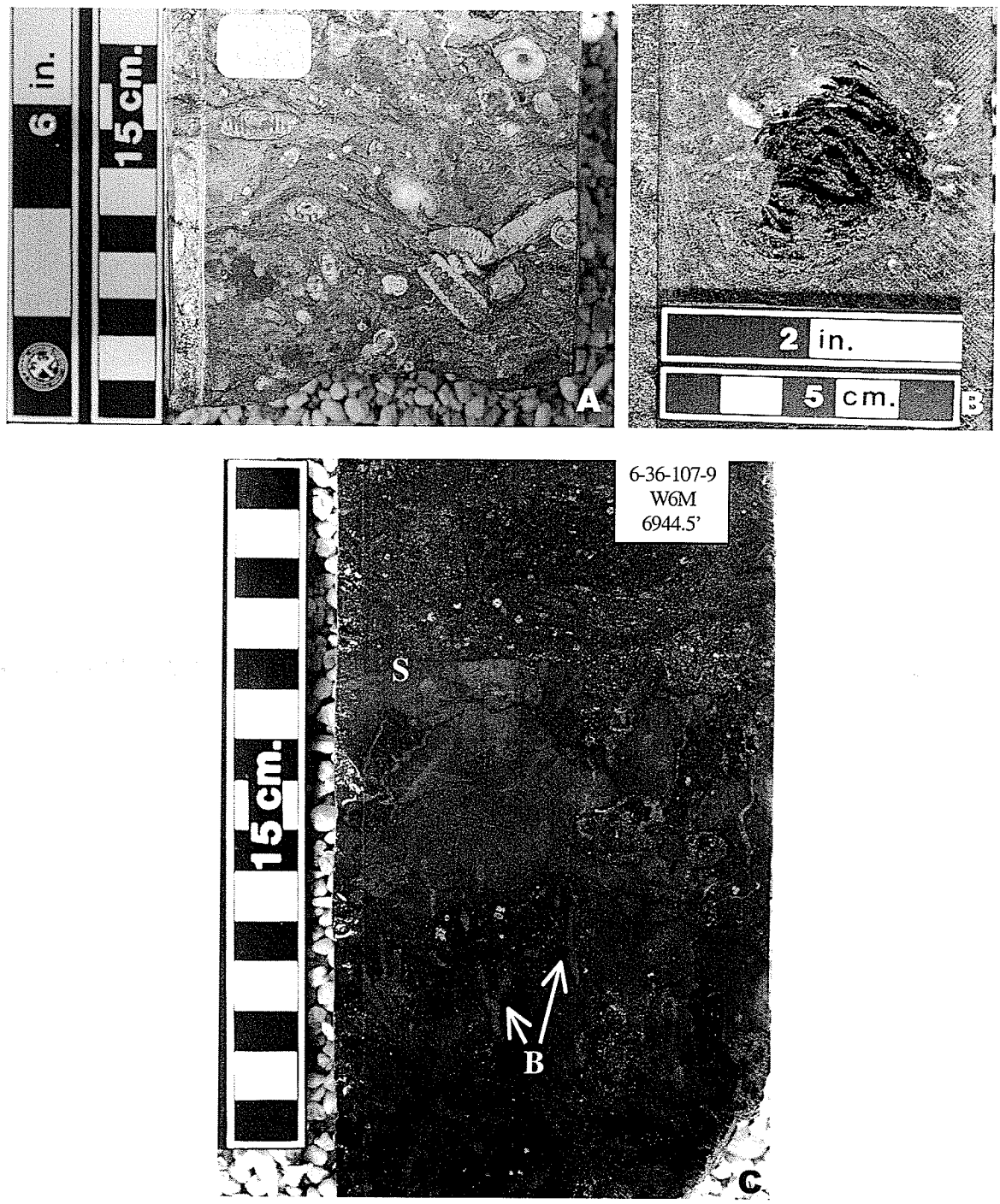

Figure 3.8 Core photographs of Lithofacies E: bioturbated crinoid-brachiopod floatstone. A) Crinoid floatstone to rudstone showing large articulated ossicles. 4-19-116-4 W6M, 1564.8 m (5134 ft). B) Brachiopod-crinoid-stromatoporoid floatstone exhibiting biomoldic porosity created by leaching of a nodular stromatoporoid. 4-16-108-8 W6M, 1987.9 m (6522 ft). C) Pervasively bioturbated crinoid-brachiopod wackestone displaying well-defined vertical burrows (B) and scour surface (S). 6-36-107-9 W6M, 2116.7 m (6944.5 ft).

terrigenous clays and OM. Locally, the matrix is peloidal (up to 5%). All samples exhibit partial to complete dolomitization, making accurate identification of matrix and allochemical constituents problematic. However, the use of diffused plane-polarized light microscopy facilitated allochem identification in a number of samples (Fig. 3.9, Appendix C.2).

Lithofacies E contains abundant (35-75%) and diverse allochems, with crinoids and brachiopods being the most abundant. Crinoid ossicles are commonly large (up to 1 cm diameter), and may remain articulated (Fig. 3.8A). Brachiopod tests (up to 2 cm long) are articulated or disarticulated, have a random orientation, and show little evidence of shell fragmentation and/or bioerosion (Fig. 3.7B). Typically, matrix wackestones contain smaller crinoid ossicles and brachiopod fragments (<2 mm size). Other important skeletal constituents include styliolinids and ostracods. Bivalves, gastropods, stromatoporoid fragments (Fig. 3.9B), peloids, and intraclasts are minor constituents. Oncoids and ovoid grapestones (up to 1.5 mm x 1 mm), composed of peloid and microbial structures including *Girvanella*, occur only locally.

Finely crystalline, inclusion-rich dolomite is associated with argillaceous matrix and medium crystalline, inclusion-free dolomite is associated with poorly argillaceous matrix. Coarsely crystalline, planar-euhedral dolomite and minor, extremely coarsely crystalline saddle dolomite fill fractures and vugs in partially dolomitized lithologies such as in burrows. Porosity is minor and consists of vuggy, biomoldic (Fig. 3.8B) and

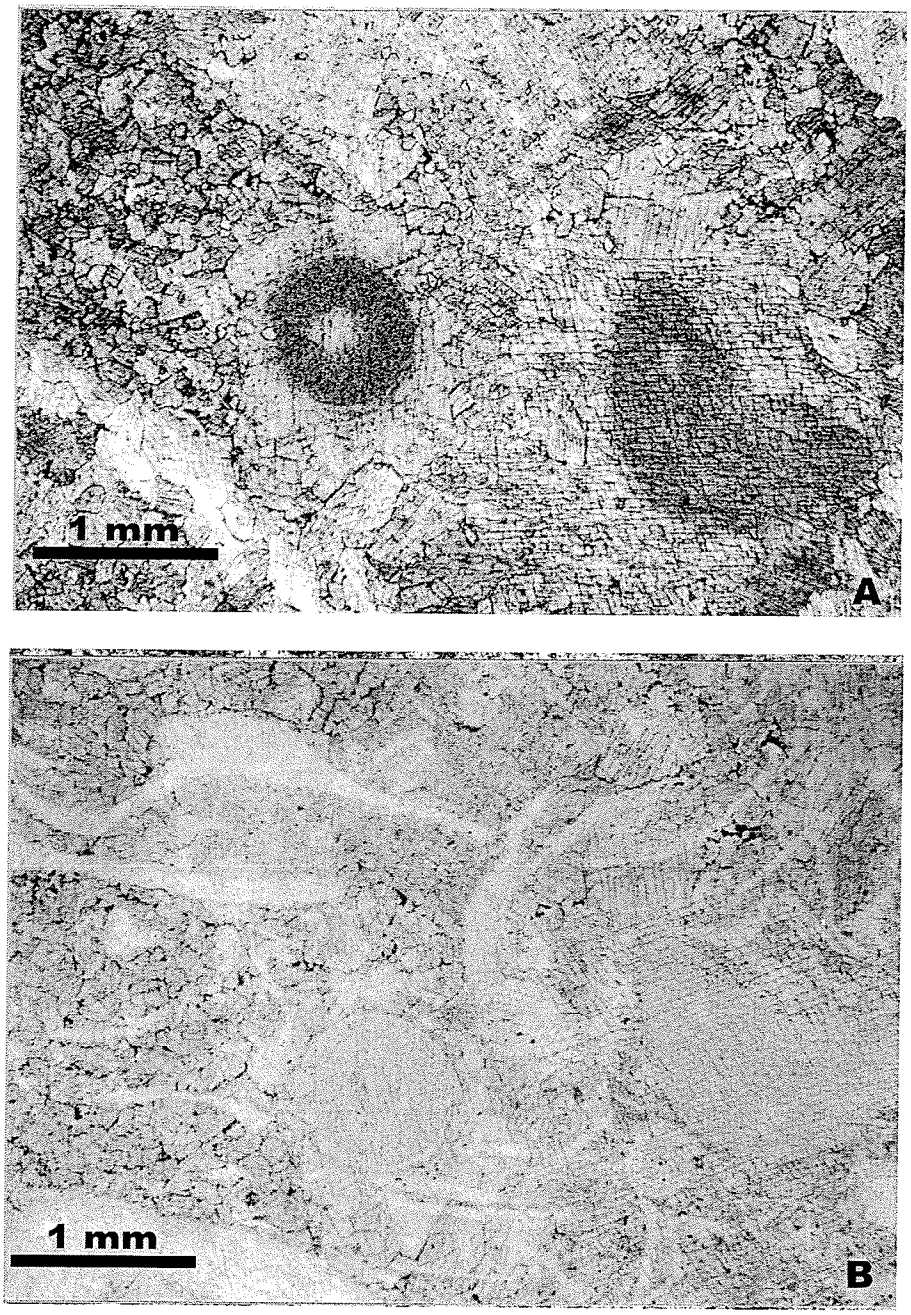

Figure 3.9 Thin section photomicrographs of lithofacies E: bioturbated crinoid-brachiopod floatstone. 4-9-109-8 W6M, 1999.8 m (6561 ft). A) Plane-polarized light microscopy, showing some skeletal allochems (white and light brown in photo). B) Diffused plane-polarized light microscopy of (A) revealing additional skeletal allochems that are obscured by dolomitization.

intercrystalline. Prismatic calcite cements are present inside brachiopod and bivalve tests. Rare, laterally discontinuous microstylolites contain argillaceous sediment and OM and drape around carbonate grains. Minor pyrite (up to 5%) occurs as euhedral, very fine crystals associated with silicified fossils, and disseminated through the matrix in the same forms as those observed in lithofacies A, B, C, and D. Chalcedonic quartz also occurs in the same forms as observed in other lithofacies. Euhedral microquartz replaces allochems and locally even partially replaces microbial coatings on oncoids. Trace anhydrite laths are associated with vuggy pores and pyrite.

3.6.2 Interpretation

Lithofacies E is interpreted to have been deposited in a moderate energy, subtidal environment between storm and fairweather wave-base. The prevalence of peloids and the occurrence of sharp-based beds of crinoid and brachiopod rudstones are evidence for moderate energy conditions episodically influenced by storm events (cf. Jones and Desrochers, 1992). The articulated crinoid ossicles (Fig. 3.8A) and brachiopod tests in the tempestites suggest that rapid deposition and burial of storm-transported sediments prevented significant postmortem degradation of these allochems by physical or biological processes (Jones and Desrochers, 1992).

The abundance and diversity of fauna in lithofacies E are comparable to that of lithofacies D and therefore is interpreted similarly to be indicative of open-marine conditions (refer to Section 3.5.2). The presence of locally abundant oncolites (oncoid floatstones) may provide evidence for somewhat shallower conditions than lithofacies D (i.e., an

intermediate depth subtidal environment) where cyanobacterial coatings could form readily around skeletal grains, well within the photic zone (James and Bourque, 1992). Conversely, the association of coarse oncolites (which probably formed in turbulent, well oxygenated waters) with delicate styliolinids may suggest that the oncolites formed in shallow, higher energy environments and were transported down depositional slope prior to deposition (cf. Stanford, 1989). Oxygenated conditions in the water column and within sea floor sediments are further evidenced by the pervasive bioturbation in lithofacies E.

3.7 Lithofacies F: Bituminous Peloidal Laminite

3.7.1 Description

This buff to very light grey lithofacies, 0.5 – 4.5 m thick, ranges from peloidal-skeletal dolopackstone to dolograinstone and contains abundant black, organic-rich laminae (Figs. 3.10A and B). These laminae comprise 5-35% of the lithofacies, are horizontal to irregular, and are typically stylolitized (Fig. 3.10C). They are commonly concentrated into microstylolite swarms, up to 5 mm thick, which drape around carbonate layers forming irregular laminae and/or a nodular texture (Fig. 3.10D). This lithofacies contains little micrite and terrigenous clastic sediment. Dolomitization obscures primary textures and makes allochem identification tenuous. However, one sample studied was only partially (25%) dolomitized facilitating allochem determinations. Diffused plane-polarized light microscopy was used to discern primary fabrics in dolomitized samples (Appendix C.2).

Allochems are diverse and abundant (40-60%) with the most common skeletal allochems

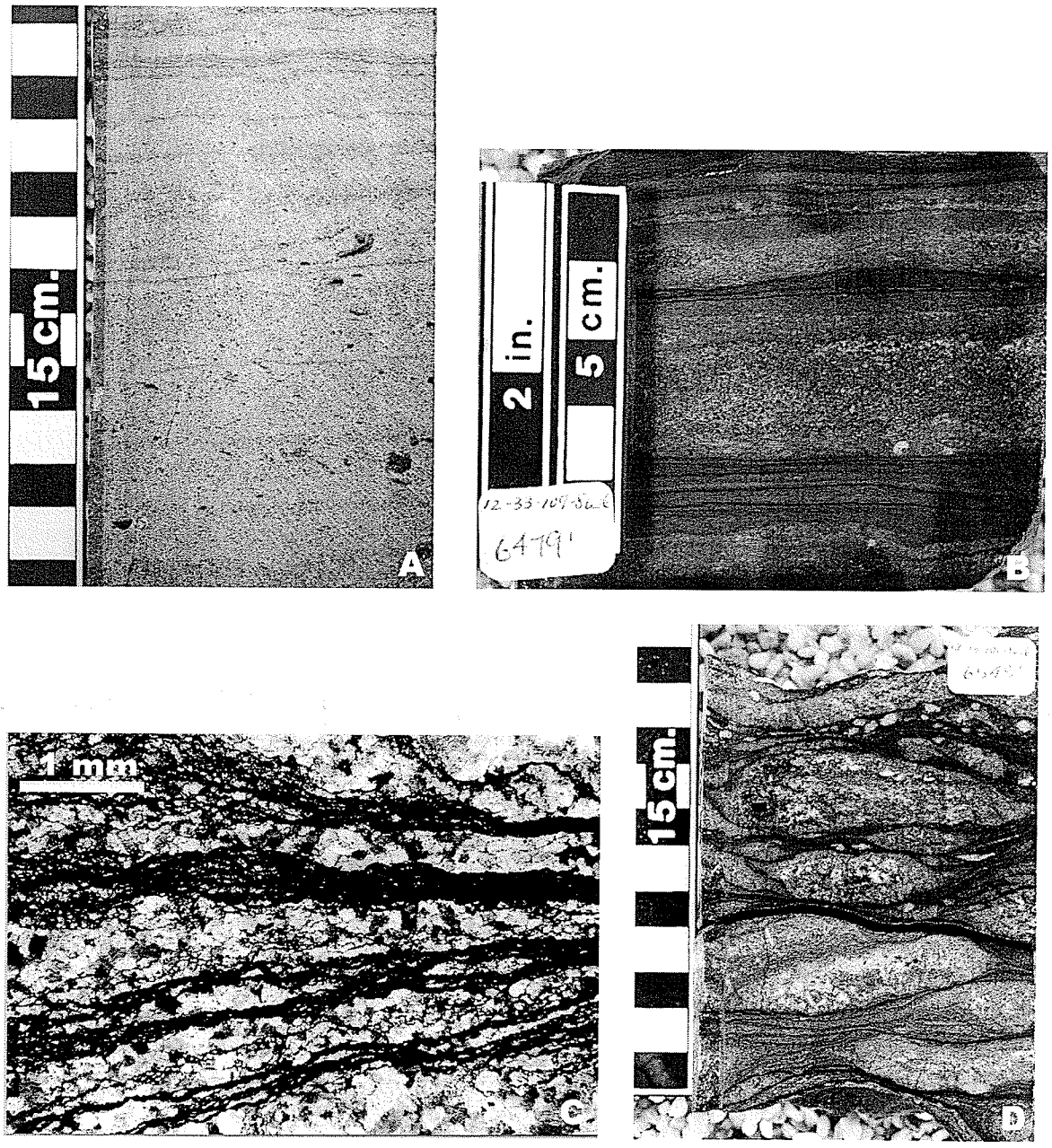

Figure 3.10 Lithofacies F: bituminous-peloidal laminite. A) Core photograph of laminated peloidal-skeletal dolopackstone to dolograinstone displaying sparse organic-rich laminae. Intercrystalline and biomoldic porosity are well developed. 6-32-109-8 W6M, 1964 m (6444 ft). B) Core photograph of laminated peloidal-skeletal dolopackstone to dolograinstone exhibiting a relatively high concentration of organic-rich laminae. 12-33-109-8 W6M, 1974.8 m (6479 ft). C) Thin-section photomicrograph of very thin microstylolite swarms in dolostone composed of coarsely crystalline saddle dolomite and medium crystalline, nonplanar dolomite. D) Core photograph showing organic-rich microstylolites draping around the peloidal-skeletal packstone to grainstone to form very irregular laminae and a nodular texture. 12-33-109-8 W6M 1994.9 m (6545 ft).

being tentaculitids, styliolinids, undifferentiated brachiopods and bivalves, and crinoids. Other minor constituents include gastropods, ostracods, stromatoporoid fragments, and *Coenites*. Abundant peloids and ovoid grapestones composed of lumps of peloids are distinctive constituents.

Primary textures are replaced with a coarse dolomite mosaic and the matrix ranges from nonplanar, coarsely crystalline saddle dolomite to planar-subhedral, medium crystalline dolomite (Fig. 3.10C). Inclusion-rich allochem ghosts in nonplanar dolomite observed using diffused plane-polarized light represent nonmimic replacement of bioclastic material. Void-filling coarsely crystalline saddle dolomite and planar-euhedral coarsely crystalline dolomite are also common. Biomoldic porosity (~5% average) was created by the dissolution of most commonly crinoids, styliolinids, and brachiopods. Minor intercrystalline porosity (1-5%) is present and trace fracture porosity occurs locally. Trace euhedral anhydrite laths are associated with vuggy and biomoldic porosity, and trace pyrite occurs as very finely crystalline grains in framboids. Bitumen is abundant within microstylolites, intercrystalline and intraparticle porosity.

3.7.2 Interpretation

The bituminous peloidal laminite lithofacies is interpreted to have been deposited in a moderate energy, intermediate to deep-subtidal environment. Evidence suggests that lithofacies F was deposited above storm wave-base and was influenced by frequent storm-induced sediment gravity flows and pervasive current reworking. Episodic dysoxic to anoxic conditions are interpreted to have developed during deposition of lithofacies F.

The lack of micrite and terrigenous mud in lithofacies F provides evidence for deposition in moderate energy conditions frequently affected by periodic storm activity and/or indirect storm effects (i.e., sediment gravity flows). Fine-grained sediments would have been prevented from settling out of suspension and/or would have been removed subsequently by storm and current reworking (cf. James and Kendall, 1992). The presence of abundant peloids, assuming that they are derived from the faecal pellets of organisms such as gastropods, worms, and shrimp-like organisms (e.g., Scoffin, 1987; Jones and Desrochers, 1992) suggests that bottom waters and sediments were oxygenated enough to support the activities of these organisms. However, storm waves, gravity flows, and currents also could have transported peloidal sands from upslope and redeposited these sediments in deeper water (e.g., Jones and Desrochers, 1992; Wendte, 1992c).

The abundant, diverse fauna of this lithofacies indicates oxygenated, open-marine conditions. However, the predominance of styliolinids (up to 30%) suggests deposition of planktonic organisms in a relatively deep-subtidal setting where the balance of sediment was transported into this setting from upslope positions by sediment gravity flows. Alternatively, the abundance of styliolinids may be attributed to mass kills and fallout of pelagic organisms during periodic anoxic conditions (cf. Chow *et al.*, 1995a).

Preservation of organic-rich laminae in lithofacies F required episodes of dysoxia to anoxia. It is interpreted that oxygen-reduced conditions developed in response to high

primary productivity rather than in response to depth-related anoxia. This will be discussed in further detail in Chapter 6: Organic Petrology.

3.8 Lithofacies G: Massive Peloidal-Skeletal Dolopackstone to Dolograinstone

3.8.1 Description

Lithofacies G is buff colored, massive, and ranges from peloidal-skeletal dolopackstone to dolograinstone, 0.5 to 14.5 m thick (Fig. 3.11). It lacks organic-rich laminae (Fig. 3.11A), but otherwise appears compositionally similar to lithofacies F. Argillaceous material and OM are rare and tend to be concentrated into very thin microstylolites which lend a slightly mottled appearance to the lithofacies (Fig. 3.11B).

Allochem identification was based on partially (10-25%) dolomitized samples and diffused plane-polarized light microscopy was employed on pervasively dolomitized samples (Appendix C.2). Allochems comprise up to 85% of this lithofacies with the most abundant allochems being crinoids, peloids, and undifferentiated brachiopods and bivalves. Other significant carbonate grains include ostracods and styliolinids. Molds of whole and fragmented nodular stromatoporoids are locally abundant (Fig. 3.11A).

Dolomite in lithofacies G occurs in the same modes as observed in lithofacies F (refer to Section 3.7.1). Porosity ranges from 1-20% and includes intercrystalline porosity which is ubiquitous and occurs as "pinpoint" pores between dolomite crystals; and minor intraparticle, biomoldic, vuggy, and fracture porosity (Figs. 3.11A and C). Quartz content ranges from 0-30% and consists of finely crystalline, anhedral microquartz associated

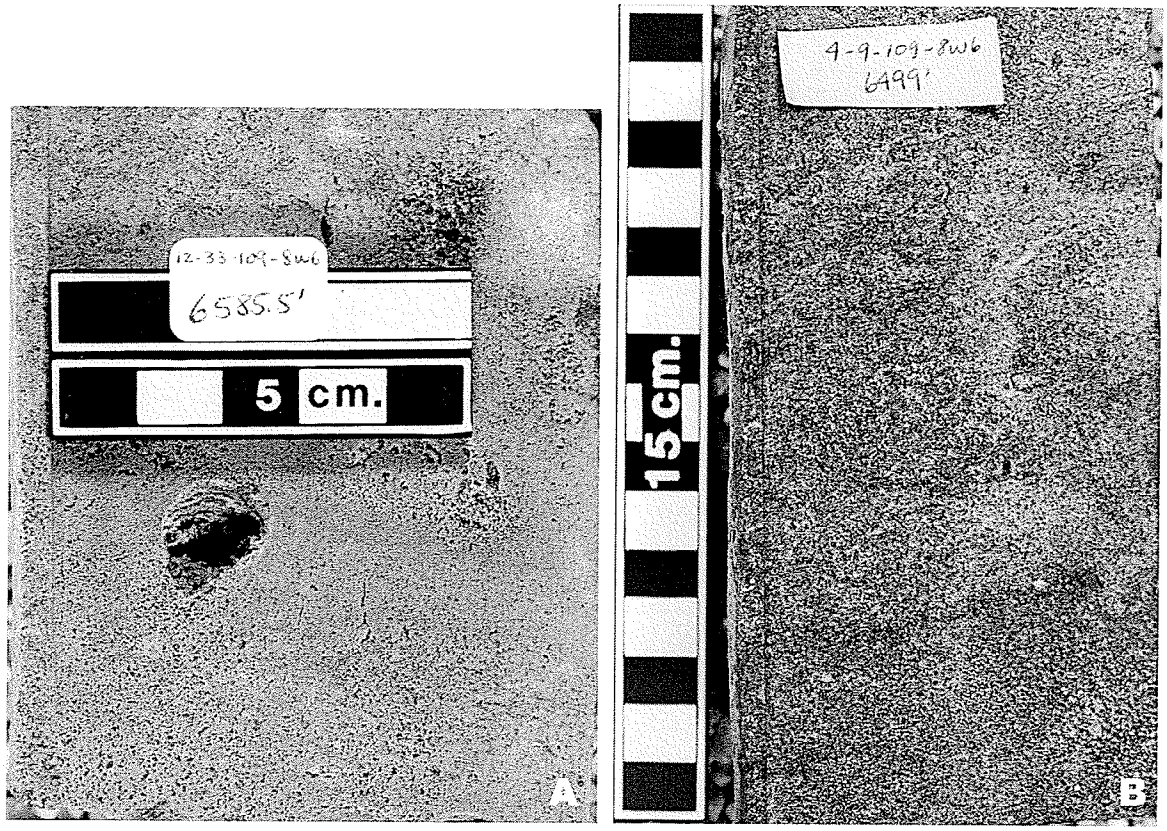

Figure 3.11 Lithofacies G: massive peloidal-skeletal dolopackstone to dolograinstone. A) Core photograph of well developed intercrystalline and biomoldic porosity (leached stromatoporoid fragments) in massive peloidal-skeletal dolograinstone. 12-33-109-8 W6M, 2007.3 m (6585.5 ft). B) Core photograph of massive peloidal-skeletal dolopackstone to dolograinstone with slightly mottled coloration and lack of significant moldic porosity. Intercrystalline porosity is well developed. 4-9-109-8 W6M, 1980.9 m (6499 ft). C) Thin-section photomicrograph of B showing nonplanar, coarsely crystalline saddle dolomite formed during nonmimic replacement of allochems and other primary textures. Intercrystalline porosity (blue in photo) is well developed. 4-9-109-8 W6M, 1980.9 m (6499 ft).

with silicified allochems, porosity, and pyrite framboids, as well as zoned, subhedral to anhedral megaquartz and chalcedonic quartz. Coarsely crystalline, subhedral anhydrite and bitumen line or completely occlude intercrystalline, vuggy, and biomoldic porosity.

3.8.2 Interpretation

The depositional environment of lithofacies G is interpreted as a moderate energy, intermediate-subtidal environment. It was situated between storm and fairweather wave-base in fully oxygenated conditions.

As in lithofacies F, moderate energy conditions for lithofacies G are indicated by a lack of fine sediment and the presence of abundant peloids suggests that storm waves, sediment gravity flows, and/or currents transported peloidal sediments down depositional slope (refer to Section 3.7.2). In contrast to lithofacies F, lithofacies G lacks OM which lends support to an interpretation of deposition above storm wave-base where storm-related high-energy events occurred frequently enough to prevent the accumulation and/or removal of fine-grained OM (cf. James and Kendall, 1992; Jones and Desrochers, 1992). Fully oxygenated conditions promoting the activities of bioturbating and scavenging organisms also would have destroyed any accumulated OM. The diverse, abundant fauna of this lithofacies supports the interpretation of oxygenated, open-marine conditions.

3.9 Lithofacies H: Stromatoporoid-Coral Dolofloatstone to Dolorudstone

3.9.1 Description

Lithofacies H is buff to medium brown in color, 10 cm - 26 m thick, and ranges from stromatoporoid-coral floatstone to rudstone with peloidal-skeletal packstone to grainstone matrix. This lithofacies is predominantly pervasively dolomitized but is locally limestone or only partially dolomitized (10-20%). Diffused plane-polarized light microscopy was utilized to detect primary fabrics in dolomitized samples (Appendix C.2). The matrix of lithofacies H is compositionally similar to lithofacies G (refer to Section 3.8.1).

Lithofacies H has the most abundant (30-80%) and diverse fauna of all the lithofacies examined in this study. The most abundant allochems are stromatoporoid fragments (>2 cm size) that have ragged edges, irregular shape, and display either wafer (<1 cm thick), thin tabular (1-5 cm thick), thick tabular (>5 cm thick), small hemispherical (up to 5 cm thick), or small bulbous (1 cm diameter) morphology (Figs. 3.12A, B, and C). Dolomitization obscures the internal structure of stromatoporoid fragments but they are discernible because they have been replaced by coarsely crystalline dolomite and are more porous than the matrix. Other abundant allochems include crinoids, peloids, and various corals including *Alveolites*, *Coenites*, solitary rugose, tabulate (Fig. 3.12D) and thamnoporid corals. *Alveolites* (up to 7 cm size) and thamnoporid fragments (~1.5 cm long) are ubiquitous. Many stromatoporoids and corals appear to have been transported, although a number of wafer, tabular and hemispherical stromatoporoids with enveloping form were observed in original growth position. Ostracods, gastropods, undifferentiated brachiopods and bivalves, styliolinids, intraclasts and oncoids are minor constituents.

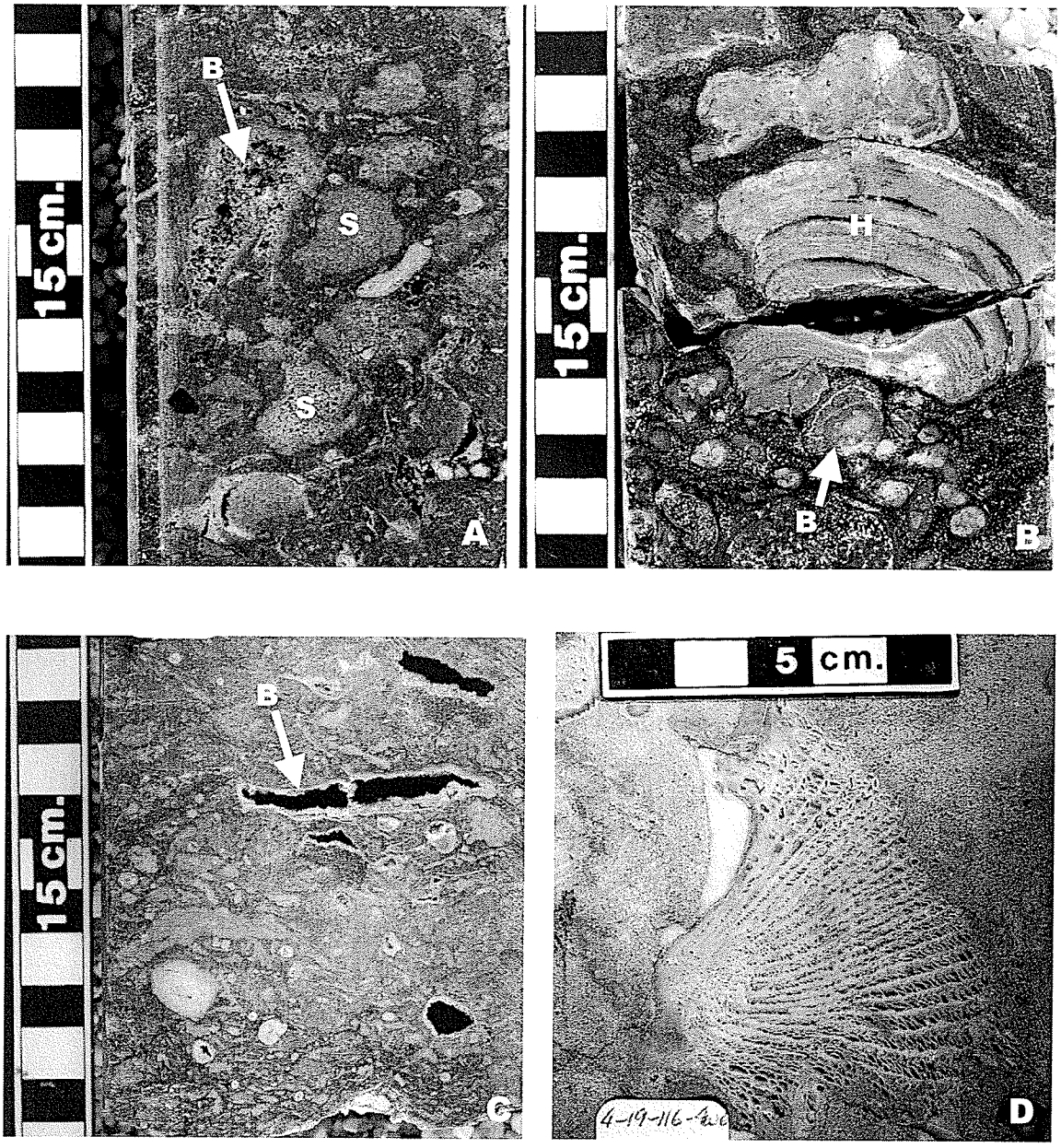

Figure 3.12 Core photos of lithofacies H: stromatoporoid-coral dolofloatstone to dolorudstone. A) stromatoporoid-coral dolofloatstone with abundant stromatoporoid fragments (S) in a peloidal-skeletal dolopackstone to dolograinstone matrix. Biomoldic porosity (B) is present in leached stromatoporoid fragments. 12-33-109-8 W6M, 1985.8 m (6515 ft). B) Hemispherical (H) and small bulbous (B) stromatoporoid fragments in stromatoporoid-coral dolorudstone. 12-33-109-8 W6M, 1982.8 m (6505.15 ft). C) Well-developed biomoldic porosity (B) (leached stromatoporoid fragments) lined by saddle dolomite in stromatoporoid-coral dolofloatstone. 5-36-117-6 W6M, 1675.2 m (5496 ft). D) Large solitary tabulate coral in stromatoporoid-coral dolorudstone. The white mineral at the edge of the coral is anhydrite and intraparticle porosity is visible within the coral. 4-19-116-4 W6M, 1536 m (5039.5 ft).

Finely crystalline pseudospar calcite matrix and fibrous prismatic calcite cements have been observed in limestone samples. Finely to medium crystalline, nonplanar, inclusion-rich dolomite appears to have preferentially replaced matrix material that contained argillaceous sediment or OM. Coarse and very coarse-crystalline dolomite is inclusion-free and has replaced allochems. Accessory components include chalcedonic quartz, quartz replacing allochems, very fine-crystalline pyrite, and void-filling very coarse-crystalline, euhedral anhydrite. Thin microstylolites containing argillaceous material and OM are widespread.

Porosity is ~10% on average but ranges up to 25% locally. Intercrystalline porosity is dominant, although fracture, intraparticle (in coral skeletons), vuggy, and biomoldic porosity are also present. Porosity is lined with bitumen, very coarse-crystalline anhydrite, saddle and coarse-crystalline planar-euhedral dolomite, and coarse-crystalline euhedral quartz.

3.9.2 Interpretation

Lithofacies H is interpreted to have been deposited in an open-marine, moderate energy, intermediate-subtidal environment that was fully oxygenated and located between storm and fairweather wave-base.

As in lithofacies F and G, the lack of micrite and terrigenous clay, and the presence of abundant peloids indicate deposition under moderate energy conditions above storm wave-base (refer to Section 3.7.2 and 3.8.2). Lithofacies H lacks abundant OM and

contains abundant and diverse fauna suggesting oxygenated bottom-waters (refer to Section 3.8.2). The abundance of reworked, fragmented coral and stromatoporoid fossils, probably transported to their current position from an upslope environment, indicate a depositional setting that was shallower than that of lithofacies F and G. The presence of in situ wafer, tabular, and small hemispherical stromatoporoids indicate periods of low sedimentation and low wave-energy (cf. James and Bourque, 1992; Wendte, 1992c).

3.10 Lithofacies I: Non-Fossiliferous Dolomudstone

3.10.1 Description

The non-fossiliferous dolomudstone lithofacies is relatively thin (1 to 1.5 m thick), and is associated only with anhydrite units of the Muskeg and Chinchaga formations. It ranges from buff to light grey in color and massive (Fig. 3.13A) to brecciated in structure (Fig. 3.13C). Locally, this lithofacies has highly irregular structures tentatively identified as haloturbation which is defined as disruption of sediments as a result of the precipitation of salts within surface sediment layers (White *et al.*, 2000) (Fig. 3.13B).

Lithofacies I is composed of pseudospar, dolomicrite, finely crystalline planar-euhedral dolomite, and medium crystalline planar-subhedral dolomite. Intraclasts and skeletal grains occur only locally (up to 30%) and include minor crinoids, undifferentiated brachiopods and bivalves, and trace ostracods and styliolinids. Coarse to very coarse-crystalline, subhedral anhydrite is relatively abundant (up to 15%) in patches and trace pyrite, bitumen, terrigenous clays, and OM are also present. Intercrystalline, vuggy, and

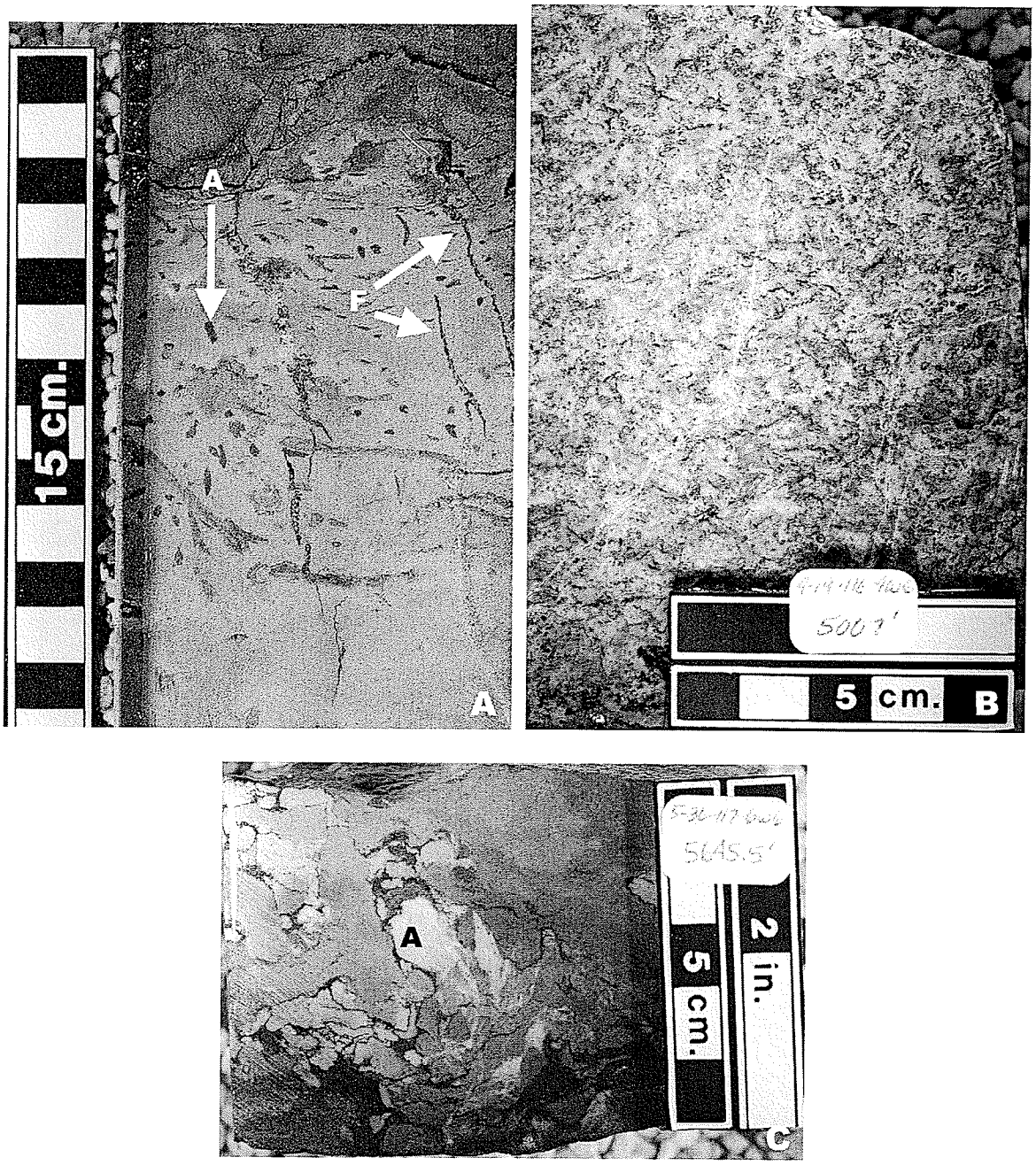

Figure 3.13 Core photos of lithofacies I: non-fossiliferous dolomudstone. A) Massive dolomudstone showing abundant anhydrite laths (A) and dolomite-filled fractures (F). 4-9-109-8 W6M, 2042.2 m (6700.11 ft). B) Haloturbated dolomudstone. Buff-colored areas are pseudospar and nonplanar dolomite. Darker grey areas are coarse to very coarse-crystalline, subhedral anhydrite. 4-19-116-4 W6M, 1526.1 m (5007 ft). C) Brecciated dolomudstone exhibiting patches of extremely coarsely crystalline anhydrite (A). 5-36-117-6 W6M, 1720.8 m (5645.5 ft).

fracture porosity comprise <1% total porosity. Some porosity is cemented by coarse-crystalline, planar-subhedral dolomite and extremely coarse-crystalline saddle dolomite.

3.10.2 Interpretation

The non-fossiliferous dolomudstone lithofacies is interpreted to have been deposited in a low energy, high salinity, restricted environment. This interpretation is supported by the fine sediment size, absence of fauna and bioturbation, and the presence of anhydrite and haloturbation.

The association of lithofacies I with the Chinchaga and Muskeg formations suggests deposition took place during a transition from evaporitic to open marine conditions and vice versa. Dolomicrite in lithofacies I is considered to be analogous to dolomicrites that form in crusts or within sediments of modern carbonate intertidal and supratidal environments (cf. Morrow, 1990). Dolomitic crusts in tidal flats in the Caribbean and sabkha sediments in the Persian Gulf are usually interpreted to be the result of the replacement of aragonitic mud during very early diagenesis (Morrow, 1990). However, overlying or laterally adjacent evaporites can also provide hypersaline solutions that bear Mg^{2+} by seepage-refluxion to adjacent carbonates (Wilson, 1975). These solutions are capable of dolomitizing adjacent or underlying carbonates. Therefore, the reflux model is evoked to explain the association of lithofacies I with adjacent evaporites of the Chinchaga and Muskeg formations. Anhydrite may represent recrystallization of gypsum, replacement of allochems, or void-filling anhydrite.

3.11 Lithofacies Associations

Eight of the nine lithofacies in the Keg River Formation, as previously described, can be grouped genetically into three lithofacies associations: 1) outer ramp – lithofacies A, B, and C; 2) mid-ramp – lithofacies D and E; and 3) reef foreslope – lithofacies F, G, and H (Table 3.2). The remaining lithofacies (lithofacies I: non-fossiliferous dolomudstone) is related to temporally restricted events of increased salinity associated with the onset and termination of Keg River carbonate sedimentation, and therefore, will not be discussed further in this section. The outer and mid-ramp lithofacies associations comprise the Lower Keg River Member and the reef foreslope lithofacies association comprises part of the Upper Keg River Member.

Table 3.2 Organization of lithofacies into representative lithofacies associations.

	LITHOFACIES NAME	LITHOFACIES ASSOCIATION	STRATIGRAPHIC UNIT
H	Stromatoporoid-coral dolofloatstone to dolorudstone	Reef Foreslope	Upper Keg River Member
G	Massive peloidal-skeletal dolopackstone to dolograinstone		
F	Bituminous peloidal laminite		
E	Bioturbated crinoid-brachiopod floatstone	Mid ramp	Lower Keg River Member
D	Massive crinoid-brachiopod wackestone		
C	Nodular crinoid-brachiopod wackestone	Outer Ramp	
B	Irregular-bedded lime mudstone		
A	Bituminous laminite		

3.11.1 Outer Ramp Lithofacies Association

Lithofacies A (bituminous laminite), lithofacies B (irregular-bedded lime mudstone), and lithofacies C (nodular crinoid-brachiopod wackestone) are interpreted to comprise the outer ramp lithofacies association (Fig. 3.1). A carbonate ramp, is defined as a large carbonate body that extends away from positive areas and down gentle regional paleoslopes (Wilson, 1975). Facies patterns in such an environment generally form wide, regular belts because there are no sharp breaks in slope. The outer ramp, as defined by Burchette and Wright (1992), extends from the basin plain up to storm wave-base and is dominated by carbonate and terrigenous mud deposited from suspension. Evidence of storm or wave reworking is sparse in outer ramp environments where only the most powerful storms affect the sea floor (Wilson, 1975; Burchette and Wright, 1992). In the deepest zones of the outer ramp, organic-rich facies can develop due to oxygen-reduced basinal waters which result from restricted bottom conditions triggered by density stratification in the basin. Deposits from the upper part of the outer ramp can exhibit a variety of storm-related features including uncommon, graded distal tempestites (Burchette and Wright, 1992). However, these features were not observed in lithofacies A, B, or C.

The three lithofacies that comprise the outer ramp lithofacies association are laterally gradational. Lithofacies A is interpreted to represent the deeper part of the outer ramp facies and lithofacies C represents the shallower part of the outer ramp facies, having been deposited just below normal storm wave-base (Fig. 3.1). Lithofacies B is transitional between lithofacies A and C. Interpretation of the relative positions of these

lithofacies is based on increasing faunal abundance and diversity, increasing bioturbation, and decreasing OM content from lithofacies A to B to C.

3.11.2 Mid-Ramp Lithofacies Association

Lithofacies D (massive crinoid-brachiopod wackestone), and lithofacies E (bioturbated crinoid-brachiopod floatstone) constitute the mid-ramp lithofacies association (Fig. 3.1). The mid-ramp, as defined by Burchette and Wright (1992), is the zone between fairweather wave-base and storm wave-base. Facies deposited in the mid-ramp exhibit evidence of frequent reworking by bioturbation, storm waves, and swells (Burchette and Wright, 1992). However, suspension settling of carbonate and terrigenous mud contributes significant sediment during fairweather periods.

The depositional environment of the mid-ramp lithofacies association is interpreted as open marine, characterized by a diverse fauna including abundant crinoids, brachiopods, and bivalves, as well as minor gastropods, cricoconarids, and coral and stromatoporoid fragments. Allochems are more diverse and abundant than in the outer ramp lithofacies association, and skeletal constituents are typically larger in size (> 2 mm). Bedding and laminations are absent in this lithofacies association indicating increased oxygenation, bioturbation and scavenging activity that are typical of shallower open-marine environments. Evidence of storm activity, including graded beds, interbedded mudstones and grainstones composed of peloids and/or bioclasts, scoured bases, and preservation of articulated tests (Jones and Desrochers, 1992), was also observed in this lithofacies association.

Lithofacies D and E are laterally gradational. Lithofacies D is interpreted to represent the deeper mid-ramp, whereas lithofacies E is interpreted to have accumulated in the shallower mid-ramp (Fig. 3.1). The relative position of these two lithofacies is indicated by an increase in faunal abundance and diversity, evidence of storm activity, and bioturbation from lithofacies D to E.

3.11.3 Reef Foreslope Lithofacies Association

Lithofacies F (bituminous peloidal laminite), lithofacies G (massive peloidal-skeletal dolopackstone to dolograinstone), and lithofacies H (stromatoporoid-coral dolofloatstone to dolorudstone) comprise the reef foreslope lithofacies association (Fig. 3.2). Reef foreslope refers to an accumulation of in situ and reef-derived, bedded carbonate sand and gravel that encircles a reef, dipping and thinning away from the reef core facies (James and Bourque, 1992). The reef foreslope lithofacies association is interpreted as having accumulated in a moderate-energy environment between storm and fairweather wave-base which was frequently affected by storm events. Sediment gravity flows triggered by storm waves reworking upper foreslope peloidal-skeletal sand and gravel are postulated to have provided the balance of sediment comprising this lithofacies association (cf. Campbell, 1992). Sedimentary structures suggest that bioturbation and scavenging were active in these sediments indicating well oxygenated, open marine waters.

Lithofacies F, G, and H are all laterally gradational (Fig. 3.2). Lithofacies F and G are interpreted as having been deposited in the gently dipping, distal positions of the Upper Keg River foreslope, whereas lithofacies H is interpreted as having been deposited in

shallower, more proximal positions of the foreslope. Proximity to reef core facies is suggested by the higher abundance of debris from reef building organisms such as stromatoporoids and corals in lithofacies H than in lithofacies F and G.

CHAPTER 4: CYCLICITY & DEPOSITIONAL HISTORY

4.1 Introduction

The Keg River Formation in the Rainbow and Zama sub-basins exhibits vertical and lateral lithofacies variations related to second and third-order Devonian depositional cycles as defined by Wendte (1992b). Depositional histories of the Rainbow and Zama sub-basins are considered in the context of these cycles.

4.2 Depositional Cycles

Depositional cycles recognized within Devonian strata of the WCSB are transgressive-regressive sequences that can be grouped into three relative levels of organization which are readily defined (Wendte, 1992b). First-order cycles involve the most significant facies shifts and can be correlated across the WCSB. These cycles generally coincide with group level stratigraphy and they include, in ascending order, the Upper Elk Point Megacycle, Beaverhill Lake Megacycle, Woodbend Megacycle, Winterburn Megacycle, and the Wabamun Megacycle (Fig. 2.1). Second-order cycles consist of shoaling-upward successions and may involve significant lateral facies shifts related to allocyclic processes such as eustatic sea-level rise and/or subsidence. Individually or when grouped, these cycles approximate formation level stratigraphy. Third-order cycles are also composed of shoaling-upward successions and are generally thin (meters to 10s of meters). They represent stages of carbonate ramp deposition or reef growth which reflect minor variations in depositional environment including allocyclic processes (eustasy, subsidence) and autocyclic processes (sediment supply). Third-order cycles are more

commonly expressed in environments with low sedimentation rates such as distal carbonate ramp, distal reef foreslope and lagoonal settings than in environments with higher sediment supply such as reef cores and proximal reef foreslopes.

4.3 Keg River Cycles

The Keg River Formation comprises the lowermost second-order cycle of the Upper Elk Point Megacycle (Fig. 2.1) (Wendte, 1992b). In this study, two shoaling-upward third-order cycles (R1 and R2) are recognized in the Lower Keg River Member in the Rainbow Sub-basin and one such cycle (Z1) in the Lower Keg River Member in the Zama Sub-basin. The reef succession of the Upper Keg River Member is also composed of a number of third-order depositional cycles representing stages of reef growth and demise (Wendte, 1992b). However, this study focuses primarily on reef foreslope and off-reef deposits and only the lowermost portion of the basal third-order cycle in the Upper Keg River Member in the Rainbow Sub-basin (R3), and in the Zama Sub-basin (Z2) are described.

4.4 Third-Order Cycles in the Rainbow Sub-basin

4.4.1 Cycle R1

This basal third-order cycle, R1, contains lithofacies (A to E) of the outer ramp to mid-ramp lithofacies associations as well as lithofacies I (Fig. 4.1 and Encl. 2). Cycle R1 ranges from ~24 to 35 m thick. In the Rainbow area the gradational contact from the Chinchaga Formation to the overlying Lower Keg River Member was observed in core from the 6-32-107-9 W6M well at 2117.7 m (6947.8') and the 4-9-109-8 W6M well at

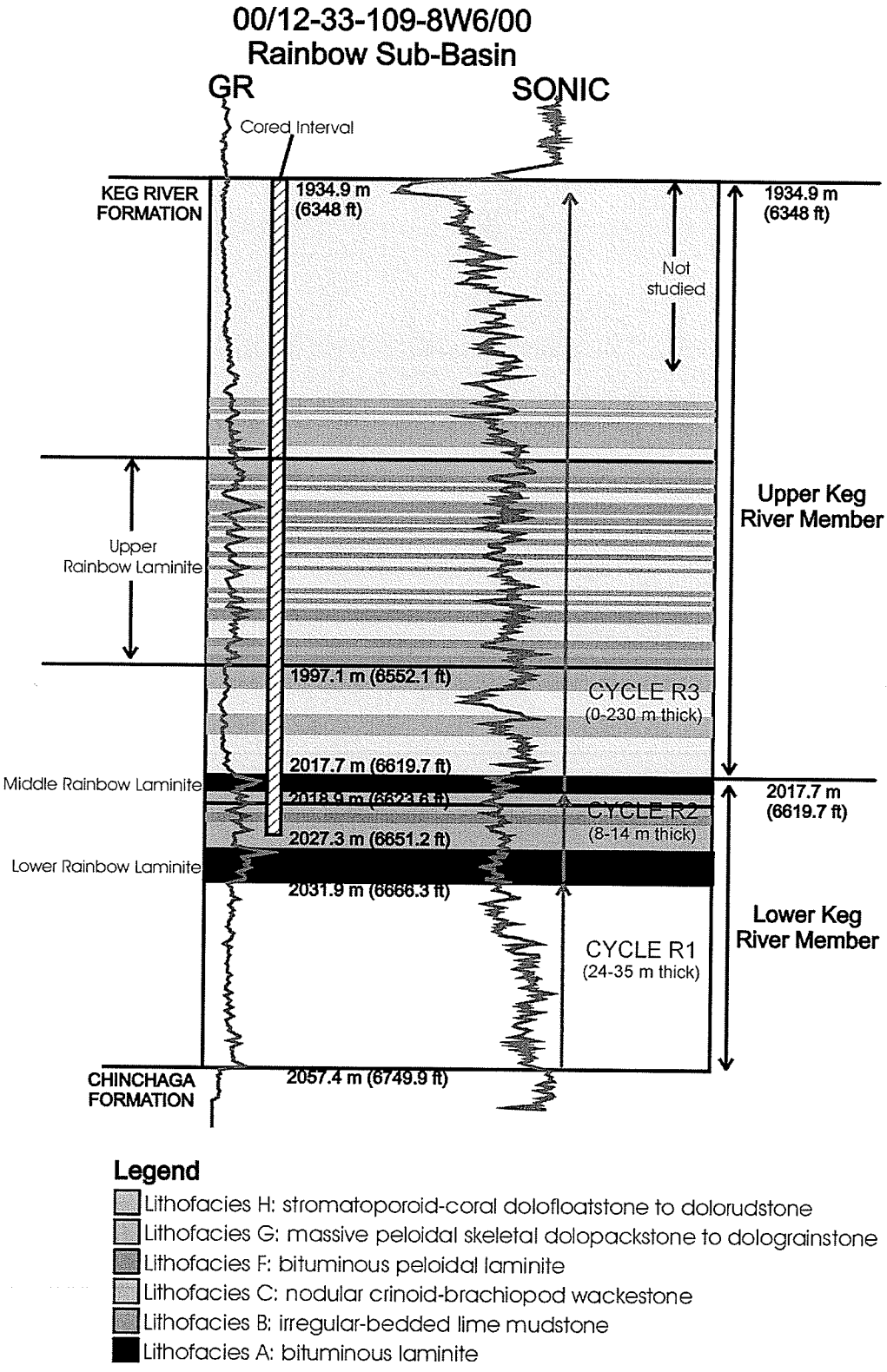

Figure 4.1 Summary of cyclicity in the Rainbow Sub-basin utilizing well 12-33-109-8 W6M to illustrate third-order cycle distribution (R1, R2, and R3), thickness, and petrophysical log response (GR = gamma ray).

2043 m (6702.7'). In both these cores, ~1 - 1.5 m of non-fossiliferous dolomudstone (lithofacies I) marks the transition from anhydrite to open marine carbonate rocks. The lithofacies that comprise the outer ramp lithofacies association (A: bituminous laminite, B: irregular-bedded lime mudstone, and C: nodular crinoid-brachiopod wackestone) and the mid-ramp lithofacies association (D: massive crinoid-brachiopod wackestone, and E: bioturbated crinoid-brachiopod floatstone) overlie lithofacies I and alternate in an apparently non-systematic manner. No single core exhibits all the lithofacies recognized in cycle R1.

The presence of alternating lithofacies A to E indicates that cycle R1 was deposited in an outer to mid-ramp environment with laterally shifting, gradational facies. Although the vertical succession of lithofacies appears almost random, certain relationships can be drawn between the various lithofacies (Encl. 2). In the 6-32-107-9 W6M well (2117.7 - 2089.1 m, 6947.8 - 6853.9' depth), the lower part of cycle R1 is largely composed of lithofacies A, C, and D, whereas the upper part of the cycle is composed of lithofacies C and E. Lithofacies E represents shallower positions on the ramp than lithofacies A and D suggesting a subtle, overall shoaling-upward succession. However, evidence for an overall shoaling-upward is not as apparent in cycle R1 of the 4-9-109-8 W6M (2043 - 2015.9 m, 6702.7 - 6613.8' depth) or 4-30-110-9 W6M (1982.4 – 1957.1 m, 6503.9-6420.9' depth) wells.

4.4.2 Cycle R2

The basal ~3 - 6 m of cycle R2 is typically comprised of interbedded lithofacies of the outer ramp lithofacies association (A: bituminous laminite, B: irregular-bedded lime mudstone, and C: nodular crinoid-brachiopod wackestone) and less commonly lithofacies of the mid-ramp lithofacies association (D: massive crinoid-brachiopod wackestone, and E: bioturbated crinoid-brachiopod floatstone). This unit is referred to as the lower Rainbow laminite (LRL) in this study. It is recognized on petrophysical logs by a prominent gamma-ray deflection (Fig. 4.1 and Encl. 2). Cycle R2 is ~8 - 14 m thick in total. The character of cycle R2 is best seen in the 4-30-110-9 W6M well (1957.1 – 1948.5 m, 6420.9 – 6392.6' depth) in which alternating lithofacies A and B grade up into lithofacies C (Encl. 2). Cycle R2 appears to be a better developed shallowing-upward succession that is expressed across the Rainbow area than cycle R1. The presence of alternating lithofacies A to E indicates that cycle R1 was deposited in an outer to mid-ramp environment with laterally shifting, gradational facies.

4.4.3 Cycle R3 (Basal Portion)

The base of cycle R3 is marked by deposition of the middle Rainbow laminite (MRL), which is composed largely of lithofacies A (bituminous laminite), ~2 m thick, at the top of the Lower Keg River Member (Fig. 4.1 and Encl. 2). This shoals upward into reef foreslope facies of the Upper Keg River Member including, massive peloidal-skeletal dolopackstone to dolograinstone (lithofacies G), and stromatoporoid-coral dolofloatstone to dolorudstone (lithofacies H). A relatively thin (~3 m) oncoidal unit, interpreted as equivalent to lithofacies E, was observed in one well (4-30-110-9 W6M; 1945.5 - 1947.5

m, 6389.4 – 6383' depth) immediately overlying the MRL (Encl. 2). This unit is anomalous in cycle R3, and is interpreted to represent the basin to buildup transition (refer to Section 3.6.2). Bituminous peloidal laminite (lithofacies F) occurs 15 m to 25 m above the base of cycle R3 and is interbedded with lithofacies G and H. These beds comprise the upper Rainbow laminite (URL), which ranges from at least 10 m thick (in the 4-9-109-8 W6M well) to at least 30 m thick (in the 6-32-109-8 W6M well) (Fig. 4.1). However, in the Rainbow Sub-basin, none of the core intervals that were studied completely span the Upper Keg River Member. It is possible that the URL is present throughout the Upper Keg River Member foreslope succession up to the contact with the overlying Muskeg Formation although this was not observed in this study. Based on petrophysical log signatures indicating high gamma ray values and high interval transit times, the interpreted top of the URL has been indicated on logs (Encl. 1 and 2) and recorded in Appendix A: Formation Tops.

Cycle R3 lithofacies reflect the reef foreslope expression of adjacent, shoaling-upward reefs of the Upper Keg River Member in the Rainbow Sub-basin. The MRL is interpreted to have been deposited in response to the onset of the relative sea level rise that facilitated initiation of the Upper Keg River Member reefs. Following this relative sea level rise, reefs grew vertically, contributing reef debris (i.e., lithofacies F, G, and H) to the reef foreslope. Although not observed directly in this study, it is hypothesized that the thickness of cycle R3 is dependent on its position relative to newly forming reef and inter-reef environments. This cycle would be expected to be thickest at the center of fully

developed Upper Keg River Member reefs (up to a maximum of 230 m thick) and have no expression (i.e., zero thickness) in off-reef positions (pers. comm. J. Wendte, 2001).

4.5 Third Order Cycles in the Zama Sub-basin

4.5.1 Cycle Z1

In the observed cores from the Zama area cycle Z1 is composed of nodular brachiopod-crinoid wackestone to floatstone (lithofacies C), and massive brachiopod-crinoid wackestone to floatstone (lithofacies D), which are parts of the outer ramp and mid-ramp lithofacies associations respectively (Fig. 4.2 and Encl. 2). Cycle Z1 is ~35 to 40 m thick. As in cycle R1, ~1.5 m of lithofacies I (non-fossiliferous dolomudstone) occurs at the base of cycle Z1 and marks the transition from Chinchaga Formation anhydrite rocks to Keg River Formation carbonate rocks. Lithofacies I grades up into alternating metre-scale units of lithofacies D and lithofacies C (Encl. 2). No overall shoaling-upwards of facies is apparent.

4.5.2 Cycle Z2 (Basal Portion)

The base of cycle Z2 is marked by the occurrence of ~1.5 – 2.5 m of Lower Keg River Member deposits including lithofacies A (bituminous laminite) which is locally interbedded with lithofacies C (nodular brachiopod-crinoid wackestone) that collectively comprise the lower Zama laminite (LZL) (Fig. 4.2 and Encl. 2). These lithofacies pass upward into reef foreslope lithofacies of the Upper Keg River Member, including, massive peloidal-skeletal dolopackstone to dolograinstone (lithofacies G) and stromatoporoid-coral dolofloatstone to dolorudstone (lithofacies H). Lithofacies F

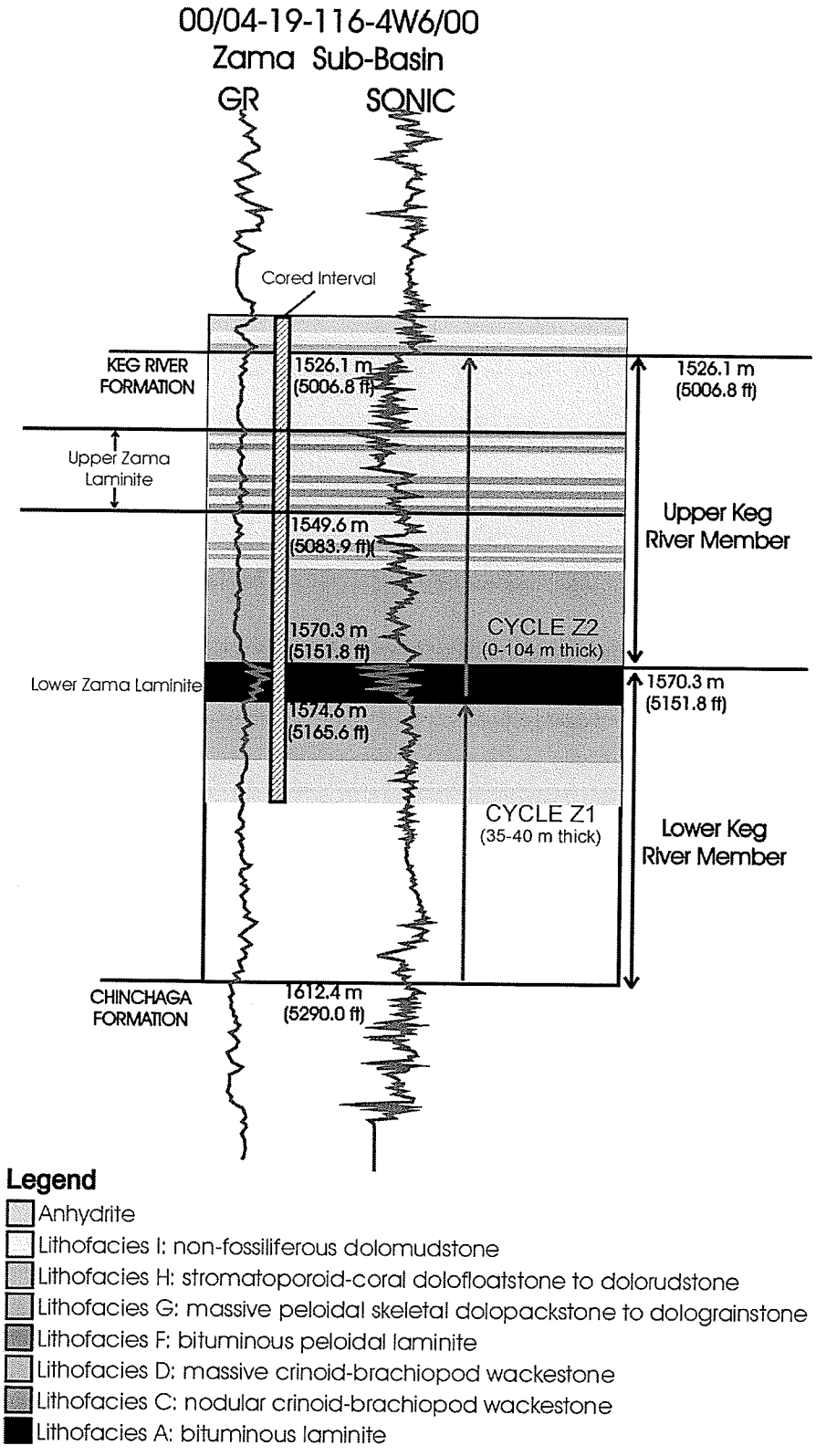

Figure 4.2 Summary of cyclicity in the Zama Sub-basin utilizing well 4-19-116-4 W6M to illustrate third-order cycle distribution (Z1 and Z2), thickness, and petrophysical log response (GR = gamma ray).

(bituminous peloidal laminite) occurs ~25 m above the base of cycle Z2 in the 4-19-116-4 W6M well where it was observed interbedded with lithofacies G. Interbedded lithofacies F, G, and H comprise the upper Zama laminite (UZL) which ranges from an estimated minimum of 0 m in true off-reef positions to at least 10 m thick (in the 4-19-116-4 W6M well) (Fig. 4.2). However, in the Zama Sub-basin, only one of the core intervals that was studied completely spans the Upper Keg River Member (in the 4-19-116-4 W6M well). It is conceivable that the URL is present throughout the Upper Keg River Member foreslope succession up to the contact with the overlying Muskeg Formation, although this was not observed in this study. The top of the UZL has been estimated based on high gamma ray values and high interval transit times on petrophysical logs (Encl. 1 and 2). The estimated top of the UZL has been recorded in Appendix A.

The LZL is interpreted to have been deposited during the onset of the relative sea level rise that resulted in reef development in the Upper Keg River Member in the Zama Sub-basin. Reef foreslope deposits that comprise cycle Z2 were derived from sediment shed off adjacent, shoaling-upward reefs onto the reef flank. As in cycle R3 in the Rainbow Sub-basin, the full thickness of cycle Z2 was not observed directly in this study. However, the thickness of cycle Z2 is also considered to be dependent on its position relative to newly forming reef and inter-reef environments with zero thickness in off-reef positions ranging up to ~104 m thick where maximum reef development occurred (e.g., 13-7-116-4 W6M well) (McCamis and Griffith, 1967).

4.6 Correlation Between the Rainbow and Zama Sub-basins

Two possible schemes for the correlation of the Keg River Formation in the Rainbow and Zama sub-basins were considered in this study. In the first correlation, cycle R1 in the Rainbow Sub-basin correlates to cycle Z1 in the Zama Sub-basin and the LRL correlates to the LZL (Fig. 4.3A). Cycles R2 and R3 in the Rainbow Sub-basin correspond to cycle Z2 in the Zama Sub-basin. This correlation suggests that the MRL could be correlative with the UZL and that the URL has no correlative unit in the Zama Sub-basin. This interpretation would suggest that two cycles of ramp development in the Rainbow area (R1 and R2) correlate to only one such cycle in the Zama area (Z1) and that reef growth in the Upper Keg River Member initated earlier in the Zama Sub-basin than in the Rainbow Sub-basin.

Regional studies indicate that the Rainbow and Zama areas are part of the extensive Elk Point Embayment, (e.g., Meijer Drees, 1994) and that initiation of Upper Keg River Member reefs in both areas occurred at approximately the same time, controlled by significant geological events (Campbell, 1992). Walsh (1986) described a regional subsidence that occurred at the close of Lower Keg River deposition that affected the entire Elk Point Embayment, creating sub-basins such as Rainbow, Meander, La Crete, Shekilie, and Zama.

A more plausible correlation between the Rainbow and Zama sub-basins connects cycles R1 and R2 in the Rainbow area to only one such cycle in the Zama area (Z1) (Fig. 4.3B).

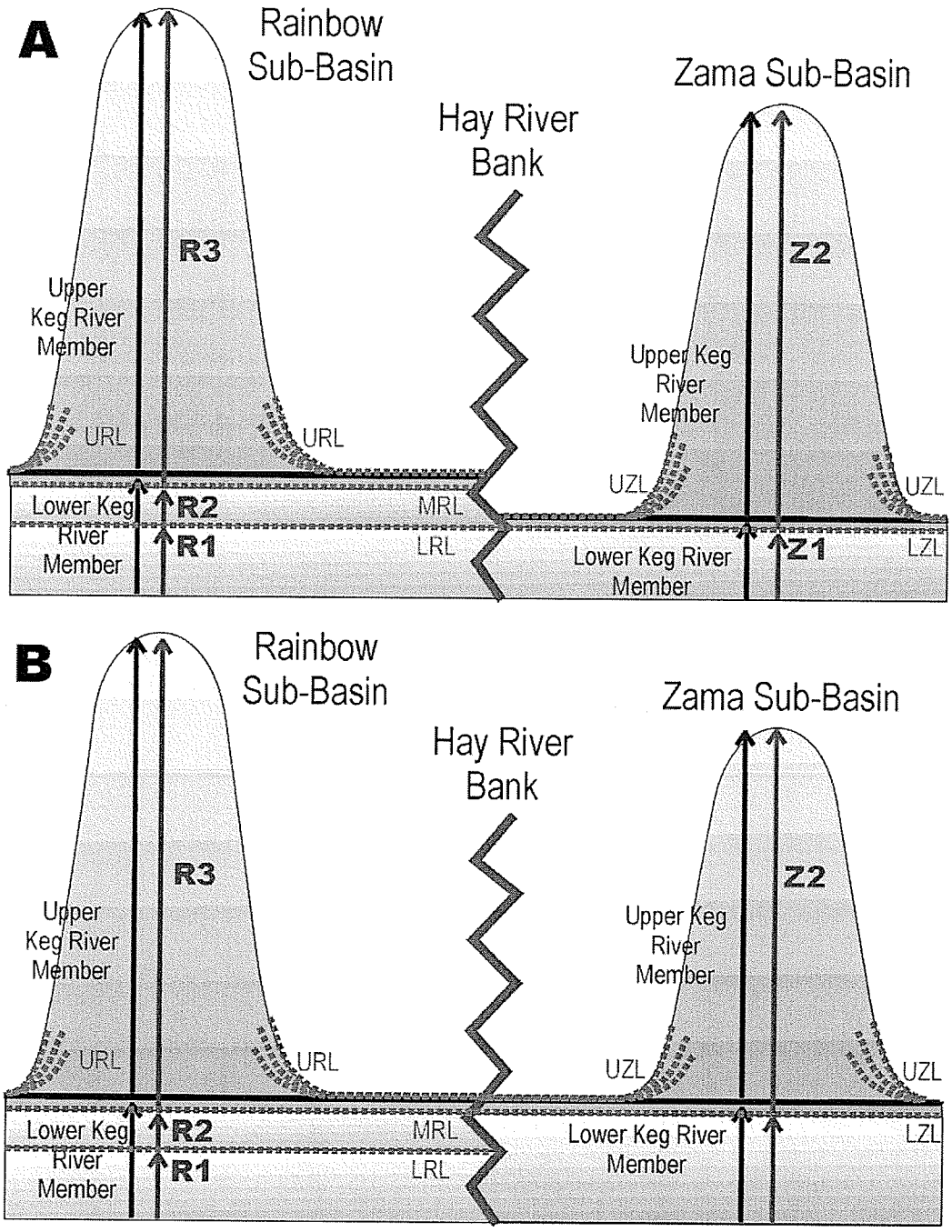

Figure 4.3 Possible correlations between the Rainbow and Zama sub-basins, red represents depositional cycles, blue represents stratigraphy, and green represents organic rich laminites (LRL=lower Rainbow laminite, MRL=middle Rainbow laminite, URL=upper Rainbow laminite, LZL=lower Zama laminite, and UZL=upper Zama laminite). A) This correlation assumes that reef initiation occurred earlier in the Zama Sub-basin than in the Rainbow Sub-basin. B) The favored correlation suggests coeval reef initiation in both sub-basins. See text for details.

The LRL has no correlative laminite in the Zama area. This succession is followed by cycles R3 and Z2, which suggests coeval initiation of Upper Keg River Member reefs in both the Rainbow and Zama sub-basins. Based on this correlation, the MRL correlates to the LZL and the URL is correlative with the UZL.

4.7 Depositional History

Deposition of the Lower Keg River Member began during a relative sea-level rise that transformed the Rainbow and Zama areas from an evaporitic setting, represented by the Chinchaga Formation, to an widespread carbonate ramp represented by cycle R1 in the Rainbow area and cycle Z1 in the Zama area.

This marine transgression corresponds to the initial incursion of open-marine waters into the Elk Point Embayment (Campbell, 1992). Cycle R2 developed in response to a relative sea-level rise attributed to relatively local subsidence in the Rainbow area. A correlative cycle is not present in the Zama Sub-basin suggesting that the subsidence responsible for initiating R2 was less pronounced or did not occur in the Zama area. Cycle R2 has not been recognized previously by other workers.

Following deposition of the Lower Keg River Member ramp, another relative sea-level rise attributed to subsidence resulted in growth of shelfal carbonates on a platform fringing the Peace River Arch and on banks connected to this platform that were positioned over basement highs (e.g., Hay River Fault Zone) (Campbell, 1992). Lower lying areas were drowned at this time to form discrete sub-basins such as the Rainbow,

Zama, and Shekilie sub-basins. In these sub-basins, isolated reefs of the Upper Keg River Member developed on paleotopographic highs where greater light intensity and higher energy conditions were favorable for coral and stromatoporoid growth (Campbell, 1992). In the Rainbow Sub-basin, crinoidal shoals formed at the top of the Lower Keg River Member ramp and are the proposed initiation sites for reefs (Campbell, 1992). Basement structures such as faults, folds, and topography caused by dissolution of underlying Lower Elk Point salts may have influenced the distribution of crinoidal shoals and, in turn, reef distribution (Langton and Chin, 1968). In the Zama Sub-basin, McCamis and Griffith (1967) observed a dolomitized crinoid bank forming the basal 12 m of Upper Keg River Member reefs and suggested this bank formed initiation sites for the reefs. Walsh (1986) postulated that reefs in the Rainbow and Zama sub-basins developed along platform highs related to basement structure.

In off-reef and foreslope positions, the deepening event responsible for sub-basin differentiation corresponds to the base of cycle R3 in the Rainbow Sub-basin and the base of cycle Z2 in the Zama Sub-basin where the deep-water facies of the MRL and the LZL, respectively, were deposited in response to drowning of the Lower Keg River Member ramp. These facies pass upwards into allochthonous foreslope debris near Upper Keg River Member reefs (Campbell, 1992). Subsequently, a relative sea-level drop, due to either evaporitic drawdown or regional sea-level lowering, halted carbonate growth in the Rainbow and Zama sub-basins as reefs were exposed and hypersaline conditions were established (Campbell, 1992).

CHAPTER 5: ORGANIC MATTER ACCUMULATION & PRESERVATION

5.1 Introduction

The hydrocarbon source potential of organic-rich marine deposits has sparked interest in characterization of the paleoecology and paleoenvironment of organic-rich facies (e.g., Chow *et al.*, 1995a). A number of factors influence OM accumulation and preservation including: 1) bottom-water oxygenation that is independent of phytoplankton productivity, 2) primary phytoplankton productivity in surface waters, 3) bulk sedimentation rates, 4) supply of terrestrial OM, and 5) sediment texture and mineralogy (summarized in Tyson, 1987; Pederson and Calvert, 1990; Wetzel, 1991)). The major debate revolves around whether enhanced preservation due to anoxia or high primary phytoplankton productivity is the primary control on accumulation and preservation of OM (e.g., Demaison and Moore, 1980; Pederson and Calvert, 1990; Calvert *et al.*, 1996). Other factors are considered secondary to preservation and productivity.

Determination of the primary control on accumulation of OM in specific petroleum systems, using organic petrology, has far-reaching implications for the petroleum industry. Once the primary control is determined for a number of source rocks, models for source rock distribution firmly rooted in direct observation can be constructed and previously developed models can be evaluated.

5.2 Anoxia (Preservation)

Bottom-water anoxia has been considered by many studies to be the primary control for accumulation and preservation of OM (e.g., Demaison and Moore, 1980; Jenkyns, 1980; Tyson, 1987; Canfield, 1989; Demaison, 1991; Tyson and Pearson, 1991; Van Cappellen and Canfield, 1993). Anoxia has historically been the model that most geologists and others have used to explain source rock occurrence. This study adopts the definition of anoxia presented by Demaison and Moore (1980) that defines water containing less than 0.5 mL of oxygen per liter of water as anoxic. At this low oxygen concentration, benthic metazoan biomass and, therefore, bioturbation is appreciably reduced. Demaison and Moore (1980) suggested that this oxygenation level marks the boundary between poor and good preservation of OM, with respect to both quality and quantity. However, many researchers do not agree with this statement as will be discussed subsequently.

5.2.1 Development of Anoxic Layers

Anoxia can develop in response to a number of factors, including water-column stratification, high OM flux, and water depth (Demaison and Moore, 1980). Anoxia ultimately reflects a higher demand for oxygen than can be met by the current supply in the water column. Oxygen demand is directly related to the amount of OM in the water column that needs to be oxidized (degraded). Approximately 80% of OM degradation occurs in the euphotic zone where free oxygen is supplied from the atmosphere and from photosynthesis in surface waters (Demaison and Moore, 1980). The remaining 20% that sinks below the euphotic zone must also be degraded, creating additional oxygen demand.

The oxygen supply available to degrade OM below the euphotic zone depends largely on ocean circulation. Density differences, high-latitude cooling, surface winds, and the Coriolis force drive ocean circulation, which facilitates the downward movement of aerated surface waters and the upward movement of oxygen-rich, colder, denser bottom-waters (Parrish, 1982). Density stratification in the water column (pycnocline) develops when cooler water underlies warmer water (thermocline), or when saline water underlies fresher water (halocline) restricting vertical mixing. This can lead to development of anoxic layers, or an oxygen minimum zone (OMZ) in the water column (Fig. 5.1A). Vertical mixing can also be restricted when a physical barrier exists between the open ocean and an isolated body of water (Pederson and Calvert, 1990). Such a barrier prevents the replenishment of oxygen in the body of water below the barrier depth due to the presence of a strong pycnocline.

Increased flux of OM from terrestrial sources and/or elevated primary productivity can overwhelm the oxygen supply in the water column, resulting in the creation of an anoxic layer that favors OM accumulation and preservation (Chow *et al.*, 1995a). However, Demaison and Moore (1980) observed no systematic correlation between elevated productivity and OM content in modern marine sediments and concluded that factors other than productivity must control OM accumulation and preservation.

Water-column oxygenation can also change dramatically with increasing depth (Demaison and Moore, 1980). This is because oxygen is only produced in the upper water column by photosynthesis within the photic zone and the atmosphere only

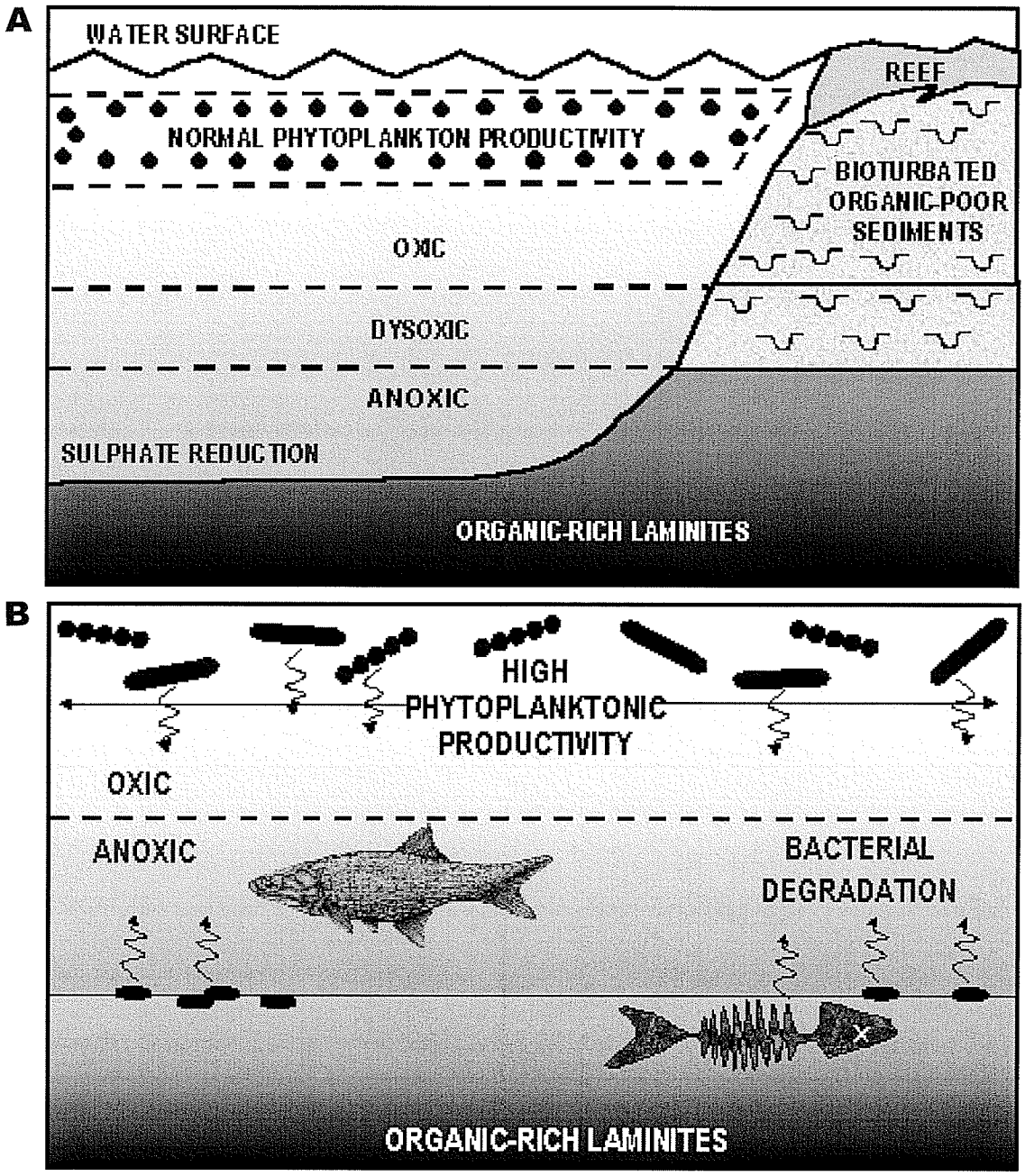

Figure 5.1 Schematic diagrams illustrating preservation and productivity as primary controls on OM accumulation. A) Preservation: A stratified water column inhibits or eliminates benthic scavenging and bioturbation favoring the accumulation and preservation of organic-rich facies on the seafloor. B) Productivity: High phytoplanktonic productivity in surface waters produces an increased flux of OM settling to the seafloor. Elevated rates of aerobic bacterial decay and phytoplanktonic respiration create an oxygen minimum zone. Where this oxygen minimum zone impinges on the continental margin, anoxic bottom-waters result which favor the accumulation and preservation of OM (modified from Chow *et al.*, 1995b; Stasiuk *et al.*, 1995).

oxygenates surface waters. However, deeper waters can be oxygenated periodically by agitation. Lack of circulation can lead to the development of anoxic waters, sometimes due to water depth, but also related to topography of deep areas creating regions with sluggish circulation such as amongst reefs within intracratonic basins. Oxygen consumption is greatest at the sediment water interface where settled OM is degraded by aerobic bacteria (e.g., Rhoads, 1974). These conditions lead to a deficit of dissolved oxygen at depth resulting in bottom-water dysoxia or anoxia.

5.2.2 Anoxia: Accumulation and Preservation of OM

In an oxygenated water column, OM is subjected to biochemical degradation before, during, and after reaching the sediment-water interface. During settling, OM is a source of energy and nutrients for living organisms including zooplankton, larger invertebrates, and fish (Arthur and Sageman, 1994). At the sediment-water interface suspension feeders and benthic organisms consume a proportion of the OM that reaches the sediment surface. Following shallow burial, deposit feeders such as polychaetes, holothurians, and bivalves further consume and degrade OM (Demaison and Moore, 1980). OM degradation is further enhanced by mobile deposit feeders, which aerate and irrigate sediments through burrowing activity. Therefore, the total benthic metazoan biomass is a controlling factor on accumulation and preservation of OM.

Oxygen levels directly affect the benthic metazoan biomass. Studies show that the benthic metazoan biomass is active down to oxygen concentrations of 1 mL of oxygen per litre of water (Rhoads, 1974). From 0.7 to 0.3 mL/L oxygen concentration, the

benthic metazoan biomass decreases, directly affecting the rate of OM degradation (Rosenberg, 1977). Below 0.3 mL/L deposit feeders are rare, sluggish, and soft-bodied if present at all. Below 0.1 mL/L, no suspension feeders can survive and only anaerobic bacteria remain to carry out OM degradation. Benthic metazoan biomass decreases with decreasing oxygenation levels, therefore, favoring preservation of OM in oxygen-poor environments.

Although benthic metazoans are largely responsible for OM degradation, bacteria also degrade OM in the water column and at the sediment surface (Demaison and Moore, 1980). Aerobic bacteria utilize oxygen to breakdown OM by the reaction:

(1) $CH_2O + O_2 \rightarrow CO_2 + H_2O$

Once free oxygen is used up, anaerobic bacteria replace aerobic bacteria. Anaerobic bacteria use nitrate to degrade OM by the reaction:

(2) $CH_2O + 4NO_3 \rightarrow 6CO_2 + 6H_2O + 2N_2$

Once all free nitrate has been consumed, anaerobic bacteria resort to sulfate reduction reactions to degrade OM:

(3) $CH_2O + SO_4 \rightarrow CO_2 + H_2O + H_2S$

Finally, when the supply of sulfate is exhausted, anaerobic bacteria must use carboxyl groups and organic acids derived from the OM itself to breakdown OM further via fermentation reactions.

The significance of this series of reactions is that efficiency is reduced with each progressive step rendering anaerobic degradation much less efficient than aerobic

decomposition. Anaerobic degradation, the process predominant in anoxic water columns, produces more lipid-rich, hydrogen-rich OM than aerobic degradation. Bacterial biomass, a large contributor to total OM content, is also disproportionately high in anoxic environments. Inefficient anaerobic degradation favors preservation of OM in oxygen-poor environments.

5.3 Phytoplankton Productivity

Based on recent oceanographic studies, elevated primary productivity in surface waters has been proposed as an alternative to bottom-water anoxia as a primary control on OM accumulation (Fig. 5.1B) (e.g., Müller and Suess, 1979; Suess, 1980; Parrish, 1982; Calvert, 1987; Pederson and Calvert, 1990; Calvert and Pederson, 1992; Tribovillard *et al.*, 1994). A number of studies have shown that bottom-water oxygen concentration has little effect on the quantity or quality of OM that accumulates and is preserved (e.g., Harvey *et al.*, 1986; Calvert *et al.*, 1991; Calvert *et al.*, 1992; Cowie and Hedges, 1992; Lee, 1992; Pederson *et al.*, 1992).

5.3.1 Development of Algal Blooms

Modern algal blooms develop in response to changes in environmental parameters including nutrient levels, temperature, salinity, light, turbidity, and water-column stratification (summarized in Fritsch, 1959; Calvert, 1987; South and Whittick, 1987; www.dlwc.nsw.gov.au/care/water/bga/causes.html, accessed January 14, 2002). Algal blooms are favored by elevated levels of dissolved nutrients, such as phosphorous and nitrogen, in a body of water (eutrophication). Nutrients may be derived from terrestrial

erosion and runoff from laterally adjacent landmasses. Upwelling, which brings nutrients into the photic zone from deeper, more nutrient-rich environments is another mechanism for elevating nutrient levels. Two major types of upwelling currents are recognized: a) coastal upwelling and b) open-ocean divergence.

Coastal upwelling occurs when prevailing winds cause transport of surface waters away from the coast and replacement of these waters from below (Parrish, 1982). In the Northern Hemisphere, coastal upwelling requires steady winds parallel to the coast with the coast positioned such that net water transport offshore occurs due to the Coriolis effect. Upwelling, and consequently algal blooms, are ubiquitous off the west coasts of continents (Parrish, 1982). Trade winds, which blow from east to west and towards the equator in both hemispheres, are responsible for this distribution because they drive surface water away from west-facing coastlines causing upwelling (Pederson and Calvert, 1990). Shallow upwelling near the equator, as surface water is warmed and moves away from the equator, is correlated with moderate primary productivity throughout the year (Pederson and Calvert, 1990).

Open-ocean divergence upwelling occurs under low-pressure systems, where air rises relative to surrounding air and adjacent, high-pressure air flows in to replace the rising air (Parrish, 1982). Water is driven away from the center of the low-pressure system and is replaced by upwelling waters from below.

Modern algal blooms develop during warmer seasons (spring and summer) when water temperatures are elevated and more sunlight is available for the phytoplankton (www. dlwc.nsw.gov.au/care/water/bga/causes.html, accessed January 14, 2002). Temperature sensitivity explains why algal blooms can persist in tropical regions throughout the year but do not occur in temperate regions during the winter months.

Brackish or hypersaline waters can also encourage the development of algal blooms. Different species of algae have different salinity requirements; therefore, changes in salinity can trigger blooms of specific algae species (www. dlwc.nsw.gov.au/care/water/bga/causes.html, accessed January 14, 2002). For example, modern blooms of *Aureococcus anophagefferens*, a picoplanktonic algae responsible for "brown tides" along the midwestern Atlantic coast of the U.S.A, are triggered by elevated salinities resulting from reduced estuarine flushing rates (Bricelj and Lonsdale, 1997).

Intermittent, high-intensity light favors the development of modern algal blooms although long periods of high intensity light can be detrimental to phytoplankton (www. dlwc.nsw.gov.au/care/water/bga/causes.html, accessed January 14, 2002). Modern cyanobacteria can thrive even under low light conditions, such as in turbulent waters, where other algae are unable to flourish (Bricelj and Lonsdale, 1997). This is because cyanobacteria can control their position in the water column (and therefore their exposure to light) by deflating and inflating a gas vesicle. In general, light conditions are more favorable to algal blooms in tropical regions throughout the year or during spring and

summer in temperate regions. Turbidity is generally detrimental to most phytoplankton because turbid waters contain suspended particles of sediment and OM that limit light penetration necessary for phytoplanktonic productivity (www.dlwc.nsw.gov.au/care/water/bga/causes.html; accessed January 14, 2002). Therefore, algal blooms are favored in slow moving waters, affected only by light surface winds, and limited sediment load from terrestrial sources.

Water column stratification, such as thermal stratification, can also promote algal blooms (www.dlwc.nsw.gov.au/care/water/bga/causes.html; accessed January 14, 2002). Stable surface waters in stratified water columns are warm and clear, have excellent light penetration, and extend to greater depths than surface waters in mixed water columns. Stratification also often leads to decreased oxygenation of bottom-water layers. Bottom-water dysoxia or anoxia may lead to increased release of nutrients from the sediments.

5.3.2 Productivity: Accumulation and Preservation of OM

During periods of elevated phytoplankton productivity (algal blooms), high rates of phytoplanktonic respiration and aerobic bacterial decay of settling OM depletes oxygen levels in the surrounding water, creating an oxygen minimum zone which results in anoxic bottom-waters where the oxygen minimum zone impinges on the continental margin (Fig. 5.1B) (Demaison and Moore, 1980). In addition to reducing or eliminating scavengers and bioturbators, an oxygen minimum zone can also result in mass kills of pelagic organisms trapped within this zone. In these scenarios, large amounts of OM

cannot be oxidized (degraded) and therefore accumulates and is preserved as a direct result of high productivity.

5.4 Sedimentation Rates

A number of studies have indicated that that the dominant second-order control on OM content in marine sediments is bulk sedimentation rate (e.g., Müller and Suess, 1979; Canfield, 1989; Betts and Holland, 1991). Elevated inorganic sediment accumulation rates reduce the residence time of OM at the sediment-water interface, increase the burial efficiency of the system (the amount of ultimately buried OM as a percentage of the OM flux that reaches the sediment-water interface) (Arthur and Sageman, 1994), and decrease benthic degradation loss, all of which serve to promote preservation of OM. However, if OM flux rates remain constant, total OM content of sediment will decrease with increasing inorganic sedimentation rate because of a "clastic dilution" effect. Clastic dilution can occur in both oxic and anoxic depositional environments.

5.5 Supply of Terrestrial OM

The main source of allochthonous OM is from terrestrial environments (Meybeck, 1982). The contribution of terrestrial OM by precipitation, wind, and rivers is modest compared to the significant amounts of OM produced by marine phytoplankton, but it is still an important control on the accumulation of OM. Less than 1% of the total OM in modern marine environments is derived from terrestrial sources, although modern rivers transport 7.0×10^8 metric tons of OM into the oceans and seas annually (Skopintsev, 1950 *in* Bordovskiy, 1965). The OM content of any river depends on a number of factors,

including climate, erosion, relief, and turbidity. Modern research indicates that rivers draining swamps and other poorly drained areas have the highest OM content (25 mg/L) (Meybeck, 1982). Rvers in taiga (moist subarctic forests dominated by conifers) have the second highest OM content (10 mg/L), followed by rivers in the wet tropics (6 mg/L), and rivers in temperate zones (3 mg/L). Rivers that flow through tundra or other semi-arid environments have the lowest OM contents.

OM content is also high in rivers with relatively high erosion rates that result in leaching and erosion of organic soil components, organic-rich sedimentary rock, and metamorphosed OM (Bordovskiy, 1965; Meybeck, 1982). Rivers flowing through areas of high relief may contain more OM than those flowing through areas of limited relief due to their higher potential for erosion. However, rivers flowing through plains typically contain more OM than those in mountainous regions because they are commonly less turbid which favors high OM contents (Meybeck, 1982). Terrestrial OM may also be transported to marine environments by winds and by precipitation but to a lesser extent than by rivers (Meybeck, 1982, Arthur and Sageman, 1994).

5.6 Sediment Texture and Mineralogy

OM content is affected by both the texture and the mineralogy of associated sediments. Aside from typically characterizing environments with lower depositional energy and higher OM flux, fine-grained sediments also favor high OM content because surface area increases exponentially with decreasing grain size and OM forms a coating of consistent thickness on clastic grains (Müller and Suess, 1979; Keil *et al.*, 1993 *in* Arthur and

Sageman, 1994). Mineralogy is another important consideration because some organic compounds are sorbed onto the surfaces of calcium carbonate grains and/or clays resulting in greater preservation potential for OM (Arthur and Sageman, 1994). The amount of OM sorbed onto these grains is dependent on surface area, and therefore fine-grained sediments favor elevated OM contents as mentioned previously.

CHAPTER 6: ORGANIC PETROLOGY

6.1 Introduction

Study of OM in sedimentary rocks, such as the organic-rich laminites within the Rainbow and Zama sub-basins, provides insight into the prevailing paleoecological and paleoenvironmental conditions during deposition. OM is transformed into kerogen, the source of hydrocarbon accumulations, by burial pressures and temperatures (Tissot and Welte, 1984; Hunt, 1996). Kerogen in organic-rich laminites in the Rainbow and Zama sub-basin were analyzed using organic petrology and organic geochemistry integrated with detailed sedimentology.

Organic petrology is the branch of earth science concerned with all aspects of the origin, occurrence, and history of sedimentary OM (Taylor *et al.*, 1998). In this study, incident-light microscopy was used to identify macerals and OF based on the morphology and fluorescence of dispersed OM particles. OF were then determined based on maceral assemblages and used to interpret paleoenvironment and paleoecology.

6.2 Overview of Maceral Types

Macerals, a term introduced by Stopes (1935), was initially used to refer to the microscopically identifiable constituents in coal. However, the maceral concept is also applicable to dispersed OM (kerogen) in organic-rich, fine-grained sedimentary rocks. Macerals are the insoluble remains of plant tissue and plant-derived substances present in coal and organic-rich sedimentary rocks and exhibit heterogeneity in both chemical

composition and physical properties, creating many challenges for their study (Stopes, 1935; Stach *et al.*, 1982). C, H, O, S, and N are the main elemental constituents of macerals (Taylor *et al.*, 1998). Morphology, hardness, and optical properties such as reflectance, fluorescence, and color are the criteria used to classify different macerals (Taylor *et al.* 1998). Macerals are classified in to three groups based on optical properties: vitrinite, liptinite, and inertinite (Taylor *et al.*, 1998). Vitrinite macerals are derived from humic substances originating from lignin and cellulose in plant cell walls and are characterized by relatively high carbon aromatic fraction and oxygen content. Liptinites originate from hydrogen-rich plant material including algaenan (algal cell walls), sporopollenin (spores and pollen), resins, cutin, suberin, waxes, oils, and fats. Liptinites have higher hydrogen content and aliphatic fraction than vitrinites. Inertinites are derived from the same original plant substances as vitrinite and liptinite, but the precursors to inertinites underwent some primary transformation (i.e., oxidation) prior to kerogen formation. Inertinites have high carbon content, low hydrogen content, and are highly aromatized. Varieties of alginite and sporinite macerals of the liptinite group have proven successful for defining OF in the Devonian of the WCSB and Ontario (Obermajer, 1997; Stasiuk, 1999).

6.2.1 Alginite Macerals

Alginite macerals are organic-walled microfossils derived from lipid-rich, resistant biomacromolecules including green algae, cyanobacteria, dinoflagellate cysts, planktonic prokaryotic and eukaryotic algae cysts (Lipps, 1993). Prasinophyte alginites, coccoidal

alginites, filamentous alginites, and acanthomorphic acritarchs are of importance in this study.

Prasinophyte Alginites

Prasinophytes are derived primarily from marine green algae (phylum Chlorophyta) (Lipps, 1993). The largest, thick-walled fossil Prasinophytes probably represent the phycoma (highly resistant, nonmotile resting stage) of the Prasinophyte life cycle. A number of different fossil genera may be distinguished in organic-rich rocks, including *Leiosphaeridia* and *Tasmanites*. *Leiosphaeridia* (considered to be an acritarch by some researchers) is characterized by thin (commonly less than 0.5 μm), smooth cell walls (pers. comm. L. Stasiuk, 2000) (Fig. 6.1A). In contrast, *Tasmanites* has relatively thick (commonly 4–5 μm), pore-bearing (punctate) cell walls (Fig. 6.1B).

Coccoidal Alginites

Coccoidal alginites are derived from unicellular green algae or cyanobacteria which, after cell division, group together in a colonial aggregate within an extracellular envelope (Golubic and Knoll, 1993). Coccoidal alginite macerals include *Gloeocapsomorpha, Botryococcus*, *Pila*, and *Reinschia* (Taylor *et al.*, 1998). The coccoidal alginite in the Devonian of the WCSB has been classified as *Gloeocapsomorpha prisca*-like (Chow *et al.*, 1995a; Stasiuk, 1999; Fowler and Stasiuk, 1999) in marine environments (Fig. 6.2A and C) and as *Botryococcus*-like in lacustrine settings (Fig. 6.2B) (Stasiuk, 1999).

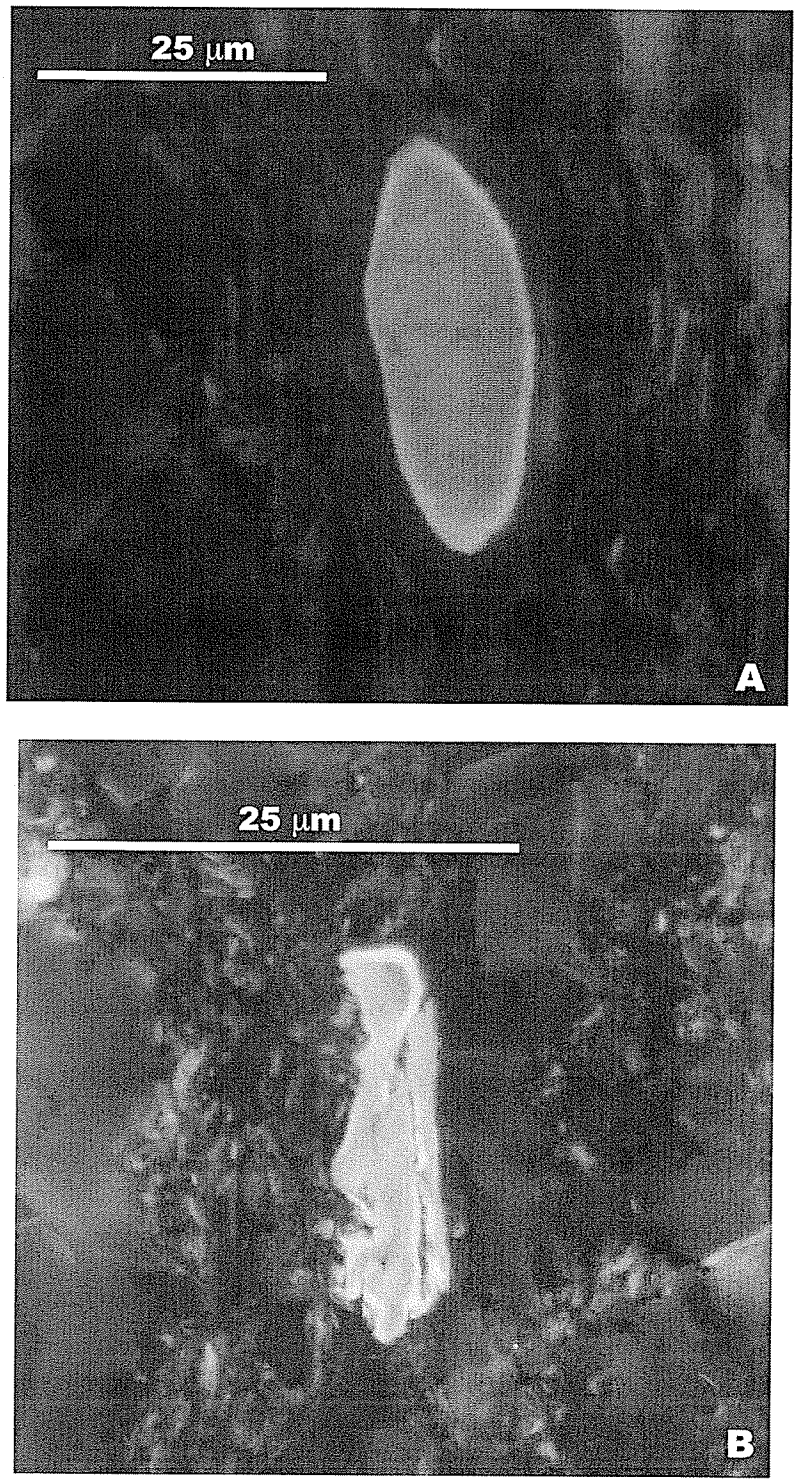

Figure 6.1 Photomicrographs of alginite macerals from the URL in the Rainbow Sub-basin taken using fluorescent incident light microscopy and water-immersion objectives. A) Large, relatively thin-walled *Leiosphaeridia* exhibiting characteristic smooth cell walls. 6-32-109-8 W6M, 1994 m (6542') depth. B) Large, thick-walled *Tasmanites* displaying contorted, punctate cell walls. 4-9-109-8 W6M, 1954.3 m (6511.75') depth.

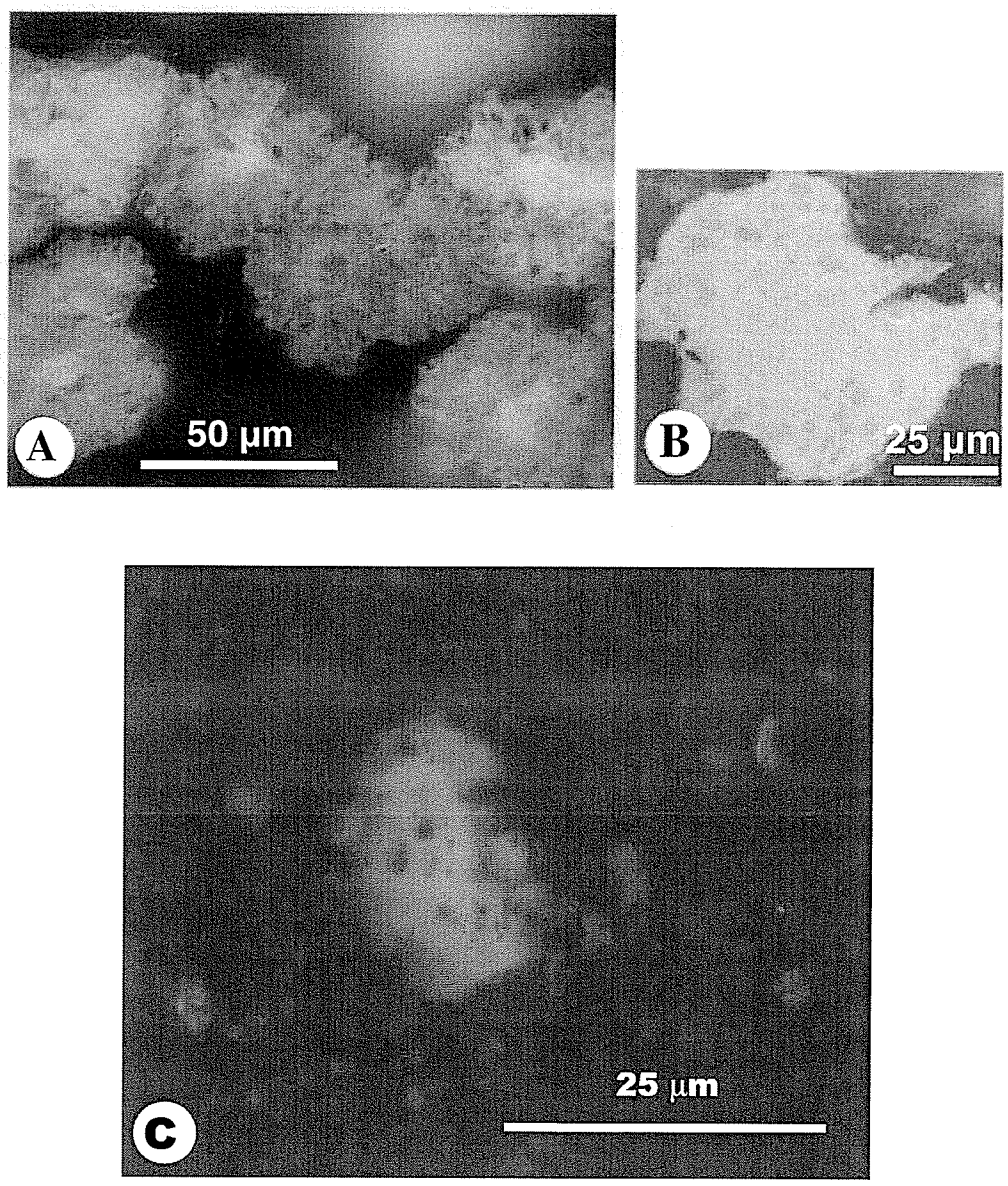

Figure 6.2 Photomicrographs of coccoidal alginites taken using fluorescent incident light microscopy and water-immersion objectives (photomicrographs A and B from Stasiuk, 1999). A) Coccoidal *Botryococcus* alginite in lacustrine marl. B) Multicellular, marine coccoidal alginite (*Gloeocapsomorpha prisca)* showing the typical appearance of colonial aggregates of coccoid cyanobacteria (from Stasiuk, 1999). C) *Gloeocapsomorpha prisca*-like coccoidal alginite from the LRL in the Rainbow Sub-basin. 6-32-107-9 W6M, (2086.7 m) 6843.3' depth.

Filamentous Alginites

Filamentous alginites are derived from multicellular cyanobacteria (Golubic and Knoll, 1993). These organisms maintain intimate contact between cells subsequent to cell division. Modern filamentous cyanobacteria are characterized by tight linear arangements of cells called trichomes. These cyanobacteria range from simple rod-shaped to more complex branching taxa that differentiate specialized cells such as reproductive cells, apical cells, heterocysts, and akinete cells. Filamentous alginites are rarely preserved due to their original cell morphology, and no filamentous alginites were identified in the Keg River Formation in this study. However, remnants of filamentous alginites in the form of algal akinete cells, interpreted as cyanophyte-derived, have been previously reported in the Keg River Formation in the La Crete Sub-basin by Chow *et al.* (1995a), and Stasiuk (1999). Akinetes are resting spores of cyanobacteria that develop in response to unfavorable conditions by increasing in size and developing thickened cell walls (Fig. 6.3). Modern and fossil akinetes have an exospore (outer wall) and an endospore (inner wall). Once environmental conditions return to normal, the exospore bursts and the endospore germinates to produce new cyanobacteria cells (Round, 1981; Stasiuk, 1999).

Acritarchs

Acritarchs are organic-walled microfossils derived from different stages in the life cycle of unicellular algae, such as cysts and vegetative cells (Mendelson, 1993). Acritarchs are sub-divided into eight main varieties based on morphology; 1) acanthomorphs which

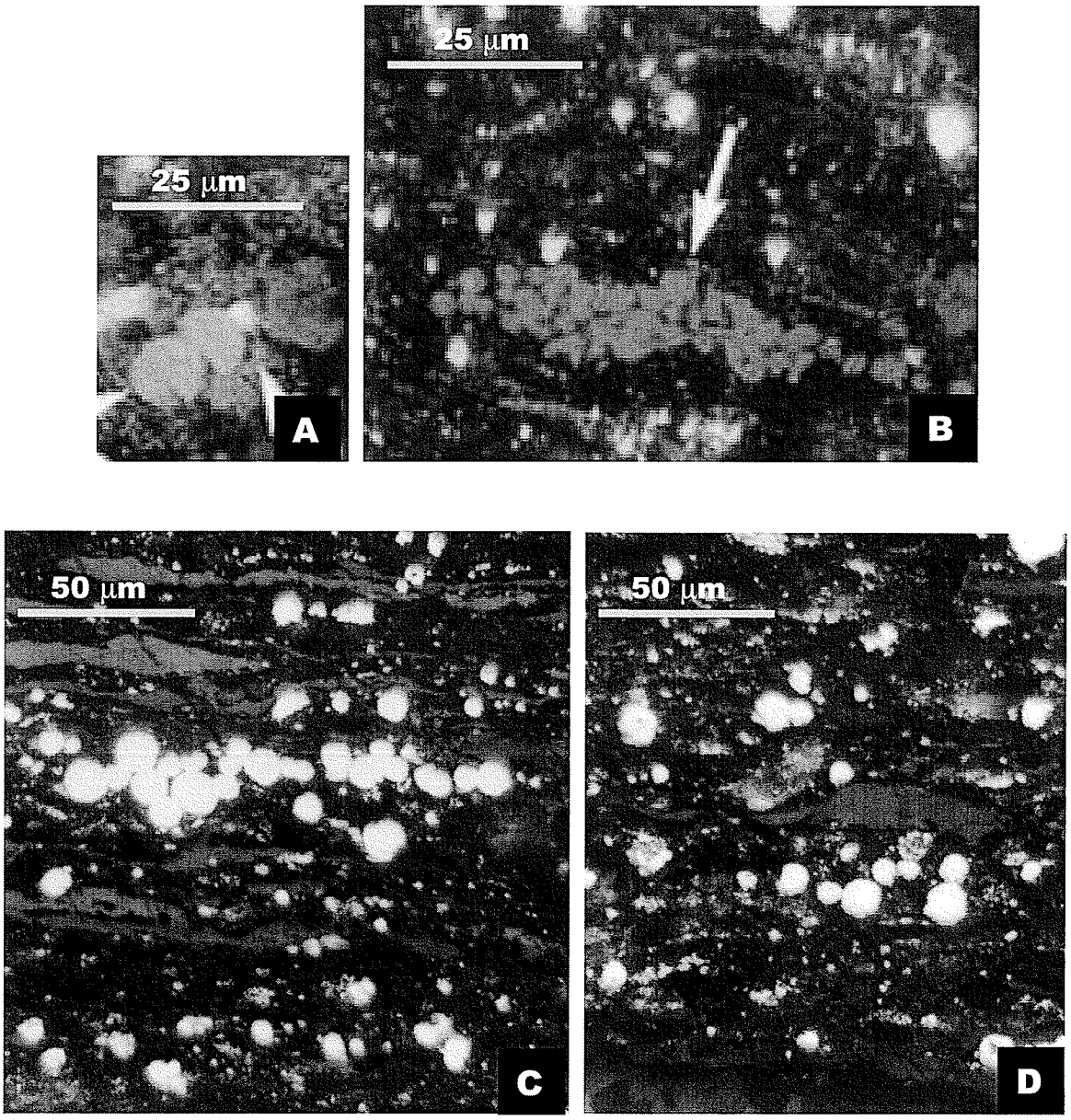

Figure 6.3 A and B) Photomicrographs from the Keg River Formation taken using fluorescent incident light microscopy and water-immersion objectives. Round vitrinite group macerals derived from micro-algal special reproductive, resting or akinete cells, indicative of algal blooms (from Stasiuk, 1999). C and D) Photomicrographs of pyrite spheres which occur in chains parallel to laminae from the UZL in the Zama Sub-basin (this study) taken using reflected white light microscopy and water-immersion objectives. These pyrite spheres are postulated to be pyritized akinete cells. 4-19-116-4 W6M, (1527.5 m) 5011.5' depth.

have spherical bodies with spiny processes (Fig. 6.4A); 2) polygonomorphs which have a body shape determined by the number and position of their spines and are often square or triangular; 3) neteromorphs which have a fusiform body and at least one spine; 4) diacromorphs which have spherical to ellipsoidal bodies with ornamentation confined to their poles; 5) prismatomorphs which have prismatic to polygonal bodies with a flange or crest at the edges; 6) oomorphs which have an egg shaped body with ornamentation at only one pole; 7) herkomorphs which have approximately spherical bodies divided into polygonal fields; and 8) sphaeromorphs which have spherical bodies (Downie *et al.*, 1961; Downie and Sarjeant, 1964; Mendelson, 1993). Acritarchs in the Keg River Formation consist mainly of acanthomorphic acritarchs including *Veryachium*-like acanthomorphic acritarchs (Fig. 6.4B).

6.2.2 Sporinite Macerals

Sporinite macerals represent the preserved remains of the cell walls of terrestrial spores and pollens. Spore/pollen fossils are tough, hollow, variably grooved or ornamented bags, balls, or cases (Traverse, 1988). The inner cell wall layers and protoplasm of fossil spores/pollen are absent and the remaining "empty cases" are usually flattened and contorted during fossilization. The outer cell wall (exine) may be variably ornamented, ranging from smooth to bumpy, spiny, grooved, polygonal or structured in some other manner (Fig. 6.4). Morphological differentiation of spores/pollen is based on such ornamentation. Sporinite has relatively high relief in polished mounts and thin sections due to the toughness of sporinite cell walls.

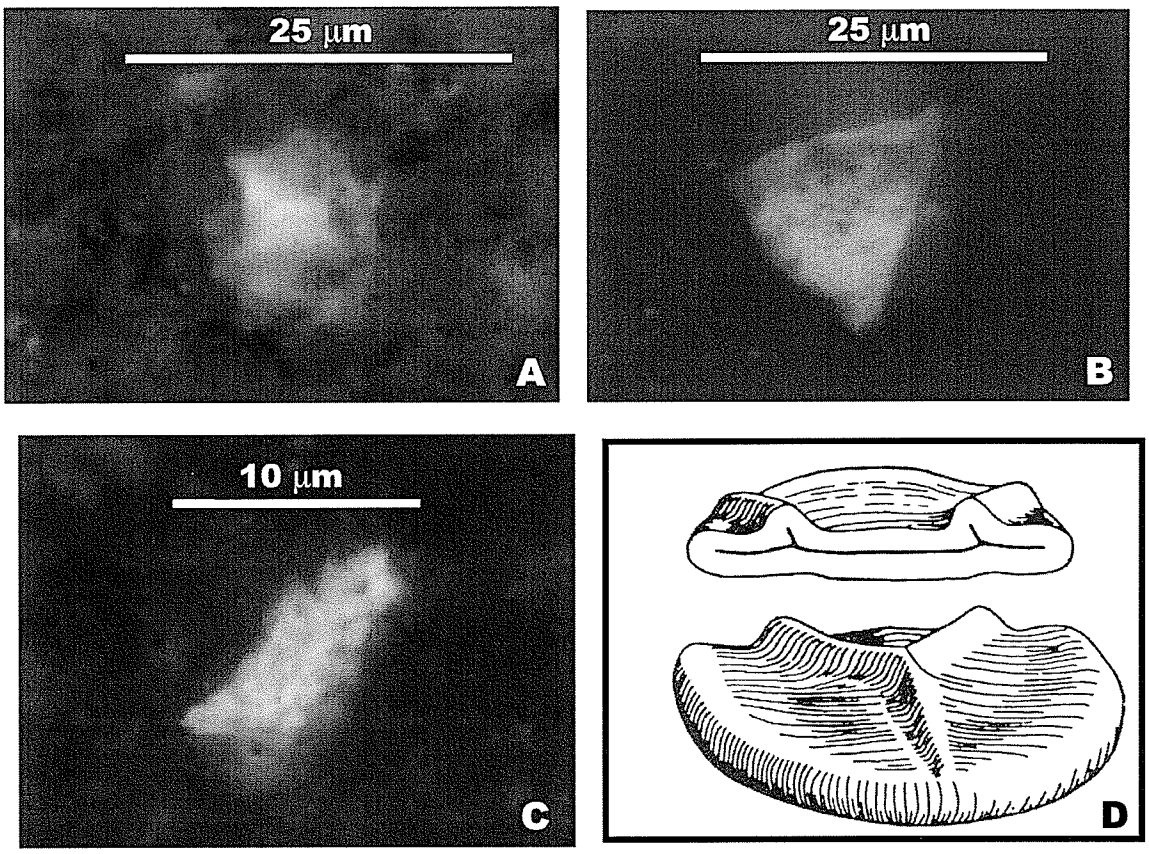

Figure 6.4 Photomicrographs of acritarchs and sporinites taken using fluorescent incident light microscopy and water-immersion objectives. A) Acanthomorphic acritarch from the MRL in the Rainbow Sub-basin. 6-32-109-8 W6M, 1994 m (6542') depth. B) *Veryachium*-like acanthomorphic acritarch from the MRL in the Rainbow Sub-basin. 4-9-109-8 W6M, 1985 m (6511.75') depth. C) Sporinite exhibiting bumpy surface ornamentation from the LRL in the Rainbow Sub-basin 4-9-109-8 W6M, 2009 m (6591') depth. D) Schematic drawing of a collapsed trilete spore with the trilete mark visible on the upper surface (after Stach *et al.*, 1982).

Some spores/pollen are morphologically distinctive due to preserved "infrasculpture" which refers to inward directed folds and structures visible inside the spore/pollen cell walls (Stach *et al.*, 1982) or surface monolete, alete, or trilete markings (Taylor *et al.*, 1998). Trilete spores have surface Y-shaped scars (Fig. 6.4D), and are the most basic spores and the first to appear in the fossil record in the early Silurian (Traverse, 1988). Other spore types appear later than trilete spores in the fossil record and were probably derived from trilete spores.

6.2.3 Other Macerals

Bituminite is a liptinite maceral that has weak brownish to no fluorescence, lacks characteristic shape or structure, and occurs as lenses and streaks in the matrix (Taylor *et al.*, 1998). Bituminite is likely derived from bacterial decomposition of algae and other OM. Micrinite is a finely granular inertinite group maceral that represents the solid carbon residues that remain when petroleum generation releases liquid hydrocarbons from bituminite and other liptinite macerals (Taylor *et al.*, 1998).

6.3 Organic Facies

Jones and Demaison (1982) formally defined an organic facies (OF) as "a mappable subdivision of a designated stratigraphic unit distinguished from the adjacent subdivisions on the basis of the character of its organic constituents, without regard to the inorganic aspects of the sediment." Alginite and acritarch distribution in marine settings has been utilized by previous authors to identify OF and to interpret the proximity of paleodepositional environments to shoreline (Dorning, 1987; Tyson, 1987, 1993; Chow *et*

al., 1995a). The OF model based on maceral assemblages utilized in this study is based on the model of Stasiuk (1999) (Fig. 6.5), which is based in part on the work of Dorning (1987). This model can be applied to the Keg River Formation in the Rainbow, Zama, and La Crete sub-basins where phytoplankton precursors (alginite varieties) and sporinites are used to define OF. The OF model illustrates the distribution of phytoplankton and sporinites in surface waters from shoreline to basin under conditions of normal phytoplanktonic productivity (Chow *et al.*, 1995a). The distribution of these diagnostic macerals indicate changes in water depth, water agitation, and trophic conditions.

The most basinward maceral assemblage is OF A (Chow *et al.*, 1995a). It is dominated by small, relatively thin-walled Prasinophyte alginites with varying amounts of larger, thick-walled Prasinophytes, ranging from minor, but persistent, to abundant (Stasiuk, 1999). OF B represents depositional environments at intermediate depths and intermediate distances from a bank margin or shore setting. OF B is dominated by small, thin-walled Prasinophytes (similar to OF A), acanthomorphic acritarchs, and may include rare to very minor sporinites. OF C represents the shallowest depositional environments, proximal to bank margin or shoreline settings. This OF is characterized by those macerals found in OF B as well as persistent sporinites and coccoidal alginite colonies.

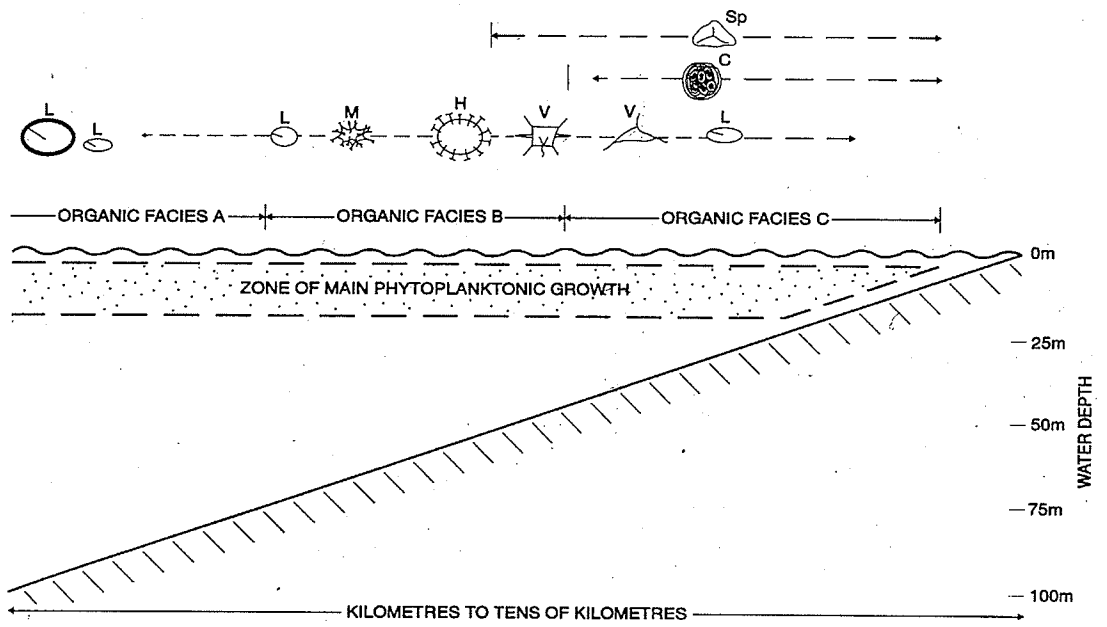

Figure 6.5 Maceral-based OF model for Devonian strata in the Western Canada Sedimentary Basin deposited during a phase of normal productivity (from Chow *et al.*, 1995a; Stasiuk, 1999). This model is based on recorded maceral abundance and position relative to the reef margin; the distribution is based in part on the work of Dorning (1987). OF A is defined by the most basinward maceral assemblage, OF B includes an "intermediate" maceral assemblage, and OF C is represented by a maceral assemblage which accumulated in the most proximal position. Maceral key: C – coccoidal alginite, H – *Hystrichosphaeridium*-like acritarchs, L – *Leiosphaeridia* alginite, M – *Micrhystridium*-like acritarch, V – *Veryachium*-like acritarcyh, Sp – terrestrial sporinites.

6.3.1 Algal Bloom Organic Facies

Organic petrology can also be used to identify periods of elevated phytoplanktonic productivity, i.e., algal blooms (Stasiuk, 1993; Chow *et al.*, 1995a; Clegg *et al.*, 1997; Stasiuk, 1999). Algal bloom conditions subject phytoplankton to a variety of environmental stresses including decreased light penetration due to the overabundance of phytoplankton in surface waters, photo-oxidation of algal cells caused by exposure to too much light when these cells are forced to the top of the algal bloom by overcrowding, and depletion of nutrient supply. During modern algal blooms, algal akinete cells form in response to unfavorable conditions and are important indicators of elevated phytoplanktonic productivity (Fritsch, 1959; Stasiuk, 1999). Large, thick-walled Prasinophytes may also develop in significant quantities during these periods of environmental stress (Fay, 1983; Lipps, 1993; Anderson, 1994). Therefore OF A with substantial amounts of large, thick-walled Prasinophyte alginite macerals could also indicate algal blooms rather than exclusively deposition in deeper water. Integration of sedimentology and organic petrology is crucial in this determination. Sedimentological evidence for shallow water deposition, combined with the identification of abundant large, thick-walled Prasinophytes using organic petrology could therefore support algal bloom activity.

6.4 Effects of Thermal Maturation

High thermal maturity in certain sedimentary basins poses challenges for organic petrological studies due to the effects of maturation on the petrographic properties of OM (Taylor *et al.*, 1998). Reflectance (% R_o), defined as "the proportion of perpendicularly

incident light which is reflected from a surface" increases with maturation (Taylor *et al.*, 1998). Therefore, measuring the reflectance of vitrinite macerals has become an accepted means of assessing the level of maturation in sedimentary OM. The Zama Sub-basin has a maturity on the order of 1% R_o vitrinite reflectance equivalent (%R_o V_E) (Fowler *et al.*, 2001) while the Rainbow Sub-basin has an even higher thermal maturity. Both sub-basins fall well within the catagenesis stage of thermal maturation (0.5% R_o to 2% R_o) (Hunt, 1996). Catagenesis occurs at temperatures ranging from 50°C to 150°C and pressures between 30 and 150 MPa (Tissot and Welte, 1984). Most oil windows ("the depth at which a petroleum source rock generates and expels most of its oil") occur between 60°C and 160°C within the catagenesis stage (Hunt, 1996). During catagenesis, kerogen is transformed into petroleum-range hydrocarbons by thermal degradation. Liquid hydrocarbons are produced first, followed by wet gas, condensates, and methane. The end of catagenesis occurs approximately at a vitrinite reflectance of 2.0% R_o after which point there is no further petroleum generation and only limited methane generation (Tissot and Welte, 1984).

Of all maceral groups, the liptinite group (i.e., sporinites and alginites) is the most sensitive to temperature increases and therefore, exhibits the most pronounced degradation as maturation progresses (Taylor *et al.*, 1998). The fluorescence intensity of liptinite macerals decreases and shifts from lower wavelengths (green and yellow) to higher wavelengths (red). At approximately 1.3% R_o when oil generation ends (oil death line), sporinite macerals typically cease fluorescing entirely or are converted to vitrinite and inertinite (secondary maceral groups). Alginites exhibit an even more pronounced

decrease in fluorescence intensity with increasing maturation than sporinites, losing all fluorescence at 0.9 to 1.0% R_o. A blue shift in fluorescene of alginites is sometimes observed once the oil window has been attained. This is due to the blue fluorescence of liquid hydrocarbons which can remain inside the alginite macerals subsequent to oil expulsion. If all hydrocarbons are expelled from the alginites, the fluorescence color shifts to red. Alginite color observed in thin sections changes from white to yellow, red and brown with maturation.

Elevated pressure and hydrocarbon expulsion during maturation results in flattening and size reduction of liptinite macerals. For example, large, thick-walled Prasinophyte alginites in the thermally mature Rainbow and Zama sub-basins rarely exceed 100 μm length and are flattened to as thin as 5 μm, whereas Prasinophytes described by Chow *et al.*, (1995a) in the thermally immature La Crete Sub-basin are much less flattened and are up to 350 μm long. Another problem encountered when examining thermally mature samples is that the number of alginites in any given volume of rock increases with increasing burial depth, thermal maturity, and oil expulsion from the alginites (concentration effect).

6.5 Organic Facies in This Study

Samples from organic-rich laminite units in the Rainbow, Zama, and Meander sub-basins were analyzed using organic petrological methods to determine maceral assemblages and to identifiy OF as described previously in Section 6.3 (Fig. 6.6A; Appendix F). In the Rainbow Sub-basin, samples from the LRL and MRL of the Lower Keg River Member

ramp, and from the URL of the Upper Keg River Member reef foreslope were examined. In the Zama Sub-basin, samples from the LZL in the Lower Keg River Member ramp and from the UZL in the Upper Keg River Member reef foreslope and off-reef were examined. In the Meander Sub-basin, only the LML from the base of the Lower Keg River Member was examined.

Maceral assemblages were determined qualitatively by determining the abundance of each diagnostic maceral (dominant, minor, rare, trace, or absent). Each sample was assigned a primary OF based on the dominant maceral assemblage and a number of samples were assigned a secondary OF which takes into account maceral assemblages present in the samples that are different from the predominant or primary OF. It is important to appreciate the discrepancies in size between the data sets for the Rainbow, Zama, and Meander sub-basins in this study (Fig. 6.6B). Fifty-seven samples were analyzed from the Rainbow Sub-basin. In contrast, only 7 samples from the Zama Sub-basin, and only 2 samples from the Meander Sub-basin were analyzed. The Zama and Meander sub-basins are underrepresented in the sample suite and require more thorough sampling.

6.5.1 Lower Rainbow Laminite (LRL)

The predominant OF in samples from the LRL is OF B (65% of samples) and a significant number of samples (35%) exhibit dominant OF B and secondary OF C (Fig. 6.6A). Total organic carbon (TOC) ranges from 0.1 to 5.0% with a mean of 1.9%.

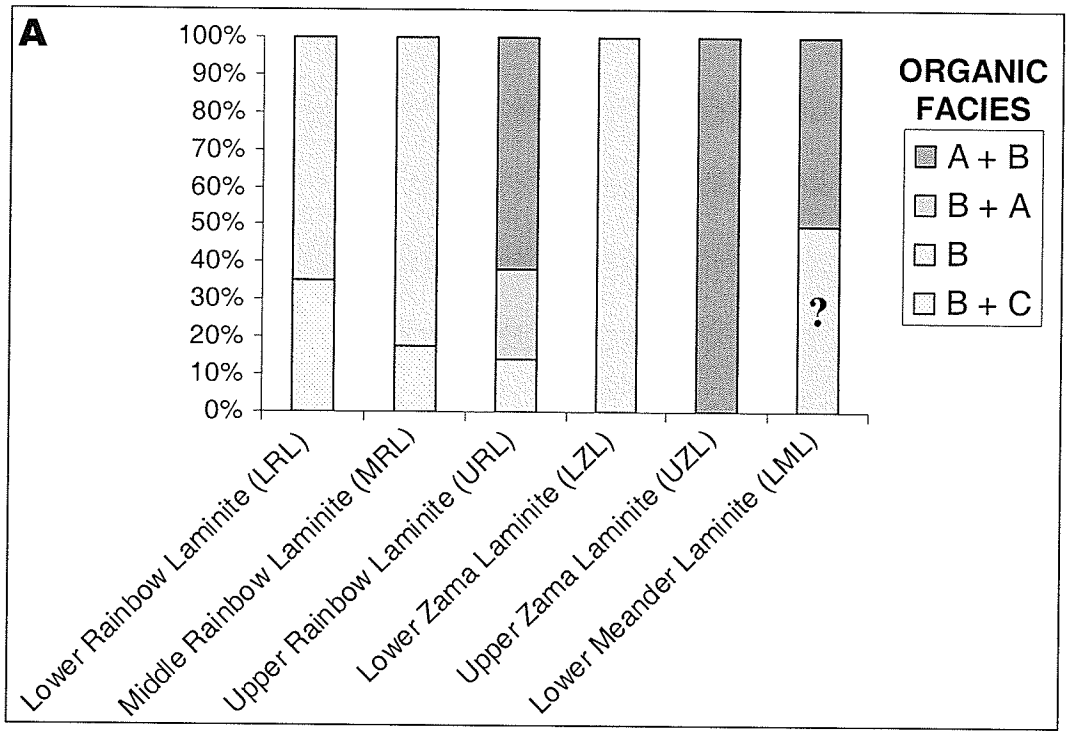

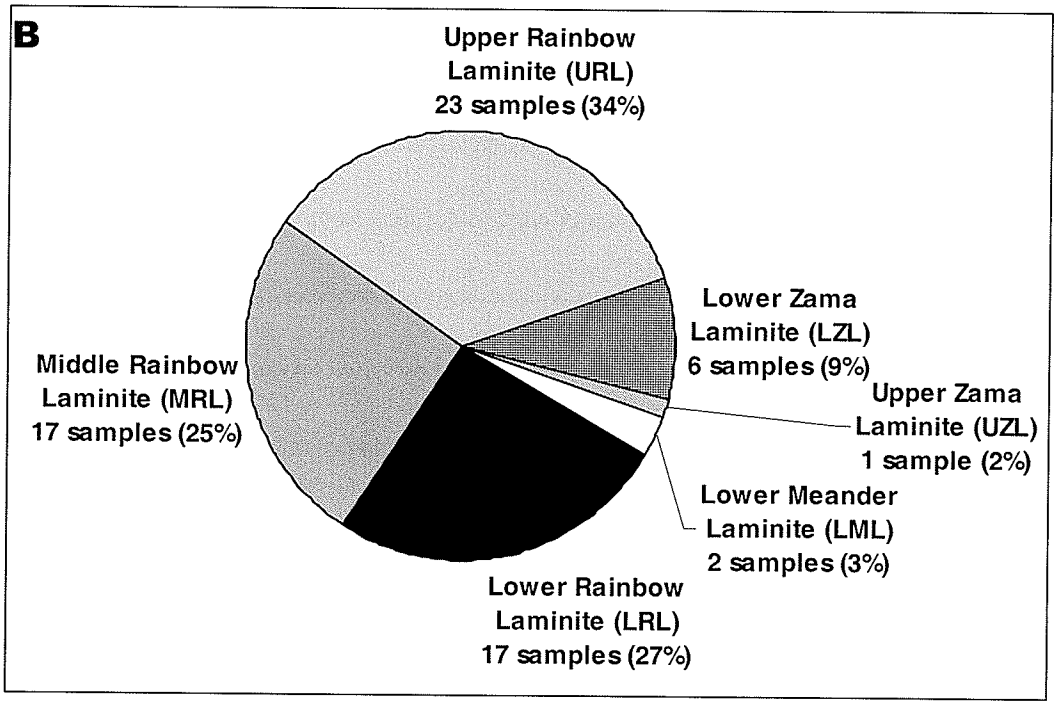

Figure 6.6 A) Percentage of each OF identified in samples of each laminite of the Rainbow, Zama, and Meander sub-basins. B) Distribution of samples analyzed using organic petrology categorized by the sub-basin and laminite unit that was sampled. Note that a large proportion of samples were derived from the Rainbow Sub-basin whereas the Zama and Meander sub-basins have low representation.

The dominant macerals are all indicative of OF B, representing depositional environments at intermediate distances from a bank margin or shore setting and intermediate water depths. The most abundant macerals are small, thin-walled Prasinophyte alginites ranging from 5 to 50 μm in length and only up to 5 μm in thickness when viewed perpendicular to bedding (Fig. 6.7A and E). Distinct cell walls are not visible in these very compacted and degraded macerals. Prasinophyte fluorescence is limited to brown-orange to dull yellow fluorescence indicating relatively high maturity. Some Prasinophytes with greenish fluorescence perhaps contain hydrocarbon liquids (which fluoresce blue). Acanthomorphic acritarchs in the LRL range from trace abundance in some samples to significant/dominant abundance in other samples. Acritarchs are highly compacted and degraded, range from 5 to 15 μm in length, and exhibit only dull to moderate yellow fluorescence making their identification problematic and potentially leading to underestimation of acritarch abundance in some samples (Fig. 6.7C). A large amount of fluorescing OM in the LRL is composed of liptodetrinite, a maceral made up of finely detrital liptinite maceral fragments which are not diagnostic of any particular OF. Liptodetrinite is derived from degradation of many macerals including alginite, sporinite, cutinite, and resinite, although identification of component macerals is impeded by the very small size of liptodetrinite fragments (Taylor *et al.*, 1998). Based on the similarity of fluorescence properties of liptodetrinite to those of alginite macerals in the Keg River Formation, it is probably mainly derived from Prasinophytes and acritarchs.

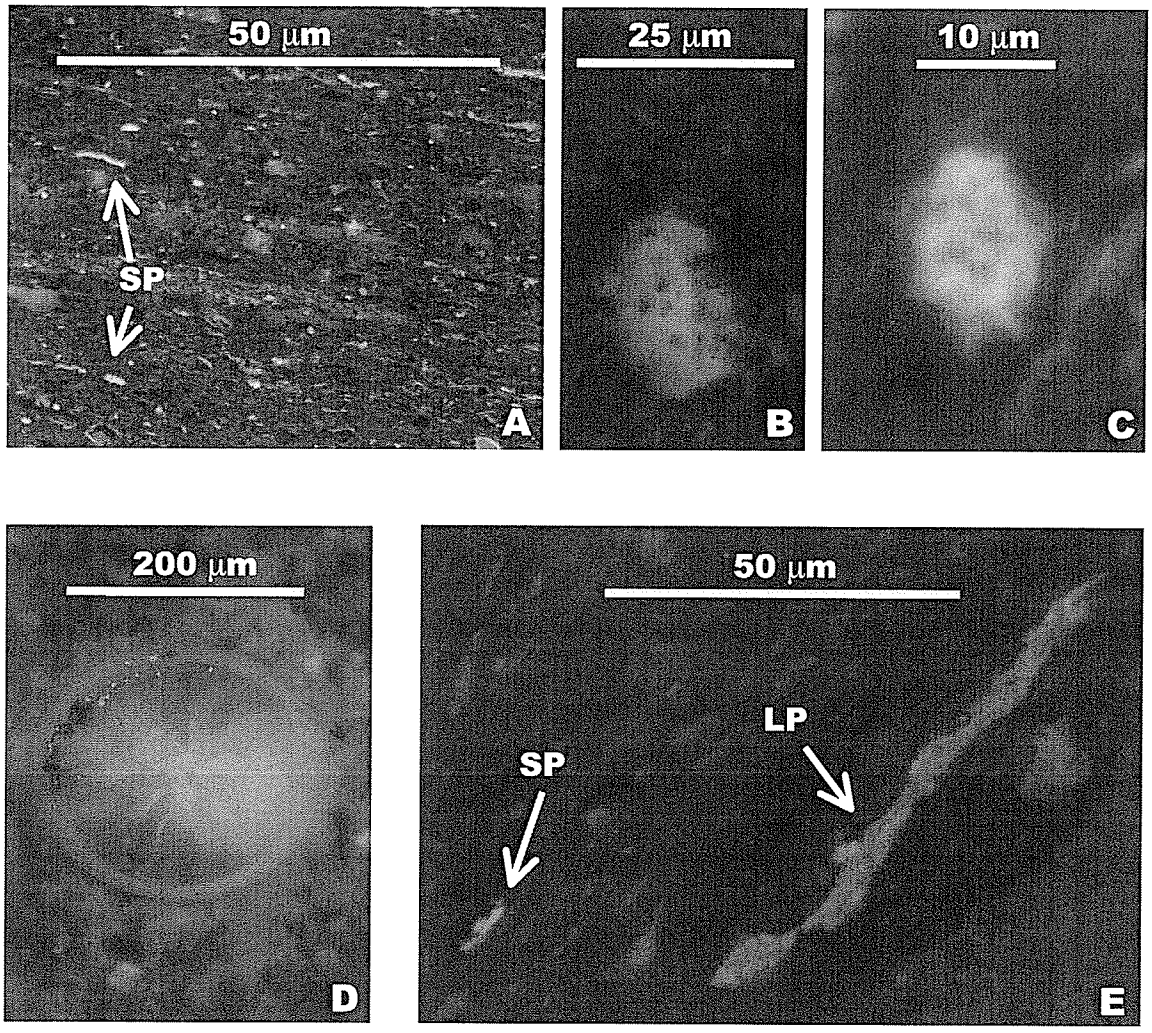

Figure 6.7 Photomicrographs from the lower Rainbow laminite (LRL) taken using fluorescence microscopy and water-immersion objectives. A) Typical appearance of the LRL showing abundant small Prasinophytes (SP) from 4-9-109-8 W6M, 2009.7 m (6593.6') depth. B) Coccoidal alginite from 6-32-107-9 W6M, 2086.7 m (6843.3') depth. C) Acanthomorphic acritarch from 4-9-109-8 W6M, 2009.7 m (6593.6') depth. D) Cross-sectional view of a styliolinid test from 6-32-107-9 W6M, 2087.7 m (6849.5') depth. E) Large, thick-walled Prasinophyte (LP) from 6-32-107-9 W6M, 2118.9 m (6951.9') depth. A small Prasinophyte (SP) is also visible on the left side of this photomicrograph.

OF C macerals, including *Veryachium*-like acritarchs, sporinites, and coccoidal alginites, were identified in low abundances in 35% of samples collected from the LRL indicating a secondary OF C. *Veryachium*-like acritarchs were identified in two samples based on roughly triangular morphology and the presence of spiny processes extending from each of the three points. Sporinites are present in only trace amounts and range from 10 to 20 μm in length. They have varied surface ornamentation, and exhibit fluorescence properties similar to those of the small Prasinophyte macerals. Trace amounts of coccoidal alginites were identified in some samples based on the recognition of cup-like structures representing individual cells within a colonial structure (Fig. 6.7B). Coccoidal alginite colonies range from 10 to 25 μm in diameter and fluoresce dull yellow to bluish-green. Bluish-fluorescing coccoidal alginites may have been impregnated with blue-fluorescing hydrocarbon liquids. Large thick-walled Prasinophytes are absent or occur in only trace amounts in the LRL discounting the possibility of algal blooms (OF A) during deposition of the laminite (Fig. 6.7E). The presence of secondary OF C may represent minor perturbations in the depositional environment (i.e., relative sea level changes) during which shallower water conditions developed or may represent macerals transported to an intermediate-depth depositional environment from areas more proximal to a bank margin or shoreline. Transported OF C macerals should exhibit oxidation features, such as red shift in the fluorescence relative to OF B macerals (pers. comm. L. Stasiuk, 2002). Such evidence was not observed indicating that relative sea level falls of short duration are a more likely explanation for secondary OF C. Other macerals in the LRL include abundant bituminite and minor to abundant micrinite. Neither bituminite nor micrinite can be used as criteria for defining OF.

6.5.2 Middle Rainbow Laminite (MRL)

The MRL is predominantly OF B (~82% of samples) but also has secondary OF C in ~18% of the samples which is comparable to the OF observed in the LRL (Fig. 6.6). TOC values for this laminite range from 0.3% to 3.3% (mean of 1%), which are slightly lower on average than those of the LRL.

Small, thin-walled Prasinophytes are typically the dominant maceral in the MRL although these macerals are only minor constituents in some samples (Fig. 6.8B). Large thick-walled Prasinophytes were absent or occurred in only trace amounts in most samples (Fig. 6.8A). Acanthomorphic acritarchs are also important macerals, ranging from minor abundance to dominant (Fig. 6.8C and D). The presence of both small Prasinophytes and acanthomorphic acritarchs indicates OF B. Sporinites and coccoidal alginites are present in trace to minor amounts in some (~18%) of the samples collected, indicating secondary OF C (Fig. 6.8E and F). Bituminite and micrinite are also present in the MRL. As in the LRL, OF B in the MRL indicates that deposition occurred primarily in intermediate depths and intermediate distances from a bank margin or shoreline setting, although evidence of secondary OF C suggests short temporal excursions to shallower water depositional environments (i.e., drop in relative sea level).

6.5.3 Upper Rainbow Laminite (URL)

The primary OF of the URL is OF A with secondary OF B (~48% of samples; Fig. 6.6). Fourteen percent of samples show primary OF B with secondary OF A constituents,

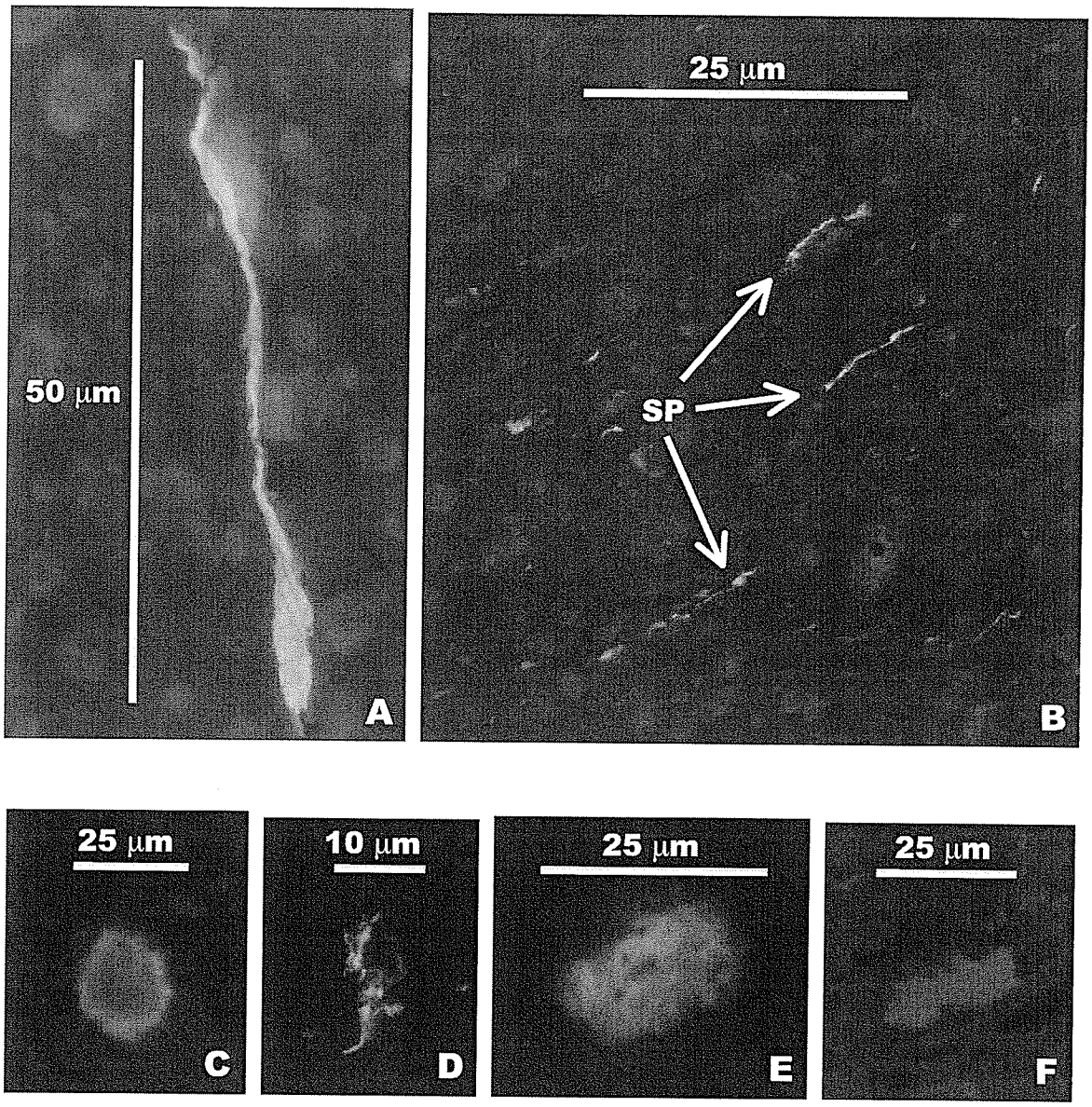

Figure 6.8 Photomicrographs of macerals from the middle Rainbow laminite (MRL) taken using fluorescence microscopy and water-immersion objectives. A) Large Prasinophyte from 4-16-108-7 W6M, 2003 m (6572') depth. B) Small Prasinophytes (SP) from 4-16-108-7 W6M, 2001.6 m (6567') depth. C and D) Acanthomorphic acritarchs from 4-16-108-7 W6M, 2017.8 m (6620.3') depth. E) Coccoidal alginite from 12-33-109-8 W6M, 2017.9 m (6620.3') depth. F) Dull yellow-brown fluorescing sporinite from 6-32-107-9 W6M, 2077.3 m (6816.4') depth.

~24% of samples show OF B only, and ~14% show OF A only. TOC values range from 1.0 to 8.6% (mean of 2.7%), somewhat higher than for the LRL and MRL.

A predominance of large, thick-walled Prasinophyte alginites indicates OF A. They range from 50 to 400 μm long and 5 to 30 μm thick when viewed perpendicular to bedding (Fig. 6.9A and D). These macerals are commonly folded over on themselves due to compaction and exhibit flattening and elongation parallel to bedding. Thick (up to 5 μm) cell walls are readily visible. Fluorescence of the large Prasinophytes ranges from dull yellow to bluish-green (attributed to absorbed or non-expelled hydrocarbon liquids within the alginites). OF B is indicated in the URL by abundant to dominant small, thin-walled Prasinophytes, trace to minor acanthamorphic acritarchs (Fig. 6.9B), *Veryachium*-like acritarchs (Fig. 6.9C), and trace sporinites. These macerals have the same physical characteristics as those observed in the LRL and MRL. No coccoidal alginites were observed in the URL but bituminite and micrinite are abundant in the matrix of this unit.

In samples where large Prasinophytes are less abundant than small Prasinophytes (Fig. 6.9D), primary OF B with secondary OF A is interpreted and in samples containing only trace amounts of large Prasinophytes, only OF B is inferred.

A significant trend has been identified in reef foreslope samples from the URL. All samples consistently exhibit some contribution of OF A macerals (large, thick-walled Prasinophytes). Of the 16 samples collected from positions where foreslope sediments are relatively thick (indicating closer proximity to the reef core), 3 samples were

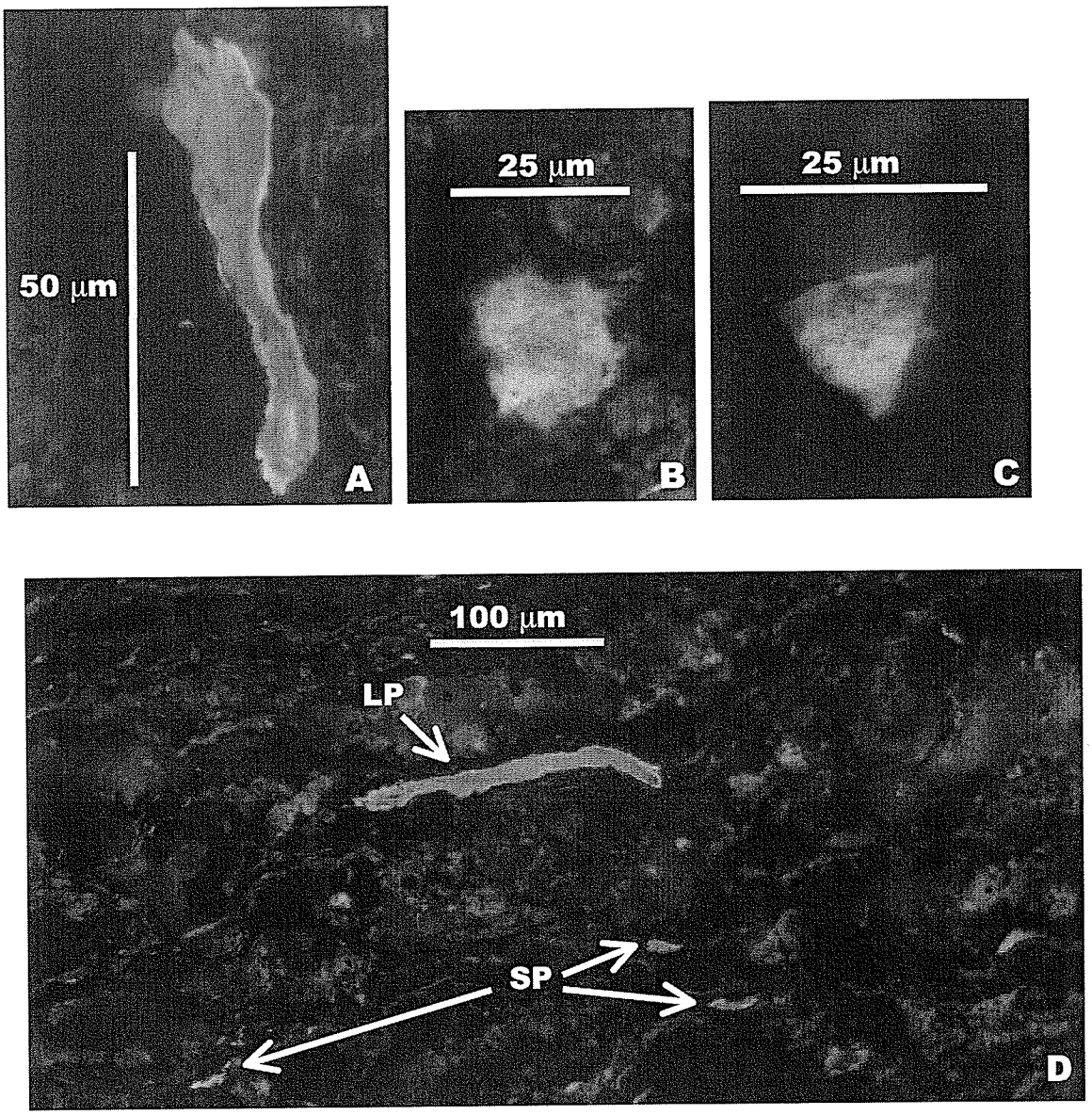

Figure 6.9 Photomicrographs of macerals from the upper Rainbow laminite (URL) taken using fluorescence microscopy and water-immersion objectives. A) Large, thick-walled Prasinophyte from 6-32-109-8 W6M, 1994 m (6542') depth. B) Acanthomorphic acritarch from 4-9-109-8 W6M, 1984.7 m (6511.5') depth. C) *Veryachium*-like acritarch from 4-9-109-8 W6M, 1984.8 m (6511.75') depth. D) Large (LP) and small Prasinophytes (SP) from 12-33-109-8 W6M, 1980.9 m (6499') depth.

identified as OF A only, 10 samples have primary OF A with secondary OF B and 3 samples have primary OF B with secondary OF A. However, the 5 samples collected from positions where foreslope sediments were relatively thin (indicating distal, toe-of-slope deposits) consistently exhibited only trace to minor amounts of OF A macerals. Three samples showed only trace amounts of large, thick-walled Prasinophytes and were therefore interpreted as OF B only, and 2 samples contained only minor amounts of large, thick-walled Prasinophytes (primary OF B and secondary OF A). The persistence of OF A in the URL, combined with sedimentological evidence for deposition in a relatively shallow water-depth (refer to Section 3.7), suggests that high phytoplanktonic productivity (algal blooms) rather than water-depth was primarily responsible for the dominance of large, thick-walled Prasinophytes.

6.5.4 Lower Zama Laminite (LZL)

OF B dominates all samples from the LZL (Fig. 6.6). This unit has relatively high TOC values ranging from 3.0% to 9.6% (mean 6.4%). Small thin-walled Prasinophytes (Fig. 6.10A) are the dominant macerals in all samples of the LZL. In individual samples they vary from rare to abundant. Acanthomorphic acritarchs (Fig. 6.10B) are rare to minor in abundance and sporinites are absent or occur in only trace amounts. Trace coccoidal alginites were observed in only two samples, and therefore may have been transported into this unit from shallower or more nearshore environments although oxidation features were not observed. Bituminite and micrinite are abundant within the matrix.

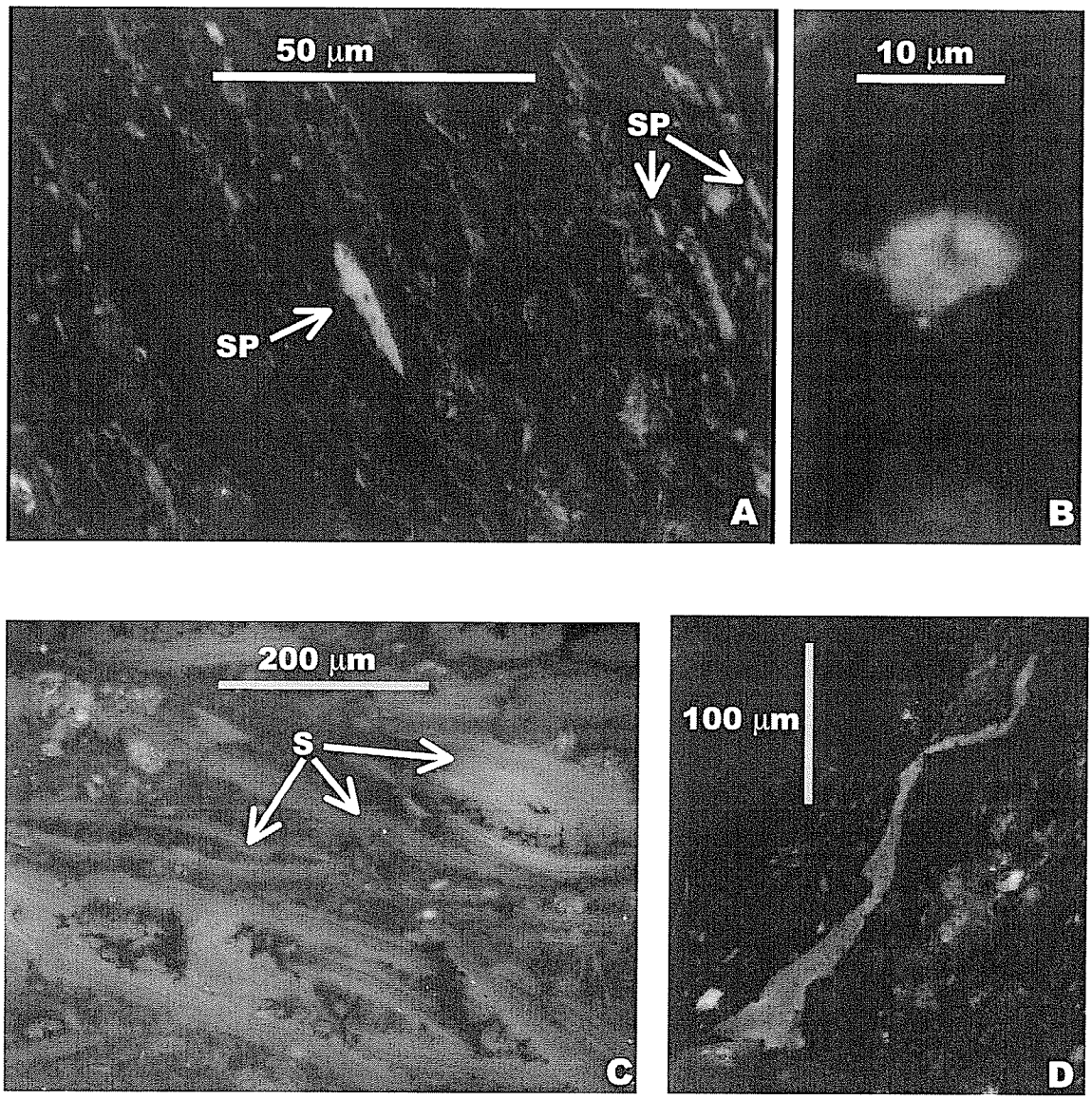

Figure 6.10 Photomicrographs from the lower Zama laminite (LZL) taken using fluorescence microscopy and water-immersion objectives. A) Abundant small Prasinophytes (SP) from 5-36-117-6 W6M, 1684.5 m (5526.5') depth. B) Acanthomorphic acritarch from 4-19-116-4 W6M, 1570.9 m (5154') depth. C) Abundant fragmented styliolinid tests (S) from 5-36-117-6 W6M, 1684.5 m (5526.5') depth. D) Large Prasinophyte from 5-36-117-6 W6M, 1680.2 m (5512.5') depth.

Large, thick-walled Prasinophytes are present in trace amounts in all but one of the samples collected from the LZL (Fig. 6.10D). Sedimentological evidence from examination of the most organic-rich portions of the LZL (i.e., lithofacies A) indicates deposition in a low-energy, deep-subtidal environment below storm wave-base, characterized by pervasive dysoxic to anoxic conditions (refer to Section 3.2). Both the organic petrology and sedimentology suggest that the OF A maceral assemblages in the organic-rich portions of the LZL accumulated in a basinward depositional environment characterized by deep water, a considerable distance from a bank margin or shoreline setting, and a low degree of water agitation. Further evidence for this depositional setting is the low faunal diversity and a predominance of cricoconarids which can indicate restricted conditions due to dysoxic or anoxic bottom waters (Fig. 6.10C).

6.5.5 Upper Zama Laminite (UZL)

OF A with secondary OF B was observed in the single sample collected from the UZL from the 4-19-116-4 W6M well at a depth of 1527.5 m (5011.5'). The TOC value for this sample is 1.5%. The sample contains abundant Prasinophytes, both the small, thin-walled, and large, thick-walled varieties (Fig. 6.11A and B), as well as rare acanthomorphic acritarchs (Fig. 6.11C). No coccoidal alginites nor sporinites are present in this unit. Pyrite spheres, 5 to 10 μm diameter, occur in this unit, commonly grouped in chains parallel to laminae (Fig. 6.3C and D). These pyrite spheres have very similar morphology to algal akinetes (Fig. 6.3A and B) and, therefore, are hypothesized to be pyritized algal akinete cells.

As in the URL, the presence of OF A in the most organic-rich parts of the UZL (i.e., lithofacies F) combined with sedimentological support for deposition in a relatively shallow water setting (refer to Section 3.7) suggests that high phytoplanktonic productivity (algal blooms) rather than water-depth was responsible for the dominance of large, thick-walled Prasinophytes.

6.5.6 Lower Meander Laminite (LML)

Only two samples were examined from the LML. The first sample collected from the 7-7-113-21 W5M well at a depth of 1403 m (4603') corresponds to OF A with secondary OF B and has predominantly large Prasinophytes. The TOC value is 13.8%. The second sample, collected from the 7-7-113-21 W5M well at a depth of 1397.5 m (4585'), has a TOC value of 1%, and has only OF B macerals, containing only trace large Prasinophytes. However, because fewer macerals in total were identified in this relatively organic-poor sample, trace amounts of large Prasinophytes may be sufficient to indicate an OF A signature for this sample also. Micrinite and bituminite are abundant in the matrix of both of these samples. Large, thick-walled Prasinophytes are 25-100 μm long and 25 μm thick with pronounced, thickened cell walls and yellow to blue-green fluorescence (perhaps indicating absorption or incomplete expulsion of hydrocarbon liquids) (Fig. 6.12A and C). They are typically less flattened and more ovoid than other large Prasinophytes observed in the Zama or Rainbow sub-basins. This morphology difference may be due to filling of Prasinophytes cells by phosphatic nodules which resisted compaction (pers. comm. L. Stasiuk, 2000), early cementation or some other process which protected the Prasinophytes from compaction.

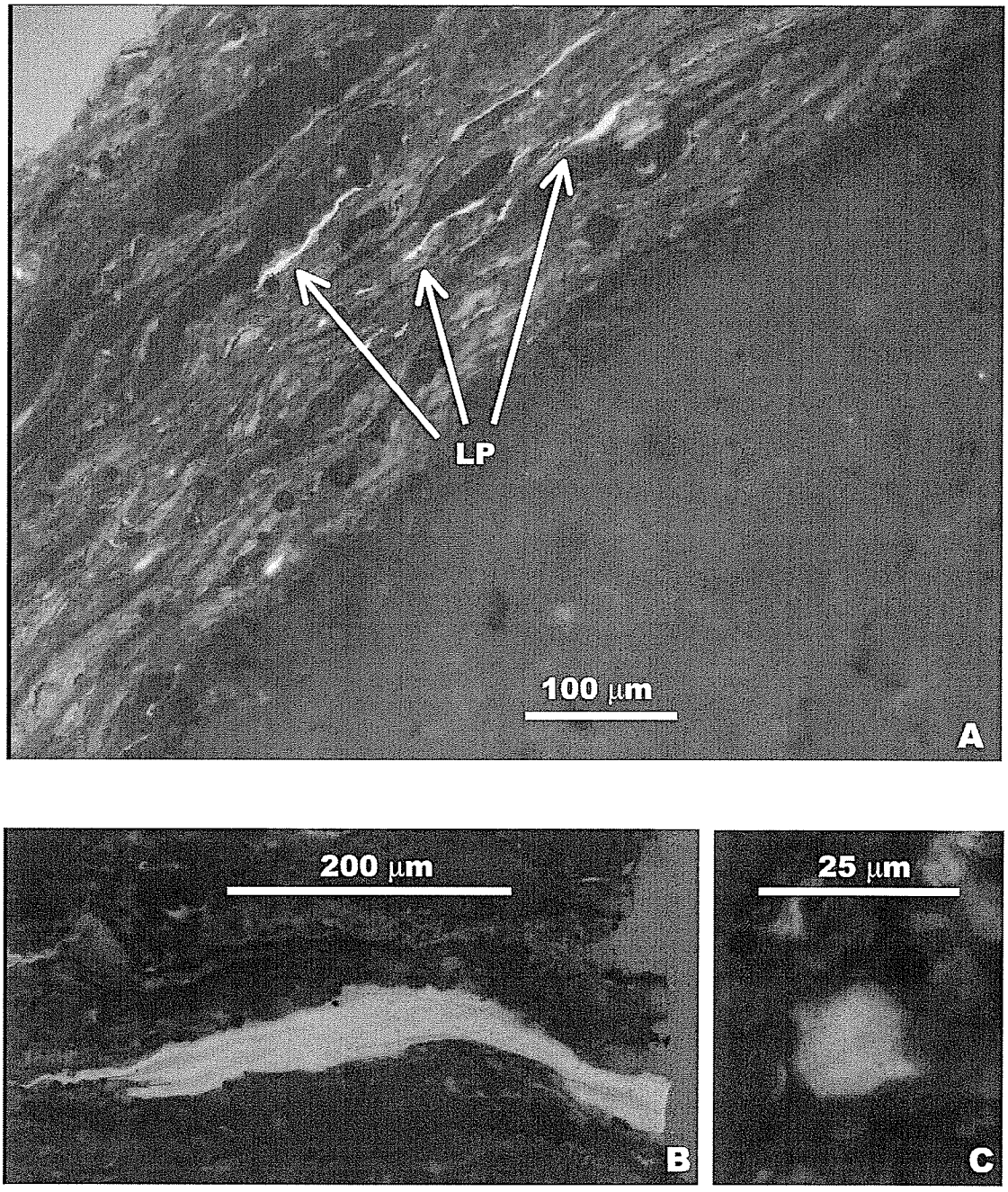

Figure 6.11 Photomicrographs of macerals from the upper Zama laminite (UZL) taken using fluorescence microscopy and water-immersion objectives. A) Abundant large Prasinophytes. B) Detailed photomicrograph of a large Prasinophyte. C) Acanthomorphic acritarch. All photomicrographs from 4-19-116-4 W6M, 1527.5 m (5011.5') depth.

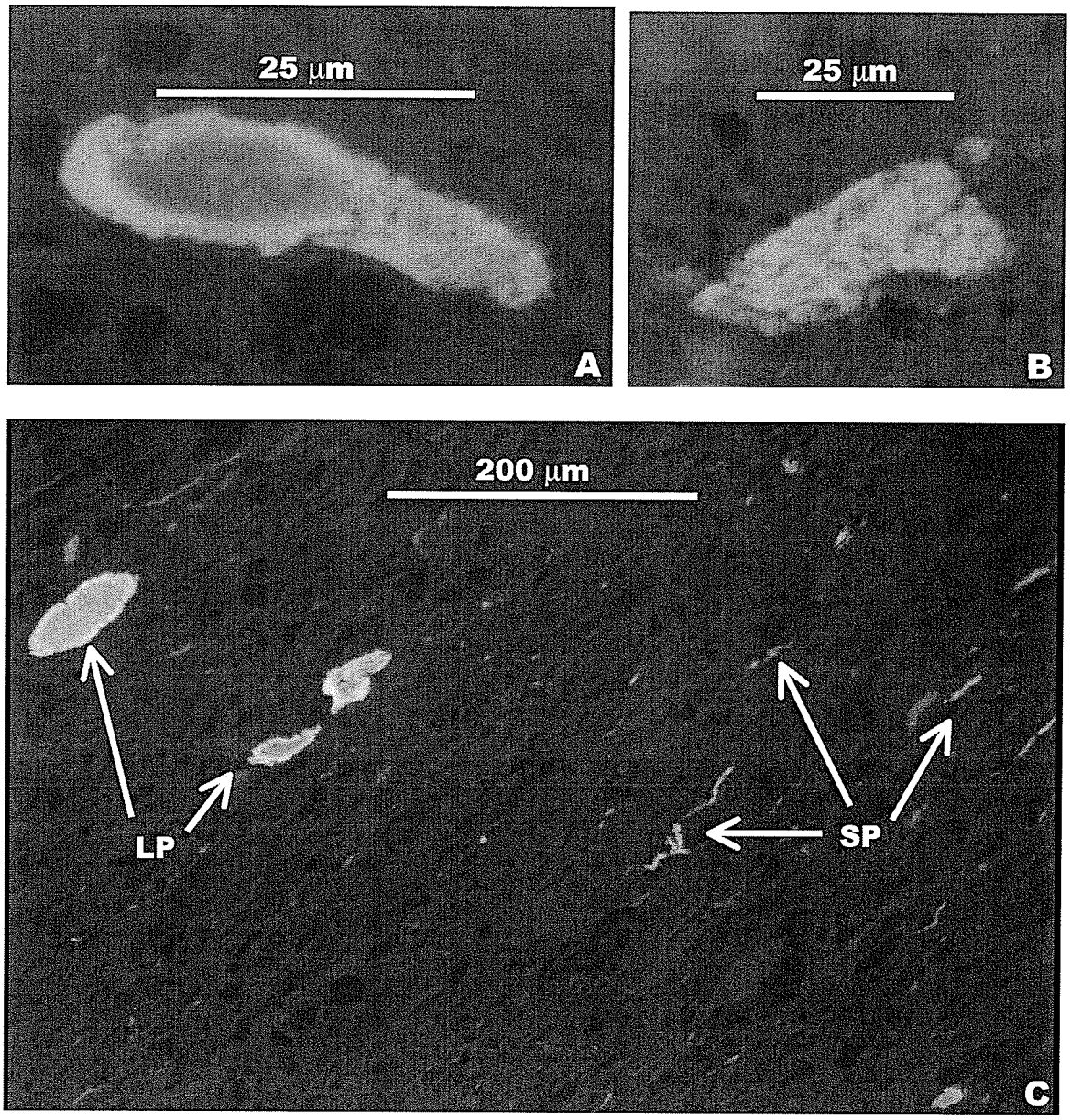

Figure 6.12 Photomicrographs of macerals from the lower Meander laminite (LML) taken using fluorescence microscopy and water-immersion objectives. A) Large, thick-walled, *Tasmanites* Prasinophyte exhibiting punctate cell walls. B) Coccoidal alginite. C) Large (LP) and small Prasinophytes (SP). All photomicrographs from 7-7-113-21 W5M, 1403 m (4603') depth.

Small, thin-walled Prasinophytes alginites are relatively abundant in both samples indicating OF B (Fig. 6.12C). Acanthomorphic acritarchs, coccoidal alginites (Fig. 6.12B), and sporinites are present in trace amounts only in the 1403 m sample (exhibiting OF A with secondary OF B) which is probably due to the comparatively low amount of OM in this sample as discussed previously.

CHAPTER 7: ORGANIC GEOCHEMISTRY

7.1 Introduction

Organic geochemistry involving Rock-Eval pyrolysis was used to quantify the petroleum potential and to help assess the origin of organic-rich laminites in the Rainbow and Zama sub-basins. A total of 74 samples were analyzed using Rock-Eval6 pyrolysis at the Organic Geochemistry Lab at the Geological Survey of Canada in Calgary (Appendix G).

7.2 Kerogen Types

Kerogen is classified into four main types based on organic geochemistry (Tissot *et al.*, 1974). Type I, II, III, and IV kerogen are defined based on hydrogen/carbon (H/C) and oxygen/carbon (O/C) ratios from elemental analysis or from the hydrogen index (HI) and oxygen index (OI) from Rock-Eval pyrolysis. Each kerogen type is composed of different maceral components derived from OM deposited in different depositional environments, and produces hydrocarbons of varying compositions (Brooks, 1981; Killops and Killops, 1993). Type I (liptinite-type) kerogen, derived from algal material, is highly oil-prone and exhibits high hydrogen and low oxygen contents. It typically accumulates in organic-rich muds deposited in anoxic, low-energy, shallow lagoons or lakes and is relatively rare in the geologic record. Type II (exinite-type) kerogen is oil-prone and derived from a variety of organic precursors including zooplankton, phytoplankton, bacterial OM, as well as spores, pollen, cuticles, resins, and waxes from higher plants. This relatively high carbon and low oxygen content kerogen accumulates primarily in marine environments and is the most common kerogen type. Type III

(vitrinite-type) kerogen is carbon-enriched with low hydrogen content, low oxygen content and it is gas-prone. Type III kerogen is formed predominantly from OM derived from vascular plants, and therefore has a terrestrial, rather than aquatic, origin. Hydrocarbon generation from type III kerogen is typically poor. Type IV (inertinite-type) kerogen has high carbon content, low oxygen and hydrogen content, and no potential to produce oil or gas. Type IV kerogen is derived from altered (i.e., oxidized) higher plant matter or from oxidized OM of any origin (marine or terrestrial). For a more thorough discussion of kerogen types refer to Brooks (1981), Tissot and Welte (1984), Killops and Killops (1993), Taylor *et al.* (1998), and Stasiuk (1999).

7.3 Results of Rock-Eval Pyrolysis

Rock-Eval pyrolysis is a method by which powdered samples are gradually heated in the absence of oxygen to yield organic compounds (Peters, 1986). It provides rapid determination of kerogen type, kerogen evolution, and hydrocarbon source potential of samples (Tissot, 1984). A more detailed description of this technique and explanation of data parameters are provided in Appendix E.3.

Of the 81 samples collected for the purpose of organic petrology, 74 were analyzed using Rock Eval pyrolysis. The samples that were not analyzed were cuttings, and therefore lacked sufficient material for pyrolysis. Forty-eight samples produced results that were judged reliable for the purposes of graphic representation. The other 26 samples were not plotted graphically for one or more of the following reasons: 1) low TOC values ($\leq$ 0.5%); 2) low S1 values ($<$ 0.2%) where S1 represents any free hydrocarbons in the rock

present at the time of deposition or generated from the kerogen since deposition; 3) low production index (PI) values (< 0.1) suggesting immature samples; 4) temperature of maximum liberation of hydrocarbons (T_{max}) < 435°C suggesting thermal immaturity, and 5) anomalously high TOC values (>10%) due to contamination by secondary bitumen constituents (Appendix G).

Excluding anomalous samples, 1 sample from the Meander Sub-basin, 3 samples from the Zama Sub-basin, and 43 samples from the Rainbow Sub-basin were considered (Fig. 7.1). The sample from the Meander Sub-basin was derived from the UML. In the Zama Sub-basin, all three samples were derived from the LZL. In the Rainbow Sub-basin 18 samples were derived from the LRL, 11 samples were from the MRL, and 14 were from the URL. The most reliable geochemical interpretations are obtained from large data sets. Peters (1986) suggested one sample at every 30-60 ft (9-18 m) of depth in a well for best results. Therefore, no reliable results were obtained by Rock-Eval pyrolysis for the Upper laminite units in the Zama or Meander Sub-basins. The results of the Rock-Eval pyrolysis are provided in Appendix G.

7.3.1 HI versus OI plots

Data were plotted on hydrogen index/oxygen index (HI/OI) graphs, "pseudo-Van Krevelin plots", for each of the laminites (LRL, MRL, URL, LZL, and UML) in order to determine kerogen types (Fig. 7.2) (Peters, 1986). Kerogen types are indicated on the HI/OI plot by maturation lines labelled I, II, and III. Moving to the left and down any one

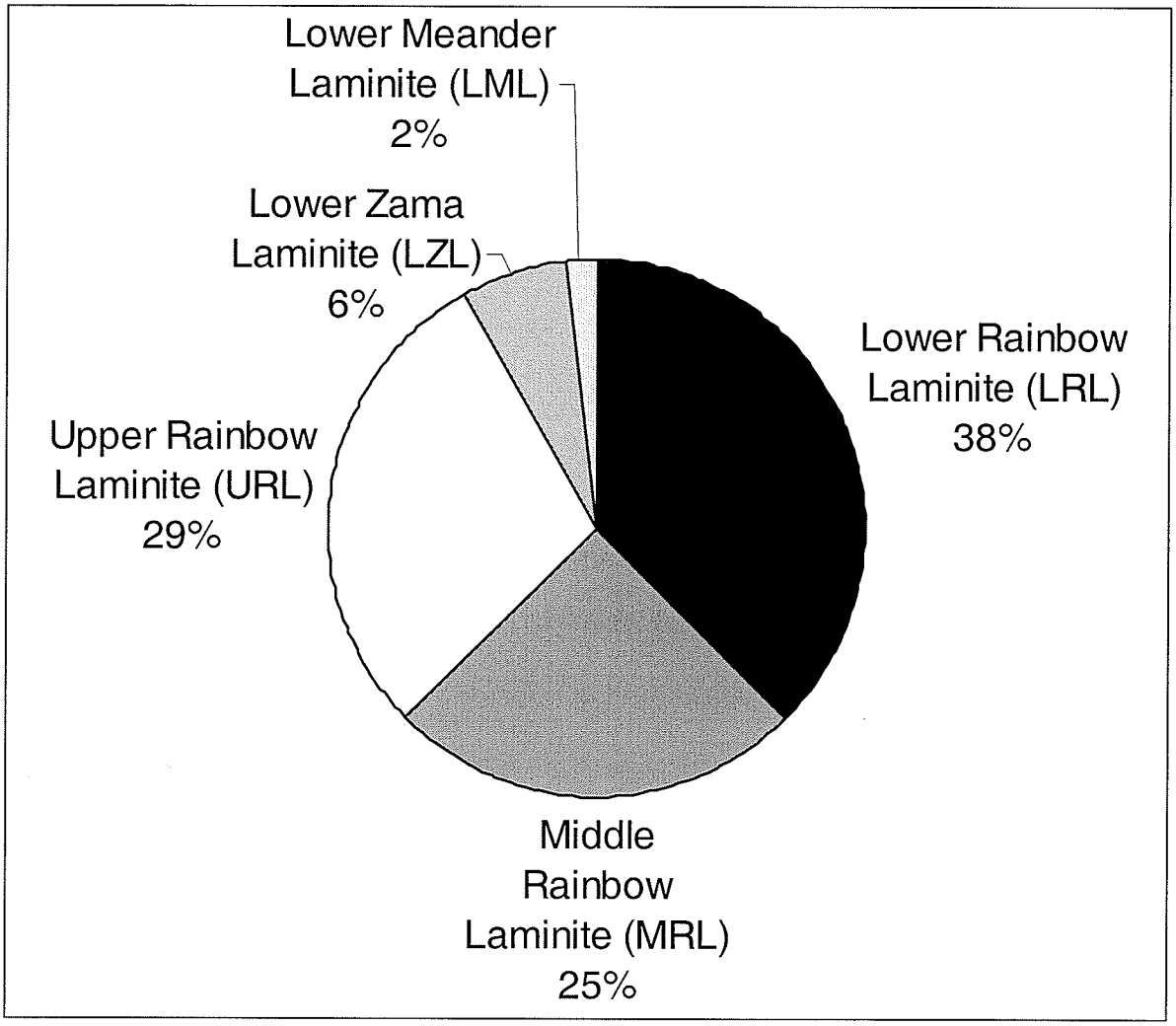

Figure 7.1 Distribution of samples analyzed by Rock-Eval pyrolysis according to the laminite sampled. Note that 92% of the samples analyzed by Rock-Eval pyrolysis were from the Rainbow Sub-basin and that only 6% and 2% of samples came from the Zama and Meander sub-basins respectively.

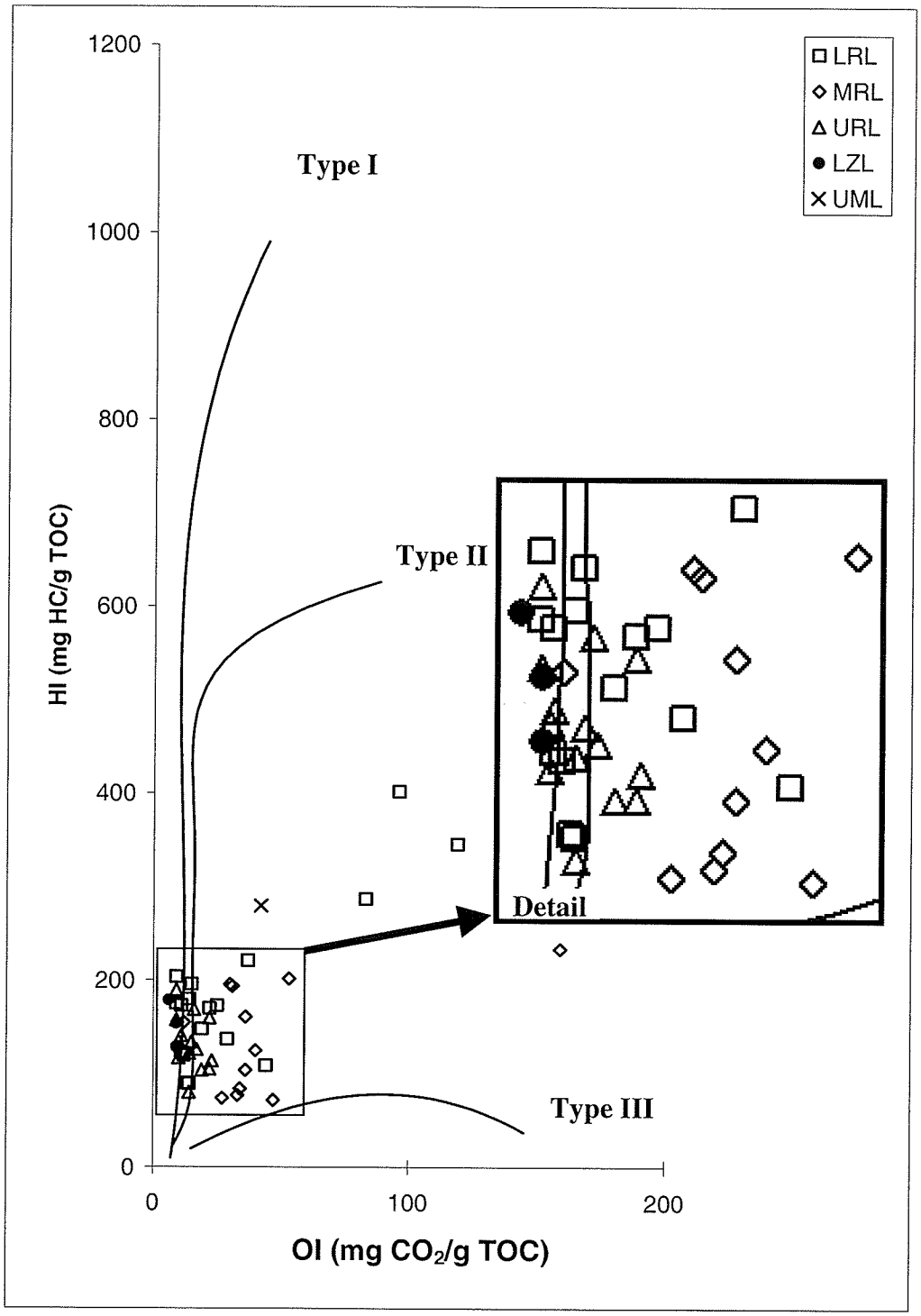

Figure 7.2 HI vs. OI for samples from the study area. Lines labeled Types I, II, and III kerogen are from Peters (1986).

of these idealized maturation lines indicates increasing maturation along the evolutionary pathway for each type of kerogen (Hunt, 1996). The vast majority of samples in this study, regardless of the laminite from which they were collected, cluster very tightly near the origin of the HI/OI plot indicating high thermal maturity. Samples predominantly fall between kerogen type II (marine, oil-prone) and type III (terrestrial, gas-prone). Kerogen type III can also be formed due to the oxidation of marine type II OM in shallow water, near bank margins or shoreline settings, during deposition and early diagenesis (pers. comm. L. Stasiuk, 2003). Organic petrology did not indicate significant amounts of terrestrial OM in any of the organic-rich laminites. Therefore, type III kerogen is probably the result of oxidation of marine OM, and not terrestrial OM. Samples from the URL and the LZL cluster closer to the kerogen type II maturation pathway than samples from the LRL, MRL, and UML, perhaps indicating that marine OM was more subject to oxidation during deposition of the LRL, MRL, and UML. This distribution may be artificial due to very limited data from the Zama Sub-basin. If more data were available, samples from this sub-basin may display the same distribution of data between type II and type III kerogen as seen in other laminites with more representative sampling.

7.3.2 HI versus T_{max} plots

Data were plotted on a hydrogen index/maximum temperature (HI/T_{max}) plot for each of the laminites (LRL, MRL, URL, LZL, and UML) (Fig. 7.3). Kerogen types are indicated on the HI/T_{max} plot by maturation pathways labelled I, II, and III, corresponding to kerogen type. However, kerogen type determinations are better indicated by the HI/OI

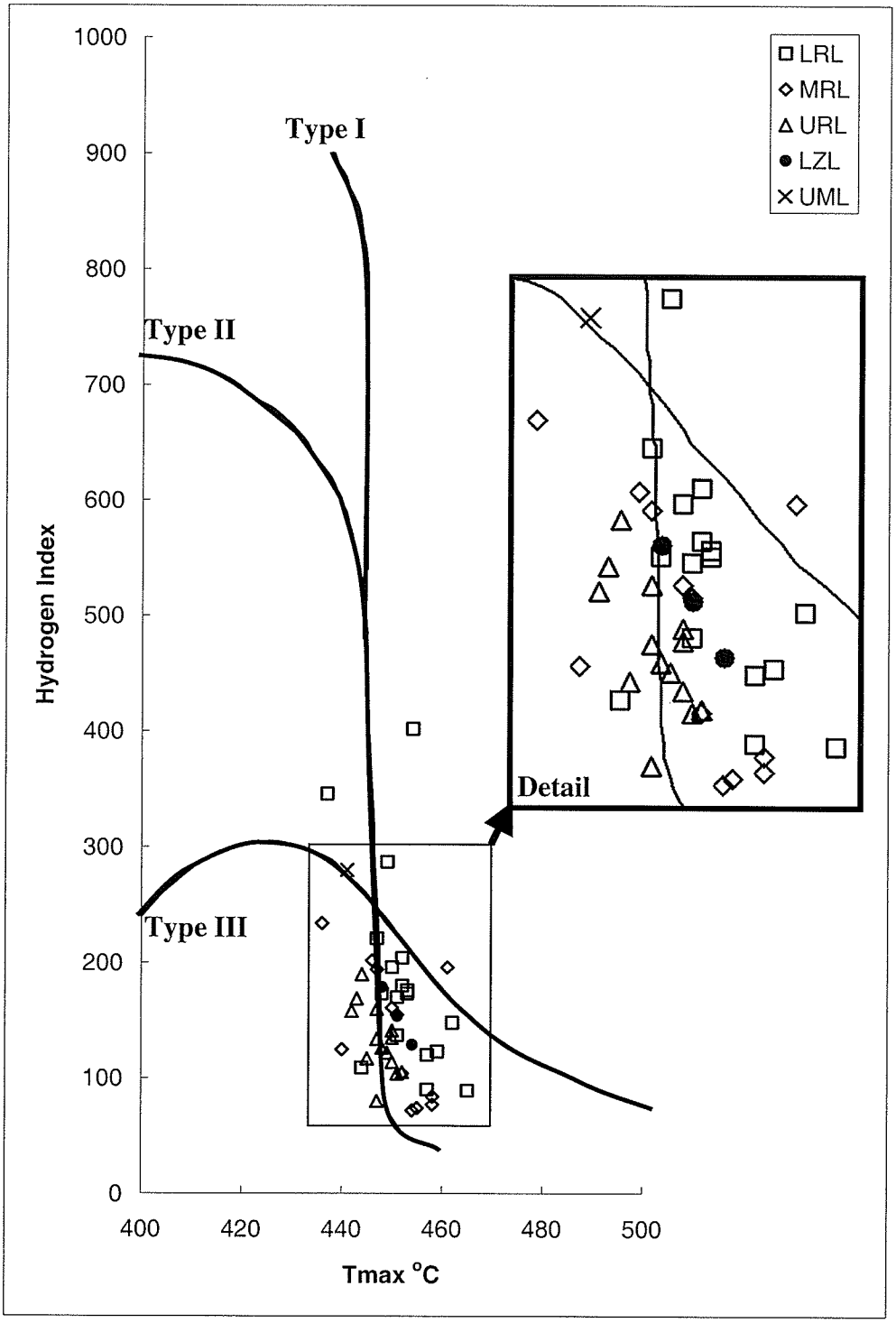

Figure 7.3 HI vs. T_{max} plot of samples from the study area. Lines indicating Types I, II, and III kerogen are from Peters (1986).

plot than by the HI/T_{max} plot (Peters, 1986). Moving to the right and down any one of the maturation pathways indicates increasing maturation. All samples once again plot relatively far down the maturation pathway indicating high thermal maturity.

The HI/T_{max} plot exhibits the same predominance of type II and III kerogen as observed in the HI/OI plot. As discussed previously, samples that plot close to the kerogen type III maturation pathway probably represent oxidized marine OM rather than terrestrial OM.

CHAPTER 8: DISCUSSION

8.1 Introduction

Stratigraphy, sedimentology, organic petrology, and organic geochemistry are integrated in this study to aid in the assessment of the paleoenvironment and paleoecology in the Rainbow and Zama sub-basins during late Middle Devonian times. A key aspect of this work is evaluation of the primary controls (productivity versus preservation) on accumulation of organic-rich laminites in the Rainbow and Zama sub-basins. Secondary controls are also considered and they include 1) bulk sedimentation rate, 2) supply of terrestrial OM, and 3) sediment texture and mineralogy. The findings are summarized in Table 8.1. The organic-rich laminites in the Lower Keg River Member in the Rainbow and Zama sub-basins are compared to coeval units in the La Crete Sub-basin and the Williston Basin to provide a regional perspective on source rock accumulation.

An impetus for understanding the controls on OM accumulation and preservation is the potential for better prediction of source rock distribution through geologic time. Parrish (1982) postulated that the distribution of Paleozoic source beds closely corresponds to the distribution of predicted upwelling zones. This model can be evaluated by using organic petrology to examine the relationships between high productivity, upwelling, and reef growth.

This study also has interesting implications for understanding Devonian reef growth, particularly related to the nutrient levels that stromatoporoid reefs could tolerate. In

Table 8.1 Summary of the interpreted controls on OM accumulation and preservation in the Rainbow and Zama sub-basins as determined by stratigraphy, sedimentology, organic petrology, and organic geochemistry. "Primary" indicates a primary control, "secondary" indicates a secondary control, and "minor" or "very minor" indicate less predominant influences on OM accumulation and preservation. "N/A" indicates that the factor in question had no positive influence on OM accumulation and preservation.

	Rainbow Sub-basin				**Zama Sub-basin**	
	LRL	**MRL**	**URL (off-reef)**	**URL (foreslope)**	**LZL**	**UZL (foreslope)**
Preservation (Anoxia)	primary	primary	primary	secondary	primary	secondary
Productivity	N/A	N/A	secondary	primary	N/A	primary
Sedimentation Rate	minor	minor	minor	N/A (dilution)	minor	N/A (dilution)
Supply of Terrestrial OM	N/A	N/A	N/A	N/A	N/A	N/A
Sediment Texture and Mineralogy	minor	minor	minor	very minor	minor	very minor

recent years the debate has been between those researchers who believe that Devonian reefs existed in low nutrient environments similar to modern coral reefs and those who believe that stromatoporoid reefs could tolerate higher nutrient conditions than modern reefs (e.g., Hallock and Schlager, 1986; Wood, 1993, 1995; Kiessling *et al.*, 1999). Evidence from this study suggests that Devonian stromatoporoid reefs may have been able to tolerate episodic high nutrient conditions.

8.2 Preservation vs. Productivity in the Rainbow and Zama Sub-basins

8.2.1 Controls on LRL, MRL, and LZL: Anoxia

Based on the integration of sedimentology and organic petrology, the organic-rich beds in the LRL and MRL in the Rainbow Sub-basin and in the LZL in the Zama Sub-basin are interpreted to have accumulated primarily in response to bottom-water anoxia. The most organic-rich lithofacies (A: bituminous laminite) of the LRL, MRL, and LZL is part of the outer ramp lithofacies association (refer to Section 3.11.1). These laminites are interpreted to have been deposited during relative sea level rises that initiated third-order shallowing-upward cycles R2, R3, and Z2 (refer to Sections 4.6 and 4.7). The base of cycles R3 and Z2 represent the deepening event responsible for basin differentiation that created the Rainbow and Zama sub-basins (refer to Section 4.5). The predominance of OF B and lack of bloom indicators in the LRL, MRL, and LZL (refer to Sections 6.5.1, 6.5.2, and 6.5.4) supports an interpretation of OM accumulation and preservation being primarily due to depth-related anoxia.

During LRL deposition in the Rainbow area anoxia could have developed in response to depth and/or restricted vertical mixing. Sedimentological evidence suggests depth was probably sufficient for anoxia to develop on the outer ramp (refer to Section 3.11.1). Anoxia may also have developed in response to barriers around the Rainbow-Zama region that restricted vertical mixing. The Peace River Arch formed a barrier to the south, the Precambrian Shield formed the eastern barrier, the Tathlina High bounded the region to the north, and the Western Alberta Ridge formed the western boundary that isolated the Rainbow-Zama area from the main Elk Point Embayment (Fig. 1.2) (Bassett and Stout, 1967).

Anoxia attributed to depth and/or restricted vertical mixing could also explain deposition of the MRL and LZL in the Rainbow and Zama areas. Initiation of basin differentiation and associated relative sea level rise may have created sufficient topography within the sub-basins to create deep water conditions and/or sluggish circulation that could have led to the development of anoxic waters.

8.2.2 Controls on Distal Reef Foreslope URL: Anoxia

The most organic-rich beds in the URL (lithofacies F: bituminous peloidal laminite) in distal reef foreslope and off-reef positions in the Rainbow Sub-basin are also interpreted to have accumulated primarily in response to anoxia. The URL is coeval with reef growth during cycle R3. Reefs in the Rainbow Sub-basin have a maximum thickness of 230 m (Campbell, 1992), suggesting that the URL in off-reef positions may have been deposited in water up to a maximum of ~230 m deep. Anoxia is able to develop much

shallower in the water column than this. For example, modern Lake Kivu, part of the East African rift-lake system, is 500 m deep and entirely anoxic below ~60 m (Degens *et al.*, 1973).

Although true off-reef samples were not available for examination, a number of wells in the Rainbow Sub-basin have a relatively thin Upper Keg River Member interpreted as distal reef foreslope deposits. Two cuttings samples from the URL in the 4-16-108-7 W6M well (1975 - 1978 m, 6480 - 6490' depth and 1978 - 1981 m, 6490 - 6500' depth), where the Upper Keg River Member is only 57 m thick, were assessed and found to contain dominant OF B (non-bloom) macerals, along with only rare to minor amounts of OF A (bloom) macerals. Similarly, of the three cuttings samples analyzed from the 4-30-110-9 W6M well (1917 - 1920 m, 6290 - 6300' depth; 1923 - 1926 m, 6310 - 6320' depth; and 1926 - 1929 m, 6320 - 6330' depth) where the Upper Keg River Member is only 68 m thick, two samples contain minor OF B macerals and only trace OF A macerals, and one sample has minor OF B macerals and rare OF A macerals. The interpretation of this OF signature is that the large volume of OM in the URL was preserved due to depth-related anoxia in the relatively deep off-reef and distal reef foreslope positions. Oxygenation due to storm activity and sediment gravity flows would not occur as frequently in these distal positions as it would in more proximal reef foreslope positions. Episodic algal blooms occurred but were overwhelmed by the "anoxia" signature in off-reef and distal reef foreslope positions.

8.2.3 Controls on Proximal Reef Foreslope URL and UZL: Productivity

Accumulation of OM in the URL in proximal reef foreslope positions (characterized by relatively thick, ≥80 m, Upper Keg River Member deposits) is primarily attributed to anomalously high phytoplanktonic productivity. Anoxia is interpreted to be of only secondary importance. OF A (bloom) macerals are predominant and OF B (non-bloom) macerals comprise only a secondary signature. OM in the only UZL sample assessed contains dominant OF A macerals and abundant OF B macerals. This anomalously high abundance of OF A macerals suggests phytoplankton blooms were the primary control on OM accumulation. The abundance of OF B macerals, in the UZL suggests that anoxia may also have influenced accumulation and preservation of OM.

In the Rainbow and Zama sub-basins, the URL and UZL are comprised of lithofacies F (bituminous peloidal laminite) interbedded with lithofacies G (massive peloidal-skeletal dolopackstone to dolograinstone) and H (stromatoporoid-coral dolofloatstone to dolorudstone). Based on stratigraphic and sedimentological evidence, lithofacies G and H are interpreted to have been deposited in fully oxygenated, moderate energy conditions, above storm wave-base (3.8.2, and 3.9.2). The organic-rich lithofacies F is interpreted in the same way aside from evidence that suggests episodic dysoxic to anoxic conditions developed during its deposition (Section 3.7.2). Algal blooms are the most likely cause of episodic anoxia during the deposition of organic-rich beds in the URL and UZL because high phytoplanktonic productivity can produce anoxic conditions due to increased respiration rates and high OM flux to the sea floor (Sections 3.7.2 and 5.3.2) (Chow *et al.*, 1995a). Therefore, episodic anoxia induced by algal blooms is interpreted

as a secondary control on OM accumulation and preservation in organic-rich beds in both the URL and UZL.

Modern algal blooms can develop in response to a number of factors including 1) increases in nutrient supply, 2) warm temperatures, 3) salinity increases, 4) intermittent, high intensity light, 5) relatively low turbidity, and 6) water-column stratification (refer to Section 5.2.2). For the URL and UZL, triggering mechanisms for algal blooms are difficult to ascertain. However, increased nutrient supply may have occurred in the Rainbow and Zama sub-basins due to coastal upwelling or open-ocean divergence upwelling (refer to Section 5.3.1). Locations of modern coastal upwelling correlate to sites of elevated primary productivity (Parrish, 1982), and Golonka *et al.*, (1994) modeled favorable conditions for coastal upwelling near the Rainbow and Zama sub-basins during the Givetian. Although modern divergences are unfavorable settings for organic-rich sediment accumulation, in Devonian intracratonic seas and more local sub-basins, divergence could have triggered algal blooms (Parrish, 1982). OM created during algal blooms in the Rainbow and Zama sub-basins would have had better preservation potential than OM produced at modern open-ocean divergences because of shallower water, higher sedimentation rate, and the increased likelihood that the oxygen minimum layer would have impinged on the sediment-water interface (cf. Parrish, 1982).

Terrestrial input is another possible source of nutrients. The early stages of tree evolution occurred during the late Middle Devonian (Givetian) (Flanagan, 1995). As root-bearing plants initially spread into dry, upland areas previously devoid of plants, they would have

chemically and physically broken up the land surface making it susceptible to weathering and erosion (Flanagan, 1995). This would have facilitated the movement of large quantities of soil and dissolved nutrients from land into adjacent marine environments which, in turn, may have triggered algal blooms.

The UZL sample assessed in this study from the 4-19-116-4 W6M well (1527.5 m, 5011.5' depth) was taken from just below the contact (~1.5 m) with the overlying Muskeg Formation. Since the Muskeg Formation was deposited in an evaporitic basin, is hypothesized that increased salinity may have triggered the algal blooms contributing to the formation of the UZL.

Low turbidity and water-column stratification can probably be discounted as triggering mechanisms for algal blooms in the study area due to sedimentological evidence that suggests that the URL and UZL were deposited in a well oxygenated, moderate-energy, open marine environment between storm wave-base and fairweather wave-base. This depositional environment, which was frequently affected by storm events, storm-triggered sediment gravity flows, and active bioturbation and scavenging would probably have been characterized by relatively high turbidity and vertical mixing.

8.3 Sedimentation Rate in the Rainbow and Zama Sub-basins

Sedimentation rates for the LRL, MRL, and LZL are postulated to have been relatively low based on their interpretation as outer ramp deposits. Einsele (2000) estimated a sedimentation rate of ~20 cm/ka for carbonate shelves, ~10cm/ka for black shale settings,

and ~5 cm/ka for pelagic carbonate environments. Tyson (2001) determined that bulk sedimentation rates of <20 cm/ka exert a positive influence on OM preservation and that clastic dilution effects are not significant at these relatively low sedimentation rates. Therefore, abundant OM present in the LRL, MRL, and LZL may be attributed in part to bulk sedimentation rates that increased burial efficiency, decreased residence time, and decreased benthic degradation loss of OM at the sediment-water interface.

The URL and UZL were deposited in reef foreslope and off-reef settings. It has been estimated that these types of depositional environments had relatively high bulk sedimentation rates, ranging up to 500 cm/ka or more in proximal reef foreslope positions (Einsele, 2000). Clastic dilution effects are significant at high sedimentation rates (>20cm/ka) and have a negative influence on the accumulation of OM (Tyson, 2001). Clastic dilution increases with bulk sedimentation rate, indicating that the effects should be most pronounced in the proximal reef foreslope and least pronounced in distal reef foreslope to off-reef positions. Pronounced clastic dilution effects were observed in the URL in proximal foreslope positions where sparse, organic-rich laminae were separated by relatively thick beds (1-5 cm) of organic-poor, peloidal-skeletal dolopackstone to dolograinstone. Clastic dilution effects were less pronounced but still apparent in distal foreslope positions where organic-poor beds were thinner and less abundant than in proximal reef foreslope deposits.

8.4 Supply of Terrestrial OM in the Rainbow and Zama Sub-basins

Minor amounts of terrestrial sediments were transported via rivers into the Elk Point Embayment and deposited in a narrow but extensive coastal plain around the Peace River Arch (Nelson, 1970). The Arch had very low relief, an arid climate, and little to no vegetation during the Middle Devonian. Rivers flowing over the Arch were probably dry for much of the year and carried little to no terrestrial OM. This interpretation is supported by the lack of significant type III (terrestrial) kerogen in organic-rich laminites of the Rainbow and Zama sub-basins (refer to Sections 6.5 and 7.3.1). Therefore, terrestrial OM can be eliminated as a significant source of OM in the Rainbow and Zama sub-basins.

8.5 Sediment Texture and Mineralogy in the Rainbow and Zama Sub-basins

Sediment texture and mineralogy are probably important factors affecting OM accumulation in the Rainbow and Zama sub-basins. The organic-rich sediments of the LRL, MRL, URL, LZL, and UZL contain both carbonate minerals and clay minerals providing sorption sites for OM (Müller and Suess, 1977; Keil *et al.*, 1993 *in* Arthur and Sageman, 1994). The organic-rich beds of the LRL, MRL, and LZL (lithofacies A) are characterized by very fine-grained (micritic and clay) components, which provide large surface areas for sorption of OM (refer to Section 3.2.1). The organic-rich beds of the URL and UZL (lithofacies F) are also characterized by somewhat fine-grained sediments although the matrix is mainly peloidal (refer to Section 3.7.1).

8.6 Summary of OM Accumulation and Preservation Controls in the Rainbow and Zama Sub-basins

Table 8.1 summarizes the interpreted controls on OM accumulation and preservation in the LRL, MRL, URL, LZL, and UZL of the Rainbow and Zama sub-basins.

(1) The primary control on accumulation and preservation of OM in the LRL and MRL of the Rainbow Sub-basin and in the LZL of the Zama Sub-basin is interpreted to be anoxia. Low sedimentation rate, sediment texture, and mineralogy may have acted as secondary controls.

(2) The primary control on OM accumulation in the URL and UZL in distal reef foreslope and off-reef positions is hypothesized to be anoxia, while primary productivity acts as only a subsidiary control.

(3) In proximal reef foreslope positions, the primary control on OM accumulation and preservation in the URL and UZL is interpreted to be primary productivity. High primary productivity probably created short-lived anoxic conditions which then acted as a secondary control on OM preservation.

8.7 Comparison to La Crete Sub-basin and Williston Basin

Organic-rich laminated deposits, similar to those observed in the Rainbow and Zama sub-basins, occur elsewhere in the Elk Point Embayment. The bituminous marker in the Lower Keg River Member in the La Crete Sub-basin (Chow *et al.*, 1995a), and the

Brightholme Member of the Winnipegosis Formation of the Williston Basin in Saskatchewan (Jin and Bergman, 1999, 2001) are explored in the context of their relationship to the organic-rich laminites examined in this study.

8.7.1 Bituminous Marker: Lower Keg River Member, La Crete Sub-basin

In the La Crete Sub-basin (Fig. 1.2), the Lower Keg River Member consists of two shoaling upwards successions, referred to as the lower ramp sequence and the upper ramp sequence (Chow *et al.*, 1995a). An organic-rich laminite, called the bituminous marker, occurs at the base of the upper ramp sequence. In the Rainbow Sub-basin the LRL also occurs at the base of the second (cycle R2) of two shallowing-upward cycles that comprise the Lower Keg River Member. This suggests a possible correlation between the LRL and the bituminous marker although further work is needed to support this correlation.

The bituminous marker is generally 1 m thick but ranges up to 5 m thick locally and has TOC values from 5.3 to 18.3% (Chow *et al.*, 1995a). It is composed of finely laminated, carbonate-rich and bituminous layers. The bituminous laminae contain abundant compacted cricoconarids and ostracods, as well as lenses and thin beds of cricoconarid-ostracod grainstone-packstone. The bituminous marker is known to extend throughout the La Crete Sub-basin based on recognition of a characteristic "shale spike" on gamma ray–sonic or neutron petrophysical logs (Corrigan, 1975; Chow *et al.*, 1995a).

Organic petrology of the bituminous marker indicates a dominant "bloom" OF (similar to OF A of this study) containing abundant large, thick-walled Prasinophyte alginites and persistent algal akinete cells in organic-rich laminae (Chow *et al.*, 1995). OM in the bituminous marker is interpreted to have accumulated primarily in response to elevated phytoplanktonic productivity in surface waters. As a result of such algal blooms, anoxic bottom-waters developed in response to high respiration rates and high OM flux to the seafloor. Very low sedimentation rate was a secondary control. In contrast, OM in the LRL in the Rainbow Sub-basin is interpreted to have accumulated in response to anoxia as the primary control. This may suggest that specific paleoecological conditions, such as algal blooms, could have been confined locally to sub-basins due to physical barriers or environmental differences between adjacent sub-basins.

8.7.2 Brightholme Member: Winnipegosis Formation, Southern Saskatchewan

The Upper Elk Point Subgroup in the Williston Basin in southern Saskatchewan is very similar to stratigraphically equivalent strata in the Rainbow, Zama, and La Crete sub-basins. The Winnipegosis Formation forms an extensive carbonate platform around the southern extent of the Elk Point Embayment (Campbell, 1992). The Lower Winnipegosis Member is composed of open-marine carbonate ramp deposits equivalent to the Lower Keg River Member in the Rainbow, Zama, and La Crete sub-basins. Isolated banks and reefs in the Upper Winnipegosis Member developed in basinal areas of the southern region of the Elk Point Embayment and are equivalent to Upper Keg River Member reefs and banks in the Rainbow, Zama, and La Crete sub-basins (Martindale and MacDonald, 1989; Campbell, 1992). The Brightholme Member is a laminated, bituminous carbonate

unit that occurs in off-reef positions between Upper Winnipegosis reefs (Campbell, 1992; Jin and Bergman, 1999, 2001). Osadetz *et al.*, (1990) established that the Brightholme Member is one of the source rocks for oil produced from Winnipegosis reefs in southeastern Saskatchewan. Deposition of the Brightholme Member preferentially occurred where the Lower Winnipegosis carbonate ramp was relatively thin, suggesting that OM accumulation was in response to local development of anoxic conditions in parts of the basin (Campbell, 1992). The Brightholme Member interfingers with reef-derived deposits providing evidence that it was deposited coevally with the Upper Winnipegosis Member (Jin and Bergman, 1999, 2001). In the Rainbow and Zama sub-basins, the URL and UZL were deposited coevally with Upper Keg River Member reef. Therefore, it is postulated that the Brightholme Member may be statigraphically equivalent to the URL and UZL. However, further work is needed to assess this correlation.

OM in the Brightholme Member is dominated by an OF indicative of algal blooms which is nearly identical to that in the Lower Keg River Member laminites in the La Crete Sub-basin (Fowler *et al.*, 2001). The URL and UZL also contain algal bloom OF (refer to Section 8.2). The Brightholme Member, URL, and UZL provide evidence of at least episodic, high phytoplankton productivity coeval with reef growth during the Middle Devonian.

8.8 Assessment of Upwelling Models

A number of studies have attempted to use models to predict source rock distribution through geologic time (e.g., Parrish, 1982; Parrish and Curtis, 1982; Scotese and

Summerhayes, 1986; Parrish, 1987; Golonka *et al.*, 1994; Kiessling *et al.*, 1999). Parrish (1982) used a theoretical approach to model upwelling zones through geologic time based on paleogeography and general principles of atmospheric circulation. Source bed occurrences were used as paleoclimatic indicators to test the validity of the model. Golonka *et al.* (1994) used paleogeographic maps to model global atmospheric pressure, paleowind direction, and potential sites of coastal upwelling for the Cambrian to the present during both winter and summer. The paleogeographic maps illustrate air pressure, wind direction, humid zones, and probable upwelling zones with respect to paleogeographic configurations. Kiessling (1999) created a database of Phanerozoic reefs and then utilized numerical processing of coded reef characteristics to recognize reef properties and trends in reef evolution, as well as to create paleoreef distribution maps.

Models such as those described above could be effectively evaluated by using organic petrology to determine the primary control on OM accumulation in organic-rich facies. Based on the correlation of modern upwelling zones with elevated primary productivity (algal blooms), one would expect to find macerals indicative of algal blooms in ancient deposits located where coastal upwelling is predicted to have occurred. If, however, modeled upwelling zones have source rocks that do not show evidence of elevated productivity, the validity of the paleoclimate model may be suspect.

Parrish (1982) did not model the distribution of upwelling and source beds for the Givetian (Middle Devonian), so an evaluation of this model using the data from the present study is not possible. Golonka *et al.* (1994) formulated a paleoclimate model for

the Givetian (~377 m.y.a.) that predicts over 70% favorable conditions for coastal upwelling in the Elk Point Embayment north and south of the Rainbow and Zama sub-basins during the summer months (Fig. 8.1A). The paleoclimate map for Givetian winter predicts that conditions favorable to coastal upwelling are more widespread in the Elk Point Embayment extending throughout the Rainbow and Zama sub-basins (Fig. 8.1B).

Organic petrology results from this study support the model of Golonka *et al.* (1994). Algal blooms are interpreted as the primary control on OM accumulation and preservation in the URL in the Rainbow Sub-basin and the UZL in the Zama Sub-basin in reef foreslope positions. These sub-basins are situated within areas modeled as being favorable to upwelling. However, if upwelling in the Rainbow and Zama areas occurred throughout the winter months as modeled by Golonka *et al.*, (1994), one might expect evidence of more persistent and widespread algal blooms than was seen in this study.

Modelling by Kiessling *et al.* (1999), based partly on the work of Golonka *et al.*, (1994), also suggests that many Givetian-Frasnian reefs are located at or close to sites that have >70% probability of coastal upwelling (Fig. 8.2). Kiessling *et al.*, (1999) go on to conclude that Givetian-Frasnian reefs could thrive in or near to coastal upwelling sites, and that Devonian reef builders could cope with higher nutrient levels than modern reefs. Although organic petrology in this study did find evidence of episodic algal blooms, potentially triggered by upwelling, a thorough study of reef core facies, correlated to the URL and UZL, is required in order to determine the effect of upwelling on reefs in the Rainbow and Zama sub-basins. The duration and intensity of the upwelling events

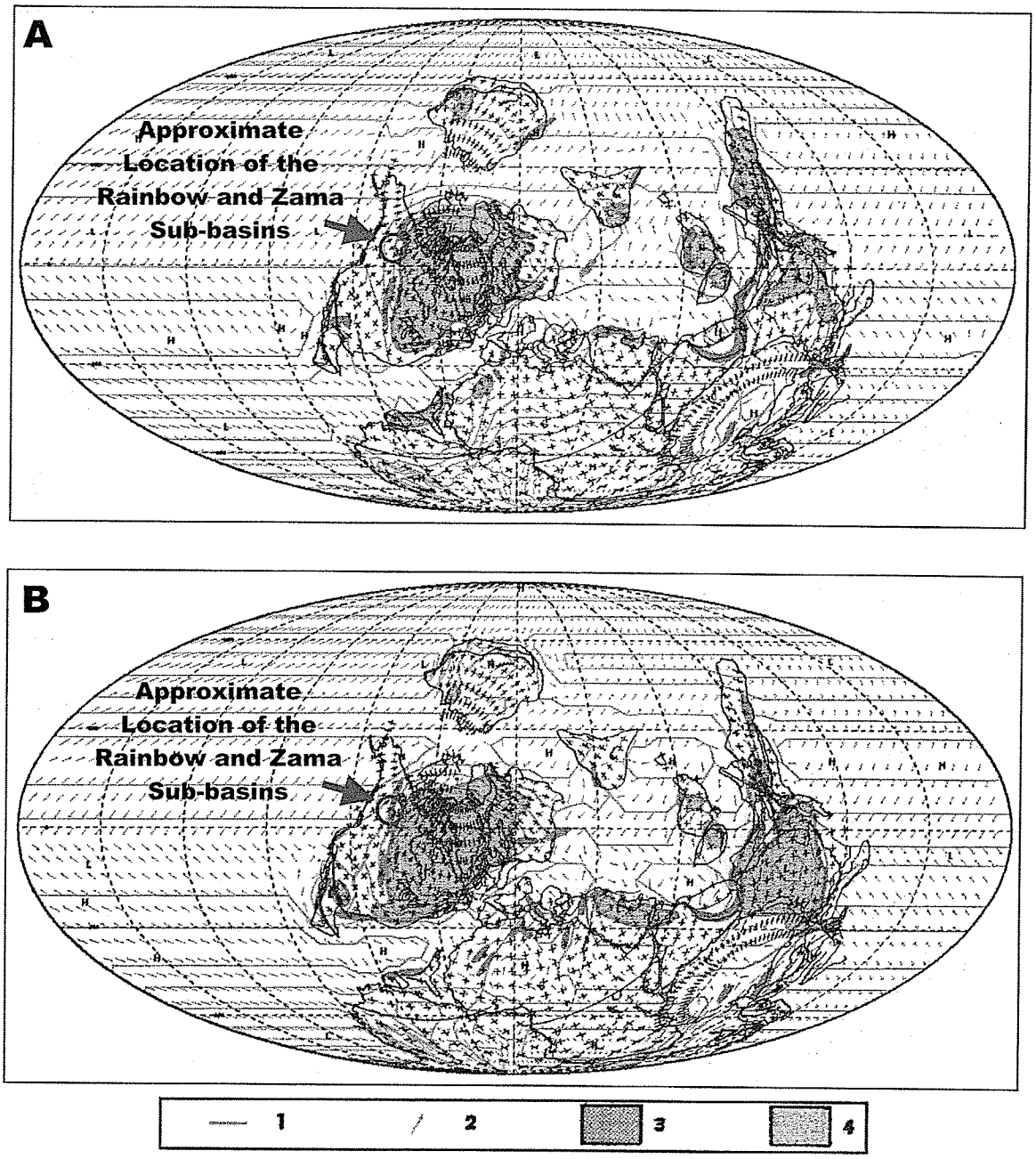

Figure 8.1 Model for paleogeography during the Givetian (Middle Devonian – 377 m.y.a) highlighting the location of the Rainbow and Zama sub-basins (modified from Golonka *et al.*, 1994). A) Summer in the Northern Hemisphere. B) Winter in the Northern Hemisphere. 1-pressure contours ("H"-High, "L"-Low), 2-wind vectors, 3-over 70% probability of favorable conditions for coastal upwelling, 4-over 70% probability of favorable conditions for equatorial humid environs.

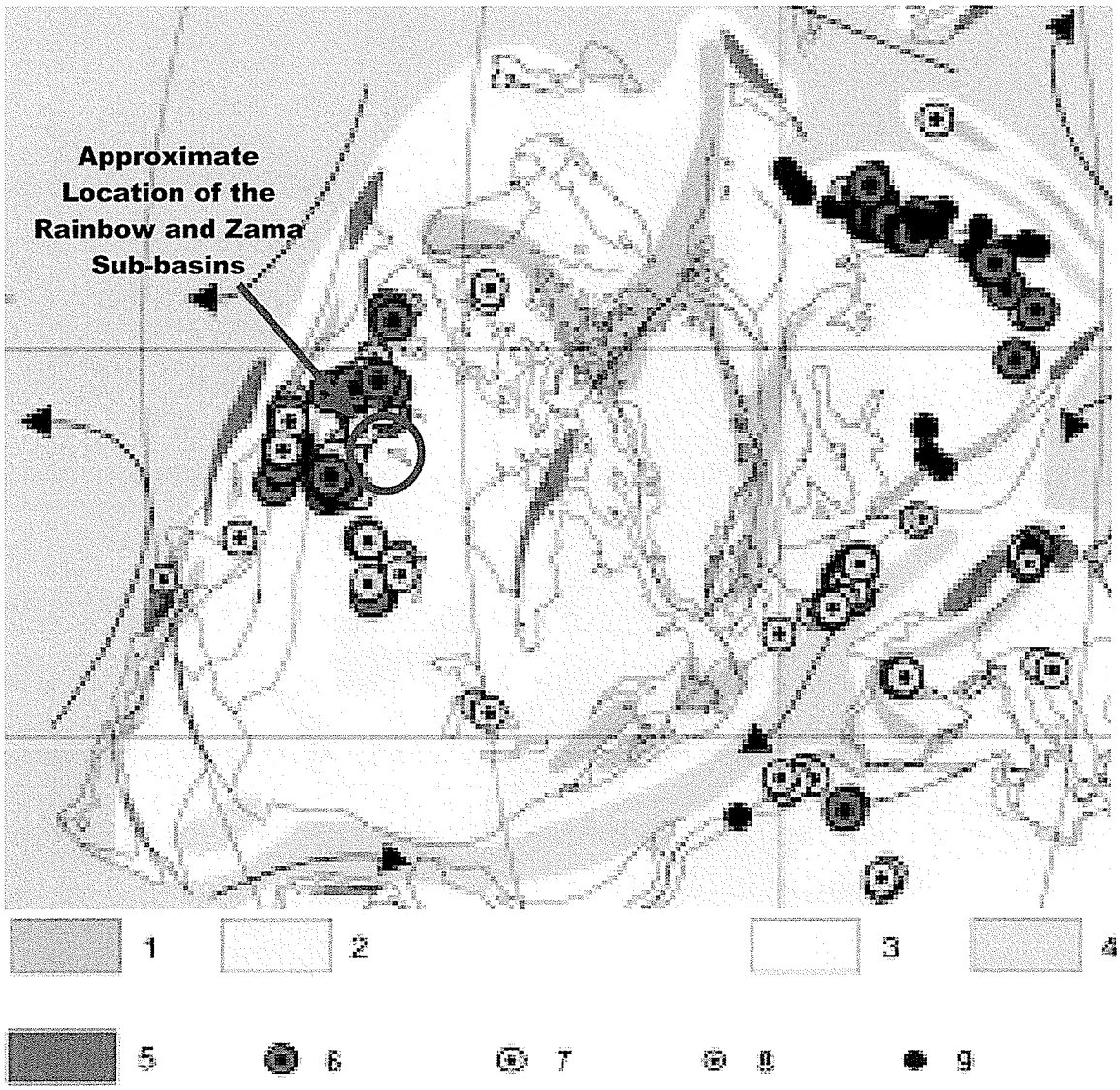

Figure 8.2 Distribution of Givetian-Frasnian reefs (modified from Kiessling *et al.*, 1999). Ocean surface currents (black arrows) were derived from the plate tectonic configuration. 1 = mountains, 2 = land, 3 = shelf, 4 = deep water, 5 = predicted upwelling zones, slightly modified from Golonka et al. (1994), 6 = reefs thicker than 100 m, 7 = reefs between 10 and 100 m thickness, 8 = reefs thinner than 10 m, 9 = reefs without thickness data. Note the close association of many reefs with predicted upwelling sites and the wide latitudinal distribution of reefs

postulated to have triggered the algal bloom events in the study area are unknown. Keg River reefs may have thrived, as suggested by Kiessling *et al.*, (1999), or the reefs could have been harmed by upwelling but were able to recover or recolonize once upwelling ceased.

8.9 Implications for Devonian Reef Growth

Increased nutrient levels accompanied by elevated phytoplanktonic productivity have typically been considered detrimental to reef growth (James and Bourque, 1992). This is due to the increased abundance of "fouling organisms", such as fleshy algae and suspension feeders, as well as decreased water clarity and effective light penetration. These consequences of eutrophication are detrimental to photosymbionts which require effective light penetration to carry out photosynthesis. However, various studies have suggested that Devonian stromatoporoid reefs could tolerate higher nutrient levels than modern reefs (e.g., Hallock and Schlager, 1986; Wood, 1993, 1995; Kiessling *et al.*, 1999).

In order to understand the implications of trophic regimes to Devonian stromatoporoid reefs, it is important to discuss their biological relationship to their environment (autecology). Evidence for photosymbiosis in Silurian to Devonian stromatoporoid sponges is equivocal. Wood (1995) suggested that some Paleozoic tabulate corals and stromatoporoids harbored symbionts based on indications that Silurian to Devonian stromatoporoids grew to large sizes, possessed a thin layer of tissue, and could competitively outgrow a number of other metazoans. If stromatoporoid autecology was

the same as that of modern reef builders, photosymbiosis and an intolerance of eutrophic conditions stemming from their photosymbiosis would be expected.

However, other evidence indicates that stromatoporoids had a different autecology than modern reef builders, likely the absence of photosymbiosis prior to the Late Triassic (Stanley and Swart, 1995). No algal fractionation signal has been found in carbon isotope results from their skeletons (Wood, 1993) and, as discussed previously, some research suggests that stromatoporoid reefs could tolerate eutrophic conditions based on reef occurrences coincident with modeled upwelling zones.

This study finds no unequivocal evidence to support the hypothesis that Devonian stromatoporoid reefs could tolerate extended periods of high nutrient concentrations. However, this study presents evidence, as previously discussed, that Middle Devonian reefs in the Rainbow and Zama sub-basins may have grown during prevailing conditions of relatively low-nutrient influx which were punctuated by episodic eutrophic conditions characterized by elevated phytoplanktonic productivity. This research suggests that the reefs in the Rainbow and Zama sub-basins were relatively unaffected or had ample time to recover and thrive between episodes of short-lived eutrophic conditions.

8.10 Future Work

This study has laid the groundwork for future sedimentological and organic petrological studies in the Rainbow and Zama sub-basins and elsewhere. The following summarizes some recommendations for future work:

1) More representative sampling of the Zama Sub-basin is needed for organic petrological and organic geochemical analysis to test the interpretations made in this study.

2) Stratigraphic correlations between the Rainbow and Zama sub-basins need to be tested with additional work in these sub-basins. In particular the thickness and lateral extent of the URL and UZL require further examination. Biostratigraphy is needed to help refine correlations.

3) Studies that integrate sedimentology and organic petrology should be done in other areas that have been modeled as being favorable for upwelling conditions in order to "ground truth" these theoretical models.

4) The impact of eutrophication on Devonian reefs should be further explored. Studies similar to this one should be carried out in areas where upwelling may have increased trophic resources and triggered phytoplankton blooms coeval with reef growth.

CHAPTER 9: SUMMARY & CONCLUSIONS

9.1 Sedimentology

Based on core examination, eleven lithofacies were identified in the ramp, reef foreslope, and off-reef successions of the Keg River Formation in the Rainbow and Zama sub-basins:

1) Lithofacies A, the bituminous laminite lithofacies, is a dark brown to black, argillaceous lime mudstone to styliolinid wackestone interlaminated with black, bituminous laminae. This lithofacies is interpreted to have been deposited in a low-energy, deep-subtidal environment below storm wave-base, characterized by pervasive dysoxic to anoxic conditions.

2) Lithofacies B, the irregular-bedded mudstone lithofacies, is composed of dark brown lime mudstone to styliolinid wackestone interbedded with medium to light brown, argillaceous lime mudstone to argillaceous styliolinid wackestone. Bed contacts are very irregular and laterally discontinuous imparting a nodular to mottled appearance to the lithofacies. This lithofacies is interpreted to have been deposited in a low-energy, deep-subtidal environment below storm wave-base, similar to the depositional environment interpreted for lithofacies A.

3) Lithofacies C, the nodular crinoid-brachiopod wackestone lithofacies, consists of dark grey to medium brown, nodular skeletal wackestone to floatstone. Nodules have gradational contacts with the matrix which tends to be darker in color, more

argillaceous and organic-rich, and locally less skeletal-rich than the nodules. Lithofacies C is interpreted to have been deposited in a low-energy, deep-subtidal environment below storm wave-base, similar to lithofacies A and B. However, lithofacies C appears to have accumulated in a setting with more oxygenated conditions than those of lithofacies A or B.

4) Lithofacies D, the massive crinoid-brachiopod wackestone lithofacies, consists of dark grey to black, crinoid-brachiopod wackestone to floatstone in an argillaceous and organic-rich matrix containing micrite and dolomicrite. This partially to pervasively dolomitized lithofacies is predominantly massive although vague laminations occur locally, defined by concentrations of OM and clay material, and by skeletal fragments and peloids. Lithofacies D is interpreted to have been deposited in a low to moderate energy, deep-subtidal environment near storm wave-base.

5) Lithofacies E, the bioturbated crinoid-brachiopod floatstone lithofacies, is highly variable and composed of medium brown to grey, crinoid-brachiopod floatstone to rudstone showing pervasive bioturbation (mottled appearance). Burrows are preferentially dolomitized. This lithofacies is interpreted to have been deposited in a moderate energy, subtidal environment between storm and fairweather wave-base.

6) Lithofacies F, the bituminous peloidal laminite lithofacies, is buff to very light grey in color and ranges from peloidal-skeletal dolopackstone to dolograinstone. Abundant black, organic-rich, stylolitized laminae comprise 5-35% of the lithofacies. Primary textures are replaced by a coarse dolomite mosaic in this pervasively dolomitized lithofacies. Lithofacies F is interpreted to have been deposited in a moderate energy, intermediate to deep-subtidal environment. Evidence suggests that this lithofacies was deposited above storm wave-base and was influenced by frequent storm-induced sediment gravity flows and pervasive current reworking. Episodic dysoxic to anoxic conditions are interpreted to have developed during deposition of lithofacies F due to algal blooms.

7) Lithofacies G, the massive peloidal-skeletal dolopackstone to dolograinstone lithofacies, is buff colored and massive. It lacks organic-rich laminae, but otherwise is compositionally similar to lithofacies F. Porosity ranges from 1-20% and includes intercrystalline porosity, which is ubiquitous and occurs as "pinpoint" pores between dolomite crystals; and minor intraparticle, biomoldic, vuggy, and fracture porosity. Lithofacies G is interpreted to have been deposited in a moderate energy, intermediate-subtidal environment situated between storm and fairweather wave-base in fully oxygenated conditions.

8) Lithofacies H, the stromatoporoid-coral dolofloatstone to dolorudstone lithofacies, is buff to medium brown and has a peloidal-skeletal packstone to grainstone matrix which is compositionally similar to lithofacies G. This lithofacies is

predominantly pervasively dolomitized but is locally limestone or partially dolomitized. Lithofacies H has the most abundant (30-80%) and diverse fauna of all the lithofacies examined in this study. Major allochems include stromatoporoid fragments, crinoids, peloids, thamnoporid fragments, and *Alveolites*. Porosity ranges from 10-25% and includes intercrystalline, fracture, intraparticle (in coral skeletons), vuggy, and biomoldic porosity. Lithofacies H is interpreted to have been deposited in an open-marine, moderate energy, intermediate-subtidal environment that was fully oxygenated and located between storm and fairweather wave-base.

9) Lithofacies I, the non-fossiliferous dolomudstone lithofacies, is associated with anhydrite units of the Muskeg and Chinchaga formations. It ranges from buff to light grey in color and from massive to brecciated to haloturbated in structure. Lithofacies I is composed of pseudospar, dolomicrite, finely crystalline planar-euhedral dolomite, and medium crystalline planar-subhedral dolomite. This lithofacies is interpreted to have been deposited in a low energy, high salinity, restricted environment.

These lithofacies were grouped into three lithofacies associations:

1) The outer ramp lithofacies association includes lithofacies A, B, and C. The outer ramp extends from the basin plain up to storm wave-base and is dominated by carbonate and terrigenous mud deposited from suspension. Evidence of storm or wave reworking is sparse. In the deepest parts of the outer ramp, organic-rich

facies can develop due to oxygen-poor bottom-water conditions triggered by density stratification.

2) The mid ramp lithofacies association includes lithofaces D and E. The mid ramp encompasses the zone between storm and fairweather wave-base. Facies deposited in the mid-ramp exhibit evidence of frequent reworking by bioturbation, storm waves, and swells. However, suspension settling of carbonate and terrigenous mud contributes significant sediment during fairweather periods.

3) The reef foreslope lithofacies association includes lithofacies F, G, and H. The reef foreslope lithofacies association represents an accumulation of in situ and reef-derived, bedded carbonate sand and gravel that dip and thin away from the reef core facies. The foreslope lithofacies association is interpreted as having accumulated in a moderate-energy environment between storm wave-base and fairweather wave-base which was frequently affected by storm events and sediment gravity flows. Pervasive bioturbation indicates well oxygenated, open marine waters.

The Lower Keg River Member consists of the mid-ramp to outer ramp lithofacies associations (lithofacies A to E). The Upper Keg River Member in reef-foreslope and off-reef positions is composed of the reef foreslope lithofacies association (lithofacies F to H). Lithofacies I occurs at two stratigraphic positions in the Keg River Formation that are associated with evaporite deposits: 1) at the base of the Lower Keg River Member

overlying the Chinchaga Formation; and 2) at the top of the Upper Keg River Member overlain by the Muskeg Formation.

9.2 Depositional Cycles

Three shallowing-upward, third-order cycles were identified in the Rainbow Sub-basin:

1) Cycle R1 (~24 - 35 m thick) marks the onset of Lower Keg River Member deposition as a relative sea level rise transformed the Rainbow area from evaporitic to open marine conditions. This transition is marked by lithofacies I, ~1 –1.5 m thick, at the base of cycle R1 which shoals up into alternating lithofacies A to E indicating a mid to outer-ramp depositional environment with laterally shifting, gradational facies.

2) Cycle R2 (~8 - 14 m thick) has the lower Rainbow laminite (LRL), ~3 – 6 m thick, at the base. The LRL is composed of lithofacies A interbedded with lithofacies B, C and less commonly D and E. The LRL typically shoals up into alternating lithofacies A to E representing a mid to outer-ramp setting with laterally shifting, gradational facies.

3) The base of cycle R3 (~0 - 230 m thick) was deposited in response to subsidence which created the Rainbow Sub-basin. This relative sea-level rise resulted in Upper Keg River Member reef initiation and deposition of the organic-rich middle Rainbow laminite (MRL), ~2 m thick, at the base of the cycle. The MRL, composed largely of lithofacies A, shoals up into alternating lithofacies F to H of

the reef foreslope lithofacies association. Occurrences of lithofacies F interbedded with lithofacies G and H comprise the upper Rainbow laminite (URL).

Only two such depositional cycles were identified in the Zama Sub-basin:

1) Cycle Z1 (~35 – 40 m thick) occurs at the base of the Lower Keg River Member, and was deposited in response to a relative sea level rise that transformed the Zama area from evaporitic to open marine conditions. This transition is marked by ~1.5 m of lithofacies I at the base of cycle Z1 which grades up into alternating lithofacies C and D of the outer and mid-ramp lithofacies associations respectively.

4) Cycle Z2 (~0 – 104 m thick) deposited in response to subsidence which created the Zama Sub-basin. This relative sea-level rise resulted in Upper Keg River Member reef initiation and deposition of the lower Zama laminite (LZL), ~1.5 – 2.5 m thick, at the base of the cycle. The LZL is composed of lithofacies A locally interbedded with lithofacies C. These lithofacies pass upward into alternating lithofacies F to H of the reef foreslope lithofacies association. Occurrences of lithofacies F interbedded with lithofacies G and H comprise the upper Zama laminite (UZL).

The correlation between the Rainbow and Zama sub-basins is interpreted as follows:

1) Cycles R1 and R2 in the Rainbow Sub-basin correlate to cycle Z1 in the Zama Sub-basin. The LRL has no correlative expression in the Zama Sub-basin.
2) Cycle R3 correlates to cycle Z3 and, therefore, the MRL correlates to the LZL and the URL correlates to the UZL.

9.3 Depositional History

The depositional history of the Keg River Formation in the Rainbow and Zama sub-basins is interpreted as follows within the framework of cycles R1, R2, and R3 in the Rainbow Sub-basin and cycles Z1 and Z2 in the Zama Sub-basin:

1) A relative sea-level rise transformed the Rainbow and Zama areas from an evaporitic setting, represented by the Chinchaga Formation, to an open marine environment in which deposition of the outer and mid-ramp successions (lithofacies A to E) of the Lower Keg River Member began. This initial incursion of open-marine waters into the Elk Point Basin is represented by the correlative cycles R1 and Z1 in the Rainbow and Zama areas respectively.

2) Local subsidence in the Rainbow area resulted in deposition of cycle R2, the base of which is marked by the LRL which shoals upward into lithofacies of the outer and mid-ramp lithofacies associations (lithofacies B to E). A correlative cycle is not present in the Zama area suggesting that little or no subsidence occurred in the area at this time.

3) Another relative sea-level rise attributed to subsidence in the study area resulted in the formation of discrete sub-basins including the Rainbow and Zama sub-basins. This subsidence resulted in drowning of the Lower Keg River Member ramp, which is marked by deposition of the MRL at the base of cycle R3 in the Rainbow Sub-basin. In the Zama Sub-basin, this drowning event is marked by deposition of the LZL at the base of cycle Z2. Cycles R3 and Z2 are interpreted to be correlative, and therefore, it follows that the organic-rich MRL and LZL are also correlative.

4) Isolated reefs of the Upper Keg River Member developed on paleotopographic highs in both the Rainbow and Zama sub-basins during cycles R3 and Z2. Reef development is expressed in the reef foreslope by deposition of lithofacies F to H. The URL in the Rainbow Sub-basin and the UZL in the Zama Sub-basin were deposited in off-reef and reef foreslope positions and are interpreted to be correlative.

5) A relative sea-level drop, due either to evaporitic drawdown or to regional sea-level fall, halted carbonate production in the study area as Upper Keg River Member reefs were exposed and hypersaline conditions were established. Evaporitic conditions at this time resulted in deposition of the Muskeg Formation.

9.4 Organic Petrology

Based on organic petrology, organic facies were identified in the five laminite units: the LRL, MRL and URL in the Rainbow Sub-basin; and the LZL and UZL in the Zama Sub-basin.

1) The LRL, MRL, and LZL are all interpreted as primarily OF B, characterized by small, thin-walled alginites and acanthomorphic acritarchs indicative of deposition in intermediate water depths and intermediate distances from a bank margin or shore setting.

2) The URL and UZL in off-reef positions are interpreted as primarily OF B with secondary OF A signatures, characterized by dominant large, thick-walled alginites. This is indicative of deposition in a low energy, deep-water setting, a considerable distance from a bank margin or shoreline in which OM contributed by algal blooms was overwhelmed by OM which accumulated in response to bottom-water anoxia.

3) The URL and UZL in reef foreslope positions are interpreted as primarily OF A, characterized by dominant large, thick-walled alginites and indicative of accumulation and preservation of OM due to algal blooms.

9.5 Organic Geochemistry

Rock-Eval6 pyrolysis was used to quantify the petroleum potential and to help assess the origin of organic-rich laminites in the Rainbow and Zama sub-basins.

1) HI versus OI plots indicate that all of the organic-rich laminites (LRL, MRL, URL, LZL, and UZL) were thermally mature and were composed of type II (marine, oil-prone) kerogen.
2) HI versus T_{max} plots also indicated high thermal maturity and type II kerogen.

9.6 Preservation versus Productivity Controls

Based on sedimentology and organic petrology, preservation due to bottom-water anoxia is interpreted to be the primary control on OM accumulation in the LRL, MRL, LZL, and URL in distal reef foreslope and off-reef positions.

1) During LRL deposition, anoxia could have developed in response to depth and/or restricted vertical mixing and sluggish circulation caused by barriers around the Rainbow-Zama region.

2) During MRL and LZL deposition, anoxia could have developed in response to the depth of the newly differentiated Rainbow and Zama sub-basins. Anoxia may have also developed due to restricted vertical mixing and sluggish circulation caused by incipient reefs, barriers, and banks within the sub-basins and limited wind fetch over these sub-basins.

3) During URL deposition in distal reef foreslope and off-reef positions, anoxia could have also developed in response to depth and/or restricted vertical mixing and sluggish circulation. Isolated reefs in the Rainbow and Zama sub-basins,

banks and barriers around them, and limited wind fetch may have impeded circulation and vertical mixing in the sub-basins.

Elevated phytoplanktonic productivity (algal blooms) is interpreted to be the primary control on OM accumulation in the URL and UZL in more proximal reef foreslope positions. The triggering mechanisms for algal blooms are difficult to ascertain. A number of potential mechanisms may have been active in the Rainbow and Zama sub-basins during deposition of the URL and UZL including: 1) coastal upwelling; 2) open-ocean divergence upwelling; 3) increases in nutrient supply, potentially derived from terrestrial sources; and 4) restriction due to hypersalinity. Algal blooms could have induced episodic anoxia in normally oxygenated sediments due to increased phytoplanktonic respiration rates and high OM flux to the sea floor.

Sedimentation rate and sediment texture and mineralogy were secondary controls on OM accumulation and preservation in organic-rich laminites in the Rainbow and Zama sub-basins.

1) Relatively low sedimentation rates (estimated <20 cm/ka) during deposition of the LRL, MRL, and LZL probably exerted a positive influence on OM accumulation and preservation. Such low bulk sedimentation rates increased burial efficiency, decreased residence time, and decreased benthic degradation loss of OM at the sediment-water interface. Relatively high sedimentation rates (estimated >20 cm/ka) during deposition of the URL and UZL probably had a negative influence

on OM accumulation and preservation because clastic dilution effects increase with bulk sedimentation rates.

2) Very fine-grained micrite and clay mineral components characteristic of the LRL, MRL, and LZL would have provided large surface areas for sorption of OM. Relatively fine-grained peloids in the URL and UZL would have also provided sorption sites for OM.

9.7 Comparison to the La Crete Sub-basin and Williston Basin

1) In the La Crete Sub-basin the Lower Keg River Member consists of two shoaling-upward ramp successions with an organic-rich laminite, the bituminous marker, present at the base of the upper succession. The similar stratigraphic position of the LRL in the Rainbow Sub-basin and the bituminous marker suggests a possible correlation. However, the organic petrology of the bituminous marker indicates a dominant "bloom" organic facies suggesting that OM accumulated primarily in response to elevated phytoplanktonic productivity, whereas OM in the LRL is interpreted to have accumulated primarily in response to anoxia. This difference suggests that specific paleoecological conditions, such as algal blooms, may have been confined locally to sub-basins due to physical barriers or environmental differences between adjacent sub-basins.

2) The Brightholme Member of the Winnipegosis Formation in southern Saskatchewan is a laminated, bituminous carbonate unit that occurs in the off-reef

areas between the Upper Winnipegosis reefs and is coeval with the reefs. The URL and UZL of this study are coeval with Upper Keg River reefs in the Rainbow and Zama sub-basins suggesting that these two units may be stratigraphically equivalent to the Brightholme Member. However, considerably more work is required to test this hypothesis. OM in the Brightholme Member and the URL and UZL are interpreted to have accumulated primarily in response to algal blooms providing evidence of at least episodic high phytoplankton productivity during reef growth in the Middle Devonian.

9.8 Assessment of Upwelling Models and Implications for Devonian Reef Growth

A number of studies have developed upwelling models to predict source rock distribution through geologic time. Based on the correlation of modern upwelling zones with algal blooms, one would expect macerals indicative of algal blooms in ancient settings where coastal upwelling is predicted to have occurred.

1) Golonka *et al.* (1994) formulated a paleoclimate model for the Givetian that predicts: a) over 70% favorable conditions for coastal upwelling in the Elk Point Basin north and south of the Rainbow and Zama sub-basins during the summer months; and b) conditions favorable to coastal upwelling that are more widespread during the winter months, extending throughout the Rainbow and Zama sub- basins. The present study supports the model because algal blooms are interpreted as the primary control on OM accumulation and preservation in the URL of the Rainbow Sub-basin and the UZL of the Zama Sub-basin in reef foreslope positions which coincide with modeled sites favorable to upwelling.

2) The model of Kiessling *et al.* (1999) suggests that many Givetian-Frasnian reefs are located at or close to sites that have >70% probability of coastal upwelling. The present study found evidence of episodic algal blooms in the URL and UZL in reef foreslope successions, potentially triggered by upwelling, which supports the model.

3) No unequivocal evidence was found in the Keg River Formation in the Rainbow and Zama sub-basins to support the theory that Devonian stromatoporoid reefs could tolerate extended periods of high nutrient concentrations. However, evidence was found for episodic, high nutrient conditions coeval with reef growth suggesting that the reefs in the Rainbow and Zama sub-basin were relatively unaffected by or were able to recover between episodes of short-lived eutrophic conditions.

REFERENCES

Adams, A.E., Mackenzie, W.S., and Guilford, C. 1984. Atlas of Sedimentary Rocks Under the Microscope. John Wiley and Sons Inc., New York, 104p.

Adams, A.E., Mackenzie, W.S. 1998. A Color Atlas of Carbonate Sediments and Rocks Under the Microscope. John Wiley and Sons Inc., New York, 192p.

Aigner, T. 1985, Storm Depositional Systems. Lecture Notes in Earth Science. Springer-Verlag Inc., New York, v. 3, p. 1-174.

Aller, R.C. 1982. Chapter 2 - The effects of macrobenthos on chemical properties of marine sediment overlying water. *In:* Animal-Sediment Relations – The Biogenic Alteration of Sediments. P.L. McCall and J.S. Tevesz (eds.). Plenum Press, New York, p. 53-102.

Aller R.C. 1984. Preservation of reactive organic matter in marine sediments. Earth and Planetary Science Letters, v. 70 (2), p. 260-266.

Anderson, D.M. 1994. Red Tides. Scientific American, August, 1994, p. 62-68.

Arthur, M.A. and Sageman, B.B. 1994. Marine black shales: depositional mechanisms and environments of ancient deposits. Annual Review of Earth and Planetary Sciences, v. 22, p. 499-551.

Baillie, A.D. 1953. Devonian names and correlation in Williston Basin area. American Association of Petroleum Geologists Bulletin, v. 37 (2), p. 444-447.

Barss, D.L., Copland, A.B. and Ritchie, W.D. 1970. Geology of Middle Devonian reefs, Rainbow area, Alberta, Canada. *In:* Geology of Giant Petroleum Fields. M.T. Halbouty (ed.). American Asociation of Petroleum Geologists Memoir 14, p. 19-49.

Bassett, H.G. and Stout, J.G. 1967. Devonian of western Canada *In:* International Symposium on the Devonian System. D.H. Oswald (ed.). Calgary, v. 1, p. 717-752.

Behar, F., Beaumont, V., and De B. Penteado, H.L. 2001. Rock-Eval 6 technology: performance and developments. Oil & Gas Science and Technology-Review IFP, v. 56 (2), p. 111-134.

Belyea, H.R. 1952. Notes on the Devonian system of the north-central plains of Alberta. Geological Survey of Canada, Paper 52-27. 66p.

Belyea, H.R. and Norris, A.W. 1962. Middle Devonian and older Palaeozoic formations of southern District of Mackenzie and adjacent areas. Paper – Geological Survey of Canada, Paper 62-15. 82p.

Betts, J.N. and Holland, H.D. 1991. The oxygen content of ocean bottom waters, the burial efficiency of organic carbon, and the regulation of atmospheric oxygen. Palaeogeography, Palaeoclimatology, Palaeoecology (Global and Planetary Change Section), v. 97, p. 5-18.

Bordovskiy, O.K. 1965. Accumulation and transformation of organic substances in marine sediments 2 - sources of organic matter in marine basins. Marine Geology, v. 3, p. 5-31.

Bricelj, V.M. and Lonsdale, D.J. 1997 *Aureococcus anophagefferens*: causes and ecological consequences of brown tides in U.S. mid-Atlantic coastal waters. Limnology and Oceanography, v. 42(5), part 2, p. 1023-1038.

Brooks, J. 1981. Some chemical and geochemical studies on sporopollenin. *In:* Sporopollenin. J. Brooks (ed.). Academic Press, London, p. 351-407.

Brooks and Fleet, 1987. Marine Petroleum Source Rocks. J. Brooks and A.J. Fleet (eds.). Geological Society Special Publication No. 26, 444p.

Burchette, T.P. and Wright, V.P. 1992. Carbonate ramp depositional systems. Sedimentary Geology, v. 79 (1-4), p. 3-57.

Burrowes, O.G. and Krause, F.F. 1987. Overview of the Devonian system: subsurface of Western Canada Basin. *In*: Devonian Lithofacies and Reservoir Styles in Alberta. F.F. Krause, and O.G. Burrowes (eds.). 13th Canadian Society of Petroleum Geologists Core Conference and Second Symposium on the Devonian System, p. 1-20.

Calvert, S.E. 1987. Oceanographic controls on the accumulation of organic matter in marine sediments. *In:* Marine Petroleum Source Rocks. J. Brooks and A.J. Fleet (eds.). Geological Society Special Publication No. 26. p. 137-151.

Calvert, S.E., Karlin, R.E., Toolin, L.J., Donahue, D.J., Southon, J.R. and Vogels, J.S. 1991. Low organic carbon accumulation rates in Black Sea sediments. Letters to Nature, April 1991, v. 350, p. 692.

Calvert, S.E., Bustin, R.M. and Pederson, T.F. 1992. Lack of evidence for enhanced preservation of sedimentary organic matter in the oxygen minimum of the Gulf of California. Geology, v. 20, p. 757-760.

Calvert, S.E. and Pederson, T.F. 1992. Organic carbon accumulation and preservation in marine sediments: how important is anoxia? *In:* Organic Matter, Productivity, Accumulation, and Preservation in Recent and Ancient Sediments. J.K. Whelan and J.W. Farrington (eds.). Columbia University Press, New York., p. 231-263.

Calvert, S.E., Bustin, R.M., Ingall, E.D. 1996. Influence of water column anoxia and sediment supply on the burial and preservation of organic carbon in marine shales. Geochimica et Cosmochimica Acta, v. 60 (9), p. 1577-1593.

Campbell, C.V. 1987. Stratigraphy and facies of the Upper Elk Point Subgroup, Northern Alberta. *In:* Second International Symposium on the Devonian System - Devonian Lithofacies and Reservoir Styles in Alberta – 13th CSPG Core Converence & Display, August 19. 20, & 21, p. 274

Campbell, C.V. 1992. Chapter 6 – Upper Elk Point megasequences. *In:* Devonian-Early Mississippian Carbonates of the Western Canada Sedimentary Basin: A Sequence Stratigraphic Framework. J. Wendte, F.A. Stoakes and C.V. Campbell (authors). Society for Sedimentary Geology (SEPM) Short Course No. 28, p. 145-162.

Canfield, D.E. 1989. Sulfate reduction and oxic respiration in marine sediments; implications for organic carbon preservation in euxinic environments. Deep-Sea Research Part A: Oceanographic Research Papers, v. 36 (1A), p. 121-138.

Chen, Z., Osadetz, K.G., Gao, H., Hannigan, P. and Watson, C. 2000. Characterizing the spatial distribution of an undiscovered hydrocarbon resource: the Keg River Reef play, Western Canada Sedimentary Basin. Bulletin of Canadian Petroleum Geology, v. 48 (2), p. 150-163.

Cheng, Y.C., Lee, P.J. and Lee, T.Y. 2000. Estimating exploration success ratio by fractal geometry. Bulletin of Canadian Petroleum Geology, v. 48 (2), p. 116-122.

Chernyk, J.F. 1994. Horizontal drilling in the Keg River carbonate reefs. The Journal of Canadian Petroleum Technology, September 1994, v. 33 (7), p. 22-26.

Choquette, P.W. and Pray, L.C. 1970. Geological nomenclature and classification of porosity in sedimentary carbonates. The American Association of Petroleum Geologists Bulletin, v. 54 (2), p. 207-250.

Chow, N., Wendte, J. and Stasiuk, L.D. 1995a. Productivity versus preservation controls on two organic-rich carbonate facies in the Devonian of Alberta: sedimentological and organic petrological evidence. Bulletin of Canadian Petroleum Geology, v. 43, p. 433-460.

Chow, N., Wendte, J. and Stasiuk, L.D. 1995b. Productivity versus preservation controls on potential carbonate source rocks in the Devonian of the Alberta Basin. CSPG Reservoir, v. 22 (9), p. 2-3.

Clegg, H., Horsfield, B., Stasiuk, L.D., Vliex, M. and Fowler, M.G. 1997. Geochemical characterization of facies variations in the Keg River Formation (Elk Point Group, Middle Devonian) La Crete Basin, Western Canada. Organic Geochemistry, v. 26, p. 627-643.

Clough, J.G. and Blodgett, R.B. 1984. Lower Devonian basin to shelf carbonates in outcrop from the western Ogilvie Mountains, Alaska and Yukon Territory. *In:* Canadian Society of Petroleum Geologists Core Conference - Carbonates in subsurface and outcrop. L.L. Eliuk, (chair), J. Kaldi, N. Watts and G. Harrison (eds.). Calgary, Alberta, p. 57-81.

Coniglio, M and Dix, G.R. 1992. Carbonate Slopes. *In:* Facies Models; response to sea level change. R.G. Walker and N.P. James (eds.). Geological Association of Canada, St. Johns, Newfoundland, Canada, p. 349-373.

Corrigan, A.F. 1975. The evolution of cratonic basin from carbonate to evaporite deposition, and the resulting stratigraphic and diagenetic changes, Elk Point Subgroup, northeastern Alberta. Unpublished Ph.D. thesis, University of Calgary. 274p.

Cowie, G.L. and Hedges, J.I. 1992. The role of anoxia in organic matter preservation in coastal sediments; relative stabilities of the major biochemicals under oxic and anoxic depositional conditions. Organic Geochemistry, v. 19 (1-3), p. 229-234.

Davison, R.J., Mayder, A., Hladiuk, D.W., Jarrell, J. 1999. Zama acid gas disposal/miscible flood implementation and results. Journal of Canadian Petroleum Technology, February 1999, v. 38 (2), p. 45-54.

Degens, E.T., Von Herzen, R.P., Wong, H., Deuser, W.G. and Jannasch, H.W. 1973. Lake Kivu; structure, chemistry and biology of an East African rift lake. Geologische Rundschau, v. 62 (1), p. 245-277.

Degens, E.T. and Stoffers, P. 1976. Stratified waters as a key to the past. Nature, v. 263, p. 22-27.

Delgado, F. 1977. Primary textures in dolostones and recrystallized limestones: a technique for their microscopic study. Journal of Sedimentary Petrology, v. 47 (3), p. 1339-1341.

Demaison, G.J. 1991. Anoxia vs. productivity: what controls the formation of organic-rich sediments and sedimentary rocks?: Discussion. American Association of Petroleum Geologists Bulletin, v. 75(3), p. 499.

Demaison, G.J. and Moore, G.T. 1980. Anoxic environments and oil source bed genesis. American Association of Petroleum Geologists Bulletin, v.64, p. 1179-1209.

Dickson, J.A.D. 1966. Carbonate identification and genesis as revealed by staining. Journal of Sedimentary Petrology, v. 36, p. 491-505.

Dorning, K.J. 1987. The organic paleontology of Paleozoic carbonate environments. *In:* Micropaleontology of Carbonate Environments. M.B. Hart (ed.). Ellis Horwood, Chichestor, p. 256-265.

Downie, C., Williams, G.L. and Sarjeant, W.A.S. 1961. Classification of fossil microplankton. Nature (London), v. 192 (4801), p. 471.

Downie, C. and Sarjeant, W.A.S. 1964. Bibliography and index of fossil dinoflagellates and acritarchs. Memoir – Geological Society of America, 180p.

Dravis, J.J. 1991. Carbonate petrography – update on new techniques and applications. Journal of Sedimentary Petrology, v. 61, p. 626-628.

Dunham, R.J. 1962. Classification of carbonate rocks according to depositional texture. Classification of carbonate rocks - a symposium. American Association of Petrolgeum Geologists Memoir 1. p. 108-121.

Einsele, G. 2000. Sedimentary Basins - Evolution, Facies, and Sediment Budget (2nd Edition). Springer, Berlin, 792p.

Embry, A.F. and Klovan, J.E. 1971. A late Devonian reef tract on northeastern Banks Island, N.W.T. Bulletin of Canadian Petroleum Geology, v. 19 (4), p. 730-781.S

Enos, P. and Moore, C.H. 1983. Fore-reef Slope Environment. *In:* Carbonate Depositional Environments. P.A. Scholle, D.G. Bebout and C.H. Moore (eds.). American Association of Petroleum Geology Memoir 33, p. 507-537.

Fay, P. 1983. The Blue-Greens. The Institute of Biology's Studies in Biology 160, Camelot Press Ltd., Southampton, 88p.

Flanagan, R. 1995. Killer trees choked ocean life. New Scientist, April 1995. p. 17.

Folk, R.L. 1957. Petrology of Sedimentary Rocks – Web Version 1.0. Austin, Texas, 111p.

Folk, R.L. 1987. Detection of organic matter in thin-sections of carbonate rocks using a white card. Sedimentary Geology, v. 54, p. 193-200.

Fong, D.K., Wong, F.Y., McIntyre, F.J. 1996. An unexpected benefit of horizontal wells on offset vertical well productivity in miscible floods. Journal of Canadian Petroleum Technology, November 1996, v. 35 (9), p. 70-79.

Fowler, M.G. and Stasiuk, L.D. 1999. Presence of *Gloeocapsomorpha prisca* in Devonian sediments of the Western Canada Sedimentary Basin. 19th International Meeting on Organic Geochemistry, September 1999, Istanbul, Turkey, p. 163-164.

Fowler, M.G., Stasiuk, L.D., Hearn, M. and Obermajer, M. 2001. Devonian hydrocarbon source rocks and their derived oils in the Western Canada Sedimentary Basin. Bulletin of Canadian Petroleum Geology, v. 49 (1), p. 117-148.

Fritsch, F.E. 1959. The Structure and Reproduction of the Algae, Volume 1. Cambridge University Press, Cambridge, 791p.

Galloway, W.E. 1989. Genetic stratigraphic sequences in basin analysis; I, Architecture and genesis of flooding-surface bounded depositional units. American Association of Petroleum Geologists Bulletin, v. 73 (2), p. 125-142.

Glass, D.J. (ed.). 1990. Lexicon of Canadian Stratigraphy Volume 4 Western Canada, Including Eastern British Columbia, Alberta, Saskatchewan and Southern Manitoba. Canadian Society of Petroleum Geologists.

Golonka, J., Ross, M.I. and Scotese, C.R. 1994. Phanerozoic paleogeographic and paleoclimatic modeling maps. *In:* Pangea: Global Environments and Resources – Canadian Society of Petroluem Geologists Memoir 17. A.F. Embry, B. Beauchamp and D.J. Glass (eds.). p. 1-47.

Golubic, S. and Knoll, A.H. 1993. 5 Prokaryotes. *In:* Fossil Prokaryotes and Protists. J.H. Lipps (ed.). Blackwell Scientific Publications, Boston, p. 51-76.

Gray, F.F. and Kassube, J.R. 1963. Geology and stratigraphy of Clarke Lake gas field, British Columbia, Bulletin of the American Association of Petroleum Geologists, v. 47 (3) p. 467-483.

Gregg, J.M. and Sibley, D.F. 1984. Epigenetic dolomitization and the origin of xenotopic dolomite texture. Journal of Sedimentary Petrology, v. 54 (3), p. 908-931.

Hallam, A. 1964. Origin of the limestone-shale rhythm in the Blue Lias of England; a composite theory. Journal of Geology, v. 72 (2), p. 157-169

Hallock, P. and Schlager, W. 1986. Nutrient excess and the demise of coral reefs and carbonate platform. Palaios, v. 1, p. 389-398

Harvey, H.R., Fallon, R.D. and Patton, J.S. 1986. The effect of organic matter and oxygen on the degradation of bacterial membrane lipids in marine sediments. Geochimicia et Cosmochimica Acta, v. 50, p. 795-804.

Hedges, J.I. 1976. Land-derived organic matter in surface sediments from the Gulf of Mexico, Geochimica et Cosmochimica Acta, v. 40 (9), p. 1019-1029.

Hollander, D, J. 1990. Environmental factors controlling the preservation and accumulation of organic matter. Chemical Geology, v. 84 (1-4), p. 215-216.

Hopkins, J.C. 1972. Petrography, distribution and diagenesis of foreslope, nearslope and basin sediments, Miette and ancient wall carbonate complexes (Devonian), Alberta. Unpublished Ph.D. thesis, McGill University, Montreal, Quebec, Canada.

Hriskevich, M.E. 1966. Stratigraphy of Middle Devonian and older rocks of Banff Aquitaine Rainbow West 7-32 discovery well, Alberta. Bulletin of Canadian Petroleum Geology, v. 14 (2), p.241-265.

Hunt, J.M. 1996. Petroleum geochemistry and geology (2nd Edition), 743p.

James, N.P. and Bourque, P. 1992. Reefs and mounds. *In:* Facies Models; response to sea level change. R.G. Walker and N.P. James (eds.). Geological Association of Canada, St. Johns, Newfoundland, Canada, p. 323-347.

James, N.P. and Kendall, A.C. 1992. Introduction to carbonate and evaporite facies models. *In:* Facies Models; response to sea level change. R.G. Walker and N.P. James (eds.). Geological Association of Canada, St. Johns, Newfoundland, Canada, p. 265-275.

Jenkyns, H.C. 1980. Cretaceous anoxic events: from continents to oceans. Journal of the Geological Society of London, v. 137, p. 171-188.

Jin, J. and Bergman, K.M. 1999. Sequence stratigraphy of the Middle Devonian Winnipegosis carbonate-prairie evaporite transition, southern Elk Point Basin. Carbonates and Evaporites, v. 14 (1), p. 64-83.

Jin, J. and Bergman, K.M. 2001. Canadian Society of Petroleum Geologists Bulletin, v. 49, p. 441-457.

Jones, R.W. and Demaison G.J. 1982. Proceedings of the Second ASCOPE Conference and Exhibition. Saldivar-Sali, A. (ed.). Manilla, October 7-11th, 1981, p. 51-68.

Jones, B. and Desrochers, A. 1992. Shallow Platform Carbonates. *In:* Facies Models; response to sea level change. R.G. Walker and N.P. James (eds.). Geological Association of Canada, St. Johns, Newfoundland, Canada, p. 349-373.

Kennedy, W.J. and Garrison, R.E. 1975. Morphology and genesis of nodular chalks and hardgrounds in the upper Cretaceous of southern England. Sedimentology, v. 22 (3), p. 311-386.

Kiessling, W., Flügel, E. and Golonka, J. 1999. Paleoreef maps: evaluation of a comprehensive database on phanerozoic reefs. American Association of Petroleum Geologists Bulletin, v. 83 (10), p. 1552-1587.

Killops, S.D. and Killops, V.J. 1993. An Introduction to Organic Geochemistry. Longman, Harlow, 265p.

Klingspor, A.M. 1969. Middle Devonian Muskeg evaporites of western Canada. American Association of Petroleum Geologists Bulletin, v. 53 (4), p. 927-948.

Klovan, J.E. 1974. Development of western Canadian Devonian reefs and comparison with Holocene analogues. The American Associatoin of Petroleum Geologists Bulletin, v. 58 (5), p. 787-799.

Langton, J.R. and Chin, G.E. 1968. Rainbow Member facies and related reservoir properties, Rainbow Lake, Alberta. Bulletin of Canadian Petroleum Geology, v. 16 (1), p. 104-143.

Law, J. 1955. Geology of northwestern Alberta and adjacent areas. American Association of Petroleum Geologists Bulletin, v. 39 (10), p. 1927-1978.

Lee, C. 1992. Controls on organic carbon preservation: the use of stratified water bodies to compare intrinsic rates of decomposition in oxic and anoxic systems. Geochimica et Cosmochimica Acta, v. 56, p. 3323-3335.

Leggett, J.K. 1985. Deep-sea pelagic sediments and palaeo-oceanography; a review of recent progress. *In:* Sedimentology; Recent Developments and Applied Aspects. P.J. Brenchley and B.P.J. Williams (eds.). Meeting: British Sedimentological Research Group Annual Meeting, p. 95-118.

Lipps, J.H. 1993. 1 Introduction to fossil prokaryotes and protists. *In:* Fossil Prokaryotes and Protists. J.H. Lipps (ed.). Blackwell Scientific Publications, Boston, p. 1-10.

Maiklem, W.R., Bebout, D.G. and Glaister, R.P. 1969. Classification of anhydrite – a practical approach. Bulletin of Canadian Petroleum Geology, v. 17 (2), p. 194-233.

Martindale, W. and MacDonald, R.W. 1989. Sedimentology and diagenesis of the Winnipegosis Formation, Tableland area, Southeast Saskatchewan. *In:* Geology and Reservoir Heterogeneity. P.G. Aukes (chair), J. den Haan and T. Webb (eds.). Canadian Society of Petroleum Geologists Core Conference, p. 2.1-2.52.

McCamis, J.G. and Griffith, L.S. 1967. Middle Devonian facies relations, Zama area, Alberta. American Association of Petroleum Geologsists, Bulletin, v. 52 (10), p. 1899-1924.

McCrossan, R.G. 1958. Sedimentary "boudinage" structures in the Upper Devonian Ireton Formation of Alberta. Journal of Sedimentary Petrology, v. 28 (3), p. 316-320.

McIntyre, F.J., Hunter, D.S., Wong, F. and Fong, D. 1996. Redeveloping mature miscible flood reservoirs with horizontal wells: a summary of six years of experience. Journal of Canadian Petroleum Technology, v. 35 (3), p. 54-62.

Meijer Drees, N.C. 1994. Devonian Elk Point Group of the Western Canada Sedimentary Basin. *In:* Geological Atlas of the Western Canada Sedimentary Basin. G.D. Mossop and I. Shetsen (comps.). Canadian Society of Petroleum Geologists and the Alberta Research Council, p. 129-147.

Mendelson, C.V. 1993. 6 – Acritarchs and prasinophytes. *In:* Fossil Prokaryotes and Protists. J.H. Lipps (ed.). Blackwell Scientific Publications, Boston, p. 77-104.

Meybeck, M. 1982. Carbon, nitrogen, and phosphorus transport by world rivers. American Journal of Science, v. 282, p. 401-450.

Moore, P.F. 1988. Devonian geohistory of the western interior of Canada. *In*: Devonian of the World. N.J. McMillan, A.F. Embry and D.J. Glass, (eds.). Canadian Society of Petroleum Geologists, Memoir 14, v. 1, Calgary, p. 67-84.

Morrow, D.W. 1990. Dolomite – Part 1: the chemistry of dolomitization and dolomite precipitation. *In:* Diagenesis. I.A. McIlreath, D.W. Morrow (eds.). Geoscience Canada Reprint Series 4, p. 113-123.

Müller, P.J. and Suess, E. 1979. Productivity and sedimentation rate, and sedimentary organic matter in the oceans – I. Organic carbon preservation. Deep-Sea Research, v. 26A, p. 1347-1362

Mullins, H.T., Neumann, A.C., Wilber, R.J. and Boardman, M.R. 1980. Nodular carbonate sediment on Bahamian slopes; possible precursors to nodular limestones. Journal of Sedimentary Petrology, v. 50 (1), p. 117-131.

Nelson, S.J. 1970. The face of Ttime; the Geological History of Western Canada. Alberta Society of Petroleum Geologists, Calgary, Alberta, Canada, p. 133.

Nikakhtar, B., Kantzas, A., De Wit, P., Pow, M. and George, A. 1996. On the characterization of rock/fluid and fluid/fluid interactions in carbonate rocks using the ultracentrifuge. Journal of Canadian Petroleum Technology, v. 35 (1), p. 47-56.

Noble, J.P.A. and Howells, K.D.M. 1974. Early marine lithification of the nodular limestones in the Silurian of New Brunswick. Sedimentology, v. 21 (4), p. 597-609.

Obermajer, M.R. 1997. Thermal maturity and petroleum potential of the Paleozoic strata in southwestern Ontario, Unpublished Ph.D. Thesis, University of Western Ontario, London, Ontario, Canada, p. 330.

Osadetz K.G., Snowdon, L.R., Brooks, P.W. and Rygh, M.E. 1990. Progress identifying oil families and effective sources in Williston Basin. American Association of Petroleum Geologists Bulletin, v. 74 (8), p. 1340.

Osadetz, K.G., Brooks, P.W. and Snowdon, L.R. 1992. Oil families and their sources in Canadian Williston basin (southeastern Saskatchewan and southwestern Manitoba). Bulletin of Canadian Petroleum Geology, v. 40, p. 254-273.

Parrish, J.T. 1982. Upwelling and petroleum source beds, with reference to Paleozoic. American Association of Petroleum Geologists Bulletin, v. 66, p. 750-774.

Parrish, J.T. 1987. Paleo-upwelling and the distribution of organic-rich rocks. *In:* Marine Petroleum Source Rocks. J. Brooks and A.J. Fleet (eds.). Geological Society Special Publication No. 26, p. 199-205.

Parrish, J.T. and Curtis, R.L. 1982. Atmospheric circulation, upwelling, and organic-rich rocks in the Mesozoic and Cenozoic Eras. Palaeogeography, Palaeoclimatology, Palaeoecology, v. 40, p. 31-66.

Pederson, T.F. and Calvert, S.E. 1990. Anoxia vs. productivity: what controls the formation of organic-carbon-rich sediments and sedimentary rocks? American Association of Petroleum Geologists Bulletin, v. 74, p. 454-466.

Pederson, T.F., Shimmield, G.B. and Price, N.B. 1992. Lack of enhanced preservation of organic matter in sediments under the oxygen minimum on the Oman Margin. Geochimica et Cosmochimica Acta, v. 56, p. 545-551.

Peters, K.E. 1986. Guidelines for evaluating petroleum source rock using programmed pyrolysis. American Association of Petroleum Geologists Bulletin, v. 70 (3), p. 318-329.

Podruski, J.A., Barclay, J.E., Hamblin, A.D., Lee, P.H., Osadetz, K.G., Proctor, P.M. and Taylor, W.C. 1987. Part I: Resource endowment of conventional oil resources of

Western Canada (light & medium). Geological Survey of Canada, Paper 87-26, p. 1-26.

Reijers, T.J.A. and Hsu, K.J. 1986. Manual of Carbonate Sedimentology; a Lexicographical Approach. Academic Press, London, United Kingdom, 302p.

Reinson, G.E., Lee, P.J., Warters, W., Osadetz, K.G., Bell, L.L., Price, P.R., Trollope, F. and Barclay, J.E. 1993. Part I: Geological play analysis and resource assessment. Geological Survey of Canada, Bulletin 452, p. 1-127.

Rhoads, D.C. 1974. Organism-sediment relations on the muddy sea floor. Oceanography and Marine Biology, v. 12, p. 263-300.

Rosenberg, R. 1977. Benthic macrofaunal dynamics, production and dispersion on an oxygen-deficient estuary of west Sweden. Journal of Experimental Marine Biology and Ecology, v. 26, p. 107-133.

Round, F.E. 1981. The Ecology of Algae. Cambridge University Press, Cambridge, 653p.

Sami, T. and Desrochers, A. 1992. Episodic sedimentation on an Early Silurian, storm-dominated carbonate ramp, Becscie and Merrimack formations, Anticosti Island, Canada. Sedimentology, v. 39 (3), p. 355-381.

Sarjeant, W.A.S. and Downie, C. 1974. The classification of dinoflagellate cysts above generic level; a discussion and revisions. Special Publication – Birbal Sahni Institute of Palaeobotany, (3), p. 9-32.

Schmidt, V., McIlreath, I.A. and Budwill, A.E. 1985. Origin and diagenesis of Middle Devonian pinnacle reefs enclosed in evaporates, "A" and "E" Pools, Rainbow field, Alberta. *In:* Carbonate Petroleum Reservoirs. P.O. Roehl and P.W. Choquette (eds.). Springer-Verlag, New York, p. 143-160.

Scoffin, T.P., 1987. Chapter 7 – reef growth. *In:* An Introduction to Carbonate Sediments and Rocks (1st Edition). Chapman and Hall, New York, p. 77-88

Scotese, C.R. and Summerhayes, C.P. 1986. Computer model of paleoclimate predicts coastal upwelling in the Mesozoic and Cenozoic. Geobyte, v. 1 (3), p. 28-42.

Sherwin, D.F. 1962. Lower Elk Point section in east-central Alberta. Journal of the Alberta Society of Petroleum Geologists, v. 10 (4), p. 185-191.

Sibley, D.F. and Gregg, J.M. 1987. Classification of dolomite rock textures. Journal of Sedimentary Petrology, v. 57 (6), p. 967-975.

South, G.R. and Whittick, A. 1987. Introduction to Phycology. Blackwell, Oxford, 341p.

Stach, E., Mackowsky, M.-Th., Teichmüller, M., Taylor, G.H., Chandra, D. and Teichmüller, R. 1982. Stachs Textbook of Coal Petrology, 3rd edition. Gebrüder Bomtraeger, Berlin, 535p.

Stanford, R.L. 1989. Sedimentology and diagenesis of the Winnipegosis Formation, southeastern Saskatchewan. Unpublished M.Sc. Thesis, University of Alberta, Edmonton, Alberta, Canada, 137p.

Stanley, G.D. and Swart, P.K. 1995. Evolution of the coral-zooxanthellae symbiosis during the Triassic; a geochemical approach. Paleobiology, v. 21 (2), p. 179-199.

Stasiuk, L.D. 1993. Algal bloom episodes and the formation of bituminite and micrinite in hydrocarbon source rocks: evidence from the Devonian and Mississippian, northern Williston Basin, Canada. International Journal of Coal Geology, v. 24. p. 195-210.

Stasiuk, L.D. 1994. Oil prone alginite macerals from organic-rich Mesozoic and Paleozoic strata, Saskatchewan, Canada. Marine and Petroleum Geology, v. 11, p. 208-218.

Stasiuk, L.D. 1999. Microscopic studies of sedimentary organic matter: key to understanding organic-rich strata, with Paleozoic examples from Western Canada Basin. Geoscience Canada, v. 26 (4), p. 149-172.

Stasiuk, L.D., Osadetz, K.G., Goodarzi, F. and Gentzis, T. 1991. Organic microfacies and basinal tectonic control on source rock accumulation; a microscopic approach with examples from an intracratonic and extensional basin. International Journal of Coal Geology, v. 19, p. 457-481.

Stasiuk, L.D., Osadetz, K.G. and Potter, J. 1990. Fluorescence spectral analysis and hydrocarbon exploration; examples from Paleozoic potential source rocks, Saskatchewan. Meeting: Modern Exploration Techniques. L.S. Beck and C.T. Harper (eds.). Special Publication – Saskatchewan Geological Society, v. 10, p. 242-251.

Stasiuk, L.D., Wendte, J. and Chow, N. 1995. The application of organic petrography in evaluating productivity versus preservational controls on accumulation of

organic-rich carbonate successions. Abstracts with Programs – Geological Society of America, v. 27 (6), p. 442.

Stearn, C.W. and Carroll, R.L. 1989. Paleontology; The Record of Life. John Wiley and Sons, New York, NY, United States, 453p.

Stoakes, F.A. 1980. Nature and control of shale basin fill and its effect on reef growth and termination: Upper Devonian Duvernay and Ireton formations of Alberta, Canada. Bulletin of Canadian Petroleum Geology, v. 28, p. 345-410.

Stopes, M.C. 1935. On the petrology of banded bituminous coal. Colliery Guardian, v. 150 (3864), p. 111-113.

Suess, E. 1980. Particulate organic carbon flux in the oceans – surface productivity and oxygen utilization. Nature, v. 288, p. 260-263.

Taylor, G.H., Teichmüller, M., Davis, A., Diessel, C.F.K., Littke, R. and Robert, P. 1998. Organic Petrology. Gebrüder Bomtraeger, Berlin, 704p.

Terry, R.D. and Chilingar, G.V. 1955. Summary of "Concerning some additional aids in studying sedimentary formations," by M. S. Shvetsov. Journal of Sedimentary Petrology, 25 (3), p. 229-234.

Tissot, B.P. 1984. Recent advances in petroleum geochemistry applied to hydrocarbon exploration. American Association of Petroleum Geologists, v. 68 (5), p. 545-563.

Tissot, B., Durand, B., Espitalié, J., and Combaz, A. 1974. Influence of nature and diagenesis of organic matter in formation of petroleum. AAPG Bulletin, v. 58, p. 488-506.

Tissot, B.P. and Welte, D.H. 1984. Petroleum Formation and Occurrence, 2nd edition. Springer-Verlag, Berlin, 699p.

Traverse, A. 1988. Paleopalynology, Unwin Hyman, Boston, 600p.

Tribovillard, N., Desprairies, A., Lallier-Vergès, E., Bertrand, P., Moureau, N., Ramdanai, A., Ramanampisoa, L. 1994. Geochemical study of organic-matter rich cycles from the Kimmeridge Clay Formatoin of Yorkshire (UK): productivity versus anoxia. Palaeogeography, Palaeoclimatology, Palaeoecology, v. 108, p. 165-181.

Tucker, M.E., Kendall, A.C. 1973. The diagenesis and low-grade metamorphism of Devonian styliolinid-rich pelagic carbonates from West Germany; possible

analogues of recent pteropod oozes. Journal of Sedimentary Petrology, v. 43 (3), p. 672-687.

Tyson, R.V. 1987. The genesis and palynofacies characteristics of marine petroleum source rocks. *In:* Marine Petroleum Source Rocks. J. Brooks and A.J. Fleet (eds.). Geological Society Special Publication No. 26, p. 47-67.

Tyson, R.V. 1993. Palynofacies analysis. *In:* Applied Micropaleontology. D.G. Jenkins (ed.). Kluwer Academic, Netherlands, p. 153-191.

Tyson, R.V. 1995. Sedimentary Organic Matter: Organic Facies and Palynofacies. Chapman and Hall, London, 615p.

Tyson, R.V. 2001. Sedimentation rate, dilution, preservation and total organic carbon: some results of a modeling study. Organic Geochemistry, v. 32, p. 333-339.

Tyson, R.V. and Pearson, T.H. 1991. Modern and ancient continental shelf anoxia: an overview. *In:* Modern and Ancient Continental Shelf Anoxia. R.V. Tyson and T.H. Pearson (eds.). Geological Society Special Publication No. 58, p. 1-24.

Van Cappellen, P. and Canfield, D.E. 1993. Lack of evidence for enhanced preservation of sedimentary organic matter in the oxygen minimum of the Gulf of California: Comment. Geology, Boulder, v. 21 (6), p. 570-571.

Walsh, P.R.H. 1986. Technical paper number twelve - development of the Zama basin and Upper Keg River reefs. *In:* Ontario Petroleum Institute Inc. Twenty-Fifth Annual Conference, p. 1-43

Wanless, H.R. 1979. Role of physical sedimentation in carbonate-bank growth. American Association of Petroleum Geologists Bulletin, v.63 (3), p. 547.

Wendte, J.C. 1992a. Chapter 1 – Overview of the Devonian of the Western Canada Sedimentary Basin. *In:* Devonian-Early Mississippian Carbonates of the Western Canada Sedimentary Basin: A Sequence Stratigraphic Framework. J. Wendte, F.A. Stoakes and C.V. Campbell (authors). Society for Sedimentary Geology (SEPM) Short Course No. 28, p. 1-24.

Wendte, J.C. 1992b. Chapter 2 – Cyclicity of Devonian strata in the Western Canada Sedimentary Basin. *In:* Devonian-Early Mississippian Carbonates of the Western Canada Sedimentary Basin: A Sequence Stratigraphic Framework. J. Wendte,

F.A. Stoakes and C.V. Campbell (authors). Society for Sedimentary Geology (SEPM) Short Course No. 28, p. 25-40.

Wendte, J.C. 1992c. Chapter 3 – Platform evolution and its control on reef inception and localization. *In:* Devonian-Early Mississippian Carbonates of the Western Canada Sedimentary Basin: A Sequence Stratigraphic Framework. J. Wendte, F.A. Stoakes and C.V. Campbell (authors). Society for Sedimentary Geology (SEPM) Short Course No. 28, p. 41-88.

Wentworth, C.K., 1922. A scale of grade and class terms for clastic sediments. Journal of Geology, v. 30, p. 377-392.

Wetzel, A. 1991. Stratification in black shales; depositional models and timing; an overview. *In:* Cycles and Events in Stratigraphy. G. Einsele, W. Ricken, A. Seilacher (eds.). Springer Verlag, Berlin, Federal Republic of Germany, p. 508-523.

White, A., Cannell, M.G.R., and Friend, A.D., 2000. The high-latitude terrestrial carbon sink: A model analysis. Global Change Biol. v. 6, p. 227-245

Williams, G.K. 1984. Some musings on the Devonian Elk Point Basin, western Canada. Bulletin of Canadian Petroleum Geology, v. 32 (2), p. 216-232.

Wilson, J.L. 1969. Microfacies and sedimentary structures in 'deeper water' lime mudstones, Depositional environments in carbonate rocks; a symposium. Special Publication – Society of Economic Paleontologists and Mineralogists, v. 14, p. 4-19.

Wilson, J.L. 1975. Carbonate Facies in Geologic History. Springer-Verlag, New York, N.Y., United States, 471p.

Wong, F.Y. and Fong, D.K. 1997. Developing a field strategy to eliminate crossflow along a horizontal well. Journal of Canadian Petroleum Technology, v. 36 (9), p. 26-35.

Wood, R. 1993. Nutrients, predation and the history of reef-building. Palaios, v. 8, p. 526-543.

Wood, R. 1995. The changing biology of reef-building. Palaios, v. 10, p. 517-529.

Zenger, D.H. 1979. Primary textures in dolostones and recrystallized limestones: a technique for their microscopic study. Journal of Sedimentary Petrology, v. 49, p. 677-678.

APPENDIX A: FORMATION TOPS

The following table presents; 1) tops picks for the Chinchaga Formation, Lower Keg River Member, and Upper Keg River Member, 2) picks for the base and top of all organic-rich laminites identified in the study, 3) base and top of described core intervals, and 4) base and top of described cuttings intervals. Depths are provided in imperial and metric units and data is organized by sub-basin.

	Rainbow Sub-basin											
	00/6-32-107-09W6/0		00/04-16-108-07W6/0		00/04-09-109-08W6/0		00/06-32-109-08W6/0		00/12-33-109-08W6/0		00/04-30-110-09W6/0	
	meters	feet	meters	feet	meters	feet	meters	feet	meters	feet	meters	feet
Kelly Bushing (K.B.)	487.1	1598.1	498.3	1634.8	488.6	1603.0	535.5	1756.9	533.4	1750.0	438.0	1437.0
Top of Upper Keg River Member	1950.2	6398.2	1946.0	6384.4	1917.2	6289.9	1922.4	6307.0	1934.9	6348.0	1880.4	6169.2
Top of upper Rainbow laminite	1997.7	6554.1	1961.6	6435.6	1947.6	6389.7	1954.9	6413.6	1973.0	6473.0	1898.4	6228.3
Base of upper Rainbow laminite	2047.6	6717.8	1983.6	6507.8	1987.3	6519.9	1995.3	6546.2	1997.1	6552.1	1928.6	6327.4
Top of middle Rainbow laminite	2076.4	6812.3	2001.7	6567.2	2002.2	6568.8	2018.0	6620.7	2017.7	6619.7	1947.5	6389.4
Top of Lower Keg River Member	2076.4	6812.3	2001.7	6567.2	2002.2	6568.8	2018.0	6620.7	2017.7	6619.7	1947.5	6389.4
Base of middle Rainbow laminite	2077.8	6816.8	2003.1	6571.8	2003.6	6573.4	2019.4	6625.2	2018.9	6623.6	1948.5	6392.6
Top of lower Rainbow laminite	2084.3	6838.2	2010.0	6594.4	2011.4	6599.0	2027.0	6650.2	2027.3	6651.2	1953.9	6410.4
Base of lower Rainbow laminite	2089.1	6853.9	2012.2	6601.6	2015.9	6613.8	2033.1	6670.2	2031.9	6666.3	1957.1	6420.9
Top of Chinchaga	2117.7	6947.8	2047.6	6717.8	2043.0	6702.7	2057.4	6749.9	2057.4	6749.9	1982.4	6503.9
Top of cored interval described	2040.6	6695.0	1984.9	6512.0	1976.3	6484.0	1978.2	6490.0	1946.8	6387.0	1941.6	6370.0
Base of cored interval described	2122.3	6963.0	2003.1	6572.0	2048.0	6719.0	2048.0	6719.0	2023.9	6640.0	1956.8	6420.0
Top of cuttings interval described	n/a	n/a	1975.1	6480.0	n/a	n/a	n/a	n/a	n/a	n/a	1917.2	6290.0
Base of cuttings interval described	n/a	n/a	1981.2	6500.0	n/a	n/a	n/a	n/a	n/a	n/a	1929.4	6330.0

	Meander Sub-basin	
	00/07-07-113-21W5/0	
	meters	feet
Kelly Bushing (K.B.)	398.7	1308.1
Top of Upper Keg River Member	1388.3	4554.7
Top of upper Meander laminite	1389.9	4560.0
Base of upper Meander laminite	1391.7	4565.9
Top of the lower Meander laminite	1393.5	4572.0
Top of Lower Keg River Member	1403.1	4603.3
Base of lower Meander laminite	1403.1	4603.3
Top of Chinchaga	1444.8	4740.1
Top of cored interval described	1375.3	4512.0
Base of cored interval described	1449.6	4756.0
Top of cuttings interval described	n/a	n/a
Base of cuttings interval described	n/a	n/a

	Zama Sub-basin					
	00/04-19-116-04W6/0		00/10-21-116-05W6/0		00/05-36-117-06W6/0	
	meters	feet	meters	feet	meters	feet
Kelly Bushing (K.B.)	377.0	1236.9	382.2	1253.9	470.9	1544.9
Top of Upper Keg River Member	1526.1	5006.8	1584.9	5199.7	1641.8	5386.4
Top of upper Zama laminite	1538.6	5047.8	1586.4	5204.7	1653.3	5424.1
Base of upper Zama laminite	1549.6	5083.9	1587.2	5207.3	1661.3	5450.4
Top of Lower Zama Laminite	1570.3	5151.8	1598.2	5243.4	1680.1	5512.1
Top of Lower Keg River Member	1570.3	5151.8	1598.2	5243.4	1680.1	5512.1
Base of lower Zama laminite	1574.5	5165.6	1601.5	5254.2	1685.8	5530.8
Top of Chinchaga	1612.4	5290.0	1638.0	5374.0	1723.9	5655.8
Top of cored interval described	1525.5	5005.0	n/a	n/a	1970.2	6464.0
Base of cored interval described	1588.6	5212.0	n/a	n/a	1727.0	5666.0
Top of cuttings interval described	n/a	n/a	1612.4	5290.0	n/a	n/a
Base of cuttings interval described	n/a	n/a	1627.6	5340.0	n/a	n/a
Top of cuttings interval described	n/a	n/a	1585.0	5200.0	n/a	n/a
Base of cuttings interval described	n/a	n/a	1603.2	5260.0	n/a	n/a

APPENDIX B: CORE DESCRIPTIONS

This appendix contains completed core logging sheets for the core intervals that were described in each of the wells studied. Core logging sheets are arranged by well location in ascending order. Lithofacies designations are indicated on Encl. 2.

Well Location	Sub-basin	Core Interval Examined (depth in feet)	Page #'s
00/06-32-107-09W6/0	Rainbow	6695 - 6963	B3 - B12
00/04-16-108-07W6/0	Rainbow	6512 - 6572	B13 – B16
00/04-09-109-08W6/0	Rainbow	6484 - 6719	B17 – B29
00/06-32-109-08W6/0	Rainbow	6490 - 6719	B30 - B40
00/12-33-109-08W6/0	Rainbow	6387 - 6640	B41 - B53
00/04-30-110-09W6/0	Rainbow	6370 - 6420	B54 – B56
00/07-07-113-21W5/0	Meander	4512 - 4756	B57 – B68
00/04-19-116-04W6/0	Zama	5005 - 5212	B69 – B80
00/05-36-117-06W6/0	Zama	5464 - 5666	B81 – B91

LEGEND

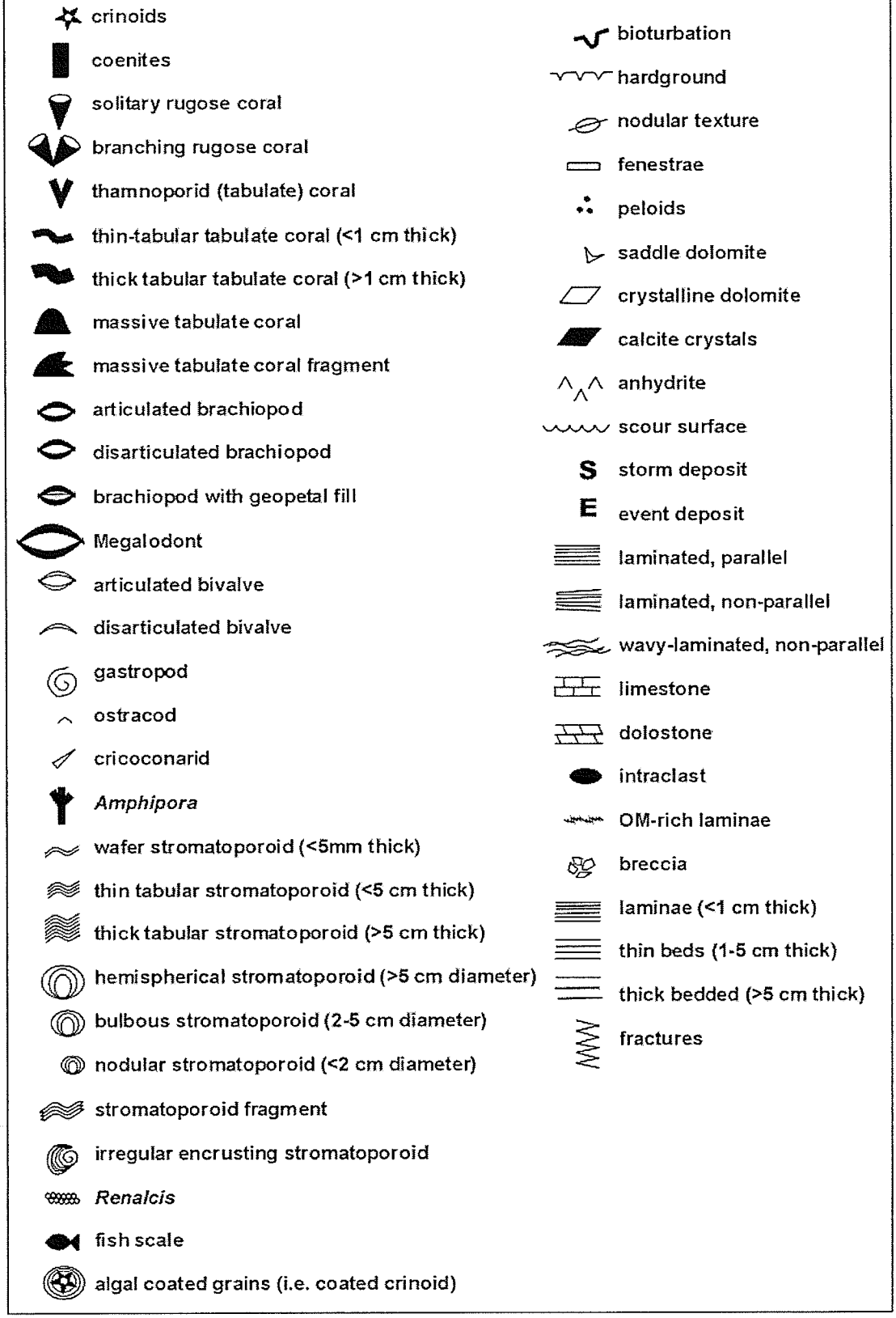
crinoids
coenites
solitary rugose coral
branching rugose coral
thamnoporid (tabulate) coral
thin-tabular tabulate coral (<1 cm thick)
thick tabular tabulate coral (>1 cm thick)
massive tabulate coral
massive tabulate coral fragment
articulated brachiopod
disarticulated brachiopod
brachiopod with geopetal fill
Megalodont
articulated bivalve
disarticulated bivalve
gastropod
ostracod
cricoconarid
Amphipora
wafer stromatoporoid (<5mm thick)
thin tabular stromatoporoid (<5 cm thick)
thick tabular stromatoporoid (>5 cm thick)
hemispherical stromatoporoid (>5 cm diameter)
bulbous stromatoporoid (2-5 cm diameter)
nodular stromatoporoid (<2 cm diameter)
stromatoporoid fragment
irregular encrusting stromatoporoid
Renalcis
fish scale
algal coated grains (i.e. coated crinoid)
bioturbation
hardground
nodular texture
fenestrae
peloids
saddle dolomite
crystalline dolomite
calcite crystals
anhydrite
scour surface
S storm deposit
E event deposit
laminated, parallel
laminated, non-parallel
wavy-laminated, non-parallel
limestone
dolostone
intraclast
OM-rich laminae
breccia
laminae (<1 cm thick)
thin beds (1-5 cm thick)
thick bedded (>5 cm thick)
fractures

Date: July

Well Location: 6-3[illegible]-107-9W6

Core Interval:

Correction Factor (Log to Core Conversion): Core -2.5 = log

Log Depth	Colour	Structures	Skeletal	Lithology: Graphic Log	Limestone	Dolostone	Anhydrite	Mudstone	Wackestone	Packstone	Grainstone	Rudstone	Floatstone	Boundstone	Porosity: Interparticle	Intraparticle	Moldic	Vuggy	Fenestral	Fracture	Other: Anhydrite	Oil/Bitumen	% Dol.: Low	Moderate	High	Samples	Comments	Depositional Environment
6690																												
																											TOP OF CORE OBSERVED	
6695																											LAMINATED	DISTAL RAMP
																											LIME MUDSTONE?	
6697																											F	
																										-116		
6699																											CRINOIDAL PACKSTONE	REEF TOE OF SLOPE
																											↑	TOE
																											Foreslope Rubble	OF SLOPE
																											and Sands	
																									?	-115	Interfingering	
																										↓Not	logged	
																											but good G&H	
																											op. for fossil ID.	
																											↓	
6688																											CRINOIDAL GRAINSTONE	FORESLOPE
6689																											G	SANDS

Date:

Core Interval:

Well Location: 6-32-107-9W6

Correction Factor (Log to Core Conversion): Core -2.5 = log depth

2

Log Depth	Colour	Structures	Skeletal	Lithology: Graphic Log	Limestone	Dolostone	Anhydrite	Mudstone	Wackestone	Packstone	Grainstone	Rudstone	Floatstone	Boundstone	Porosity: Interparticle	Intraparticle	Moldic	Vuggy	Fenestral	Fracture	Other: Anhydrite	Oil/Bitumen	% Dol.: Low	Moderate	High	Samples	Comments	Depositional Environment
6790																											CRINOID GRAINSTONE	FORESLOPE SANDS
																										G	TOE-OF SLOPE
																										~~CRINOID PACKSTONE~~	~~TOE OF SLOPE~~
																										CRINOID GRAINSTONE	FORESLOPE SANDS
6793																											G	TOE OF SLOPE
																									-114		
																										CRINOIDAL	REEF TOE-
																										PACKSTONE	-OF-SLOPE
6796																										-113		
																										H	
6798																												
6800																											-low interparticle	
																										porosity ~1%	
																										" "	
																										-trace anhydrite	
																										~2% in places	

Date:

Core Interval:

Well Location: 6-32-107-9W6

Correction Factor (Log to Core Conversion): Core -2.5 = log depth

3

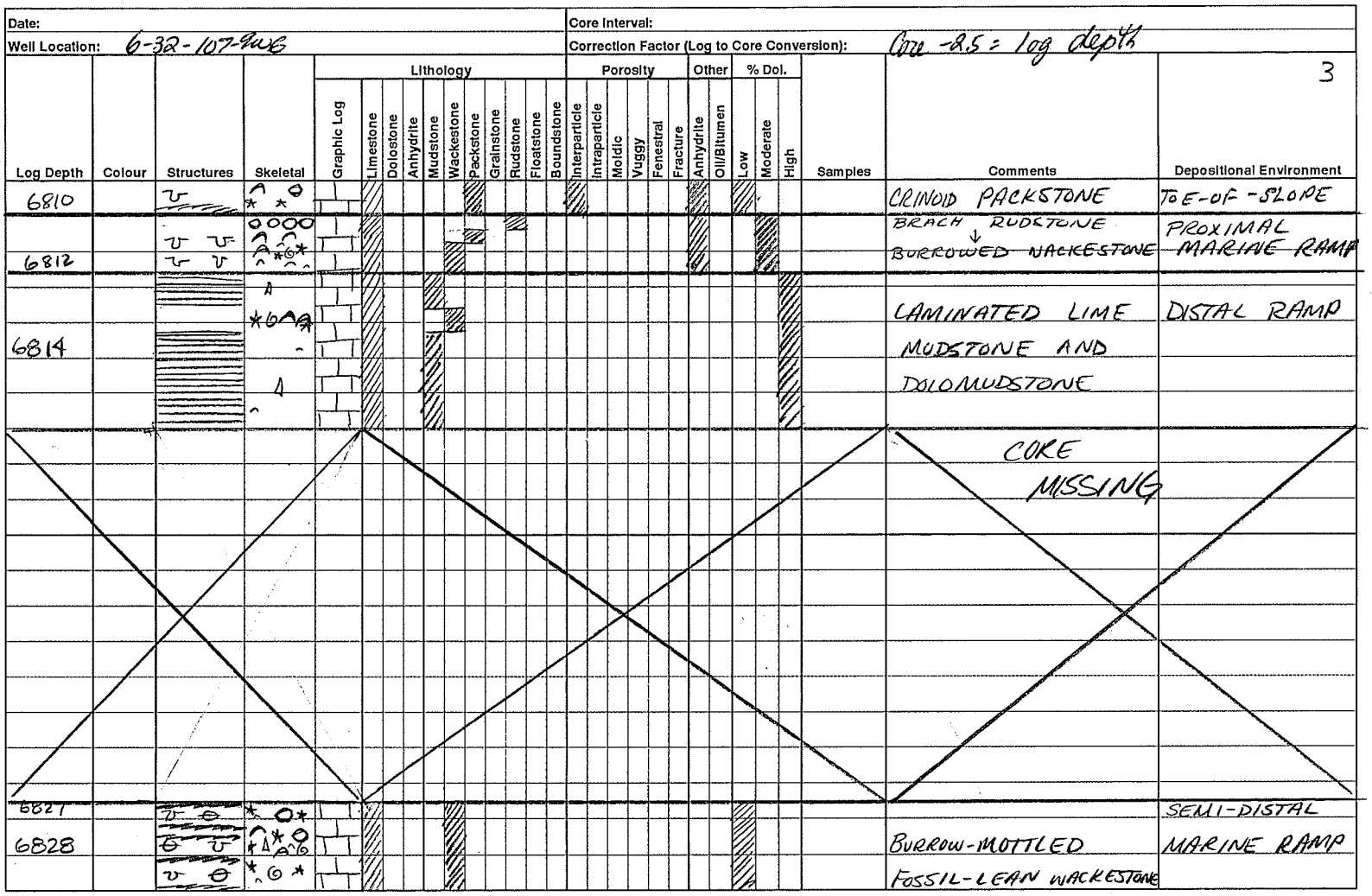

Date:

Core Interval:

Well Location: 6-32-107-9W6

Correction Factor (Log to Core Conversion): Core -2.5 = log depth

4

Log Depth	Colour	Structures	Skeletal	Lithology: Graphic Log	Limestone	Dolostone	Anhydrite	Mudstone	Wackestone	Packstone	Grainstone	Rudstone	Floatstone	Boundstone	Porosity: Interparticle	Intraparticle	Moldic	Vuggy	Fenestral	Fracture	Other: Anhydrite	Oil/Bitumen	% Dol.: Low	Moderate	High	Samples	Comments	Depositional Environment
6830	dk grey																										BURROW-MOTTLED FOSSIL-LEAN WACKESTONE	SEMI-DISTAL MARINE RAMP
6836																												
	black and tan																									109	LAMINATED LIME MUDSTONE -mod. dolomitization	DISTAL RAMP
6840																											BURROW MOTTLED FOSSIL-LEAN WACKESTONE	SEMI-DISTAL MARINE RAMP
6843																										108	only low degree of partial dolomitization	
6847																										107		

Date:

Well Location: 6-32-107-9W6

Core Interval:

Correction Factor (Log to Core Conversion): Core -2.5 = log depth

5

Log Depth	Colour	Structures	Skeletal	Lithology: Graphic Log	Limestone	Dolostone	Anhydrite	Mudstone	Wackestone	Packstone	Grainstone	Rudstone	Floatstone	Boundstone	Porosity: Interparticle	Intraparticle	Moldic	Vuggy	Fenestral	Fracture	Other: Anhydrite	Oil/Bitumen	% Dol.: Low	Moderate	High	Samples	Comments	Depositional Environment
6850																											LAMINATED LIME-	DISTAL RAMP
																										-106	MUDSTONE	
6852																											(Partially Dolomitized)	
6853																										-105		
6854																											LIME-MUDSTONE TO VERY FOSSIL-LEAN CRINOIDAL WACKESTONE	DISTAL RAMP
6857																											BURROW MOTTLED CRINOIDAL WACKESTONE	OPEN MARINE RAMP
																										-104		
6860																											- Partially Dolomitized	- slightly shallower than previous
6863																										-103	LIME MUDSTONE TO VERY FOSSIL- LEAN WACKESTONE	DISTAL RAMP
6865																												
6866																											Bedded - somewhat disrupted	

Date:

Core Interval:

Well Location: 6-32-107-9W6

Correction Factor (Log to Core Conversion): Core - 2.5 = log depth

6

Log Depth	Colour	Structures	Skeletal	Lithology: Graphic Log	Limestone	Dolostone	Anhydrite	Mudstone	Wackestone	Packstone	Grainstone	Rudstone	Floatstone	Boundstone	Porosity: Interparticle	Intraparticle	Moldic	Vuggy	Fenestral	Fracture	Other: Anhydrite	Oil/Bitumen	% Dol.: Low	Moderate	High	Samples	Comments	Depositional Environment
6870																											LIME MUDSTONE	DISTAL RAMP
																											TO VERY FOSSIL-	
6872																										-102	LEAN WACKESTONE	
																											Bedded - somewhat disrupted	
6876																												
6879	lt grey																										LAMINATED LIME MUDSTONE	SEMI-DISTAL RAMP
6880	brown																										Partially Dolomit-	MARINE RAMP
6881	and																										ized Crinoidal	PROXIMAL
	lt grey																										Wackestone	
6883																												
																											partially dolomitized ~50%	
																											-fossils more abundant than below	

B8

Date: | Core Interval:

Well Location: 6-32-107-9w6 | Correction Factor (Log to Core Conversion): Core -2.5 = log depth

7

Log Depth	Colour	Structures	Skeletal	Lithology: Graphic Log	Limestone	Dolostone	Anhydrite	Mudstone	Wackestone	Packstone	Grainstone	Rudstone	Floatstone	Boundstone	Porosity: Interparticle	Intraparticle	Moldic	Vuggy	Fenestral	Fracture	Other: Anhydrite	Oil/Bitumen	% Dol.: Low	Moderate	High	Samples	Comments	Depositional Environment
6890	Brown																										Partially Dolomitized	PROXIMAL TO
6891	and																										Fossil Lean	SEMI-DISTAL
	Blk																										Crinoidal	MARINE RAMP
6893	Grey																									#01	Wackestone	
																											>30% dolomitized	
																											Nodular &	
																											BURROW MOTTLED	
6900																												
6902																											LAMINATED TO THIN	BEDDED
																											FOSSIL-LEAN	SEMI-DISTAL
																											CRINOIDAL	MARINE
																											WACKESTONE	RAMP
																											<20% dolomitized	-still deeper
6907																											-partially	than prev.
																											dolomitized matrix	facies
6909																												

Date: July 4/2000
Well Location: 6-38-107-9W6

Core Interval:
Correction Factor (Log to Core Conversion): -Core -2.5 = Log Depth-

8

Log Depth	Colour	Structures	Skeletal	Graphic Log	Lithology: Limestone	Dolostone	Anhydrite	Mudstone	Wackestone	Packstone	Grainstone	Rudstone	Floatstone	Boundstone	Porosity: Interparticle	Intraparticle	Moldic	Vuggy	Fenestral	Fracture	Other: Anhydrite	Oil/Bitumen	% Dol.: Low	Moderate	High	Samples	Comments	Depositional Environment
6905									See Next Sheet																			
6909	v.dk grey																										CRINOIDAL WACKESTONE - FOSSIL-LEAN - Partially Dolomitized Bedded to massive OM-rich wisps // bedding	SEMI-DISTAL MARINE RAMP - bedded - fossil-lean - non burrowed
6916																												
6920																												
6920																												
6921									CORE MISSING - INCOMPLETE																		RECOVERY	
6923	dk grey																										CRINOIDAL WACKESTONE - Fossil LEAN	PROXIMAL MARINE RAMP - slightly deeper - less fossils - less bioturbation
6924																												
6926																												

Date: July 9/2000
Well Location: 6-3[illegible]-107-9W6
Core Interval:
Correction Factor (Log to Core Conversion): Core −2.5 = Log

Log Depth	Colour	Structures	Skeletal	Graphic Log	Lithology: Limestone	Dolostone	Anhydrite	Mudstone	Wackestone	Packstone	Grainstone	Rudstone	Floatstone	Boundstone	Porosity: Interparticle	Intraparticle	Moldic	Vuggy	Fenestral	Fracture	Other: Anhydrite	Oil/Bitumen	% Dol.: Low	Moderate	High	Samples	Comments	Depositional Environment
6928																											CRINOIDAL WACKESTONE	PROXIMAL MARINE RAMP
																											Minor Anhydrite ↳replacive.	
6934																											- FOSSIL LEAN	
6936																												
6938																											↙ OM-rich	
																										0098 0097	BURROW MOTTLED TO NODULAR FOSSIL-RICH WACKESTONE	PROXIMAL MARINE RAMP
6942																												
6944																											Minor anhydrite -matrix partially dolomitized	

9

B11

Date: July 4/2000 | Core Interval:

Well Location: 6-38-107-9W6 | Correction Factor (Log to Core Conversion): CORE −2.5 = LOG

Log Depth	Colour	Structures	Skeletal	Lithology: Graphic Log	Limestone	Dolostone	Anhydrite	Mudstone	Wackestone	Packstone	Grainstone	Rudstone	Floatstone	Boundstone	Porosity: Interparticle	Intraparticle	Moldic	Vuggy	Fenestral	Fracture	Other: Anhydrite	Oil/Bitumen	% Dol.: Low	Moderate	High	Samples	Comments	Depositional Environment
6948																											DOLOMUDSTONE	MESOSALINE
																											-Anhydrite laths	BASIN
6951																											OM-rich laminae	HYPERSALINE
																											BEDDED MASSIVE	HYPERSALINE
																											ANHYDRITE	BASIN
																											CHINCHAGA	
6958																												
6963																												
																											BASE OF CORE	DESCRIBED

Date: June 15/2000 | Core Interval:

Well Location: 4-16-108-7W6 | Correction Factor (Log to Core Conversion): add 2.5' to core

Log Depth	Colour	Structures	Skeletal	Lithology: Graphic Log	Limestone	Dolostone	Anhydrite	Mudstone	Wackestone	Packstone	Grainstone	Rudstone	Floatstone	Boundstone	Porosity: Interparticle	Intraparticle	Moldic	Vuggy	Fenestral	Fracture	Other: Anhydrite	Oil/Bitumen	% Dol.: Low	Medium	High	Samples	Comments	Depositional Environment
																											Add 2.5' to all depths recorded for correction factor	
6510																												
																										TOP	OF CORE	
6512																											Pelloidal/Skeletal	OPEN
6513																											Packstone?	MARINE RAMP
																												-shifting
																											- becomes slightly nodular.	carbonate
																												sands
																											Moldic - Partial Moldic	
6519																											porosity ~1%	

Date: June 15 /2000 | Core Interval:

Well Location: 4-16-108-7W6 | Correction Factor (Log to Core Conversion): 2.5' (add 2.5' to core)

2

Log Depth	Colour	Structures	Skeletal	Lithology: Graphic Log	Limestone	Dolostone	Anhydrite	Mudstone	Wackestone	Packstone	Grainstone	Rudstone	Floatstone	Boundstone	Porosity: Interparticle	Intraparticle	Moldic	Vuggy	Fenestral	Fracture	Other: Anhydrite	Oil/Bitumen	% Dol.: Low	Medium	High	Samples	Comments	Depositional Environment
6520																											Pelloidal / Skeletal Packstone? - white card. Vuggy Porosity ~1%. Interparticle = Intercrystalline ~1% porosity	OPEN MARINE RAMP - shifting sand input / limits biota
6525	med grey																										CRINOID - BRACH - STROM WACKESTONE	OPEN MARINE RAMP - fossil rich
6527																												
6530																												
6532																												
6537																											Strom fragments house fenestral pores - Vugs: bitumen-lined	

Date: June 15/2000

Well Location: 4-16-108-7W6

Core Interval:

Correction Factor (Log to Core Conversion): 2.5' (add 2.5 to core

3

Log Depth	Colour	Structures	Skeletal	Lithology: Graphic Log	Limestone	Dolostone	Anhydrite	Mudstone	Wackestone	Packstone	Grainstone	Rudstone	Floatstone	Boundstone	Porosity: Interparticle	Intraparticle	Moldic	Vuggy	Fenestral	Fracture	Other: Anhydrite	Oil/Bitumen	% Dol.: Low	Medium	High	Samples	Comments	Depositional Environment
6540	med.																											OPEN MARINE
	grey																											RAMP
6542																												
																											Vuggy Porosity ~2%	
																											Intercrystalline porosity ~1%	
6546																												
6547	H-																										Crinoidal Dolowackestone	PROXIMAL
	med																										-bitumen in inter-par	MARINE RAMP
	grey																										ticle porosity	
6550																												
6553																											Vuggy porosity ~1%	
																											Anhydrite & Bitumen	
																											infill	
6557																											Intercrystalline	
																											porosity ~1%	
6559																												

Date: June 15/2000

Well Location: 4-16-108-7W6

Core Interval:

Correction Factor (Log to Core Conversion): Add 2.5' to core

4

Log Depth	Colour	Structures	Skeletal	Graphic Log	Lithology: Limestone	Dolostone	Anhydrite	Mudstone	Wackestone	Packstone	Grainstone	Rudstone	Floatstone	Boundstone	Porosity: Interparticle	Intraparticle	Moldic	Vuggy	Fenestral	Fracture	Other: Anhydrite	Oil/Bitumen	% Dol.: Low	Medium	High	Samples	Comments	Depositional Environment
6560																											Crinoidal Dolowackestone	PROXIMAL MARINE
																											relatively fossil lean	RAMP
6562	H.																										Laminated Dolomudstone	DISTAL RAMP
6563	grey																									0051	4% vuggy porosity	
6564	dk																									0050	Laminated to	DISTAL RAMP
	grey and																										Bedded Lime	
	brown																									0049	Mudstone	
6567																											- <10% fossils	
																											-fossils in concentrations	
																										0048 0047	only - Not in matrix	
6570	med.																									0046	Crinoidal Wackestone	PROXIMAL
	grey																										Anhydrite fracture fill <1% fracture porosity	MARINE RAMP
6572																										BASE	OF CORE	
6579																												

B16

Date: June /2000
Well Location: 4-9-109-8W6

Core Interval:
Correction Factor (Log to Core Conversion): 9.75 (add 9.75 to core depth

Log Depth	Colour	Structures	Skeletal	Lithology: Graphic Log	Limestone	Dolostone	Anhydrite	Mudstone	Wackestone	Packstone	Grainstone	Rudstone	Floatstone	Boundstone	Porosity: Interparticle	Intraparticle	Moldic	Vugay	Fenestral	Fracture	Other: Anhydrite	Oil/Bitumen	% Dol.: Low	Medium	High	Samples	Comments	Depositional Environment
6470																												①
6480																												
6484																										TOP OF CORE DESCRIBED		
		S																									Crinoidal Dolowackestone -Fossil lean.	Semi-Distal/RAMP ↓
6487																											Thamnoporid-Stromatoporoid Dolopackstone -Fossil-rich	REEF FORESLOPE ↓
	?																											
6489																												

B17

Date: June 1200
Well Location: 4-9-109-8W6

Core Interval:
Correction Factor (Log to Core Conversion): core +9.75 = log

Log Depth	Colour	Structures	Skeletal	Lithology: Graphic Log	Limestone	Dolostone	Anhydrite	Mudstone	Wackestone	Packstone	Grainstone	Rudstone	Floatstone	Boundstone	Porosity: Interparticle	Intraparticle	Moldic	Vuggy	Fenestral	Fracture	Other: Anhydrite	Oil/Bitumen	% Dol.: Low	Medium	High	Samples	Comments	Depositional Environment
6490																											Thamnoporid - Strom Dolopackstone - brecciated and fragmented base	REEF FORESLOPE OR (TOE OF SLOPE) (Rubble)
6495																											Peloidal Skeletal Dolograinstone? - microcrystalline → storm event or in situ → burrow mottled	REEF FORESLOPE - burrow mottled - crinoid dominated fauna (Sand)
6498																												
6500																											check classification using white card	
6506																											Interparticle = Intercrystalline porosity ~10% - Moldic porosity ~5% - Vuggy porosity ~5% Total porosity ~20%	
6509	red grey brn																										Crinoid-Brach Dolowackestone	TOE OF REEF

B18

7

Date:

Well Location: 4-9-109-8w6

Core Interval:

Correction Factor (Log to Core Conversion): Core +9.25 = log

(3)

Log Depth	Colour	Structures	Skeletal	Lithology: Graphic Log	Limestone	Dolostone	Anhydrite	Mudstone	Wackestone	Packstone	Grainstone	Rudstone	Floatstone	Boundstone	Porosity: Interparticle	Intraparticle	Moldic	Vuggy	Fenestral	Fracture	Other: Anhydrite	Oil/Bitumen	% Dol.: Low	Medium	High	Samples	Comments	Depositional Environment
6510																											Crinoid-Brach. Dolowackestone	TOE OF REEF
↑ KEG RIVER ↑																											Dolomudstone Porosity ~1% intercrystalline	DISTAL RAMP -laminated -lack of fossils
6514	med gy ↓																										Dolowackestone ?porosity ~30% -fossil lean matrix porosity ~1%	PROXIMAL RAMP ↓
6517	med gy ↓																										Dolopackstone -fossil rich -~30% porosity	OPEN MARINE RAMP ↓
6519	↓	S																										PROXIMAL RAMP ?
6520																	intercrystalline										Peloidal Skeletal Dolograinstone	↓
6521	H-med grey																										Crinoidal Dolowackestone -Fossil lean	PROXIMAL RAMP
6524	↓	S																									storm Event - large tabular coral fragment -leans towards mudstone <10% fossils -but dolomitization makes fossils hard to find	↓
6525																												

Date:

Well Location: 4-9-109-8W6

Core Interval:

Correction Factor (Log to Core Conversion): Core +9.5 = log

Log Depth	Colour	Structures	Skeletal	Lithology: Graphic Log	Limestone	Dolostone	Anhydrite	Mudstone	Wackestone	Packstone	Grainstone	Rudstone	Floatstone	Boundstone	Porosity: Interparticle	Intraparticle	Moldic	Vuggy	Fenestral	Fracture	Other: Anhydrite	Oil/Bitumen	% Dol.: Low	Medium	High	Samples	Comments	Depositional Environment
6530		S																									Crinoidal Wackestone - fossil lean	Proximal Ramp - slightly deeper than previous b/c more fossil-lean and nodular
6534		S																										
6535		S																										
6540																											-bitumen in large pores -many porosity types -also intercrystalline porosity -moldic, vuggy, and fenestral porosity only 10%	
6543		S																										
6546	H - med gry																										Crinoidal Dolowackestone -anhydrite in some vugs -abundant tabular corals (tabulates)	Prox. Ramp to open marine ramp

B20

Date:

Well Location: 4-9-109-8W6

Core Interval:

Correction Factor (Log to Core Conversion): Core +9.5=log

5

Log Depth	Colour	Structures	Skeletal	Lithology: Graphic Log	Limestone	Dolostone	Anhydrite	Mudstone	Wackestone	Packstone	Grainstone	Rudstone	Floatstone	Boundstone	Porosity: Interparticle	Intraparticle	Moldic	Vuggy	Fenestral	Fracture	Other: Anhydrite	Oil/Bitumen	% Dol.: Low	Medium	High	Samples	Comments	Depositional Environment
6550	med to																									-0031	dolomitized wackestone	Proximal Ramp
6551	lt grey																										high porosity ~20%	to open marine
																											-less nodular than prev.	ramp.
																											-fenestral in tabular coral	
																											-vugs lined w dolomite or anhydrite	
6555																											Crinoidal Wackestone	Proximal Ramp
																											Nodular.	shallower
																											-high porosity (~15%)	than prev.
																											in vugs	facies
																											-Vugs lined by	
6560																											dolomite, bitumen	
																											and occasionally	
																											anhydrite	
																											-fossil lean	
																											↳dolomitization shrouds	
																											fossils	
	↓	S																								-0030	Packstone - Storm concentration	
6567	v.dk grey/ brn																										Lime Mudstone - Wackestone calcite and anhydrite	Semi-Distal Ramp
																											filled articulate bivalve and brach. shells	-slight burrow mottling
6569																												Distal Ramp

B21

Date:

Core Interval:

Well Location: 4-9-109-8W6

Correction Factor (Log to Core Conversion): Core +9.5 = log

6

Log Depth	Colour	Structures	Skeletal	Lithology: Graphic Log	Limestone	Dolostone	Anhydrite	Mudstone	Wackestone	Packstone	Grainstone	Rudstone	Floatstone	Boundstone	Porosity: Interparticle	Intraparticle	Moldic	Vuggy	Fenestral	Fracture	Other: Anhydrite	Oil/Bitumen	% Dol.: Low	Medium	High	Samples	Comments	Depositional Environment
6570			*																								-fossil poor (<5%)	Distal Ramp
			⌒																								laminated lime mdst	-thin laminae
			*																								-partly dolomitized	undisturbed
6573																											Wackestone to Packstone	Proximal Ramp
6574																											depending on fossil	-continued
																											concentrations ie.	shallowing
6576																											in storm deposits	-more biota
																												-more storm
6578																											-crinoid holdfasts seen here	influence
6579																											anhydrite filled vug	
6580																												Semi-Distal Ramp
																												-bioturbated
																												more
																											anhydrite filled vugs	-more fossils
																											low porosity ~1%	∴ shallower than↓
6585			*																								Crinoidal Wackestone	Distal Ramp
			*																								- burrow mottled /	-laminated
			*																								nodular	-fossil lean
6588	med		*																								CRINOIDAL WACKESTONE	MARINE RAMP
	grey		*																								Massive to slightly mottled	SEMI-DISTAL

Date:

Well Location: 4-9-109-8 W6

Core Interval:

Correction Factor (Log to Core Conversion): Core 49.85 = log

7

Log Depth	Colour	Structures	Skeletal	Lithology: Graphic Log	Limestone	Dolostone	Anhydrite	Mudstone	Wackestone	Packstone	Grainstone	Rudstone	Floatstone	Boundstone	Porosity: Interparticle	Intraparticle	Moldic	Vuggy	Fenestral	Fracture	Other: Anhydrite	Oil/Bitumen	% Dol.: Low	Medium	High	Samples	Comments	Depositional Environment
6590																												
6592																												
6594																											Crinoidal Wackestone - Nodular / Burrow Mottled	PROXIMAL MARINE RAMP
6596																												
6600	dk grey																										Carbonaceous Shale - paucity of fossils	DISTAL MARINE RAMP
	to																											
	brown																											
	med																										Crinoidal Wackestone - burrow mottled and nodular - OM / clay "wisps"	PROXIMAL MARINE RAMP
	to dk																											
	grey																											
6606	and																											
6607	brown																											
	↓																											

B23

Date:

Well Location: 49-109-8W6

Core Interval:

Correction Factor (Log to Core Conversion): Core +9.75 = log

8

Log Depth	Colour	Structures	Skeletal	Lithology: Graphic Log	Limestone	Dolostone	Anhydrite	Mudstone	Wackestone	Packstone	Grainstone	Rudstone	Floatstone	Boundstone	Porosity: Interparticle	Intraparticle	Moldic	Vuggy	Fenestral	Fracture	Other: Anhydrite	Oil/Bitumen	% Dol.: Low	Medium	High	Samples	Comments	Depositional Environment
6610	med-dk grey																										Crinoidal wackestone - Nodular / Burrow Mottled	PROXIMAL MARINE RAMP
6612	dk grey to black																										Crinoidal wackestone - Massive to Bedded	MARINE RAMP SEMI-DISTAL ↓
6615	med to dk grey and brown																										Crinoidal wackestone - Nodular and Burrow Mottled	PROXIMAL MARINE RAMP
6617																												
6620																												
6627																												↓

B24

Date:

Well Location: 4-9-109-8W6

Core Interval:

Correction Factor (Log to Core Conversion): Core +9.75 = log

Log Depth	Colour	Structures	Skeletal	Lithology: Graphic Log	Limestone	Dolostone	Anhydrite	Mudstone	Wackestone	Packstone	Grainstone	Rudstone	Floatstone	Boundstone	Porosity: Interparticle	Intraparticle	Moldic	Vuggy	Fenestral	Fracture	Other: Anhydrite	Oil/Bitumen	% Dol.: Low	Medium	High	Samples	Comments	Depositional Environment
6630	dk grey																										Crinoidal wackestone -occassional om-rich wisps, nodules and storm events -generally massive and crinoidal	9 Open Marine Ramp
6640																												
6641																												
6643																											fracture porosity <1% -occluded by anhydrite fracture fill	
6648																											Anhydrite fracture fills	
6649	↓																											↓

Date:

Well Location: 4-9-109-8W6

Core Interval:

Correction Factor (Log to Core Conversion): Core +9.75 = log

10

Log Depth	Colour	Structures	Skeletal	Lithology: Graphic Log	Limestone	Dolostone	Anhydrite	Mudstone	Wackestone	Packstone	Grainstone	Rudstone	Floatstone	Boundstone	Porosity: Interparticle	Intraparticle	Moldic	Vugay	Fenestral	Fracture	Other: Anhydrite	Oil/Bitumen	% Dol.: Low	Medium	High	Samples	Comments	Depositional Environment
6650	dk grey																										Crinoidal Dolo-wackestone	Open Marine Ramp
6653																											- undolomitized equivalent of facies below	
6660																												
6664	med grey	S																								009	Crinoidal wackestone	
																										008		
6669																										007		

B26

Date:

Core Interval:

Well Location: 4-9-109-8W6

Correction Factor (Log to Core Conversion): Core + 9.75 = log

Log Depth	Colour	Structures	Skeletal	Lithology: Graphic Log	Limestone	Dolostone	Anhydrite	Mudstone	Wackestone	Packstone	Grainstone	Rudstone	Floatstone	Boundstone	Porosity: Interparticle	Intraparticle	Moldic	Vuggy	Fenestral	Fracture	Other: Anhydrite	Oil/Bitumen	% Dol.: Low	Medium	High	Samples	Comments	Depositional Environment
6670																										006	Crinoidal Wackestone	Open Marine Ramp
		S																										
6672																										005		
6678																												
6680	med.																											
	grey																											
6683																												
																				1%								
6686																												
6688																				20%							- high porosity - saddle filled vugs	

Date:

Core Interval: C6

Well Location: 4-9-109-8W6

Correction Factor (Log to Core Conversion): Core +9.75 = log

12

Log Depth	Colour	Structures	Skeletal	Lithology: Graphic Log	Limestone	Dolostone	Anhydrite	Mudstone	Wackestone	Packstone	Grainstone	Rudstone	Floatstone	Boundstone	Porosity: Interparticle	Intraparticle	Moldic	Vuggy	Fenestral	Fracture	Other: Anhydrite	Oil/Bitumen	% Dol.: Low	Medium	High	Samples	Comments	Depositional Environment
6690	med.																		20%								Crinoidal Dolowackestone	Open Marine
6691	grey.																									-004	Crinoids indicate	Ramp
6692																											normal marine	
6693																											salinity	
																			N	%								
6696																												
6700	light grey																									003	-Paucity of fossils -laminated	Mesosaline Basin
6704	grey to tan laminated																									002	Bedded Massive Anhydrite	Hypersaline V. shallow restricted basin

B28

Date:

Core Interval:

Well Location: 4-9-109-8W6

Correction Factor (Log to Core Conversion): Core + 9.75 = log

13

Log Depth	Colour	Structures	Skeletal	Lithology: Graphic Log	Limestone	Dolostone	Anhydrite	Mudstone	Wackestone	Packstone	Grainstone	Rudstone	Floatstone	Boundstone	Porosity: Interparticle	Intraparticle	Moldic	Vuggy	Fenestral	Fracture	Other: Anhydrite	Oil/Bitumen	% Dol.: Low	Medium	High	Samples	Comments	Depositional Environment
6710	grey to tan laminated			^ ^																							CHINCHAGA ANHYDRITE - subaqueous deposition - Paucity of fossils	V. Shallow Restricted Hypersaline Basin
				^ ^																								
				^ ^																								
				^ ^																								
6714				^ ^																						001		
				^ ^																								
6716				^ ^																								
				^ ^																								
				^ ^																								
																											BASE OF CORE	
6720																												

Date: July 12 /2000
Well Location: 6-32-109-8W6

Core Interval: 6387-6640 core (
Correction Factor (Log to Core Conversion): Cores 14-11 (core -1.6=log) Cores 9-10 (core -.7=log

Log Depth	Colour	Structures	Skeletal	Lithology: Graphic Log	Limestone	Dolostone	Anhydrite	Mudstone	Wackestone	Packstone	Grainstone	Rudstone	Floatstone	Boundstone	Porosity: Interparticle	Intraparticle	Moldic	Vuggy	Fenestral	Fracture	Other: Anhydrite	Oil/Bitumen	% Dol.: Low	Moderate	High	Samples	Comments	Depositional Environment
6430																											Fossil-Rich Rudstones and Cemented Rudstones	UPPER EXTENT OF CORE DESCRIBED	
6435	light brown-grey	v v	* * *																								Pelloidal Skeletal DOLOGRAINSTONE Minor Intercrystalline porosity ~10%	Toe of Slope -foreslope sands
6440		v v	* *																								Vuggy: 1% Moldic: 5%	
6443	light grey to black lami-nae		* * *																							-146 -145	LAMINATED TO BEDDED DOLOGRAINSTONE	TOE OF SLOPE -foreslope sand, OM, and fossil debris
6448																												

Date: July 12/2000
Well Location: 6-32-109-8W6

Core Interval: 6387-6640 core
Correction Factor (Log to Core Conversion): Core 11-14 (Core-1.6=log) Cores 8-10 (Core-.7=log)

Log Depth	Colour	Structures	Skeletal	Lithology: Graphic Log	Limestone	Dolostone	Anhydrite	Mudstone	Wackestone	Packstone	Grainstone	Rudstone	Floatstone	Boundstone	Porosity: Interparticle	Intraparticle	Moldic	Vuggy	Fenestral	Fracture	Other: Anhydrite	Oil/Bitumen	% Dol.: Low	Moderate	High	Samples	Comments	Depositional Environment
6450		S																									LAMINATED TO	TOE OF SLOPE
			*																								BEDDED	-foreslope
6452		S																									DOLOGRAINSTONE	sand, OM,
6453		S	O??O																							-144		and fossil
																											Porosity-low except	debris
																											in rudstone beds	
			*																									
6457																											DOLOFLOATSTONE	TOE OF SLOPE
		None																									-moldic and vuggy	-foreslope
																											porosity dominate	rubble
6460			*																									
6461																N/A							?				LAMINATED OM AND	DISTAL TOE OF
			*																								DOLOGRAINSTONE	SLOPE?
6463	med	None																									Pelloidal/Skeletal	Toe of Slope
	brn-																										Dolofloatstone	
	grey		*																									
6466																											-high moldic porosity	
6467																										-142	near base	
																											-high vuggy porosity	
																											near upper contact	

Depositional Environment: 2

Date: July 12 / 2000
Well Location: 6-32-109-8W6
Core Interval: 6387-6640
Correction Factor (Log to Core Conversion): Cores 1A-11 (core - 1.6 = log) Cores 8-11 (core - .7 = log)

3

Log Depth	Colour	Structures	Skeletal	Lithology: Graphic Log	Limestone	Dolostone	Anhydrite	Mudstone	Wackestone	Packstone	Grainstone	Rudstone	Floatstone	Boundstone	Porosity: Interparticle	Intraparticle	Moldic	Vuggy	Fenestral	Fracture	Other: Anhydrite	Oil/Bitumen	% Dol.: Low	Moderate	High	Samples	Comments	Depositional Environment
6470	red	None!																									Pelloidal / Skeletal Dolofloatstone	Toe of Slope
	brn-grey																											
6472																												
	light brown-grey																										LAMINATED TO BEDDED PELLOIDAL SKELETAL - DOLOFLOATSTONE	TOE OF SLOPE - Foreslope Sand and Debris
6475																												
6480																												
6482	H. brown	Massive																									THAMNOPORID / DOLOFLOATSTONE	Toe of Slope
6483																											LAMINATED TO BEDDED PELLOIDAL SKELETAL DOLOFLOATSTONE	TOE OF SLOPE - Foreslope debris and Sand
6489		S																										

B32

Date: July 12/2000
Well Location: 6-32-109-8W6

Core Interval: 6387-6646
Correction Factor (Log to Core Conversion): cores 11-11 (-1.6) cores 8-10 (-0.7)

4

Log Depth	Colour	Structures	Skeletal	Lithology: Graphic Log	Limestone	Dolostone	Anhydrite	Mudstone	Wackestone	Packstone	Grainstone	Rudstone	Floatstone	Boundstone	Porosity: Interparticle	Intraparticle	Moldic	Vuggy	Fenestral	Fracture	Other: Anhydrite	Oil/Bitumen	% Dol.: Low	Moderate	High	Samples	Comments	Depositional Environment
6490	light grey																										LAMINATED TO BEDDED PELLOIDAL-SKELETAL DOLOFLOATSTONE -graphic structure log indicates beds vs. laminae Porosity in laminated parts is low ~5% increases in event beds to up to 50%!	Toe of Slope - many small event deposits of sand-fossil-debris, and OM-rich wisps carried downslope
6491																												
	w/ d'k grey lamin	S																										
6496	ae	S																										
6500																												
6503		S																										
6505	med. grey																									-138	Pelloidal Skeletal Dolofloatstone	Toe of Slope Foreslope Sand and fossil debris
6508	light grey	none																									Pelloidal Skeletal Dolograinstone	Toe of Slope Foreslope Sand

Date: July 12/2000
Well Location: 6-32-109-8w6

Core Interval: 6387-6640
Correction Factor (Log to Core Conversion): Cores 14-11 (-1.6) Cores 8-10 (-0.7)

5

Log Depth	Colour	Structures	Skeletal	Lithology: Graphic Log	Limestone	Dolostone	Anhydrite	Mudstone	Wackestone	Packstone	Grainstone	Rudstone	Floatstone	Boundstone	Porosity: Interparticle	Intraparticle	Moldic	Vuggy	Fenestral	Fracture	Other: Anhydrite	Oil/Bitumen	% Dol.: Low	Moderate	High	Samples	Comments	Depositional Environment
6510	light grey	none!																									Pelloidal/skeletal Dolograinstone?	Toe of Slope - foreslope sands
6513																												
6516	buff ↓ blck-																									-137 -136	BEDDED PELLOIDAL SKELETAL DOLOGRAINSTONE? -lam. dolograinstone	FORESLOPE - toe of slope - foreslope sands
6519	buff																									-135	PELLOIDAL SKELETAL	FORESLOPE
6520	↓ blck-																										DOLOGRAINSTONE? -laminated dolograinstone	-toe of slope foreslope sands and
6521	↑ buff	S																									-appears fossil-lam ↳May be sands not favorable ↳c. gr size may make fauna hard to see	more distal laminated grainstones
6526	↓	S																								-134		
6528		S																										
6529		S																									STROM DOLOFLOATSTONE	FORESLOPE RUBBLE

Date: July 11/2000

Well Location: 6-32-109-8W6

Core Interval: 6387-6640

Correction Factor (Log to Core Conversion): Cores 14-11 (-1.6) cores 8-10 (-0.7)

6

Log Depth	Colour	Structures	Skeletal	Samples	Comments	Depositional Environment
6530					STROM FRAGMENT DOLOFLOATSTONE	FORESLOPE RUBBLE DEPOSITED
6533				-133		
6534					} Massive @ base	
				-132	LAMINATED TOM AND DOLOGRAINSTONE	DISTAL RAMP
	grey to blk			-131		
	lam.				~10% porosity } Bedded	-onset of deepening which initiated reefs
6539						
6540					} laminated	
				130		
6542	Buff				Cemented Rudstone Skeletal Dolograinstone	OPEN MARINE RAMP: SAND SHOAL
6513						
6516					Porosity decreases from 20% in underlying unit to ~10% here b/c of cements	
				129		
6519				128		

Lithology: Graphic Log; Limestone; Dolostone; Anhydrite; Mudstone; Wackestone; Packstone; Grainstone; Rudstone; Floatstone; Boundstone

Porosity: Interparticle; Intraparticle; Moldic; Vuggy; Fenestral; Fracture

Other: Anhydrite; Oil/Bitumen

% Dol.: Low; Moderate; High

FRAMESTONE

~10%

Date: July 11/2000

Well Location: 6-32-109-8W6

Core Interval: 6387-6640

Correction Factor (Log to Core Conversion): Cores 14-11 (-1.6) cores 8-10 (-0.7)

Log Depth	Colour	Structures	Skeletal	Lithology: Graphic Log	Limestone	Dolostone	Anhydrite	Mudstone	Wackestone	Packstone	Grainstone	Rudstone	Floatstone	Boundstone	Porosity: Interparticle	Intraparticle	Moldic	Vuggy	Fenestral	Fracture	Other: Anhydrite	Oil/Bitumen	% Dol.: Low	Moderate	High	Samples	Comments	Depositional Environment
																											Cemented Pel. Skel. Grnst	OPEN MARINE RAMP
6556			*											FRAMESTONE?														
	Buff	None!	*																								Pelloidal Skeletal Dolograinstone - fossil-lean	Open Marine Ramp: high energy sand shoal on ramp - shifting sands
			*																									
			* ?																									
			*																									
			*																									
			? *																									
			*																									
			? *																									
6559			*																									
6560																										-127		
			?																									
			?																									
			?																									

Date: July 11 /2000
Well Location: 6-32-109-8W6

Core Interval: 6387 - 6646
Correction Factor (Log to Core Conversion): Cores 14-11 (-1.6) Cores 8-10 (-0.7)

8

Log Depth	Colour	Structures	Skeletal	Lithology: Graphic Log	Limestone	Dolostone	Anhydrite	Mudstone	Wackestone	Packstone	Grainstone	Rudstone	Floatstone	Boundstone	Porosity: Interparticle	Intraparticle	Moldic	Vuggy	Fenestral	Fracture	Other: Anhydrite	Oil/Bitumen	% Dol.: Low	Moderate	High	Samples	Comments	Depositional Environment
6570	Buff	None!																									Pelloidal Skeletal Dolograinstone?	OPEN MARINE RAMP: high energy sand shoal on ramp -shifting sand
6571			V																									
			?																									
6574			V ≈																								-Intercrystalline porosity ~20%.	
			?																									
6576																												
	H-																									-126	CRINOIDAL DOLOFLOATSTONE	PROXIMAL MARINE RAMP -decreased reef production or rel. sealevel rise.
	med																											
	Grey																											
6580																												
																		~10%									~10% partial moldic porosity in leached out strom fragments	
6585																												
	buff																										Pelloidal Skeletal Dolograinstone (to Dolorudstone at Top?)	OPEN MARINE RAMP: SHOAL OF SHIFTING SAND ON RAMP
6587			V															~20%										
			?																									
			?																									

Date: July 11 & 12 /2000
Well Location: 6-32-109-8W6

Core Interval: 6387-6690
Correction Factor (Log to Core Conversion): Cores 14-11 (-1.6) Cores 8-10 (-0.7)

9

Log Depth	Colour	Structures	Skeletal	Lithology: Graphic Log	Limestone	Dolostone	Anhydrite	Mudstone	Wackestone	Packstone	Grainstone	Rudstone	Floatstone	Boundstone	Porosity: Interparticle	Intraparticle	Moldic	Vuggy	Fenestral	Fracture	Other: Anhydrite	Oil/Bitumen	% Dol.: Low	Moderate	High	Samples	Comments	Depositional Environment
6590			* A?																								PELLOIDAL SKELETAL DOLOGRAINSTONE	OPEN MARINE RAMP: SHOAL ON RAMP ↳ shifting sands
6592			*																							-125	-mod. porosity	
6595																												
																										-124	STROM FRAGMENT DOLOFLOATSTONE TO DOLORUDSTONE	OPEN MARINE RAMP: SHOAL ON RAMP
																		~10%									~10% partial moldic porosity	
6600																												
6604	light grey to med grey																		~1%								DOLOFLOATSTONE -trace anhydrite and bitumen	PROXIMAL MARINE RAMP
6607																										-123		

Date: July 10/2000
Well Location: 6-32-109-8w6
Core Interval: 6387-6640
Correction Factor (Log to Core Conversion): cores 11-11 (-1.6) cores 8-10 (-0.7)

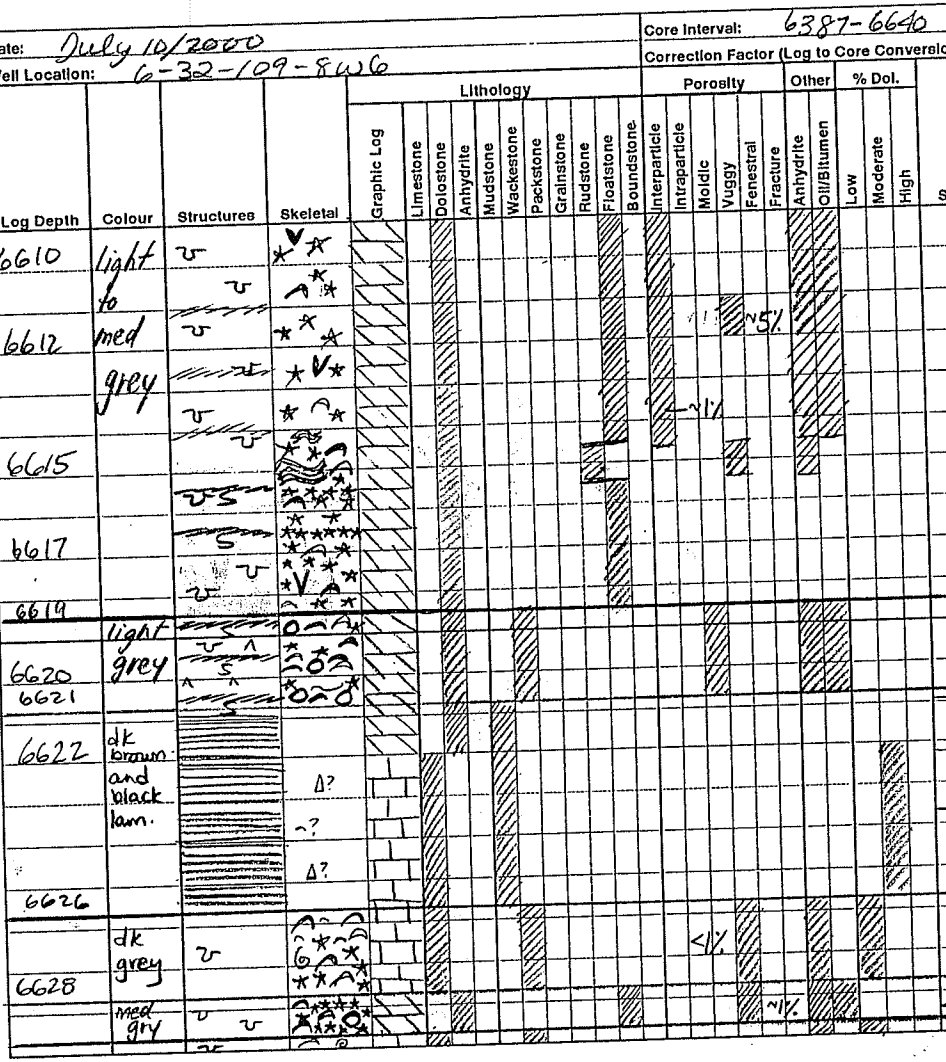

Log Depth	Colour	Structures	Skeletal	Samples	Comments	Depositional Environment
6610	light to med grey				DOLOFLOATSTONE	PROXIMAL MARINE RAMP
6612					-trace anhydrite and bitumen	
					-Variable porosity 1-5	
6615					event bed	
					-event bed	
6617						
6619					FOSSIL-LEAN DOLOWACKESTONE -porosity <1%	SEMI-DISTAL MARINE RAMP
6620	light grey					
6621				-122		
6622	dk brown and black lam.			-121	LAMINATED LIME-MUDSTONE TO DOLOMITIZED LIME-MUDSTONE	DISTAL RAMP
				-120		
6626					Partially Dolomitized Crinoid wackestone	SEMI-DISTAL RAMP or tail end of event - fines up
6628	dk grey				DOLOMITIZED CRINOID FLOATSTONE	EVENT ON DISTAL RAMP
	med grey			-119		

Date: July 10/2000

Well Location: 6-32-109-8W6

Core Interval: 6387-6640

Correction Factor (Log to Core Conversion): Core 14-11 (Core - 1.6 = log) Cores 8-10 (-0.7)

11

Log Depth	Colour	Structures	Skeletal	Graphic Log	Lithology: Limestone	Dolostone	Anhydrite	Mudstone	Wackestone	Packstone	Grainstone	Rudstone	Floatstone	Boundstone	Porosity: Interparticle	Intraparticle	Moldic	Vuggy	Fenestral	Fracture	Other: Anhydrite	Oil/Bitumen	% Dol.: Low	Moderate	High	Samples	Comments	Depositional Environment
6630	dk brn / dk grey																									-118	Partially Dolomitized Lime mudstone to Fossil-lean Wackestone	DISTAL RAMP
6634																										-117	-anhydrite infil	
6636																											- low degree dolomitization -laminated OM-rich	
6640																											BASE OF CORE	

Date: June 26 / 2000
Well Location: 12-33-109-8W6

Core Interval: 6426-6693 (corrected 6435-6655)
Correction Factor (Log to Core Conversion): +9 cores 5-7 +12 cores 8-9

Log Depth	Colour	Structures	Skeletal	Lithology: Graphic Log	Limestone	Dolostone	Anhydrite	Mudstone	Wackestone	Packstone	Grainstone	Rudstone	Floatstone	Boundstone	Porosity: Interparticle	Intraparticle	Moldic	Vuggy	Fenestral	Fracture	Other: Anhydrite	Oil/Bitumen	% Dol.: Low	Medium	High	Samples	Comments	Depositional Environment
6430																											TOP OF CORE EXAMINED	
6435																											STROMATOPOROID DOLOPACKSTONE TO DOLORUDSTONE	Foreslope Rubble
6437																												
6490																												
6499																											Peloidal Skeletal Packst.	Foreslope Sand

B41

Date: June 26/2000

Well Location: 12-33-109-8W6

Core Interval: 6426-6643 (corrected 6435-6655)

Correction Factor (Log to Core Conversion): +9. cores 5-7 +12 cores 8-9

Log Depth	Colour	Structures	Skeletal	Lithology: Graphic Log	Limestone	Dolostone	Anhydrite	Mudstone	Wackestone	Packstone	Grainstone	Rudstone	Floatstone	Boundstone	Porosity: Interparticle	Intraparticle	Moldic	Vuggy	Fenestral	Fracture	Other: Anhydrite	Oil/Bitumen	% Dol.: Low	Medium	High	Samples	Comments	Depositional Environment
6450																											PELOIDAL SKELETAL PACKSTONE?	FORESLOPE SANDS
6451																												
																											STROMATOPOROID DOLOFLOATSTONE TO DOLOPACKSTONE	FORESLOPE - rubble.
																											PELLOIDAL SKELETAL PACKSTONE?	FORESLOPE SANDS
6455	tan-ltgrey																										STROMATOPOROID DOLOFLOATSTONE	FORESLOPE Rubble
6457	light to med grey																										PELOIDAL SKELETAL PACKSTONE?	FORESLOPE - thin foreslope sands
6460																											LAMINATED LIME-MUDSTONE	
6466	ltgrey to tan																										Peloidal Skeletal Packstone? - intercrystalline porosity	Toe of Reef Slope - foreslope Sands

B42

Date: June 26/2000

Well Location: 12-33-109-8W6

Core Interval: 6426 - 6693 (Concealed 6435 - 6655)

Correction Factor (Log to Core Conversion): +9 cores 5-7 +12 cores 8,9

3

Log Depth	Colour	Structures	Skeletal	Lithology: Graphic Log	Limestone	Dolostone	Anhydrite	Mudstone	Wackestone	Packstone	Grainstone	Rudstone	Floatstone	Boundstone	Porosity: Interparticle	Intraparticle	Moldic	Vuggy	Fenestral	Fracture	Other: Anhydrite	Oil/Bitumen	% Dol.: Low	Medium	High	Samples	Comments	Depositional Environment
6470	med. grey																										FOSSIL-RICH DOLOFLOATSTONE TO DOLOPACKSTONE	REEF FORESLOPE debris on TOE OF SLOPE
6473																												
6475																											vuggy porosity upto 20%	
6477																												
																											LAMINATED DOLOMUDSTONE	DISTAL RAMP
6480																											STROM DOLOPACKSTONE TO DOLOFLOATSTONE	TOE OF SLOPE - foreslope rubble
6481																												
																											Laminated - Nodular partially dolomitized Lime Mudstone	DISTAL RAMP
6484																											ALMOST COMPLETELY DOLOMITIZED FOSSIL-RICH FLOATSTONE	TOE OF SLOPE - foreslope rubble
6486																												
6487	black and grey																										Laminated Lime Mudstone - Dolomitized	Distal Ramp
6489																											Pelloidal Skeletal Packstone	Toe of SLOPE - foreslope sand

Date: June 26/2000
Well Location: A-33-109-8W6

Core Interval: 6926-6693 (corrected 6935-6655)
Correction Factor (Log to Core Conversion): +9 cores 5-7 +12 cores 8,9

Log Depth	Colour	Structures	Skeletal	Lithology: Graphic Log	Limestone	Dolostone	Anhydrite	Mudstone	Wackestone	Packstone	Grainstone	Rudstone	Floatstone	Boundstone	Porosity: Interparticle	Intraparticle	Moldic	Vuggy	Fenestral	Fracture	Other: Anhydrite	Oil/Bitumen	% Dol.: Low	Medium	High	Samples	Comments	Depositional Environment
6490																											PELOIDAL SKELETAL	TOE OF SLOPE
																											PACKSTONE?	-foreslope sands
6492																											-low porosity	
	tan-																											DISTAL TOE OF
6493	ltgrey																										DOLOMITIZED FLOATSTONE	SLOPE
	black																										LAMINATED	DISTAL RAMP
	grey																										PARTIALLY DOLOMIT-	
	lam.																										IZED LIME-MUDSTONE	
																										0091		
6499	med																										CORAL RUDSTONE	TOE OF SLOPE
6500	grey																										-Porosity ~30%!	OR FOREREEF
6501																											FOSSIL-LEAN	TOE of Slope
																											CRINOIDAL DOLOFLOATSTONE	
6503	lt.																										FOSSIL-LEAN CRINOIDAL	TOE OF SLOPE
	grey																										DOLOWACKESTONE	
6505																											RUDSTONE	TOE OF SLOPE
																										0090	LAMINATED LIME MUDSTONE	DISTAL RAMP
6507																											PELOIDAL-SKELETAL	TOE OF SLOPE
																											DOLO PACKSTONE	-Foreslope Sand

Date: June 26/2000

Well Location: 2-33-109-8W6

Core Interval: 6426-6693 (Corrected 6435-6655)

Correction Factor (Log to Core Conversion): +9 Cores 5-7 +12 cores 8,9

5

Log Depth	Colour	Structures	Skeletal	Lithology: Graphic Log	Limestone	Dolostone	Anhydrite	Mudstone	Wackestone	Packstone	Grainstone	Rudstone	Floatstone	Boundstone	Porosity: Interparticle	Intraparticle	Moldic	Vuggy	Fenestral	Fracture	Other: Anhydrite	Oil/Bitumen	% Dol.: Low	Medium	High	Samples	Comments	Depositional Environment
6510																											PELOIDAL-SKELETAL DOLO PACKSTONE	TOE OF SLOPE - foreslope sands
6511																												
	Black																									0089	LAMINATED LIME-MUDSTONE	DISTAL RAMP
6513																											FOSSIL-RICH DOLOFLOATSTONE	TOE OF SLOPE - foreslope rubble
6516																												
6517																											PELOIDAL-SKELETAL DOLOPACKSTONE?	TOE OF SLOPE - foreslope sands
6520																										0088	Minor intercrystalline porosity	
																										0087	LAMINATED LIME-MUDSTONE	DISTAL RAMP
	Black																											
6522																				~20%							FOSSIL-RICH DOLOFLOATSTONE	TOE OF SLOPE - foreslope rubble
																										0086	LAMINATED LIME-MUDSTONE	DISTAL RAMP
	BLACK																											
6525																											FOSSIL-RICH DOLOFLOATSTONE	TOE OF SLOPE - Foreslope Rubble
6527																											Low Porosity ~5% Partial Moldic 2.5% Vuggy ~2.5% - bitumen	- strom fragments

Date: June 26/2000
Well Location: 12-33-109-8W6

Core Interval: 6426 - 6693 (corrected 6435 - 6655)
Correction Factor (Log to Core Conversion): +9 cores 5-7 +12 cores 8+9

6

Log Depth	Colour	Structures	Skeletal	Lithology: Graphic Log	Limestone	Dolostone	Anhydrite	Mudstone	Wackestone	Packstone	Grainstone	Rudstone	Floatstone	Boundstone	Porosity: Interparticle	Intraparticle	Moldic	Vuggy	Fenestral	Fracture	Other: Anhydrite	Oil/Bitumen	% Dol.: Low	Medium	High	Samples	Comments	Depositional Environment
6530																											FOSSIL-RICH DOLOWACKESTONE	TOE OF SLOPE-rubble
																											Peloidal/Skeletal Packstone?	Toe of Slope -foreslope / sand?
																											Low Porosity: ~3%	
6535																											Intercrystalline 0.5% Moldic 0.5% Vuggy 2% -thick tabular strom	
																											LAMINATED DOLOMUDSTONE	DISTAL RAMP
6538																											FOSSIL-RICH STROM DOLOFLOATSTONE	TOE OF SLOPE RUBBLE FROM FORESLOPE -fossil-rich -fragmented
6590																										-0085		
6543																										-0084	Laminated Dolomudstone	DISTAL RAMP
		S																									DOLO FLOATSTONE (crinoidal, brach, bivalve)	TOE OF REEF SLOPE
6545		S																								-0083		
6547		S																										-dynamic microfacies patterns
6549		S																										

Date: June 26/2000
Well Location: 12-33-109-8W6

Core Interval: corrected 6435-6655 unconnected 6426-6643
Correction Factor (Log to Core Conversion): +9 cores 5-7 +12 cores 8 & 9

Log Depth	Colour	Structures	Skeletal	Lithology: Graphic Log	Limestone	Dolostone	Anhydrite	Mudstone	Wackestone	Packstone	Grainstone	Rudstone	Floatstone	Boundstone	Porosity: Interparticle	Intraparticle	Moldic	Vuggy	Fenestral	Fracture	Other: Anhydrite	Oil/Bitumen	% Dol.: Low	Medium	High	Samples	Comments	Depositional Environment
6550																										0082		
6552																												
6555																												
6597																										0081	Dolowackestone-Dolomudstone	DISTAL MARINE RAMP
																										0080	Peloidal/Skeletal DOLOPACKSTONE	OPEN MARINE RAMP -Sandy Shoals
	lt grey																											
6560																												
6561																											CORE MISSING - based on correction	
6564																											See pg 8.	

Date: June 23/2000
Well Location: 12-33-109-8W6

Core Interval: 6426'-6643' (corrected 6435-6655)
Correction Factor (Log to Core Conversion): +9 cores 5-7 +12 cores 8+9

8

Log Depth	Colour	Structures	Skeletal	Lithology: Graphic Log	Limestone	Dolostone	Anhydrite	Mudstone	Wackestone	Packstone	Grainstone	Rudstone	Floatstone	Boundstone	Porosity: Interparticle	Intraparticle	Moldic	Vuggy	Fenestral	Fracture	Other: Anhydrite	Oil/Bitumen	% Dol.: Low	Medium	High	Samples	Comments	Depositional Environment
																											Due to correction difficulties.... cores 5-7 plotted separately to make depths more convenient.	to log
6563.5																											TOP OF CORE #8	(6563.7' (log)
6564.5																											FOSSIL-LEAN CRINOIDAL DOLOWACKESTONE	OPEN MARINE RAMP - SANDY SHOAL
6565.5																												
6566.5																												
6568.5																											Vugs lined w saddle dol ± anhydrite + bitumen	

B48

Date:

Well Location: 12-33-109-8W6

Core Interval: 6426'-6643'

Correction Factor (Log to Core Conversion): +9 cores 5-7 +12 cores 8&9

9

Log Depth	Colour	Structures	Skeletal	Lithology: Graphic Log	Limestone	Dolostone	Anhydrite	Mudstone	Wackestone	Packstone	Grainstone	Rudstone	Floatstone	Boundstone	Porosity: Interparticle	Intraparticle	Moldic	Vuggy	Fenestral	Fracture	Other: Anhydrite	Oil/Bitumen	% Dol.: Low	Medium	High	Samples	Comments	Depositional Environment
6573.5																											FOSSIL-LEAN	OPEN MARINE
																											CRINOIDAL DOLO-	RAMP - Sand
																											WACKESTONE	Shoal
6578.5																											DOLOFLOATSTONE	OPEN MARINE
																											WITH DOLOPACKSTONE	SHOAL
																											MATRIX	-coarse fossil
																											-vugs lined w bitumen	material
																											and anhydrite	
6583.5																											-Intercrystalline	
																											porosity b/t sand-	
																											sized dolomite xtls.	
6586.5																												
6588.5																											-Fenestral porosity	
																											within storms	
6590.5																												
																											Peloidal Skeletal	Open Marine
																											Packstone?	Ramp - sands

"Grainy" new facies?

B49

Date: June 21

Well Location: 12-33-109-8W6

Core Interval: 6426'-6643'

Correction Factor (Log to Core Conversion): +9 cores 5-7 +12 cores 8?9

Log Depth	Colour	Structures	Skeletal	Lithology: Graphic Log	Limestone	Dolostone	Anhydrite	Mudstone	Wackestone	Packstone	Grainstone	Rudstone	Floatstone	Boundstone	Porosity: Interparticle	Intraparticle	Moldic	Vuggy	Fenestral	Fracture	Other: Anhydrite	Oil/Bitumen	% Dol.: Low	Medium	High	Samples	Comments	Depositional Environment
6593.5																										-0077	Peloidal Skeletal Packstone? - grainy appearance - dolomitization destroyed skeletal grains Intergranular = Intercrystalline porosity ~5% Partial moldic porosity ~2%	OPEN MARINE RAMP - shifting carbonate sands nearshore?
6596.5																												
6597.5																												
6599.5																												
6601.5																											~~DOLOFLOATSTONE~~ WITH PELOIDAL MATRIX - fossil rich - Nodular and Burrow Mottled porosity: total ~15% max - bitumen, anhydrite in pores	OPEN MARINE RAMP - shoal on the ramp
6603.5																												
6605.5																										-0076		
6608.5																										-P	Dolowackestone - fossil lean - small storm concentration - Massive to burrow mottled <1% porosity	PROXIMAL MARINE RAMP
6609.5																				<1%						-0075P		
6611.5																										-0074P		

10

B50

Date:

Well Location:

Core Interval: 6426'-6643'

Correction Factor (Log to Core Conversion): +9 cores 5-7 +12 cores 8 & 9

Log Depth	Colour	Structures	Skeletal	Graphic Log	Limestone	Dolostone	Anhydrite	Mudstone	Wackestone	Packstone	Grainstone	Rudstone	Floatstone	Boundstone	Interparticle	Intraparticle	Moldic	Vuggy	Fenestral	Fracture	Anhydrite	Oil/Bitumen	Low	Medium	High	Samples	Comments	Depositional Environment
6613.5																											Massive to Burrow Mottled Dolowackestone - bioturbation - fossiliferous	PROXIMAL MARINE RAMP
6617.5																										-0073	Partial-Moldic Porosity <1%	
6619.5																										-0072-P -0071-P -0070-P	Laminated to thin Bedded Lime-mud-stone - partially dolomitized	DISTAL RAMP
6622.5																												
6623.5																										-0068 P	Nodular and Burrow Mottled Crinoid-Bioclastic Wackestone - increasingly fossil-rich towards top - partially dolomitized	MARINE RAMP PROXIMAL
6629.5																										-P -0069 P	↳ patches	
6630.5																										-0067 P	Laminated Lime Mudstone	DISTAL RAMP
6632.5																											Nodular to Massive Lime Mudstone	DISTAL RAMP

Date:

Well Location:

Core Interval: 6426' - 6643'

Correction Factor (Log to Core Conversion): +9 cores 5-7 +12 cores 8-9

12

Log Depth	Colour	Structures	Skeletal	Lithology: Graphic Log	Limestone	Dolostone	Anhydrite	Mudstone	Wackestone	Packstone	Grainstone	Rudstone	Floatstone	Boundstone	Porosity: Interparticle	Intraparticle	Moldic	Vuggy	Fenestral	Fracture	Other: Anhydrite	Oil/Bitumen	% Dol.: Low	Medium	High	Samples	Comments	Depositional Environment
6633.5																											Nodular/Burrow Mottled Lime Mudstone	DISTAL RAMP -shallower
6635.5																											Laminated lime-mudst. -irregular laminations -fossil lean	DISTAL RAMP -v. deep ∴ laminated
6637.5																										-P		
6638.5																											Nodular to massive Lime mudstone -Extensively burrow mottled. -fossil rich mudstone w/ -fossils increase upwards -almost wackestone -fracture fill anhydrite brimmed by calcite cement -Abundant OM wisps	DISTAL RAMP -slight base level drop in relationship to underlying facies
																										-P		
																										-P		
																										0066		
6643.5																										0065		
6644.5																										-P		
6647.5																										-0064		
6649.5																										-0063	2cm thick storm concentration of crinoids etc.	
6652.5	dk brn to blck																									-0062	laminated Mudstone	DISTAL RAMP

F

C

F

B52

Date: June 21/2000
Well Location: 12-33-109-8W6

Core Interval: 6426-6643
Correction Factor (Log to Core Conversion): +9 cores 5-7 +12 cores 8-9

13

Log Depth	Colour	Structures	Skeletal	Lithology: Graphic Log	Limestone	Dolostone	Anhydrite	Mudstone	Wackestone	Packstone	Grainstone	Rudstone	Floatstone	Boundstone	Porosity: Interparticle	Intraparticle	Moldic	Vuggy	Fenestral	Fracture	Other: Anhydrite	Oil/Bitumen	% Dol.: Low	Medium	High	Samples	Comments	Depositional Environment
6653.5	v.dk brown to black																										Laminated Lime Mudstone	DISTAL RAMP
6656.5																											BASE OF CORE	

Date: July 13/2000
Well Location: 4-30-110-9W6

Core Interval: 6370 - 6420
Correction Factor (Log to Core Conversion): Core + 9.5 = log depth

Log Depth	Colour	Structures	Skeletal	Lithology: Graphic Log	Limestone	Dolostone	Anhydrite	Mudstone	Wackestone	Packstone	Grainstone	Rudstone	Floatstone	Boundstone	Porosity: Interparticle	Intraparticle	Moldic	Vuggy	Fenestral	Fracture	Other: Anhydrite	Oil/Bitumen	% Dol.: Low	Moderate	High	Samples	Comments	Depositional Environment
6370																											TOP OF CORE	
6379																												
6380	light grey																~11%										CRINOIDAL DOLO-FLOATSTONE - low porosity - interesting anhy texture - equivalent to ↓	Proximal Marine Ramp - burrowed
6383	^ ^																									-152		
6384																												
6385	med brn.																										PARTIALLY DOLOMITIZED CRINOIDAL FLOATSTONE	PROXIMAL MARINE RAMP - burrowed
6389																											LAM. LIME MUDSTONE	DISTAL RAMP

Date: July 13/2000
Well Location: 9-30-110-9W6

Core Interval: 6420-6370
Correction Factor (Log to Core Conversion): Core +9.5 = log depth

2.

Log Depth	Colour	Structures	Skeletal	Lithology: Graphic Log / Limestone / Dolostone / Anhydrite / Mudstone / Wackestone / Packstone / Grainstone / Rudstone / Floatstone / Boundstone	Porosity: Interparticle / Intraparticle / Moldic / Vuggy / Fenestral / Fracture	Other: Anhydrite / Oil/Bitumen	% Dol.: Low / Moderate / High	Samples	Comments	Depositional Environment
6390								-151 -150 -149 -148	LAMINATED LIME MUDSTONE	DISTAL RAMP
6394	dk grey								Lime Mudstone to wackestone (laminated in places)	SEMI-DISTAL MARINE RAMP
6397									Burrow mottled except within laminated intervals	- laminated intervals = quiet distal ramp conditions
6400										
6408									Negligible porosity	- burrow mottled intervals = semi-distal ramp conditions
6406										→ both... so transitional
6409										

Date: July 13/2000
Well Location: 4-30-110-9w6

Core Interval: 6420-6430
Correction Factor (Log to Core Conversion): Core 19.5 = log depth

3.

Log Depth	Colour	Structures	Skeletal	Lithology: Graphic Log	Limestone	Dolostone	Anhydrite	Mudstone	Wackestone	Packstone	Grainstone	Rudstone	Floatstone	Boundstone	Porosity: Interparticle	Intraparticle	Moldic	Vuggy	Fenestral	Fracture	Other: Anhydrite	Oil/Bitumen	% Dol.: Low	Moderate	High	Samples	Comments	Depositional Environment
6410	dk grey																										LIME MUDSTONE TO WACKESTONE (laminated in places.)	SEMI-DISTAL MARINE RAMP
6413																	No porosity										- trace anhydrite infils leached shells etc	
6416																											- wackestone = event - Mudstone = quiet conditions	
6420																	No Porosity											
6421																											- low degree of dolomitization - ~16%	
6425																											moderate degree of dolomitization ~30%	-
6429																												
6430																											BASE OF CORE	

Date: July 28/2010
Well Location: 7-7-113-21W5

Core Interval: 4512-4756
Correction Factor (Log to Core Conversion): Core -3.5 = log

Log Depth	Colour	Structures	Skeletal	Lithology: Graphic Log	Limestone	Dolostone	Anhydrite	Mudstone	Wackestone	Packstone	Grainstone	Rudstone	Floatstone	Boundstone	Porosity: Interparticle	Intraparticle	Moldic	Vuggy	Fenestral	Fracture	Other: Anhydrite	Oil/Bitumen	% Dol.: Low	Moderate	High	Samples	Comments	Depositional Environment
4510																											TOP OF CORE DESCRIBED	
4512																											Bedded Mosaic Anhydrite - brecciated	Hypersaline
4514			None																									
4520																											Brecciated Anhydrite	
			None																									
																											Bedded Massive Anhy + Dolomudstone	
4528																											Contorted Bedded Anhy	

BEHAVES UPWARDS

B57

Date: July 28/2000
Well Location: 7-7-113-21W5

Core Interval: 4512 - 4756
Correction Factor (Log to Core Conversion): Core - 3.5 = log

2

Log Depth	Colour	Structures	Skeletal	Lithology: Graphic Log	Limestone	Dolostone	Anhydrite	Mudstone	Wackestone	Packstone	Grainstone	Rudstone	Floatstone	Boundstone	Porosity: Interparticle	Intraparticle	Moldic	Vuggy	Fenestral	Fracture	Other: Anhydrite	Oil/Bitumen	% Dol.: Low	Moderate	High	Samples	Comments	Depositional Environment
4530			None																								BRECCIATED ANHY BEDDED MOSAIC ANHYDRITE	HYPERSALINE
4532																											Bedded Massive Anhydrite & Dolomudstone	
4535			None																								Contorted Bedded anhydrite	
4539																											Bedded Massive Anhy + Dolomudstone	
4540			None																								DISTORTED NODULAR ANHYDRITE WITH LAM. DOLOMUDSTONE	
4544																											Bedded Massive Anhydrite and Dolomudstone	
4546	Brecciated		None																									

BRINING UPWARDS

Date: July 28 2000
Well Location: 7-7-113-21W6

Core Interval: 4512-4756
Correction Factor (Log to Core Conversion): Core -3.5 = log

Log Depth	Colour	Structures	Skeletal	Lithology: Graphic Log	Limestone	Dolostone	Anhydrite	Mudstone	Wackestone	Packstone	Grainstone	Rudstone	Floatstone	Boundstone	Porosity: Interparticle	Intraparticle	Moldic	Vuggy	Fenestral	Fracture	Other: Anhydrite	Oil/Bitumen	% Dol.: Low	Moderate	High	Samples	Comments	Depositional Environment
4550			None																								Bedded Massive Anhydrite and Dolomudstone / Muskeg	BRINING UPWARDS
4552																												
	lt grey																										LAM. DOLOMUDSTONE	MESOSALINE?
4555	med grey																										Burrow MOTTLED DOLOFLOATSTONE	Toe of Slope - Distal Foreslope
			None												2%												LAM. DOLOMUDSTONE	DISTAL FORESLOPE
4557																											BURROW-MOTTLED DOLOFLOATSTONE	Toe of Reef Slope - Distal Foreslope
	med. grey																											
4560																											-vuggy porosity ~10% -fracture porosity ~1%	-fine foreslope debris
4562										MISSING CORE																	Incomplete Recovery ~% missing Core	
4668	med grey & tan laminated		None												4%												LAMINATED DOLOMUDSTONE	DISTAL FORESLOPE -more O2 than prev. lagoonal interval

3

Date: July 28/2000

Well Location: 7-9-113-21W5

Core Interval: 4512 - 4756

Correction Factor (Log to Core Conversion): Core - 3.5 = log

4

Log Depth	Colour	Structures	Skeletal	Samples	Comments	Depositional Environment
4570					lami. Dolomudstone	Distal Foreslope
	med grey				BURROW MOTTLED DOLOWACKESTONE TO DOLOFLOATSTONE -low porosity ~1% fract. ~3% vuggy	REEF - semi-DISTAL FORESLOPE (TOE OF SLOPE
4573						
4576	light to med grey lami.		None		LAMINATED DOLOMUDSTONE	DISTAL MARINE RAMP
4580				-192.	<1% fracture porosity ~5% Vuggy Porosity -Brecciated Base	-non-bioturbated -No fossils -laminated -OM-rich or alternate: BRINING UP CYCLE
4587	med grey & white				FRACTURED, BURROWED DOLOWACKESTONE	PROXIMAL MARINE RAMP

B60

Date: July 27 (2000)
Well Location: 7-7-113-21W5

Core Interval: 4512 - 4756
Correction Factor (Log to Core Conversion): Core - 3.5 = log

5

Log Depth	Colour	Structures	Skeletal	Lithology: Graphic Log	Limestone	Dolostone	Anhydrite	Mudstone	Wackestone	Packstone	Grainstone	Rudstone	Floatstone	Boundstone	Porosity: Interparticle	Intraparticle	Moldic	Vuggy	Fenestral	Fracture	Other: Anhydrite	Oil/Bitumen	% Dol.: Low	Moderate	High	Samples	Comments	Depositional Environment
4590	med grey and wht												low		porosity												FRACTURED, BURROWED DOLOWACKESTONE	PROXIMAL MARINE RAMP
4591	med. grey w																	~5%									FRACTURED, BURROW MOTTLED CRINOIDAL DOLOWACKESTONE WITH BITUMINOUS WISPS AND ACCESSORY BITUMEN - vugs contain saddle dolomite, anhydrite and bitumen - low fracture por. <1%	PROXIMAL MARINE RAMP - OM-wisps suggest a less competent carbonate facies
4594	dark grey wisps & wht vugs																	~5%										
4600																										188		
4603	light grey cut by																										FRACTURED, BURROW MOTTLED, CRINOIDAL DOLOWACKESTONE - fossil-lean!	PROXIMAL MARINE RAMP
4607	white fracture																										fracture porosity ~1% vuggy porosity ~3%	

B61

Date: July 27/2000
Well Location: 7-7-113-21W5
Core Interval: 4512-4756
Correction Factor (Log to Core Conversion): Core -3.5 = log

6

Log Depth	Colour	Structures	Skeletal	Lithology: Graphic Log	Limestone	Dolostone	Anhydrite	Mudstone	Wackestone	Packstone	Grainstone	Rudstone	Floatstone	Boundstone	Porosity: Interparticle	Intraparticle	Moldic	Vuggy	Fenestral	Fracture	Other: Anhydrite	Oil/Bitumen	% Dol.: Low	Moderate	High	Samples	Comments	Depositional Environment
4610	light grey cut by white fractures																										FRACTURED, BURROW MOTTLED, CRINOIDAL DOLOWACKESTONE vuggy porosity ~15% ?trace bitumen in vugs assoc. w saddle dolomite	PROXIMAL MARINE RAMP
4613																												
4615																												
4618																											? No vugs occur here	
4620																												
4622																											Vuggy Porosity ~ 5-10% Intercrystalline porosity - mod ~10% in. crystalline dolomite Renalcis	
4624																												
4627																											Dolomitized Porous Sand Renalcis	

Date: July 27/2000
Well Location: 07-7-113-21 W5

Core Interval: 4512-4756
Correction Factor (Log to Core Conversion): Core -3.5 = log

Log Depth	Colour	Structures	Skeletal	Lithology: Graphic Log	Limestone	Dolostone	Anhydrite	Mudstone	Wackestone	Packstone	Grainstone	Rudstone	Floatstone	Boundstone	Porosity: Interparticle	Intraparticle	Moldic	Vuggy	Fenestral	Fracture	Other: Anhydrite	Oil/Bitumen	% Dol.: Low	Moderate	High	Samples	Comments	Depositional Environment
4630	light																										FRACTURED,	PROXIMAL
4631	grey																										BURROW MOTTLED	MARINE
4632	cut																										CRINOIDAL	RAMP
	by																										DOLOWACKESTONE	
	white																											
4635	fractures																										- trace bitumen in	
																											vugs assoc. w/	
																											saddle dol.	
																											- Renalcis	
																											- Absence of Oncol. Stromge	
4640																											→ Largest vug occluded!	
4641																											fracture porosity <1%	
												high % vuggy porosity - up to 20%															vuggy porosity ~10-20%	
																											→ dramatic increase	
																											due to fmt of	
																											larger vugs	
4646																											up to 9x8x6 cm!	
																											Renalcis	

7

B63

Date: July 27/2000
Well Location: 1-7-113-21W5

Core Interval: 4572-4756
Correction Factor (Log to Core Conversion): Core - 3.5 = log ✓

8

Log Depth	Colour	Structures	Skeletal	Lithology: Graphic Log	Limestone	Dolostone	Anhydrite	Mudstone	Wackestone	Packstone	Grainstone	Rudstone	Floatstone	Boundstone	Porosity: Interparticle	Intraparticle	Moldic	Vuggy	Fenestral	Fracture	Other: Anhydrite	Oil/Bitumen	% Dol.: Low	Moderate	High	Samples	Comments	Depositional Environment
4650	light grey cut																										FRACTURED,	PROXIMAL
																											BURROW MOTTLED	MARINE
																											CRINOIDAL	RAMP
4653	by white fractures																										DOLOWACKESTONE	
4656																											- Fracture Porosity ↳ low ~1% → occluded by dol. & anhydrite	
																											- Nodular & Bulbous Stroms	
4660																											- Renalcis	
																											Vuggy porosity ~5-10% ↳ rimmed by saddle dol, large anhydrite blades inside	
4665																											- Renalcis	
																											- "	
4668																												

Date: July 27/2000
Well Location: 7-7-113-21 W5

Core Interval: 4512 - 4756
Correction Factor (Log to Core Conversion): Core -3.5 = log

Log Depth	Colour	Structures	Skeletal	Lithology: Graphic Log	Limestone	Dolostone	Anhydrite	Mudstone	Wackestone	Packstone	Grainstone	Rudstone	Floatstone	Boundstone	Porosity: Interparticle	Intraparticle	Moldic	Vuggy	Fenestral	Fracture	Other: Anhydrite	Oil/Bitumen	% Dol.: Low	Moderate	High	Samples	Comments	Depositional Environment
4670	light grey cut by white fractures																										FRACTURED, BURROW MOTTLED CRINOIDAL DOLOWACKESTONE -Vuggy & Fracture Porosity ~5-10% ↳Mostly Vuggy -Renalcis -fracture & vuggy porosity on a continuum (some vugs assoc. w fractures) ↑becomes more ↑ open marine ↑ ↑-diverse fauna ↑ including stroms	PROXIMAL MARINE RAMP
4672																										few fractures		
4674																												
4677																												
4680																												
4683																												
4685																												
4688																												

Date: July 27/2000
Well Location: 7-7-113-21 W5

Core Interval: 4512 - 4756
Correction Factor (Log to Core Conversion): Core - 3.5 = log ✓

10

Lithology: Graphic Log | Limestone | Dolostone | Anhydrite | Mudstone | Wackestone | Packstone | Grainstone | Rudstone | Floatstone | Boundstone
Porosity: Interparticle | Intraparticle | Moldic | Vuggy | Fenestral | Fracture
Other: Anhydrite | Oil/Bitumen
% Dol.: Low | Moderate | High

Log Depth	Colour	Structures	Skeletal	Samples	Comments	Depositional Environment
4690	light grey cut by white fracture				FRACTURED, BURROW MOTTLED CRINOIDAL DOLOWACKESTONE	PROXIMAL MARINE RAMP
4694					} bracho/bivalves more abundant	
4697					-intercrystalline por. due to c.gr. matrix - sandy?	
4700					} saddle dol. lines vugs ~5% porosity	
4701						
4702					large vugs up to 9 cm across x 1 cm thick	
4705						
4708						

Date: July 27/2000
Well Location: 7-7-113-21W5

Core Interval: 4512 - 4756
Correction Factor (Log to Core Conversion): Core - 3.5 = log

17

Log Depth	Colour	Structures	Skeletal	Graphic Log	Limestone	Dolostone	Anhydrite	Mudstone	Wackestone	Packstone	Grainstone	Rudstone	Floatstone	Boundstone	Interparticle	Intraparticle	Moldic	Vuggy	Fenestral	Fracture	Anhydrite	Oil/Bitumen	Low	Moderate	High	Samples	Comments	Depositional Environment
4710	light grey cut by white fractures																										FRACTURED, BURROW MOTTLED CRINOIDAL DOLOWACKESTONE -scour surface? -fractures up to this depth, gap where no fractures occur from 4715-4690'	PROXIMAL MARINE RAMP
4713																										trace bitumen only		
4715																												
4717																												
4720																												
4723																											-unusual breccia -trace bitumen in matrix b/t dol. xtls -found in darker coarser grained, higher porosity matrix	

B67

Date: July 27/2000
Well Location: 7-7-113-21W5
Core Interval: 4513 - 4756
Correction Factor (Log to Core Conversion): Core -3.5 = log

12

Log Depth	Colour	Structures	Skeletal	Lithology: Graphic Log	Limestone	Dolostone	Anhydrite	Mudstone	Wackestone	Packstone	Grainstone	Rudstone	Floatstone	Boundstone	Porosity: Interparticle	Intraparticle	Moldic	Vuggy	Fenestral	Fracture	Other: Anhydrite	Oil/Bitumen	% Dol.: Low	Moderate	High	Samples	Comments	Depositional Environment
4730	light grey cut by white fractur																										FRACTURED, BURROW MOTTLED CRINOIDAL DOLOWACKESTONE	PROXIMAL MARINE RAMP
	Grey																										MASSIVE DOLOMUDSTONE	MESOSALINE
4737	Buff		None																							trace only	LAMINATED DOLOMUDSTONE	MESOSALINE SALINE
4739																											QUINTAGA	
4740	Grey Buff & Tan lamin-ated		None																								BEDDED MASSIVE ANHYDRITE - No fauna - No porosity - moderate dol. - laminated to thin bedded	HYPERSALINE BASIN - No fauna! - laminated; no bioturb-ation
																										BASE	OF CORE	

B68

Date:

Well Location: 9-19-116-4W6

Core Interval: 5212-5005

Correction Factor (Log to Core Conversion): Cores 5-7(-4.5) Core 8(-6.5) Core 9(0)

Log Depth	Colour	Structures	Skeletal	Lithology: Graphic Log	Limestone	Dolostone	Anhydrite	Mudstone	Wackestone	Packstone	Grainstone	Rudstone	Floatstone	Boundstone	Porosity: Interparticle	Intraparticle	Moldic	Vuggy	Fenestral	Fracture	Other: Anhydrite	Oil/Bitumen	% Dol.: Low	Moderate	High	Samples	Comments	Depositional Environment
4990																											TOP OF CORE	
5000	dk grey		NONE																								BEDDED MASSIVE TO DISTORTED BEDDED ANHYDRITE - buff colored dolostone	Hypersaline Basin - Evaporitic Drawdown?
5006	H. grey?																											
	v. light grey		?																								DOLOFLOATSTONE? Halofurbated?	Meso- Hypersaline Evaporitic
5009																											BRACH-CORAL FLOATSTONE	FORESLOPE

Date: July 23/2000
Well Location: 4-19-116-4W6

Core Interval: 5012-5005
Correction Factor (Log to Core Conversion): Cores 5-7 (-4.5) core 8 (-6.5) core 9 (0)

Log Depth	Colour	Structures	Skeletal	Lithology: Graphic Log	Limestone	Dolostone	Anhydrite	Mudstone	Wackestone	Packstone	Grainstone	Rudstone	Floatstone	Boundstone	Porosity: Interparticle	Intraparticle	Moldic	Vuggy	Fenestral	Fracture	Other: Anhydrite	Oil/Bitumen	% Dol.: Low	Moderate	High	Samples	Comments	Depositional Environment
5010																											BRACH-CORAL FLOATST.	FORESLOPE RUBBLE
	mid brown																						low			-178.0M -177Ts	FOSSIL-LEAN WACKE-STONE	SALINE? FORESLOPE
5012	light																										PELLOIDAL	FORESLOPE
	tan																										SKELETAL	SANDS.
	brown																										GRAINSTONE	
5015																												
																											FOSSIL-RICH	FORESLOPE
5017																											STROM-CORAL	RUBBLE
	light																										FLOATSTONE	
	brown	—E→																										
5020	to																											
	buff																											
5022																											2 thin tabular tabulate coral encrusted by and encrusting strom-interstroum	
5024																											3 Sandy fossil poor break	
5025		—E—																									7 Bitumen in fracture	
																											(Porosity - (low 2%)	
5027																											- Brecciated appearance	
		—E?—																									- Renalcis common	
5029		—E—																									- stylolitized - lots brecciated	

Date: July 28/2000 | Core Interval: 5212-5605

Well Location: 4-10-116-1W6 | Correction Factor (Log to Core Conversion): cores 5-7 (-4.5) core 8 (-6.5) core 9 (0)

3

Log Depth	Colour	Structures	Skeletal	Lithology: Graphic Log	Limestone	Dolostone	Anhydrite	Mudstone	Wackestone	Packstone	Grainstone	Rudstone	Floatstone	Boundstone	Porosity: Interparticle	Intraparticle	Moldic	Vuggy	Fenestral	Fracture	Other: Anhydrite	Oil/Bitumen	% Dol.: Low	Moderate	High	Samples	Comments	Depositional Environment
5030	light brown to buff	Cerenites?																									FOSSIL-RICH STROMATOPOROID CORAL FLOATSTONE	FORESLOPE RUBBLE
5032		Megalodont?																									-Alveolites & encrusting strom	
		Alveolites?																									-unidentified massive tab. lacks like a strom	
5035																											-wisps give brecciated appearance	
																											-abundant anhydrite	
																											-Alveolites	
																											-Favosites? ↕5cm	
5039.																												
5040																											-Number of thamnoporids encrusted by a thin strom	
																											partially dolomitized matrix	
5044																											-Favosites -massive tabulate	
5046																											-coated skeletal grains encrusted by water strom	

Alveolites

Date: July 23 / 2000 — Core Interval: 5212 - 5005

Well Location: 4-19-116-4W6 — Correction Factor (Log to Core Conversion): cores 5-7 (-4.5) core 8 (-6.5) core 9 (0)

Log Depth	Colour	Structures	Skeletal	Lithology: Graphic Log	Limestone	Dolostone	Anhydrite	Mudstone	Wackestone	Packstone	Grainstone	Rudstone	Floatstone	Boundstone	Porosity: Interparticle	Intraparticle	Moldic	Vuggy	Fenestral	Fracture	Other: Anhydrite	Oil/Bitumen	% Dol.: Low	Moderate	High	Samples	Comments	Depositional Environment
5050	light brown to buff	Alveolites?																									FOSSIL-RICH STROMATOPOROID CORAL FLOATSTONE	FORESHORE RUBBLE
5053																												
																										-175		
																											-Huge Alveolites - geopetals in branch	
5058																											-large massive tabulate	
5060		-E-																									Alveolites - very huge ~10cm x diam of core	
5062																												
																											-rugose? excavated by strom	
5067																											-geopetal fabric	
																											-Massive tabulate ↳ favosites?	
5069																												

B72

Date: July 23/2000
Well Location: 4-19-116-4W6
Core Interval: 5012 - 5005
Correction Factor (Log to Core Conversion): Core 5-7 (-4.5) Core 8 (-6.5) Core 9 (0)

5

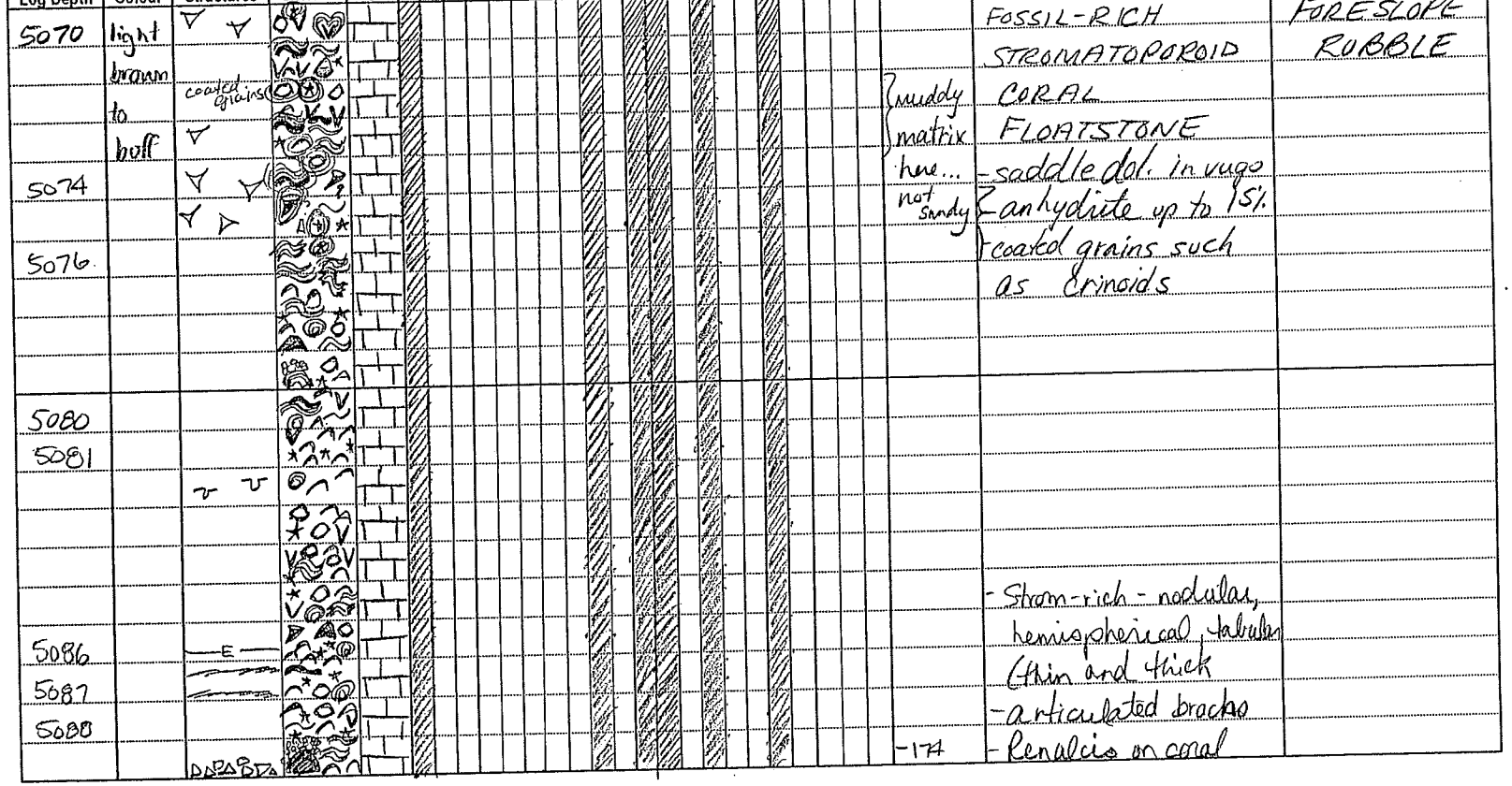

Log Depth	Colour	Structures	Skeletal	Samples	Comments	Depositional Environment
5070	light brown to buff	coated grains			FOSSIL-RICH	FORESLOPE
					STROMATOPOROID	RUBBLE
				muddy matrix	CORAL	
					FLOATSTONE	
5074				here... not sandy	- saddle dol. in vugs	
					anhydrite up to 15%	
5076					coated grains such as crinoids	
5080						
5081						
					- Strom-rich - nodular, hemispherical, tabular (thin and thick	
5086		E				
5087					- articulated brachs	
5088					- Renalcis on coral	
		DISPOSITE		-174		

B73

Date: July 23/2006 — Core Interval: 5012-5005

Well Location: 4-19-116-4W6 — Correction Factor (Log to Core Conversion): core 5-7 (-4.5) core 8 (-6.5) core 9(0)

6

Log Depth	Colour	Structures	Skeletal	Lithology: Graphic Log	Limestone	Dolostone	Anhydrite	Mudstone	Wackestone	Packstone	Grainstone	Rudstone	Floatstone	Boundstone	Porosity: Interparticle	Intraparticle	Moldic	Vuggy	Fenestral	Fracture	Other: Anhydrite	Oil/Bitumen	% Dol.: Low	Moderate	High	Samples	Comments	Depositional Environment
5090	light brown to buff																										FOSSIL-RICH STROMATOPOROID CORAL Floatstone	FORESLOPE RUBBLE
5093		-E-																										
5095																												
5098		-E-																									Partially Dolomitized Portion	
5099	buff																											
5100																										-173	Pellaidal, brach. ? Floatstone	TOE OF REEF -foreslope Sands
5103	light brown & buff																										STROM-CRINOID FLOATSTONE W GRAINSTONE MATRIX	TOE OF REEF SLOPE - Foreslope Rubble.
5107	buff														1-10%												Pelloidal, Brach. Floatstone	FORESLOPE SAND
	light brown	V															10-20%										STROM-CRINOID FLOATSTONE WITH GRAINSTONE MATRIX	FORESLOPE RUBBLE -TOE OF SLOPE

Date:

Well Location: 4-19-116-4W6

Core Interval: 5212-5605

Correction Factor (Log to Core Conversion): Cores 5-7 (-4.5) core 8 (-6.5) Core 9 (0)

7

Log Depth	Colour	Structures	Skeletal	Lithology: Graphic Log	Limestone	Dolostone	Anhydrite	Mudstone	Wackestone	Packstone	Grainstone	Rudstone	Floatstone	Boundstone	Porosity: Interparticle	Intraparticle	Moldic	Vuggy	Fenestral	Fracture	Other: Anhydrite	Oil/Bitumen	% Dol.: Low	Moderate	High	Samples	Comments	Depositional Environment
	buff																										FOSSIL-RICH	OPEN MARINE
5110	light grey																low										CRINOIDAL FLOAT-STONE	SHOAL ON RAMP (uppermost part)
5113	light brown and med grey																										BURROW MOTTLED PARTIALLY DOLOMITIZED CRINOID-BRACH. FLOATSTONE	OPEN MARINE -SHOAL ON RAMP
5120																											-anhydrite occurs infilling vugs and fractures where indicated	
5121																												
5122																												
5126																												
5128																												

Date:

Well Location: 4-19-118-7W6

Core Interval: 5212-5005

Correction Factor (Log to Core Conversion): Cores 5-7 (-4.5) one 8 (-6A) one 9 (0)

Log Depth	Colour	Structures	Skeletal	Lithology: Graphic Log	Limestone	Dolostone	Anhydrite	Mudstone	Wackestone	Packstone	Grainstone	Rudstone	Floatstone	Boundstone	Porosity: Interparticle	Intraparticle	Moldic	Vuggy	Fenestral	Fracture	Other: Anhydrite	Oil/Bitumen	% Dol.: Low	Moderate	High	Samples	Comments	Depositional Environment
5130	light																										BURROW MOTTLED	OPEN MARINE
	brown																										PARTIALLY DOLOMIT-	RAMP
	& med																										IZED CRINOID-	-SHOAL ON
	grey																										BRACHIOPOD	RAMP
																											FLOATSTONE	
5137																											-intercrystalline porosity ~5% (rel. low)	
5140																											~35-40% partially dolomitized (moderate degree)	
									grainy appearance bc noid sands																		
5145	med																										PARTIALLY DOLOMITIZED	
	brown																										BURROW-MOTTLED	PROXIMAL
	to																										CRINOIDAL WACKESTONE	RAMP
5148	med																									-170	-coated grains?	-burrowed
	grey																										oncoids	-limited OM WSDS

B

Date:

Well Location: 4-19-116-4W6

Core Interval: 5212 - 5006

Correction Factor (Log to Core Conversion): Cores 5-7 (-4.5) core 8 (-6.5) core 9 (0)

9

Log Depth	Colour	Structures	Skeletal	Lithology: Graphic Log	Limestone	Dolostone	Anhydrite	Mudstone	Wackestone	Packstone	Grainstone	Rudstone	Floatstone	Boundstone	Porosity: Interparticle	Intraparticle	Moldic	Vuggy	Fenestral	Fracture	Other: Anhydrite	Oil/Bitumen	% Dol.: Low	Moderate	High	Samples	Comments	Depositional Environment
5150	med brn to med grey																										Partially Dolomitized, Burrow Mottled CRINOIDAL WACKESTONE	PROXIMAL MARINE RAMP
5154	dk grey																									-169 -168	ALTERNATING LAMINATED AND BURROW MOTTLED WACKESTONE	SEMI-DISTAL MARINE RAMP - laminated but still burrowed in other parts - fossil-lean
5156	to med brn																											
5157																												
5158																											MISSING CORE	
5160																											CRICOCONARIDS	
5163	dk grey-																											
5164	med																											
5165	brown																									-167		
5169																											BURROW MOTLED/NODULAR WACKESTONE	PROXIMAL RAMP

B77

Date:

Well Location: 4-19-116-9W6

Core Interval: 5212-5005

Correction Factor (Log to Core Conversion): Cores 5-7 (-4.5) core 8 (-6.4) core 9 (0)

10

Log Depth	Colour	Structures	Skeletal	Lithology: Graphic Log	Limestone	Dolostone	Anhydrite	Mudstone	Wackestone	Packstone	Grainstone	Rudstone	Floatstone	Boundstone	Porosity: Interparticle	Intraparticle	Moldic	Vuggy	Fenestral	Fracture	Other: Anhydrite	Oil/Bitumen	% Dol.: Low	Moderate	High	Samples	Comments	Depositional Environment
5170	red brn lt dk grey wisps																										BURROW-MOTTLED NODULAR WACKESTONE	PROXIMAL MARINE RAMP
5180																												
5185																												
5188	v.dk grey to black																										MASSIVE TO SLIGHTLY BURROWED CRINOIDAL WACKESTONE · wafer strom ± thin tabulate	SEMI-DISTAL MARINE RAMP - v. rare

B78

Date:

Well Location: 4-19-116-4W6

Core Interval: 5212-5005

Correction Factor (Log to Core Conversion): Cores 5-7 (-4.5) core 8 (-6.5), core 9 (0)

11

Log Depth	Colour	Structures	Skeletal	Lithology: Graphic Log	Limestone	Dolostone	Anhydrite	Mudstone	Wackestone	Packstone	Grainstone	Rudstone	Floatstone	Boundstone	Porosity: Interparticle	Intraparticle	Moldic	Vuggy	Fenestral	Fracture	Other: Anhydrite	Oil/Bitumen	% Dol.: Low	Moderate	High	Samples	Comments	Depositional Environment
5190	v. dark grey to black																										MASSIVE TO SLIGHTLY BURROWED CRINOIDAL WACKESTONE	SEMI-DISTAL MARINE RAMP
																											↑ burrowed slightly and intraclasts	
5195																											- restricted fauna ↳ crinoids, bracho, bivalves, few gastropods, ostracodes etc.	
5200																											- v. thin laminated zone	
5202																												
5207																											- v. thin laminated zones	

Date: July 19/2000
Well Location: 4-19-116-4W6

Core Interval: 5212-5005
Correction Factor (Log to Core Conversion): core 5-7 (4.5), core 8 (-6.5), core 9 (0)

12

Log Depth	Colour	Structures	Skeletal	Graphic Log	Lithology: Limestone	Dolostone	Anhydrite	Mudstone	Wackestone	Packstone	Grainstone	Rudstone	Floatstone	Boundstone	Porosity: Interparticle	Intraparticle	Moldic	Vuggy	Fenestral	Fracture	Other: Anhydrite	Oil/Bitumen	% Dol.: Low	Moderate	High	Samples	Comments	Depositional Environment
5210	v. dk grey to black																										MASSIVE TO SLIGHTLY BURROWED CRINOIDAL WACKESTONE -v. thin laminated zones	SEMI-DISTAL MARINE RAMP
5215																											BASE OF CORE	

Date:

Well Location: 5-36-117-6W6

Core Interval: 5666-5464

Correction Factor (Log to Core Conversion): CORE -1 = LOG

Log Depth	Colour	Structures	Skeletal	Lithology: Graphic Log	Limestone	Dolostone	Anhydrite	Mudstone	Wackestone	Packstone	Grainstone	Rudstone	Floatstone	Boundstone	Porosity: Interparticle	Intraparticle	Moldic	Vuggy	Fenestral	Fracture	Other: Anhydrite	Oil/Bitumen	% Dol.: Low	Moderate	High	Samples	Comments	Depositional Environment
5450																												
5460																											TOP OF CORE	
5463																											CRINOID/STROM DOLOFLOATSTONE	
5465																												
5468																												

Date:

Well Location: 5-30-117-6W6

Core Interval: 5466 - 5487'

Correction Factor (Log to Core Conversion): CORE - 1 = LOG

Log Depth	Colour	Structures	Skeletal	Lithology: Graphic Log	Limestone	Dolostone	Anhydrite	Mudstone	Wackestone	Packstone	Grainstone	Rudstone	Floatstone	Boundstone	Porosity: Interparticle	Intraparticle	Moldic	Vuggy	Fenestral	Fracture	Other: Anhydrite	Oil/Bitumen	% Dol.: Low	Moderate	High	Samples	Comments	Depositional Environment
5470		E																									CRINOID / STROM DOLOFLOATSTONE	
5471		E																										
5476																												
5478		E																										
5480																												
5484		E																										
5487																												
5489		E																										

N

Date:

Well Location: 5-36-117-6W6

Core Interval: 5666 - 5464

Correction Factor (Log to Core Conversion): CORE-1 = LOG

Log Depth	Colour	Structures	Skeletal	Lithology: Graphic Log	Limestone	Dolostone	Anhydrite	Mudstone	Wackestone	Packstone	Grainstone	Rudstone	Floatstone	Boundstone	Porosity: Interparticle	Intraparticle	Moldic	Vuggy	Fenestral	Fracture	Other: Anhydrite	Oil/Bitumen	% Dol.: Low	Moderate	High	Samples	Comments	Depositional Environment
5490																											CRINOID/STROM DALOFLOATSTONE	3
5493		E																										
5495																												
5496		E																										
		E																										
5500			zebra dol																								Zebra Dolomite texture	
		E																										
5505																												
		E																										

B83

Date:

Well Location: 5-36-117-6W6

Core Interval: 5666 - 5464'

Correction Factor (Log to Core Conversion): CORE-1=LOG

Log Depth	Colour	Structures	Skeletal	Lithology: Graphic Log	Limestone	Dolostone	Anhydrite	Mudstone	Wackestone	Packstone	Grainstone	Rudstone	Floatstone	Boundstone	Porosity: Interparticle	Intraparticle	Moldic	Vuggy	Fenestral	Fracture	Other: Anhydrite	Oil/Bitumen	% Dol.: Low	Moderate	High	Samples	Comments	Depositional Environment
5510	light-med grey	E																									CRINOID / STROM DOLOFLOATSTONE	
5512	med brown & black																										BEDDED PELLOIDAL ~~DOLOGRAINSTONE~~, GRAINSTONE AND OM-RICH LAMINAE	DISTAL RAMP TO SEMI-DISTAL RAMP
															5% low											-161		
5514	light grey	m													35% low								-	low				
5515	mottled med grey and tan																										BURROW MOTTLED, PARTIALLY DOLOMITIZED CRINOIDAL WACKESTONE	PROXIMAL MARINE RAMP
5520	v. dk grey to black	m																									LAMINATED LIME MUDSTONE & laminae disrupted	DISTAL RAMP
5523																										-160		
5525	mottled tan and med. grey																									159	~~PARTIALLY DOLOMITIZED~~ BURROW MOTTLED CRINOIDAL WACKESTONE → laminated OM-rich interval ↳ distal ramp deposit - quiet waters!	PROXIMAL MARINE RAMP

4

B84

Date: July 17/2000 | Core Interval: 5666 - 5764

Well Location: 5-36-117-6w6 | Correction Factor (Log to Core Conversion): CORE-1=LOG

Log Depth	Colour	Structures	Skeletal	Lithology: Graphic Log	Limestone	Dolostone	Anhydrite	Mudstone	Wackestone	Packstone	Grainstone	Rudstone	Floatstone	Boundstone	Porosity: Interparticle	Intraparticle	Moldic	Vuggy	Fenestral	Fracture	Other: Anhydrite	Oil/Bitumen	% Dol.: Low	Moderate	High	Samples	Comments	Depositional Environment
5530	mottled buff and med. grey																										BURROW MOTTLED, PARTIALLY DOLOMITIZED CRINOIDAL WACKESTONE	PROXIMAL MARINE RAMP
5533																										-158		-burrowed -restricted fauna (no corals or strom)
5540																												
5543																												
5545																										MISSING CORE		
5546	dk brown black																										VERY FOSSIL-LEAN CRINOIDAL WACKESTONE	SEMI-DISTAL MARINE RAMP

5

Date: July 17/2000
Well Location: 5-36-117-6W6

Core Interval: 5566-5569
Correction Factor (Log to Core Conversion): Core - 1 = log

Log Depth	Colour	Structures	Skeletal	Lithology: Graphic Log	Limestone	Dolostone	Anhydrite	Mudstone	Wackestone	Packstone	Grainstone	Rudstone	Floatstone	Boundstone	Porosity: Interparticle	Intraparticle	Moldic	Vuggy	Fenestral	Fracture	Other: Anhydrite	Oil/Bitumen	% Dol.: Low	Moderate	High	Samples	Comments	Depositional Environment
5550	dk brown-black																										VERY FOSSIL-LEAN CRINOIDAL WACKESTONE	SEMI-DISTAL MARINE RAMP
5553																												
5558																											wafer strom	
5560																											Alveolites	
5563																												
5565																												

Date: July 17/2000
Well Location: 5-37-117-6W6

Core Interval: 5466-5464
Correction Factor (Log to Core Conversion): Core -1 = LOG

Log Depth	Colour	Structures	Skeletal	Lithology: Graphic Log	Limestone	Dolostone	Anhydrite	Mudstone	Wackestone	Packstone	Grainstone	Rudstone	Floatstone	Boundstone	Porosity: Interparticle	Intraparticle	Moldic	Vuggy	Fenestral	Fracture	Other: Anhydrite	Oil/Bitumen	% Dol.: Low	Moderate	High	Samples	Comments	Depositional Environment
5570	dk brown-black																										Very Fossil-lean Crinoidal Wackestone <1%-trace anhydrite	SEMI-DISTAL MARINE RAMP
5574																												
5580																											-Directum?	
5585																												
	dk brown-grey																										CRINOIDAL WACKESTONE	PROXIMAL MARINE RAMP -deeper than previous

7

B87

Date: July 17/2000
Well Location: 5-36-117-6W6

Core Interval: 5566-5569
Correction Factor (Log to Core Conversion): CORE -1 = LOG

8

Log Depth	Colour	Structures	Skeletal	Graphic Log	Lithology: Limestone	Dolostone	Anhydrite	Mudstone	Wackestone	Packstone	Grainstone	Rudstone	Floatstone	Boundstone	Porosity: Interparticle	Intraparticle	Moldic	Vuggy	Fenestral	Fracture	Other: Anhydrite	Oil/Bitumen	% Dol.: Low	Moderate	High	Samples	Comments	Depositional Environment
5590	dk brown grey																										CRINOIDAL WACKESTONE	PROXIMAL MARINE RAMP -Somewhat deeper than prev. unit -more restricted fauna -less fossil-rich
5595																										-157		
5597																												
5600																												
5602																												
5605	dk to med grey brown																										Intraclastic? Crinoidal Floatstone	OPEN MARINE RAMP -shoal on ramp
5608																												

Date: July 17 / 2000
Well Location: 5-36-117-6W6

Core Interval: 5666-5764
Correction Factor (Log to Core Conversion): CORE-1 = LOG

Log Depth	Colour	Structures	Skeletal	Lithology: Graphic Log	Limestone	Dolostone	Anhydrite	Mudstone	Wackestone	Packstone	Grainstone	Rudstone	Floatstone	Boundstone	Porosity: Interparticle	Intraparticle	Moldic	Vuggy	Fenestral	Fracture	Other: Anhydrite	Oil/Bitumen	% Dol.: Low	Moderate	High	Samples	Comments	Depositional Environment
5610	med to dk grey brown																										Intraclastic? Crinoidal Floatstone	OPEN MARINE RAMP -Crinoid shoal on the ramp
5612																												
5614																												
5616																										-156	-Alveolites?	
5618																											-Alveolites?	
5620																											-Favosites?	
5623																											-No porosity	
5626																											-	

9

Date: July 17/2000
Well Location: 5-36-117-6W6

Core Interval: 5666 - 5464
Correction Factor (Log to Core Conversion): CORE-1 = LOG

Log Depth	Colour	Structures	Skeletal	Lithology: Graphic Log	Limestone	Dolostone	Anhydrite	Mudstone	Wackestone	Packstone	Grainstone	Rudstone	Floatstone	Boundstone	Porosity: Interparticle	Intraparticle	Moldic	Vuggy	Fenestral	Fracture	Other: Anhydrite	Oil/Bitumen	% Dol.: Low	Moderate	High	Samples	Comments	Depositional Environment
5630																											Intraclastic? Crinoidal Floatstone	OPEN MARINE RAMP - Crinoid Shoal on the Ramp
5633																											- Tight: No porosity	
5635																												
5636																												
																										-155	- Amphipora	
5639																												
5640	med-																										Burrow mottled, Partially Dolomitized Fossil Lean Wackestone	PROXIMAL MARINE RAMP - Normal salinity
	grey																											
	to buff																											
5643																												
	buff																										BURROW MOTTLED DOLOMUDSTONE - breccia @ contact - scour surface	PROXIMAL MARINE RAMP - elevated salinity (fossil poor)
	and																											
	med																											
	grey																											
5648																												
	med-																										LIME MUDSTONE - Partially Dolomitized	PROXIMAL MARINE RAMP - elevated salinity
	brown															<1%												

Date: July 17/2000
Well Location: 5-36-117-6W6
Core Interval: 5666-5764
Correction Factor (Log to Core Conversion): Core -1 = LOG DEPTH

Log Depth	Colour	Structures	Skeletal	Lithology: Graphic Log	Limestone	Dolostone	Anhydrite	Mudstone	Wackestone	Packstone	Grainstone	Rudstone	Floatstone	Boundstone	Porosity: Interparticle	Intraparticle	Moldic	Vuggy	Fenestral	Fracture	Other: Anhydrite	Oil/Bitumen	% Dol.: Low	Moderate	High	Samples	Comments	Depositional Environment
5650	med brown																										LAMINATED LIME-MUDSTONE	MESOSALINE BASIN
5651	buff to med grey laminae																										LAMINATED DOLOMUDSTONE	MESOSALINE BASIN -deepening or freshening
5656	med grey to buff																										Bedded Massive Anhydrite	Hypersaline Basin
5660	lam.																											
5665																											BASE OF CORE	

11

B91

APPENDIX C: PETROGRAPHIC TECHNIQUES

C.1 Staining Techniques for Carbonates (Dickson, 1966)

A) To distinguish between calcite and dolomite:

ALIZARIN RED S - 2994 mL distilled water
16 mL conc. HCl (37%)
3 gm Alizarin Red S

B) To distinguish between ferroan carbonate and nonferroan carbonate:

POTASSIUM FERRICYANIDE - 2994 mL distilled water
16 mL conc. HCl (37%)
15 gm potassium ferricyanide

Store solution in a brown bottle, away from light. Filter before use if a precipitate develops.

1. Prepare each of the above solutions separately and allow them to stand for 24 hours before using.
2. Combine solutions in the following ratio: 2 parts Alizarin Red S to 3 parts potassium ferricyanide.
3. Staining time is approximately 2 minutes depending upon temperature and polish on the slides. The solution should be changed after approximately 24 slides are stained to maintain the effectiveness of the solution.
4. Always wash slides with distilled water; tap water contains iron and will blot on the slide. Remove slides from the stain bath and place in distilled water bath. Next rinse with distilled water.

Mineral	Effect of Etching	Stain Color with Alizarin Red S	Stain Color with Potassium Ferricyanide	Combined Result
Calcite (non-ferroan)	Considerable (relief reduced)	Pink to red-brown	None	Pink to red-brown
Calcite (ferroan)	Considerable (relief reduced)	Pink to red-brown	Pale to deep blue depending on iron content	Mauve to blue
Dolomite (non-ferroan)	Negligible (relief maintained	None	None	Colorless
Dolomite (ferroan)	Negligible (relief maintained)	None	Very pale blue	Very pale blue (appears turquoise or greenish in thin section)

Table C.1 Etching and staining characteristics of carbonate minerals (Adams *et. al*, 1984).

C.2 Diffused Plane-Polarized Light Method

Diffused plane-polarized light microscopy facilitates the delineation of relict grains and textures in massive crystalline dolomites or highly recrystallized limestones previously undetectable by standard plan-polarized light or crossed nicols (Dravis, 1991). This method also enhances recognition of stylolites, sutured grain contacts, opaque minerals, organic matter, and bitumen.

The use of diffused plane-polarized light microscopy to discern primary fabrics in dolomitized samples was first proposed by Delgado (1977), later modified by Folk (1987), and subsequently modified by Dravis (1991). This study utilized the method of Dravis (1991) which involves using a piece of white paper (standard white Xerox paper is recommended) placed beneath the thin section on a microscope stage to diffuse transmitted plane polarized light. The condenser lens was used in this study to concentrate the transmitted light for more intense light transmission and enhanced viewing conditions. An external light source was utilized to provide low angle reflected light which also enhances the appearance of relict grains and textures. Diffused plane-polarized light travels in random and indirect paths through thin sections rendering crystal boundaries nearly invisible and permitting the recognition of relict grains obscured by recrystallization. Allochem "ghosts" including peloids, ooids, and skeletal fragments may be recognized by tiny inclusions, vacuoles, and a brownish-colored stain (Zenger, 1979).

This microscopy method works equally well with unpolished, polished, uncovered, and covered thin sections. Uncovered or unpolished thin sections should be coated with a thin film of immersion oil or protective lacquer (Dravis, 1991). Buehler Metcoat Specimen Protective Lacquer worked well in this study.

APPENDIX D: THIN SECTION DESCRIPTIONS

This appendix contains a spreadsheet of thin section descriptions for all the samples analyzed petrographically in this study. Each samples was assigned a sample number which corresponds to the order it was collected and therefore corresponds closely to well location and depth.

Well Location	Sub-basin	Depth Range of Samples (feet)	Page #'s
00/06-32-107-09W6/0	Rainbow	6798.75 - 6939.1	D2 - D5
00/04-16-108-07W6/0	Rainbow	6515 - 6572.75	D4 - D7
00/04-09-109-08W6/0	Rainbow	6494 - 6714.6	D6 - D13
00/06-32-109-08W6/0	Rainbow	6453.5 - 6630.5	D12 - D17
00/12-33-109-08W6/0	Rainbow	6468.6 - 6642.5	D16 - D21
00/04-30-110-09W6/0	Rainbow	6384	D22 - D23
00/07-07-113-21W5/0	Meander	4569 - 4699.5	D22 - D23
00/04-19-116-04W6/0	Zama	5007 – 5154	D22 - D25
00/10-21-116-05W6/0	Zama	5250 – 5340	D25 - D27
00/05-36-117-06W6/0	Zama	5489 - 5651	D26 - D28

Sample	Location	Depth	Lithofacies	Allochems																										Dolomitization etc.						Accessories						
				Crinoids	Brachs	Bivalves	Undifferntiated Brach/Bivalve	Ostracodes	Gastropods	Stylolinids	Tentaculitids	Strom Fragments	Strom (Thin Tabular)	Strom (Wafer Strom)	Thamnoporids	Coenites	Alveolites	Rugose Coral	Amphipora	Tabular Tabulate Coral	Massive Tabulate Coral	Rugose Coral	Oncoids	Peloids	Intraclasts	Aggregate grains	Algal Structures	% Carbonate Grains	Non-Dolomitized	% Partially Dolomitized	Fully Dolomitized	Fracture-Filling	Vug-Filling	Saddle Dolomite	Quartz	Anhydrite	Sphalerite	Pyrite	Bitumen	Argillaceous Material	OM
115	6-32-107-9W6	6767.7	G	35	25	10		5		5											1			20				60		20					1	1					
114	6-32-107-9W6	6793.7	H	*	*	*		*		*					*	*								*				75		15					1	1					
113	6-32-107-9W6	6796.9	H	15	10	5		5		5			1		15							15		30				70		10					5	2		1	*	*	*
116	6-32-107-9W6	6798.75	F	20	10	10		10		20														30				55		25								1	10	*	*
112	6-32-107-9W6	6811.5	E	15	60	1		10	1	10																		60		15					1	5		5	*	*	*
109	6-32-107-9W6	6837.5	A	1	40					60																		25	*						1			10	*	*	*
107	6-32-107-9W6	6849.5	C	15	25			20		40	1																	10	*							1		5	*	*	*
104	6-32-107-9W6	6858.75	C	25	30	5		15	5	15	1						1								5			30	*							5		10	*	*	*

Sample	Location	Depth	Lithofacies	Matrix								Porosity											Structures									Comments
				% Non-Carbonate	Mudstone	Wackestone	Floatstone	Packstone	Grainstone	Rudstone	% Matrix	Interparticle	Intraparticle	Intercrystalline	Moldic	Fenestral	Shelter	Growth-Framework	Fracture	Channel	Vug	% Porosity	Laminations	Bedding	Nodular Texture	Microstylolites	Massive	Bioturbated	Event Concentration	Brecciated	Other	
115	6-32-107-9W6	6767.7	G	2				•			30		•	•								10					•				Similar to matrix of lithofacies H. Very grainy appearance, Favosites (massive tabulate coral fragment 1.5cm x 1.3cm rounded but not abraded)
114	6-32-107-9W6	6793.7	H	2			•	•			15			•								8					•				Very similar to Sample 113. Floatstone with packstone matrix - Coenites (avg. 3mm diam) is more common. Peloids - abundant.
113	6-32-107-9W6	6796.9	H	10			•	•			10		•	•								10					•				Floatstone with packstone matrix (peloids and bioclasts). Rugose Coral - 1.7cm diam, Encrusting Strom - on Rugose ~2mm thick, Thamnoporid fragments - 1.5cm long x 3mm thick, Stylolinids - 0.4mm diam. Fossils commonly partially silicified. Matrix dolomite (medium crystalline planar euhedral).
116	6-32-107-9W6	6798.75	F	10				•			10											0	•			•					Matrix is unusual - does not look like it had micritic precursor, matrix was probably isopachous rims and interstitial blocky carbonate cements which cemented carbonate grains (bioclasts) together. This was later dolomitized partially. Many fossils recrystallized into anhedral optically continuous xtls which contain allochem ghosts
112	6-32-107-9W6	6811.5	E	15						•	25											0				•		•			Variation of the Bioturbated Crinoid-Brachiopod Wackestone lithofacies. Abundant articulated (1.7cm x 1.3cm) and disarticulated (down to 2mm long, <1mm thick) randomly oriented brachs. Cements (prismatic carbonate cements grow inwards from bivalve shells - early), Microstylolites (relatively abundant - compress around grains and fossils), Pyrite (in matrix and in pyritized fossils -esp. stylolinids), Geopetal infil - commonly contain less fossils than matrix)
109	6-32-107-9W6	6837.5	A	25		•					50											0	•								Pyrite occurs as pyritized fossils (large brachs and stylolinids), indistinct pyritized patches of matrix, and what looks like pyrite geopetal infil of v. fine crystalline pyrite. Fossils all parallel laminae
107	6-32-107-9W6	6849.5	C	10		•					80											0			•						Buff colored micrite (this section was unstained) and brown colored argillaceous wisps - concentrate as microstylolites (bend around fossils). All fossils are more abundant in the argillaceous parts of sample.
104	6-32-107-9W6	6858.75	C	25		•					45											0			•	•				•	Unusual "burrow" structures - relatively fossil-poor wackestone forms finger-like structures which extend downwards. Between these "fingers" brecciated, fossil-rich floatstone with carbonate cements (blocky ferroan and non-ferroan) as well as euhedral v. coarsely crystalline anhydrite occurs. Wackestone could be burrow infil or could be the original lithology and the floatstone could be cavings caused by dissolution. OM wisps are common - up to 3mm thick, pyritized intraclasts (5mm x 3mm - ovoid, random orientation) also occur.

Sample	Location	Depth	Lithofacies	Allochems																								Dolomitization etc.						Accessories						
				Crinoids	Brachs	Bivalves	Undifferntiated Brach/Bivalve	Ostracodes	Gastropods	Stylolinids	Tentaculitids	Strom Fragments	Strom (Thin Tabular)	Strom (Wafer Strom)	Thamnoporids	Coenites	Alveolites	Rugose Coral	Amphipora	Tabular Tabulate Coral	Massive Tabulate Coral	Rugose Coral	Oncoids	Pelolds	Intraclasts	Aggregate grains	Algal Structures	% Carbonate Grains	Non-Dolomitized	% Partially Dolomitized	Fully Dolomitized	Fracture-Filling	Vug-Filling	Saddle Dolomite	Quartz	Anhydrite	Sphalerite	Pyrite	Bitumen	Argillaceous Material	OM
103	6-32-107-9W6	6863.9	C	40	25	5		5	1	25																	35	*									10	*	*	*
102	6-32-107-9W6	6872.6	C	40	20	5		10	5	20																	20		5								5	*	*	*
101	6-32-107-9W6	6893	C	40	20	10		10	5	20															1		1	40		5						10	1	*	*	*
100	6-32-107-9W6	6916	D	30	25	5		15	5	15																	1	70		15								1	*	*	*
99	6-32-107-9W6	6929.4	C	35	20	10		15	5	1						1								5	15		1	75		30								1	*	*	*
97	6-32-107-9W6	6939.1	H	20	10	10		5	1				20				35											70		20						1		1			
52	4-16-108-7W6	6567	A		5			20		75																		15		90								5	*	*	*
50	4-16-108-7W6	6569.5	A		5					70	25																	20	*							1		5			5
61	4-16-108-7W6	6515	G	*			*	*	*	*																		15			*				10	*	*	*	*	*	*
60	4-16-108-7W6	6519.75	G	*			*	*	*	*																		10			*				10	1	5	1	1	*	*
59	4-16-108-7W6	6523.5	G	30			50	10	1	10																		15			*				10		1	1	*	*	*

Sample	Location	Depth	Lithofacies	% Non-Carbonate	Matrix							Porosity											Structures									Comments
					Mudstone	Wackestone	Floatstone	Packstone	Grainstone	Rudstone	% Matrix	Interparticle	Intraparticle	Intercrystalline	Moldic	Fenestral	Shelter	Growth-Framework	Fracture	Channel	Vug	% Porosity	Laminations	Bedding	Nodular Texture	Microstylolites	Massive	Bioturbated	Event Concentration	Brecciated	Other	
103	6-32-107-9W6	6863.9	C	15		•					50											0			•	•					Very nodular appearance, nodules contain less OM, pyrite, fossils, and argillaceous material than the matrix (nodules appear pink, matrix looks brown). Nodules (very indistinct boundaries, irregular, up to 1.5cm long x 0.5cm wide). Matrix (contains abundant pyrite - assoc. w OM, No porosity. Fossils are more abundant in the argillaceous parts - could be due to decrease in carbonate production - this would allow more fossils and argillaceous material to settle.
102	6-32-107-9W6	6872.6	C	15		•					65											0			•	•					Relatively fossil-poor, homogenous, abundant micritic matrix - contains small amounts of argillaceous material and abundant bioclasts. Allochems replaced by ferroan and non-ferroan calcite cement (blocky) could cement moldic porosity? Very finely crystalline pyrite assoc. w calcite cement.
101	6-32-107-9W6	6893	C	15		•					45								•			1			•	•					Horsetail microstylolites wrap around burrows (range from 0.02 to 1.6 mm thick), Nodules lack OM, microstylolites, bitumen, argillaceous materials and are non-dolomitized. Intraclasts are pyritized
100	6-32-107-9W6	6916	D	10			•	•			20								•			1				•					Similar to sample 99 but no intraclats or nodules, abundant microstylolites, Girvenella present
99	6-32-107-9W6	6929.4	C	5			•	•			20								•			1			•	•					Floatstone wth packstone matrix (anhedral non-planar v. finely crystalline dolomite, micrite, argillaceous material and microstylolites), Girvenella, pyritized intraclasts, abundant microstylolites
97	6-32-107-9W6	6939.1	H	2			•	•			30											0					•				Floatstone with packstone matrix, Anhydrite (v. coarsely crystalline euhedral laths occlude vuggy porosity, subhedral laths occur in matrix), Cements (fine radial calcite-microspar, coarse calcite-pseudospar, micritized coral wall, seen in Alveolites coral), Pyrite (assoc with allochems
52	4-16-108-7W6	6567	A	10	•						75											0	•			•					Similar to sample 50 but matrix is dolomitized (light grey color), OM and argillaceous matter and fossils make up dark brown to black laminae (contain microstylolites)
50	4-16-108-7W6	6569.5	A	10		•					70											0	•								Vague laminae (0.4 to 1.2mm thick - darker=more OM, lighter=more skeletal and bioclastic fagments), allochems alligned parallel to laminations, Cemented articulated brachiopod (fibrous calcite lines shell, inside this prismatic calcite, then micrite and anhedral anhydrite occlude the pore)
61	4-16-108-7W6	6515	G	15				•			70			•							•	1				•	•				Similar to samples 59 and 60. These packstones are easier to interpret than in prev. well (4-9-109-8W6) b/c dolomitization doesn't destroy textures as much. Mottled appearance due to horsetail microstylolites (made up of brown OM)
60	4-16-108-7W6	6519.75	G	18				•			65		?	•							•	5				•	•				Similar to sample 59
59	4-16-108-7W6	6523.5	G	15				•			70			•								1				•	•				Relatively homogeneous, slightly mottled, v. pale buff color, minor microstylolites, microquartz concentrated around porosity, allochems, and assoc. with pyrite.

Sample	Location	Depth	Lithofacies	Allochems																									Dolomitization etc.						Accessories						
				Crinoids	Brachs	Bivalves	Undifferntiated Brach/Bivalve	Ostracodes	Gastropods	Stylollinids	Tentaculitids	Strom Fragments	Strom (Thin Tabular)	Strom (Wafer Strom)	Thamnoporids	Coenites	Alveolites	Rugose Coral	Amphipora	Tabular Tabulate Coral	Massive Tabulate Coral	Rugose Coral	Oncoids	Peloids	Intraclasts	Aggregate grains	Algal Structures	% Carbonate Grains	Non-Dolomitized	% Partially Dolomitized	Fully Dolomitized	Fracture-Filling	Vug-Filling	Saddle Dolomite	Quartz	Anhydrite	Sphalerite	Pyrite	Bitumen	Argillaceous Material	OM
58	4-16-108-7W6	6531	H	*			*	*	*			*	*	*		*											70			*				*			*	*	*	*
57	4-16-108-7W6	6543.5	H	*			*	*	*			*	*	*		*											70			*				*			*	*	*	*
56	4-16-108-7W6	6549.5	H	*			*	*	*			*		*		*							*				70			*				*			*	*	*	*
55	4-16-108-7W6	6558	H	10			20	5				50				10							5					70			*				10			5	*	*	*
46	4-16-108-7W6	6572.75	E	10	50	5		15	1	20	1													5	5	1		70		60			*			10		2				
39	4-9-109-8W6	6510.75	H	20			20	10		1		50																50			*		*	*				0.5	1	5	5
38	4-9-109-8W6	6511.5	F	*			*	*																				40			*							1	5	*	*
23	4-9-109-8W6	6591	A																																							
22	4-9-109-8W6	6593.62	A		40					60	1																	30										*	*	*	*
21	4-9-109-8W6	6594	A																																							
4	4-9-109-8W6	6691.45	D	*			*																					20			*		*				*	*				*
3	4-9-109-8W6	6700.11	I																					*				1			*								*	*	*
1	4-9-109-8W6	6714.6	J																																							
41	4-9-109-8W6	6494	H	*			*	*		*		*			*													50			*		*	*				*	*	*	*
40	4-9-109-8W6	6499	H	*			*	*																				30					*	*					*	*	*
37	4-9-109-8W6	6511.75	F																																							

Sample	Location	Depth	Lithofacies	% Non-Carbonate	Matrix							Porosity											Structures									Comments
					Mudstone	Wackestone	Floatstone	Packstone	Grainstone	Rudstone	% Matrix	Interparticle	Intraparticle	Intercrystalline	Moldic	Fenestral	Shelter	Growth-Framework	Fracture	Channel	Vug	% Porosity	Laminations	Bedding	Nodular Texture	Microstylolites	Massive	Bioturbated	Event Concentration	Brecciated	Other	
58	4-16-108-7W6	6531	H	20						•	10								•		•	5					•				Similar to 55 to 57. Easier to id skeletal fragments in this TS, may be intraclasts as well as strom fragments - some "strom fragments" seem to contain other allochems - these are actually intraclasts.
57	4-16-108-7W6	6543.5	H	20						•	10								•		•	5					•				Similar to sample 55 and 56, many skeletal fragments partially pyritized
56	4-16-108-7W6	6549.5	H	20						•	10			•							•	1					•				Similar to sample 55 but contains wafer stroms (2.5mm long x 1.5mm thick), gastropods (2mm diam), and oncoids visibly coat crinoid ossicles.
55	4-16-108-7W6	6558	H	20						•	10			•							•	1					•				Abundant microstylolites weave around grainy matrix (non-planar anhedral dolomicrite), Strom fragments (irregular shape, ragged edge, internal structure destroyed, 2.5 x 2cm size minimum), Chalcedonic and authigenic qtz occur at outer edges of vugs and replaces fossils, assoc. with pyrite.
46	4-16-108-7W6	6572.75	E	12						•	18			•							•	1					•				V. fossiliferous, grapestones (lumps of peloids up to 1.4mm x 1mm ovoid, anhydrite and pyrite assoc w vuggy pores, ie. In allochems). Matrix is dk brown and unstained - may be nonplanar v. finely crystalline dolomite - or inclusion rich micrite - nondolomitized)
39	4-9-109-8W6	6510.75	H	10			•	•			30			1					1		3	5				•					Dolofloatstone with Dolopackstone matrix. Matrix (polymodal non-planar anhedral medium to v. coarsely crystalline dolomite, finest dol assoc w OM and argillaceous material), Vug Filling Dolomite (medium to v. coarsely crystalline saddle dolomite)
38	4-9-109-8W6	6511.5	F	6				•			55			•							•	1	•			•					Pyrite (conc. Near bitumen, medium crystalline framboids - made up of much finer grains), Bitumen (infils vugs, also bituminous laminae up to 1mm thick, Matrix (medium to v. coarsely crystalline non-planar anhedral dolomite - finer and brown color near microstylolites, OM)
23	4-9-109-8W6	6591	A																												
22	4-9-109-8W6	6593.62	A	5			•				65											0	•								Transition from nodular wackestone to laminated floatstone up section - indicates decreased sed rate, larger fossils and OM accumulate in laminae
21	4-9-109-8W6	6594	A																												
4	4-9-109-8W6	6691.45	D	2		•					73			•					•			5								•	polymodal subhedral to euhedral planar dolomite matrix
3	4-9-109-8W6	6700.11	I	1	•						98								•		•	1				•					finely crystalline non-planar anhedral dolomite matrix
1	4-9-109-8W6	6714.6	J																												
41	4-9-109-8W6	6494	H	10			•	•			30			•							•	5				•					Similar to sample 39. Strom fragments hard to identify (remnant internal structure, high porosity, coarsely crystalline)
40	4-9-109-8W6	6499	H	1					•		45			•								25				•					V. porous and grainy. Lowest porosity in argillaceous material. Microstylolites v. sparse and poorly developed.
37	4-9-109-8W6	6511.75	F																												

Sample	Location	Depth	Lithofacies	Allochems																										Dolomitization etc.						Accessories						
				Crinoids	Brachs	Bivalves	Undifferntiated Brach/Bivalve	Ostracodes	Gastropods	Stylolinids	Tentaculitids	Strom Fragments	Strom (Thin Tabular)	Strom (Wafer Strom)	Thamnoporids	Coenites	Alveolites	Rugose Coral	Amphipora	Tabular Tabulate Coral	Massive Tabulate Coral	Rugose Coral	Oncoids	Peloids	Intraclasts	Aggregate grains	Algal Structures	% Carbonate Grains	Non-Dolomitized	% Partially Dolomitized	Fully Dolomitized	Fracture-Filling	Vug-Filling	Saddle Dolomite	Quartz	Anhydrite	Sphalerite	Pyrite	Bitumen	Argillaceous Material	OM
35	4-9-109-8W6	6519.75	G	30	20			5		5					1								40				45			•				5	1		1	5		
34	4-9-109-8W6	6520.25	G				1																				1			•				•			1	•	•	•
33	4-9-109-8W6	6535	C	40			40	20																			35			•		•	•	5			2	2		
32	4-9-109-8W6	6540.5	C	50			50	?																			10			•		•	•	2			2	•	•	•
31	4-9-109-8W6	6550	H	•	•	•			•				•		•												45			•		•					1	1		
30	4-9-109-8W6	6561	E	•	•	•			•																		65			•		•	•		5		1	1	•	•
29	4-9-109-8W6	6567.75	C		•			•		•	•																15		15								5		•	•
28	4-9-109-8W6	6570	B							1																	1		5								10			
27	4-9-109-8W6	6573.35	D	15	5	5		25	5	15													20	10			80	•									5		•	•
26	4-9-109-8W6	6575	C	15	30	10		5	15	5						20											45		5								1		1	

Sample	Location	Depth	Lithofacies	Matrix								Porosity											Structures									Comments
				% Non-Carbonate	Mudstone	Wackestone	Floatstone	Packstone	Grainstone	Rudstone	% Matrix	Interparticle	Intraparticle	Intercrystalline	Moldic	Fenestral	Shelter	Growth-Framework	Fracture	Channel	Vug	% Porosity	Laminations	Bedding	Nodular Texture	Microstylolites	Massive	Bioturbated	Event Concentration	Brecciated	Other	
35	4-9-109-8W6	6519.75	G	12				•	•		43			•					•			1					•					Peloids (coarse silt to fine sand size), Bitumen (occludes intercrystalline porosity), Quartz (minor microquartz assoc. with silicified fossils, also botroidal growths - zoned, coarsely crystalline, subhedral to anhedral), v. grainy, less homogenous than prev. sample. Matrix (polymodal planar subhedral to anhedral medium crystalline to very coarsel crystalline dolomite - finer dolomite replaces more argillaceous or OM-rich matrix)
34	4-9-109-8W6	6520.25	G	1					•		90			•					•			8				•	•					V. homogenous appearance, porous, grainy, massive, sparse brown microstylolites, Microquartz occurs assoc. with allochems., pyrite (assoc. with quartz). Matrix was probably initially bioclastic carbonate sand
33	4-9-109-8W6	6535	C	9			•				50			•							•	5				•						Grainy appearance (due to dolomitization), microstylolites v. sparse and irregular, pyrite (assoc. with microquartz botroids, subhedral finely crystalline commonly in framboids). Vugs filled with coarsely to extremely coarsely crystalline saddle dolomite, medium crystalline planar subhedral dolomite replace matrix furthest from vugs - more OM rich, therefore, finer crystals)
32	4-9-109-8W6	6540.5	C	5		•					80			•					•		•	5				•						Microquartz appears botroidal, Vugs infilled with dolomite therefore leaves only intercrystalline porosity instead of vuggy - difficult to define porosity types., sparse horsetail microstylolites
31	4-9-109-8W6	6550	H				•				45			•							•	7										planar subhedral matrix dolomite, and abundant vug-fillinmg dolomite, large vugs - up to 1mm x 3mm lined with dolomite xtlls., Bitumen in center of vugs
30	4-9-109-8W6	6561	E	7			•	•			30										•	1							•			Bitumen (occurs at center of vugs lined with planaar euhedral coarsely crystalline dolomite and coarsely crystalline subhedral saddle dolomite)
29	4-9-109-8W6	6567.75	C	10			•				75											0										No microstylolites, matrix 15% v. finely crystalline dolomite, v. coarsely crystalline anhedral calcite cement in allochems - early marine cements rim allochems (fibrous), pyrite assoc with OM.
28	4-9-109-8W6	6570	B	10	•						90											0		•								Pyrite (finely crystalline euhexdral xtlls, v. finely crystalline subhedral equant xtlls, finely to medium crystalline anhedral randomly oriented pyrite laths), ~5% matix replaced by non-planar anhedral v. finely crystalline dolostone.
27	4-9-109-8W6	6573.35	D	5				•			20											0							•			V. abundant fossils, could be event deposit with waning energy conditions upward (ie. More argillaceous material etc.), Pyrite (assoc. with allochems, single xtlls, framboids, and laminae parallel chains)
26	4-9-109-8W6	6575	C	2			•				50											0					•					Anhedral non-planar v. finely crystaline dolomite assoc. with argillaceous material. Pyrite (anhedral, equant, v. fine to coarsely crystalline - pyritized allochems), Calcite cement zoned (ferroan and non) inside articulated brach.

Sample	Location	Depth	Lithofacies	Allochems																											Dolomitization etc.						Accessories						
				Crinoids	Brachs	Bivalves	Undifferntiated Brach/Bivalve	Ostracodes	Gastropods	Stylolinids	Tentaculitids	Strom Fragments	Strom (Thin Tabular)	Strom (Wafer Strom)	Thamnoporids	Coenites	Alveolites	Rugose Coral	Amphipora	Tabular Tabulate Coral	Massive Tabulate Coral	Rugose Coral	Oncoids	Peloids	Intraclasts	Aggregate grains	Algal Structures	% Carbonate Grains	Non-Dolomitized	% Partially Dolomitized	Fully Dolomitized	Fracture-Filling	Vug-Filling	Saddle Dolomite	Quartz	Anhydrite	Sphalerite	Pyrite	Bitumen	Argillaceous Material	OM
25	4-9-109-8W6	6585	C	1	10	10		20	5	55																1	40	*				*	*				5			
24	4-9-109-8W6	6587.25	B	5				20		75																	10		2								1			
20	4-9-109-8W6	6600	C		10	5		25	20	20	20												5	?			25	*									5	*	*	10
19	4-9-109-8W6	6601	A																																					
18	4-9-109-8W6	6609.25	C	20	20			30	5	20	5											1					20										5	*	10	*
17	4-9-109-8W6	6614	B	2	2			2	2	90	1																30										5			*
16	4-9-109-8W6	6617	C	20	30	1		15	1	30														5			30	*									2	*	*	*
36	4-9-109-8W6	6619	H	30			20	25		5		20															45			*					1		1	1	*	*
15	4-9-109-8W6	6623	C	20	20	5		20	5	25																1	25		25					*		1	*	*	*
13	4-9-109-8W6	6624.5	C	40	25	1		5	1	10														20		1	50	*									*	*	*	*
14	4-9-109-8W6	6625.5	C	25	25	5		20	5	20																5	10	*									*	*	*	*
12	4-9-109-8W6	6637	C	55	35			5	1	5														*		1	50	*									*	*	*	*
11	4-9-109-8W6	6638.75	C	25	20	1		20	1	35														*		1	45	*									*	*	*	*

Sample	Location	Depth	Lithofacies	Matrix								Porosity											Structures									Comments
				% Non-Carbonate	Mudstone	Wackestone	Floatstone	Packstone	Grainstone	Rudstone	% Matrix	Interparticle	Intraparticle	Intercrystalline	Moldic	Fenestral	Shelter	Growth-Framework	Fracture	Channel	Vug	% Porosity	Laminations	Bedding	Nodular Texture	Microstylolites	Massive	Bioturbated	Event Concentration	Brecciated	Other	
25	4-9-109-8W6	6585	C	5			•				55											0								•	Huge vug fills ~85% of thin section cement zoned (outside - v. coarsely crystalline anhedral calcite cement, extremely coarsely crystalline aanhedral ferroan calcite cement, inside - extrmemely coarsely crystalline saddle dolomite, then coarsely crystalline subhedral pyrite in center).
24	4-9-109-8W6	6587.25	B	1	•						89											0		•							Similar to 17 but less fauna - could be same setting but increased sedimentation rate.
20	4-9-109-8W6	6600	C	15			•				55		•						•			1			•	•					~75% of slide is made up of nodules defined by microstylolites, intraparticle porosity - inside peloids, 10% microstylolites, peloids (0.08mm diam., ovoid, infil fossils, aggregated in intraclasts), geopetal fill common
19	4-9-109-8W6	6601	A																												
18	4-9-109-8W6	6609.25	C	15		•					65		1									1		•	•	•					Contacts bedded facies below, porosity (occluded by ferroan calcite cement, in stylolinids), pyrite (subhedral to anhedral v. finely to coarsely crystalline, assoc. w OM, dissem, or in fossils).
17	4-9-109-8W6	6614	B	6		•					65											0		•							Argillaceous wackestone (brown, dissem. OM, up to 30% stylolinids, more pyrite) interbedded with wackestone (stained pink, 15% stylolinids, less pyrite and OM). Pyrite (anhedral, v. finely crystalline, occurrence - framboids, dissem. in matrix, and pyritized stylolinids). Fauna parallel to laminae within beds defined by OM - more oriented in argillaceous material,
16	4-9-109-8W6	6617	C	2		•					55											0			•	•					Intraclasts (3mm x 2mm, irregular shape, pyritized), Horsetail microstylolites (0.01mm to 0.2mm), vug filling ferroan calcite (v. coarsely xtlline), pyrite (v. finely crystalline, assoc. with center of vugs and scattered in matrix), Nodules (less defined and larger than intraclasts - microstylolites wrap around them
36	4-9-109-8W6	6619	H	5							45			•							•	5					•				matrix (polymodal non-planar anhedral to subhedral medium to very coarsely crystalline dolomite - finer dol. is brown and inclusion rich, coarser dolomite is colorless - represents recrystallized allochems
15	4-9-109-8W6	6623	C	4		•					70											0			•	•					25% dolomitized (unimodal nonplanar anhedral v. finely crystalline dolomite) - scattered in matrix, anhydrite laths (v. coarsely crystalline euhedral), pyrite (v. finely crystalline, anhedral to spherical)
13	4-9-109-8W6	6624.5	C	5			•				45											0			•	•					Algal structure: Girvenella, charophytes, calcispheres, microstylolites concentrate at edges of nodules, intraclasts pyritized, 2mm x 1mm to 1.5cm x 7mm
14	4-9-109-8W6	6625.5	C	30		•					60											0			•	•					Very abundant microstylolites (OM, argillaceous material, bitumen), range from .08mm to 5mm thick - wrap around allochems, finely crystalline anhedral pyrite assoc. with OM in chains
12	4-9-109-8W6	6637	C	2			•	•			48											0			•	•					Algal structure: calcispheres and charophytes, intraclasts 2-3mm diameter, irregular shape, pyritized rim, zoned ferroan and non-ferroan calcite cement in vugs
11	4-9-109-8W6	6638.75	C	5		•					50											0			•	•					Similar to 13, intraclasts 7mm-1cm diam. irregular outline, sometimes pyritized, OM-rich microstylolites compress around nodules, algal structure - Girvenella

Sample	Location	Depth	Lithofacies	Allochems																												Dolomitization etc.						Accessories						
				Crinoids	Brachs	Bivalves	Undifferntiated Brach/Bivalve	Ostracodes	Gastropods	Stylolinids	Tentaculitids	Strom Fragments	Strom (Thin Tabular)	Strom (Wafer Strom)	Thamnoporids	Coenites	Alveolites	Rugose Coral	Amphipora	Tabular Tabulate Coral	Massive Tabulate Coral	Rugose Coral	Oncoids	Pelolds	Intraclasts	Aggregate grains	Algal Structures	% Carbonate Grains	Non-Dolomitized	% Partially Dolomitized	Fully Dolomitized	Fracture-Filling	Vug-Filling	Saddle Dolomite	Quartz	Anhydrite	Sphalerite	Pyrite	Bitumen	Argillaceous Material	OM
10	4-9-109-8W6	6641.5	C	31	25	20		5	3	15					1													55	*			*		*				*	*	*	*
9	4-9-109-8W6	6664.25	D	40	30	10		1	5		14																	45		20								*	*	*	*
8	4-9-109-8W6	6668	D	50			50																					20			*							*	*	*	*
7	4-9-109-8W6	6669	D	35			55										10											65			*							*	*	*	*
6	4-9-109-8W6	6670	D	72			20		2				2		2													30			*							*	*	*	*
5	4-9-109-8W6	6672	D	70			30													*								20			*							*	*	*	*
2	4-9-109-8W6	6703.99	J																																							
144	6-32-109-8W6	6453.5	?																					?				55			*			1	30		1				
143	6-32-109-8W6	6463	F	10			30			20														40				50			*		*		1			1	*	*	
141	6-32-109-8W6	6484.3	G	*			*	?		?					*									?				60			*		*		1	1		*	*	*	*
140	6-32-109-8W6	6494	G	20			30	5		5					10									30				60			*		*	*		2		1	*	*	*
139	6-32-109-8W6	6504.5	G	*			*	*		*														*				60			*							1	1	*	*
138	6-32-109-8W6	6508	G	*			*	*		*						*								*				70													

Sample	Location	Depth	Lithofacies	% Non-Carbonate	Matrix						% Matrix	Porosity										% Porosity	Structures									Comments
					Mudstone	Wackestone	Floatstone	Packstone	Grainstone	Rudstone		Interparticle	Intraparticle	Intercrystalline	Moldic	Fenestral	Shelter	Growth-Framework	Fracture	Channel	Vug		Laminations	Bedding	Nodular Texture	Microstylolites	Massive	Bioturbated	Event Concentration	Brecciated	Other	
10	4-9-109-8W6	6641.5	C	2			•	•			43											0			•	•						Fractures infilled by very coarsely crystalline saddle dolomite. Pyrite occurs as silt size spherical crystalls - sometimes framboidal, assoc. with microstylolites
9	4-9-109-8W6	6664.25	D	2		•					52								•			1				•						Contact between non-dolomitized and partially (up to 45% dolomitized) wackestone below. Microstylolites are more abundant in the partially dolomitized part - unimodal planar euhedral medium crystalline dolomite
8	4-9-109-8W6	6668	D	5		•					75											0				•						very abundant microstylolites, finely to medium crystalline unimodal planar subhedral dolomite matrix, non-mimic replacement of matrix and allochems
7	4-9-109-8W6	6669	D	1			•				35											0				•						Polymodal non-planar anhedral to planar subhedral dolomite matrix - related to primary textures
6	4-9-109-8W6	6670	D	1			•				68								•			1				•			•			polymodal planar subhedral medium to very coarsely crystalline dolomite matrix
5	4-9-109-8W6	6672	D	2			•				78															•			•			polymodal non-planar anhedral to planar subhedral dolomite matrix
2	4-9-109-8W6	6703.99	J																													
144	6-32-109-8W6	6453.5	?	32					•		10			•								1					•				•	Contains abundant large patches of anhydrite (extremely coarsely crystalline subhedral laths interlock in patches ~2cm x 1cm). Matrix (colorless material b/t peloids - could be dolomitized carbonate cement). Peloids (abundant). Qtz (assoc. with anhydrite).
143	6-32-109-8W6	6463	F	5					•		45			•								1	•			•						Diffused white light in combination with reflected light reveals pealoids. Bitumen (occludes porosity, lines intercrystalline pores). Peloids (v. abundant, ovoid). Anhydrite (assoc. with larger pores). Microstylolites (thin, irregular but horizontal and continuous).
141	6-32-109-8W6	6484.3	G	5				•			25			•							•	10		•		•						Similar to 137, 139, and 140 but slightly more stylolites. No bitumen lining pores - only in microstylolites. Microstylolites (v. thin, brown, suggests argillaceous matrix, low OM). Void-filling dolomite (planar anhedral coarsely crystalline dolomite).
140	6-32-109-8W6	6494	G	3					•		30			•								5		•		•						Similar to 137 and 139 but has coarser bed in middle. Vaguely bedded - microstylolites parallel bedding. Porosity (dissolved brachiopods and other allochems lined with saddle dolomite or planar euhedral coarsely crystalline dolomite and bitumen). Matrix (non-planar anhedral coarsely crystalline dolomite).
139	6-32-109-8W6	6504.5	G	3					•		30			•								7				•	•					V. Similar to sample 137. Microstylolites (define vague laminations). Looks like facies G with some microstylolites - transitional b/w F and G).
138	6-32-109-8W6	6508	G																													Matrix (homogeneous, medium crystalline non-planar anhedral dolomite, non-mimic allochem replacement but crinoids still behave optically as single crystal even though they have irregular shape). Microstylolites (rare, discontinuous). Fauna (estimate is very difficult b/c only allochem ghosts remain). Quartz (mimics anhydrite structure - very late stage subhedral megaquartz). Vuggy porosity (develops where allochem dissolution occurred).

Sample	Location	Depth	Lithofacies	Allochems																											Dolomitization etc.						Accessories							
				Crinoids	Brachs	Bivalves	Undifferntiated Brach/Bivalve	Ostracodes	Gastropods	Stylolinids	Tentaculitids	Strom Fragments	Strom (Thin Tabular)	Strom (Wafer Strom)	Thamnoporids	Coenites	Alveolites	Rugose Coral	Amphipora	Tabular Tabulate Coral	Massive Tabulate Coral	Rugose Coral	Oncoids	Peloids	Intraclasts	Aggregate grains	Algal Structures	% Carbonate Grains	Non-Dolomitized	% Partially Dolomitized	Fully Dolomitized	Fracture-Filling	Vug-Filling	Saddle Dolomite	Quartz	Anhydrite	Sphalerite	Pyrite	Bitumen	Argillaceous Material	OM
137	6-32-109-8W6	6516.95	G	20			10	10		10													50				60			•	•							1	•	•
135	6-32-109-8W6	6519	H	20			20	5		5					40								10				65			•	•	•	•	•				•	•	•
134	6-32-109-8W6	6525	G	•			•																				10			•								1		
133	6-32-109-8W6	6533	H	20			10	5				60				5											60			•		•	•		1			•	•	
132	6-32-109-8W6	6535.5	F	•			•	•																			60			•		•	•				1	5	•	•
129	6-32-109-8W6	6549	G	?			?					?															0			•			•				•			
128	6-32-109-8W6	6550	G	?			?																				0			•			•						•	
127	6-32-109-8W6	6560	G																					?			0			•		•	•							

Sample	Location	Depth	Lithofacies	Matrix								Porosity											Structures									Comments
				% Non-Carbonate	Mudstone	Wackestone	Floatstone	Packstone	Grainstone	Rudstone	% Matrix	Interparticle	Intraparticle	Intercrystalline	Moldic	Fenestral	Shelter	Growth-Framework	Fracture	Channel	Vug	% Porosity	Laminations	Bedding	Nodular Texture	Microstylolites	Massive	Bioturbated	Event Concentration	Brecciated	Other	
137	6-32-109-8W6	6516.95	G	2					•		30			•							•	10				•						Matrix - homogeneous, not argillaceous, probably started as carbonate cement that held grains together - later dolomitized to leave clear "matrix". Allochems - form brown shapes in matrix. Bitumen - occurs in intercrystalline pores. Microstylolites - form faint horizontal laminae. This sample could be transitional between facies G and F (the laminated equivalent to G).
135	6-32-109-8W6	6519	H	5			•	•			20			•							•	10					•					Mostly Thamnoporid corals - 5-8mm diam (larger than Coenites coral which can look similar). Matrix - peloidal packstone. Void-filling dolomite - euhedral coarsely crystalline saddle doalomite, and coarsely crystalline planar euhedral dolomite. Estimate of fauna abundance - very poor est. due to dolomitization - destroys primary fabrics.
134	6-32-109-8W6	6525	G	1					•		75			•								15					•					Very homogeneous and grainy appearance. Matrix - non-planar subhedral coarsely crystalline dolomite. Fauna - white card only helps to see a few crinoids, all other allochems masked by dolomitization. Grainy Matrix - probably made up of bioclastic material, crinoids, brachs, bivalves and possibly contains ostracods, stylolinids, gastropods, etc.
133	6-32-109-8W6	6533	H	2			•	•			35			•							•	5				•	•					non-planar anhedral medium crystalline dolomite. Void-filling dolomite - sparse, poorly developed saddle dolomite, and planar euhedral medium crystalline dolomite. Anhydrite - extremely coarsely crystalline elongate euhedral laths in large vug. Porosity - all porosity seems associated with leached out allochems (probably b/c allochems coarser crystalline than surrounding argillaceous matrix, therefore easier for dissolution to occur.
132	6-32-109-8W6	6535.5	F	10				•			30											0	•			•						Bitumen - occludes intercrystalline porosity. Pyrite - very sparse. Microstylolites - range from v. thin up to 0.8mm thick, represent period high productivity? Upper Laminite.
129	6-32-109-8W6	6549	G	0.5					•		95			•								5					•					V. similar to samples 127 and 128. Suggestion of allochem dissolution (ie. Elongate brachiopod-shaped vugs). Large porosity concentration - could be where a strom fragment was partially removed (stroms dolomitized by coarser crystalline dolomite than matrix - leads to preferential leaching). Bitumen - lines vugs. Matrix - non-planar anhedral medium crystalline dolomite.
128	6-32-109-8W6	6550	G	1					•		90			•							•	10					•					V. similar to sample 127. No allochems visible. Large vugs - could be located where strom fragments were dissolved to leave space.
127	6-32-109-8W6	6560	G	0					•		80			•								20					•					Fauna - cannot be distinguished due to dolomitization. Could be peloidal. Void-filling dolomite - minor saddle dolomite (coarsely crystalline), common planar euhedral coarsely crystalline dolomite. Matrix - non-planar anhedral coarsely crystalline (comprises most of TS).

Sample	Location	Depth	Lithofacies	Allochems																										Dolomitization etc.						Accessories						
				Crinoids	Brachs	Bivalves	Undifferntiated Brach/Bivalve	Ostracodes	Gastropods	Stylolinids	Tentaculitids	Strom Fragments	Strom (Thin Tabular)	Strom (Wafer Strom)	Thamnoporids	Coenites	Alveolites	Rugose Coral	Amphipora	Tabular Tabulate Coral	Massive Tabulate Coral	Rugose Coral	Oncoids	Pelolds	Intraclasts	Aggregate grains	Algal Structures	% Carbonate Grains	Non-Dolomitized	% Partially Dolomitized	Fully Dolomitized	Fracture-Filling	Vug-Filling	Saddle Dolomite	Quartz	Anhydrite	Sphalerite	Pyrite	Bitumen	Argillaceous Material	OM
126	6-32-109-8W6	6577	G	60			10																	30				70			*		*	*							
125	6-32-109-8W6	6593	G	*			*																					10?			*			*	1	1					
124	6-32-109-8W6	6597	H	5			5					70			10	10												60			*		*	*	*	*			*	*	*
123	6-32-109-8W6	6607.5	H	10			10	?				80																80			*							1	*	*	*
119	6-32-109-8W6	6629.8	H	35			15					50																75			*		*	*	1	1		1	*	*	*
118	6-32-109-8W6	6630.5	C	*	*	*		*	*	*	*																	20	*									1	*	*	*
94	12-33-109-8W6	6468.6	G																									0			*				30			1			
93	12-33-109-8W6	6487.25	F	10			25		5	50																		60			*								20	*	*
92	12-33-109-8W6	6496	F	10			25		5	50																		60			*								15	*	*

Sample	Location	Depth	Lithofacies	Matrix								Porosity											Structures									Comments
				% Non-Carbonate	Mudstone	Wackestone	Floatstone	Packstone	Grainstone	Rudstone	% Matrix	Interparticle	Intraparticle	Intercrystalline	Moldic	Fenestral	Shelter	Growth-Framework	Fracture	Channel	Vug	% Porosity	Laminations	Bedding	Nodular Texture	Microstylolites	Massive	Bioturbated	Event Concentration	Brecciated	Other	
126	6-32-109-8W6	6577	G	1					•		20			•								10					•					Peloidal? - difficult to tell due to dolomitization but appears to be. Matrix - coarsely crystalline non-planar anhedral dolomite. Pyrite - sparse, v. fine crystalline pyrite occurs in medium crystalline sized framboidal clusters.
125	6-32-109-8W6	6593	G	2					•		75			•								15					•					Fauna - crinoids, brachiopods/bivalves, cannot est. % of fauna b/c of dolomitization. Matrix - non-planar anhedral coarsely crystalline dolomite. Minor saddle dolomite and euhedral planar void filling dolomite.
124	6-32-109-8W6	6597	H	1			•	•			30			•							•	10				•	•					Floatstone with packstone matrix. Quartz - post-dates dolomitization, zoned, appears botroidal, megaquartz (pitted but subhedral 1.4mm diam). Matrix - difficult to describe due to dolomitization - prob. Packstone. Microstylolites - sparse.
123	6-32-109-8W6	6607.5	H	2						•	15			•							•	5				•	•					Strom fragments - coarser crystalline, therefore more porous than matrix, colorless (inclusion-free). Matrix - brown, fine crystalline dolomite due to argillaceous material, abundant bituminous microstylolites weave between strom fragments. Bitumen and pyrite - associated in microstylolites.
119	6-32-109-8W6	6629.8	H	5						•	20		•									1				•	•					Pyrite - v. finely crystalline, assoc. w microstylolites. Microstylolites - thin, OM and bitumen, squeezed together b/t strom fragments. Anhydrite - euhedral in porosity developed in the stroms. Strom fragments - coarser crystalline than matrix. Matrix - non-planar anhedral v. finely crystalline dolomite (brown, more argillaceous, finer than dolomite xtls in stroms).
118	6-32-109-8W6	6630.5	C	10		•					70		•									1			•	•						Nodules - common, have random orientations, differ from matrix because they contain less OM, argillaceous material, and pyrite. Microstylolites - sparse and thin. Porosity - assoc. with dissolution of allochems. Micritic matrix
94	12-33-109-8W6	6468.6	G	31					•		59			9					1			10					•					Large ovoid structure is silicified (microqtz) rest of matrix is not silicified and has higher intercrystalline porosity. Qtz (finely crystalline anhedral microquartz, postdates dolomitization, appears to erode edges of dolomite), Matrix (planar subhedral medium crystalline dolomite - could suggest partial dissolution prior to dolomitization or due to volume reduction during dolomitization), Pyrite (assoc. with qtz esp on edge of oval, framboids of aphanocrystalline pyrite)
93	12-33-109-8W6	6487.25	F	35				•			5											0	•			•						Similar to samle 90 and 92 but more bituminous, OM-rich laminae (1-2mm thick made up of a bundle of 0.04mm thick microstylolites), very grainy, also contains a lag grainstone (~75% bioclasts)
92	12-33-109-8W6	6496	F	30				•			10											0	•			•						Similar to sample 90, more abundant bituminous microstylolites (30% of TS, 0.04mm thick but grouped into laminae 3-5mm thick - accumulated due to algal blooms)

Sample	Location	Depth	Lithofacies	Allochems																									Dolomitization etc.						Accessories						
				Crinoids	Brachs	Bivalves	Undifferntiated Brach/Bivalve	Ostracodes	Gastropods	Stylolinids	Tentaculitids	Strom Fragments	Strom (Thin Tabular)	Strom (Water Strom)	Thamnoporids	Coenites	Alveolites	Rugose Coral	Amphipora	Tabular Tabulate Coral	Massive Tabulate Coral	Rugose Coral	Oncolds	Peloids	Intraclasts	Aggregate grains	Algal Structures	% Carbonate Grains	Non-Dolomitized	% Partially Dolomitized	Fully Dolomitized	Fracture-Filling	Vug-Filling	Saddle Dolomite	Quartz	Anhydrite	Sphalerite	Pyrite	Bitumen	Argillaceous Material	OM
90	12-33-109-8W6	6507.25	F	10			25		5	50														?				60			•								10	•	•
88	12-33-109-8W6	6520	G	1																								1			•			1	1				2		
87	12-33-109-8W6	6521	G	1																								1			•			1	1				2		
85	12-33-109-8W6	6542	H	5			30					60				5												40			•		•	•	1			1	1	•	•
83	12-33-109-8W6	6545	F	•			•	•		•		•				20												40			•	•						1	1	•	•
82	12-33-109-8W6	6550	H	10			10	10		20		30	10	10														55			•							1	1	•	•
80	12-33-109-8W6	6558	G																									0			•		•	•	•		•				
79	12-33-109-8W6	6585.5	G				•																					1			•			2	2		1				
78	12-33-109-8W6	6589.75	H	•			•						•	•	•			•										50			•		•	•	2			1	•	•	•

Sample	Location	Depth	Lithofacies	Matrix								Porosity											Structures									Comments
				% Non-Carbonate	Mudstone	Wackestone	Floatstone	Packstone	Grainstone	Rudstone	% Matrix	Interparticle	Intraparticle	Intercrystalline	Moldic	Fenestral	Shelter	Growth-Framework	Fracture	Channel	Vug	% Porosity	Laminations	Bedding	Nodular Texture	Microstylolites	Massive	Bioturbated	Event Concentration	Brecciated	Other	
90	12-33-109-8W6	6507.25	F	15				•			25											0	•			•						Buff color grainy dolopackstone with dark brown irregular OM-rich bituminous laminae. Also contains grainy lag deposits (up to 80% bioclasts, lack bituminous material, contains peloids, allochems, lens-shaped) Microstylolites wrap around these lag deposits, Bitumen (in intercrystalline and intraparticle pores)
88	12-33-109-8W6	6520	G	4					•		85			•							•	10					•					Similar to sample 87 except two types of matrix (medium crystalline non planar anhedral matrix - brownish color, homogeneous, contains more bituminous microstylolites and coarsely crystalline planar subhedral dolomite - colorless, appears as nodules in core, could be recrystallized strom fragments or intraclasts but poorly defined edges)
87	12-33-109-8W6	6521	G	4					•		80			•							•	15					•					Massive, no microstylolites, v. porous, grainy and homogeneous. Qtz (chalcedonic and coarsely crystalline), Anhydrite (in intercrystalline pores), Matrix (ranges from coarsely crystalline non-planar anhedral dolomite to coarsely crystalline planar euhedral dolomite in more porous areas - pores lined by bitumen)
85	12-33-109-8W6	6542	H	5			•				45			•	•							10				•						Porosity (intercrystalline but controlled by leached strom fragments), Quartz (chalcedonic qtz - 0.4mm diam, radial extinction, coarsely crystalline qtz - minor, zoned, not fibrous, euhedral, microqtz), Matrix (medium crystalline non-planar anhedral brown dolomite, allochems replaced by coarsely crystalline dolomite), Bitumen (lines pores), Pyrite (assoc. with allochems)
83	12-33-109-8W6	6545	F	20				•			40											0	•		•							Very abundant horsetail microstylolites (bitumen, OM, argillaceous, pyrite, range from 0.08 to 0.8mm thick, compress around lens-shaped nodules which make up matrix), Matrix (saddle dolomite, medium crystalline non-planar subhedral dolomite-occurs near microstylolites)
82	12-33-109-8W6	6550	H	10			•	•			30			•								5										Dolofloatstone with dolopackstone matrix, v. grainy matrix, abundant strom gragments, possible firmground where thin tabular strom overlies stylolite, Microstylolites (v. thin, irregular, discontinuous, 0.02mm thick, wrap around dolomite xtls in matrix), Matrix (ranges from v. finely crystalline to coarsely crystalline non-planar anhedral dolomite, also minor coarsely crystalline dolomite lines fractures)
80	12-33-109-8W6	6558	G	5					•		75			•								20					•					Very porous and homogeneous, similar to sample 79 but more porous and no allochems are discernable. Matrix (50% coarsely crystalline saddle dolomite, 50% planar subhedral coarsely crystalline dolomite)
79	12-33-109-8W6	6585.5	G	5					•		90			•								4					•					Very porous and homogeneous - carbonate sand - makes up lithofacies F and G and matrix of lithofacies H. Probably grainy due to abundance of dolomitized bioclasts.
78	12-33-109-8W6	6589.75	H	5			•				30		5	5					5			15						•				Quartz (microqtz and chalcedonic qtz, assoc. with pyrite and porosity) Microstylolites (OM, bitumen, pyrite, and argillaceous material concentration), Matrix (medium crystalline non-planar anhedral dolomite)

Sample	Location	Depth	Lithofacies	Allochems																											Dolomitization etc.						Accessories						
				Crinoids	Brachs	Bivalves	Undifferntiated Brach/Bivalve	Ostracodes	Gastropods	Stylolinids	Tentaculitids	Strom Fragments	Strom (Thin Tabular)	Strom (Wafer Strom)	Thamnoporids	Coenites	Alveolites	Rugose Coral	Amphipora	Tabular Tabulate Coral	Massive Tabulate Coral	Rugose Coral	Oncoids	Pelods	Intraclasts	Aggregate grains	Algal Structures	% Carbonate Grains	Non-Dolomitized	% Partially Dolomitized	Fully Dolomitized	Fracture-Filling	Vug-Filling	Saddle Dolomite	Quartz	Anhydrite	Sphalerite	Pyrite	Bitumen	Argillaceous Material	OM
77	12-33-109-8W6	6594	G	•			•							•	•												20			•			5	1		1				
76	12-33-109-8W6	6608	H	•			•	•									•						?				45			•			5	1		1	•	•	•
75	12-33-109-8W6	6610.27	H	20			20					30				15		15							5			48			•			1	5		1	•	•	•
74	12-33-109-8W6	6612	E	•			•	•		•																		35			•			1			1	1	•	•
68	12-33-109-8W6	6623.75	C	•	•	•		•	•	•	•														•			40	•						3		2				
69	12-33-109-8W6	6630	C	•	•	•		•	•	•																		15	•								1	•	•	•
66	12-33-109-8W6	6642.5	A		20				80	1																		30	•								1	•	•	•

Sample	Location	Depth	Lithofacies	Matrix								Porosity											Structures									Comments
				% Non-Carbonate	Mudstone	Wackestone	Floatstone	Packstone	Grainstone	Rudstone	% Matrix	Interparticle	Intraparticle	Intercrystalline	Moldic	Fenestral	Shelter	Growth-Framework	Fracture	Channel	Vug	% Porosity	Laminations	Bedding	Nodular Texture	Microstylolites	Massive	Bioturbated	Event Concentration	Brecciated	Other	
77	12-33-109-8W6	6594	G	7					•		63			•								10					•					Quartz (authigenic, zoned, euhedral, in pores), Anhuydrite (coarsely crystalline, subhedral, in matrix, not in vugs), Matrix (medium crystalline non-planar subhedral dolomite - nonmimic allochem replacement, minor saddle dolmite in vugs)
76	12-33-109-8W6	6606	H	10			•				35			•								10										V. porous (some pores are like vugs but are lined with dolomite xtls, therefore called intercrystalline), Anhydrite (occludes fracture porosity, very coarsely crystalline euhedral), Chalcedonic qtz (anhedral globular to irregular, assoc. with allochems), Microstylolites (v. thin and discontinuous), Matrix (medium crystalline non-planar anhedral dolomite)
75	12-33-109-8W6	6610.27	H	10			•				27			5							10	15						•				Strom fragments (more coarsely crystalline than matrix, more porous, difficult to distinguish, 2cm x 2cm size), Coenites (branching tabulate coral 5mm diam), Rugose (solitary, 1cm diam), Porosity (intercrystalline in stroms and inside vugs lined w v. coarsely crystalline planar euhedral dolomite, then extremely coarsely crystalline euhedral anhydrite, then bitumen), Intraclasts (similar to strom fragments but contain identifiable allochems - v. irregular, 1.3 x 1cm size), Matrix (coarsely crystalline non planar anhedral dolomite, finer crystals near argillaceous and OM)
74	12-33-109-8W6	6612	E	5		•					60			•								1						•				Bitumen (lines intercrystalline porosity), Matrix (finely crystalline non planar anhedral dolomite replaces most argillaceous matrix, medium crystalline non planar anhedral dolomite replaces matrix w/o argillaceous material or OM), Void-filling dolomite (coarsely crystalline planar euhedral - porosity b/t these xtlls), Chaledonic qtz patches randomly distributed in matrix - postdates dolomitization
68	12-33-109-8W6	6623.75	C	5			•				55											0			•							Matrix is micritic but contains abundant bioclastic debris - grainy appearance. Pyrite and anhydrite are associated with fractures and vugs - occlude porosity.
69	12-33-109-8W6	6630	C	5			•				80											0			•							Matrix similar to sample 68 - micritic with abundant bioclasts. Nodules *average 2mm x 1mm irregular, ovoid, contain less OM, argillaceous material, and pyrite than the matrix. Microstylolites (0.01mm to 0.16mm thick, contain OM, pyrite, bitumen, and argillaceous material) wrap around nodules. Pyrite (finely crystalline anhedral in matrix and masses of crystals in fractures and intercrystalline pores
66	12-33-109-8W6	6642.5	A	2		•					70											0	•									Well laminated - defined by alignment of shell fossils and OM, Pyrite (concentrates near/in fossils, dissem throughout matrix, finely crystalline, anhedral

Sample	Location	Depth	Lithofacies	Allochems																											Dolomitization etc.						Accessories						
				Crinoids	Brachs	Bivalves	Undifferntiated Brach/Bivalve	Ostracodes	Gastropods	Stylliolinids	Tentaculitids	Strom Fragments	Strom (Thin Tabular)	Strom (Wafer Strom)	Thamnoporids	Coenites	Alveolites	Rugose Coral	Amphipora	Tabular Tabulate Coral	Massive Tabulate Coral	Rugose Coral	Oncoids	Peloids	Intraclasts	Aggregate grains	Algal Structures	% Carbonate Grains	Non-Dolomitized	% Partially Dolomitized	Fully Dolomitized	Fracture-Filling	Vug-Filling	Saddle Dolomite	Quartz	Anhydrite	Sphalerite	Pyrite	Bitumen	Argillaceous Material	OM
152	4-30-110-9W6	6384	E	10			15		5	5		?										60				5	55			•			•	1				5	•	•	
194	7-7-113-21W5	4569	A	25	15	5		5		50																	50			•							5	•	•	•
189	7-7-113-21W5	4699.5	I	•			•	?		?																	5			•	•	•	•				1	•	•	•
95	16-9-116-5W6	4931	H																																						
179	4-19-116-4W6	5007	I																								0			•					15			•	•	•
178	4-19-116-4W6	5011.5	F					•		•														•		•	5			•								•	•	•
177	4-19-116-4W6	5012	G	•	•	•		•	•	•														•	•	•	70		10			•	•					•	•	•
176	4-19-116-4W6	5013	G	•	•	•		•	•	•														•			70		15			•	•		1		1			
175	4-19-116-4W6	5055	H	10	15	10		5		10			20	5										25			50	•			•	•	•					•	•	•

Sample	Location	Depth	Lithofacies	% Non-Carbonate	Matrix						% Matrix	Porosity										% Porosity	Structures									Comments
					Mudstone	Wackestone	Floatstone	Packstone	Grainstone	Rudstone		Interparticle	Intraparticle	Intercrystalline	Moldic	Fenestral	Shelter	Growth-Framework	Fracture	Channel	Vug		Laminations	Bedding	Nodular Texture	Microstylolites	Massive	Bioturbated	Event Concentration	Brecciated	Other	
152	4-30-110-9W6	6384	E	10			•				35											0			•	•					Strange variation of lithofacies. Oncoids (common, probably coated nodular stroms, 0.6 to 1cm diameter). Saddle dolomite (very well developed saddle shapes, replace oncoids partially). Microstylolites and argillaceous material (wraps around much coarser grained allochems). Bitumen (lines saddle dolomite intercrystalline porosity in oncoids). Quartz (megaquartz replaces allochems - partial silicification).
194	7-7-113-21W5	4569	A	10					•		40											0	•			•					
189	7-7-113-21W5	4699.5	I	5	•						90								•			1				•			•		V. homogeneous dolomudstone. Saddle dolomite (extremely coarsely crystalline, non-planar euhedral fills voids and fractures). Microstylolites (very minor, some small patches where microstylolites concentrate and fossils occur, could represent brecciation?). Matrix (planar subhedral medium crystalline dolomite, many small intercrystalline pores, all porosity occluded by bitumen, v. cloudy grey dolomite - may indicate argillaceous precursor.
95	16-9-116-5W6	4931	H																												
179	4-19-116-4W6	5007	I	16	•						84											0				•		?			Very mottled, disrupted appearance. Matrix (pseudospar non-planar anhedral dolomite). Anhydrite (coarsely to v. coarsely crystalline subhedral anhydrite, occurs in patches 1-4mm diam - could be holes where allochems were leached out). Microstylolites (v. sparse, discontinuous).
178	4-19-116-4W6	5011.5	F	10	•						20											0	•			•					Matrix (microspar to pseudospar, dolomudstone). Bitumen (occludes intracrystalline porosity). Diffused white light and reflected light do not reveal bioclasts or peloids - looks like homogenous dolomudstone with microstylolite laminae (from 0.02 to 1.6mm thick, irregular but continuous and horizontal). Spinose ostracod observed (0.4mm long).
177	4-19-116-4W6	5012	G	2					•		20			•								10	•			•					Transition b/t laminated skeletal grainstone below and peloidal grainstone above. Similar to 176 but contains abundant intraclasts ripped up from the underlying laminated unit. Intraclasts (dolomudstone without fossils). Bedding (parallel beds of dolomudstone 2-5mm thick, separated by v. thin OM-rich microstylolite).
176	4-19-116-4W6	5013	G	2					•		20			•					•			10					•				Partially dolomitized matrix (15% of matrix is planar subhedral medium crystalline dolomite scattered evenly, probably represents preferentially dolomitized carbonate cements b/w carbonate grains). Matrix (no real matrix exists, only cement and dolomitized cement, isopachous rims around grains).
175	4-19-116-4W6	5055	H	1			•	•			45		•	•					•		•	5				•	•				Nodular stroms (1cm diam), Thin tabular strom fragment (2.5cm x 1.3cm thick). Allochems (most allochems - esp. peloids appear blue - could be v. tiny intercrystalline pores or ferroan calcite cement - too fine to tell). Matrix (0.04mm, finely crystalline, "pseudospar" calcite cement).

Sample	Location	Depth	Lithofacies	Allochems																										Dolomitization etc.						Accessories						
				Crinoids	Brachs	Bivalves	Undifferntiated Brach/Bivalve	Ostracodes	Gastropods	Stylolilnids	Tentaculitids	Strom Fragments	Strom (Thin Tabular)	Strom (Water Strom)	Thamnoporids	Coenites	Alveolites	Rugose Coral	Amphipora	Tabular Tabulate Coral	Massive Tabulate Coral	Rugose Coral	Oncolds	Peloids	Intraclasts	Aggregate grains	Algal Structures	% Carbonate Grains	Non-Dolomitized	% Partially Dolomitized	Fully Dolomitized	Fracture-Filling	Vug-Filling	Saddle Dolomite	Quartz	Anhydrite	Sphalerite	Pyrite	Bitumen	Argillaceous Material	OM
174	4-19-116-4W6	5089.5	H		•	•		•					•											•				?	•			•	•	•								
173	4-19-116-4W6	5101.5	G	20	20	10		10	5	5														30			1	85		25					1							
172	4-19-116-4W6	5112	E	100																								75			•											
171	4-19-116-4W6	5130	E	•	•	•		•	•	•													•		•		•	45		35			•	•	5		1	•	•	•	
170	4-19-116-4W6	5148.5	E	•	•	•		•	•	•						?							•				•	60		25		•	•	•	2		3	•	•	•	
169	4-19-116-4W6	5154	A		20	5		10		40	25																	15	•								5	•	•	•	
181	10-21-116-5W6	5210-5230	D	•	•	•		•		•																		30		20						1	2	•	•	•	
182	10-21-116-5W6	5230-5240	D	•	•	•		•	•	•														•				40		10						1	1	•	•	•	
183	10-21-116-5W6	5250-5260	A	10						90																		40		10							1	•	•	•	

Sample	Location	Depth	Lithofacies	% Non-Carbonate	Matrix							Porosity											Structures									Comments
					Mudstone	Wackestone	Floatstone	Packstone	Grainstone	Rudstone	% Matrix	Interparticle	Intraparticle	Intercrystalline	Moldic	Fenestral	Shelter	Growth-Framework	Fracture	Channel	Vug	% Porosity	Laminations	Bedding	Nodular Texture	Microstylolites	Massive	Bioturbated	Event Concentration	Brecciated	Other	
174	4-19-116-4W6	5089.5	H	0			•	•			?		•	•							•	5									•	Large vug lined by extremely coarsely crystalline (up to 7mm x 3.5cm) saddle dolomite. This takes up 40% of the TS. Matrix (mostly replaced by fibrous-prismatic calcite - feathery appearance. No allochems seen in fibrous calcite. Some allochems remain between these recrystallized parts (peloids, thin tabular strom). Probably floatstone with packstone matrix.
173	4-19-116-4W6	5101.5	G	1					•		0			•								15				•						Grainstone - all of TS is carbonate grains except for porosity and calcite cement. Cement (no true matrix exists, but all the material between the carbonate grains that is not matrix dolomite or pores is cement, dolomite seems to preferentially replace coarse carbonate cement). Calcispheres - rare but present.
172	4-19-116-4W6	5112	E	0						•	25		•									1					•					Rudstone (75% crinoids). Matrix (coarsely crystalline planar subhedral dolomite). Porosity (v. small pore at the center of crinoids - intraparticle). V. homogenous, grainy appearance - suggests winnowed crinoid sands.
171	4-19-116-4W6	5130	E	2			•	•			10			•	•											•		?				V. similar to sample 170 but more dolomitized. Allochems (some are dolomitized by medium crystalline non-planar anhedral dolomite). Matrix (30% of matrix dolomitized - planar euhedral v. finely crystalline and minor saddle dolomite). Qtz (euhedral microquartz replaces allochems and even partially replaces algal coatings on oncoids). Dissolution (creates v. small pores - appear blue due to the epoxy, concentrated in algal coatings and allochems - could be ferroan calcite too fine to tell).
170	4-19-116-4W6	5148.5	E	5			•	•			35											0				•		?				Primarily oncoids (algally coated grains). Matrix dolomite (planar euhedral medium crystalline dolomite). Void-filling dolomite (extremely coarsely crystalline non-planar subhedral saddle dolomite). Quartz (anhedral chalcedonic quartz replaces allochems even in the center of coated grains). Pyrite (some oncoids partially pyritized along laminae, also euhedral v. finely crystalline pyrite assoc. with silicified fossils, minor very finely crystalline pyrite in matrix). Algal structures (Girvenella and algal coatings on oncoids). Oncoids (form around crinoids, brachiopods, bivalves, stylolinids, gastropods). Dolomitization pattern (suggests bioturbation)
169	4-19-116-4W6	5154	A	30		•					85											0	•			•						
181	10-21-116-5W6	5210-5230	D	4		•					66											0				•	•					Similar to 180 but fossils are smaller and less abundant, matrix is more micritic and there is more dolomitization.
182	10-21-116-5W6	5230-5240	D	2		•					60											0				•	•					Similar to 180 and 181. Sparse crinoids, more abundant bivalves, ostracods, and stylolinids. <1% finely crystalline anhedral pyrite.
183	10-21-116-5W6	5250-5260	A	10		•					50											0	•			•						Half of the cuttings represent lithofacies D (similar to samples 180 to 182). These cuttings not described here. Other half of cuttings represent lithofacies A and are described here. Stylolinids (most abundant fossil, some are partially pyritized). Pyrite (v. finely crystalline euhedral xtls inside stylolinids, assoc. with dolomite crystals inside the stylolinids).

Sample	Location	Depth	Lithofacies	Allochems																								Dolomitization etc.						Accessories						
				Crinoids	Brachs	Bivalves	Undifferntiated Brach/Bivalve	Ostracodes	Gastropods	Stylolinids	Tentaculitids	Strom Fragments	Strom (Thin Tabular)	Strom (Wafer Strom)	Thamnoporids	Coenites	Alveolites	Rugose Coral	Amphipora	Tabular Tabulate Coral	Massive Tabulate Coral	Rugose Coral	Oncoids	Peloids	Intraclasts	Aggregate grains	Algal Structures	% Carbonate Grains	Non-Dolomitized	% Partially Dolomitized	Fully Dolomitized	Fracture-Filling	Vug-Filling	Saddle Dolomite	Quartz	Anhydrite	Sphalerite	Pyrite	Bitumen	Argillaceous Material	OM
180	10-21-116-5W6	5330-5340	D	40	30	10		10		10						1											75		10						1		1	*	*	*
165	5-36-117-6W6	5489	H	*			*	*		*		*				*								*			65			*		*					*	*	*
164	5-36-117-6W6	5496	H	10			20	10				40				20											60			*		*						*	*	*
163	5-36-117-6W6	5501	H																								0			*	*	*	50					*	*	
161	5-36-117-6W6	5514	A							*																	?													
159	5-36-117-6W6	5526.5	A							*																	55	*									1	*		*
158	5-36-117-6W6	5534.5	C	*	*	*		*	*	*															*		50		20			*	*				2	*	*	*
157	5-36-117-6W6	5595	D	20	20	10		10	10	15			5			1	10										65	*						1			1		*	
156	5-36-117-6W6	5616.7	D	*	*	*		*	*	*	*														*		65		1					1			1	*	*	*
155	5-36-117-6W6	5638	D	*	*	*		*	*	*										*							60		10					1	1		1	*	*	*

Sample	Location	Depth	Lithofacies	Matrix								Porosity											Structures									Comments
				% Non-Carbonate	Mudstone	Wackestone	Floatstone	Packstone	Grainstone	Rudstone	% Matrix	Interparticle	Intraparticle	Intercrystalline	Moldic	Fenestral	Shelter	Growth-Framework	Fracture	Channel	Vug	% Porosity	Laminations	Bedding	Nodular Texture	Microstylolites	Massive	Bioturbated	Event Concentration	Brecciated	Other	
160	10-21-116-5W6	5330-5340	D	3				•			20											0				•	•					Micritic matrix. Fauna (crinoids, ostracods, brachs, bivalves, stylolinids - represents carbonate ramp, therefore this is a true off-reef well).
165	5-36-117-6W6	5489	H	5			•	•			20			•							•	10				•		•				Strom fragments and intraclasts primarily (irregular, up to 3.5cm x 1.5cm). Void-filling dolomite (planar euhedral coarsely crystalline dolomite). Matrix (finely crystalline non-planar anhedral dolomite, finer crystalline than dolomitized allochems which are usually medium crystalline)
164	5-36-117-6W6	5496	H	5			•	•			25			•							•	10				•		•				Strom Fragments (40%, 0.5cm x 0.5cm to 1cm x 2mm, irregular), Coenites (20%, 2mm diam avg). Void-filling dolomite (planar euhedral coarsely crystalline). Matrix (non-planar anhedral v. finely crystalline dolomite). Floatstone with packstone matrix.
163	5-36-117-6W6	5501	H	10			•				0			•								5				•						Matrix (100% anhedral non-planar v. finely crystalline dolomite). Void-filling dolomite (subhedral non-planar extremely coarsely crystalline - 3.5mm saddle dolomite - entirely fills fractures). Diagenetic feature - saddle dolomite lined fracture network.
161	5-36-117-6W6	5514	A																													Dolomite (non-planar aphanocrystalline dolomite, most abundant in bituminous beds, also occurs as lenses in carbonate beds). Bituminous beds (3mm to 1cm thick, laminated within each bed - defined by variations in porosity, bitumen, OM, and dolomite). Dolomitization - may preferentially attack allochems.
159	5-36-117-6W6	5526.5	A	30					•		5											0	•	•								Bituminous beds (up to 4mm thick, contain up to 40% stylolinids, OM, and Bitumen). Stylolinid concentration (bed ~1cm thick, 100% cemented stylolinids, internal and external prismatic cement - dog's tooth cement, also pod-shaped accumulations of stylolinids in OM-rich parts.
158	5-36-117-6W6	5534.5	C	5		•					45											0			•	•						Intraclasts and nodules (less argillaceous than the matrix). Saddle dolomite (replaces some allochems, ie. Replaced gastropod looks like it could have been leached out first then recrystallized). Matrix (planar subhedral v. finely crystalline matrix dolomite, more abundant dolomite in argillaceous parts).
157	5-36-117-6W6	5595	D	3			•	•			32											0					•					Alveolites (tabulate coral, 4cm x 1.4cm). Thin tabular strom (encrusts Alveolites, 4cm wide x 5mm thick). Pyrite (assoc. with fossils, partial pyritization, v. finely crystalline in framboids). Floatstone with packstone matrix.
156	5-36-117-6W6	5616.7	D	3				•			30											0					•					Intraclasts (abundant, not well defined, could be result of bioturbation rather than true intraclasts, v. similar to matrix, 2cm x 1cm avg., random orientation, indistinct, irregular boundaries). Fauna (v. abundant, a couple of tentaculitids seen).
155	5-36-117-6W6	5638	D	5		•					35											0				•						Pyrite (v. fine crystalline, assoc. with quartz). Quartz (silicified fossils). Amphipora? (branching delicate strom, 3mm diam, some hollow, some have internal structure)

Sample	Location	Depth	Lithofacies	Allochems																											Dolomitization etc.						Accessories						
				Crinoids	Brachs	Bivalves	Undifferntiated Brach/Bivalve	Ostracodes	Gastropods	Stylolinids	Tentaculitids	Strom Fragments	Strom (Thin Tabular)	Strom (Wafer Strom)	Thamnoporids	Coenites	Alveolites	Rugose Coral	Amphipora	Tabular Tabulate Coral	Massive Tabulate Coral	Rugose Coral	Oncoids	Peloids	Intraclasts	Aggregate grains	Algal Structures	% Carbonate Grains	Non-Dolomitized	% Partially Dolomitized	Fully Dolomitized	Fracture-Filling	Vug-Filling	Saddle Dolomite	Quartz	Anhydrite	Sphalerite	Pyrite	Bitumen	Argillaceous Material	OM
154	5-36-117-6W6	5644	I	10			10	5		5														70			50			*		*		1	1			*	*	
153	5-36-117-6W6	5651	D	10	10	5				5														70			85		40					2	1			1		

Sample	Location	Depth	Lithofacies	% Non-Carbonate	Matrix							Porosity										Structures									Comments
					Mudstone	Wackestone	Floatstone	Packstone	Grainstone	Rudstone	% Matrix	Interparticle	Intraparticle	Intercrystalline	Moldic	Fenestral	Shelter	Growth-Framework	Fracture	Channel	Vug	% Porosity	Laminations	Bedding	Nodular Texture	Microstylolites	Massive	Bioturbated	Event Concentration	Brecciated	Other	
154	5-36-117-6W6	5644	I	3			•				45			•								1								?		Matrix (finely crystalline planar euhedral dolomite - had micritic precursor). Void filling dolomite (planar subhedral coarsely crystalline dolomite). Porosity (low, 1 vug line with planar void-filling dolomite and v. coarsely crystalline euhedral anhydrite laths). Intraclasts (70% of the carbonate grains).
153	5-36-117-6W6	5651	D	4					•		10											0	•			•						Isopachous cements (early diagenetic, compose material between carbonate grains). No matrix present. Partially dolomitized (planar euhedral medium crystalline dolomite is scattered throughout the matrix, more dolomitized near microstylolites - up to 60%). Peloids (v. fine sand size 0.2mm long, ovoid). Quartz (extremely coarsely crystalline patches - 3mm x 1mm, pitted, anhedral megaquartz, postdates dolomite). Strange for this lithofacies to be peloidal - looks similar to Upper Laminite (lithofacies F) but way too deep in the well for that to make sense.

APPENDIX E: ORGANIC PETROLOGY & GEOCHEMICAL TECHNIQUES

E.1 Polished Pellet Mount Preparation

The following procedure was used for polished pellet mounts of organic-rich laminite samples.

1) Samples were crushed using a ceramic mortar and pestle to a size of less than $1cm^2$. The largest particles for pellet preparation were selected in order to best display features parallel and perpendicular to bedding. Representative particulate matter was chosen to pack into the pellet molds around these larger particles in order to maximize the sample surface available for analysis. Between each sample, the mortar and pestle were cleaned thoroughly with a damp cloth and compressed air to avoid cross contamination problems. The finest particulate matter produced during crushing was used for Rock-Eval pyrolysis (refer to Section E.2).

2) One inch "Metaserv" molds were labelled with pellet numbers and coated inside with a thin layer of vaseline in order to facilitate removal of the cured epoxy.

3) Larger sample particles were placed with the face of interest down on the base of the pellet mold. At least one large particle in each sample was oriented in order to represent a parallel to bedding view and at least one other large particle in each sample was oriented in order to represent a perpendicular to bedding view.

4) Epoxy was mixed (2 parts resin to 1 part hardener) and stirred for 2 minutes. A thin layer of epoxy was then poured over the oriented sample particles. Sample particles were lifted and set back down to ensure complete coverage by epoxy.

5) Sample particulate was introduced to the pellet mold and stirred into the epoxy to ensure complete coverage and removal of air bubbles.

6) The pellet mold was rapped firmly against a hard surface to remove any remaining air bubbles and to settle the sample particulate to the base of the pellet mold.

7) Epoxy was allowed to set for a minumum of 30 minutes before a second layer of epoxy was poured into the mold. Epoxy was mixed in the same ratio and stirred again for 2 minutes. Then epoxy was poured into the pellet molds filling the molds up to 2 mm down from the top of the mold.

8) This epoxy was allowed to set for a further 30 minutes. The third and final layer of epoxy was used to seal in a sample label which was placed on the top of the pellet and then covered with a thin (2 mm) layer of epoxy mixed in the same manner as described previously.

9) The pellet was then cured overnight before removal from the pellet mold. In order to remove the pellet from the mold, the base of the pellet mold was first removed, then the pellet was pushed out of the mold. A hammer and round-headed punch were used to

push some difficult to remove pellets. However, care was taken that the punch only contacted the top of the pellet (where the label is) and not the bottom.

10) The sharp top edges of the pellet were then beveled using a 240 grit wheel. This removed any loose epoxy and/or sample particulate prior to grinding and polishing. Samples may be ground and polished by hand or using a Buehler Automet wheel. Grinding was achieved using 240 grit paper, then 600 grit paper. The purpose of this stage was to remove enough epoxy to expose the sample particles. Between every stage of grinding pellets were rinsed and blown dry using compressed air.

11) The first step in polishing the pellets was the use of "Texmet" paper or Pelon. During this stage, 0.3 μm alpha alumina and distilled water were applied to the polishing wheel periodically using a squirt bottle. The next step involved placing the pellets on a wheel with two layers of silk attached. 0.05 μm alpha alumina mixed with distilled water was applied to the polishing wheel during this step. Between each stage of polishing, samples were rinsed with water then with a mixture of distilled water and "Kodak photo flo" solution. Cotton balls were used at this stage to clean the sample surface because other materials can scratch the polished sample surface. Care was taken not to touch the polished surface because oil from skin can stain or even etch samples. Once ground and polished, samples were stored polished side down on a piece of paper towel to avoid contact with dust and other atmospheric particles.

E.2 Rock-Eval Powdered Sample Preparation

The finest sample fraction produced during initial sample crushing for pellet preparation was further processed in order to produce the powdered sample required for Rock Eval pyrolysis. The fine material was crushed and ground using a mortar and pestle to produce a powdered sample of approximately 100 g with a flour-like consistency.

E.3 Rock-Eval Pyrolysis Technique

Values determined using Rock-Eval pyrolysis are useful indicators of source rock potential, quality, quantity, maturity, and paleoenvironment. The following discussion of Rock Eval pyrolysis follows that of Hunt (1996). During Rock-Eval pyrolysis, a stream of helium is passed through 100 mg of pulverized rock heated initially at 300°C. All free hydrocarbons from the sample (either present from the time of deposition or generated from kerogen since deposition) are released during this initial heating and analyzed with a flame ionization detector. Peak P_1 represents the measured amount of free hydrocarbons released during this phase of pyrolysis (Fig. E.1). The temperature is increased at a rate of ~ 25°C/min to a maximum of 550°C. Between 300 and 390°C, CO_2 is liberated when carboxyl groups in the kerogen break off. This CO_2 is trapped and analyzed during the cooling phase using a thermal conductivity detector. Peak P_3 represents CO_2 liberated in this manner (Fig. E.1). Continued heating between 350 and 550°C cracks the kerogen releasing hydrocarbons until only residual carbon remains in the sample. Any free bitumen of high molecular weight is also cracked to form smaller molecules during this phase of heating. Vapours are analyzed with a flame ionization detector and measured as peak P_2 (Fig. E.1).

The areas under peaks P_1, P_2, and P_3 are designated S_1, S_2, and S_3 respectively (Fig E.1). S_4 (mg C/g rock) is defined as residual carbon remaining in the sample once pyrolysis is completed. Total organic carbon (TOC), measured in weight percent, is equivalent to the sum of pyrolysis carbon (PC) and residual carbon (RC). The following equation can be used to calculate TOC:

(1) $$TOC = PC + RC$$

$$PC = 0.82\ (S_1 + S_2)/10 \qquad RC = S_4/10$$

$$\boxed{TOC = 0.083 \text{ x } (S1 + S2) + 0.10 \text{ x } (S4)}$$

Hydrogen Index (HI) is calculated using the following equation:

(2) $$HI = (S_2/TOC) \text{ x } 100$$

Oxygen Index (OI), in turn, is calculated using the following equation:

(3) $$OI = (S_3/TOC) \text{ x } 100$$

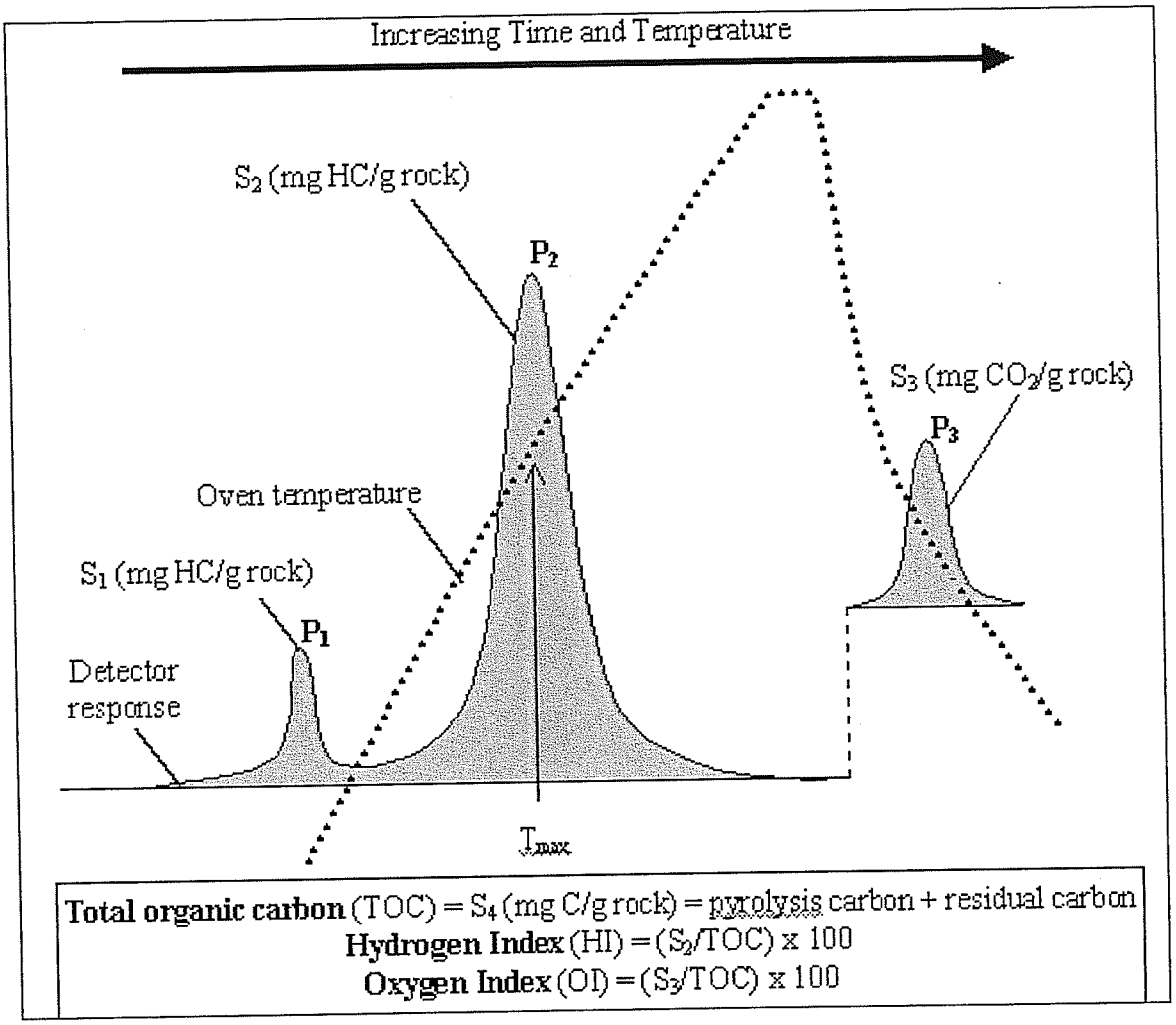

Figure E.1 Schematic diagram of pyrogram showing the evolution of hydrocarbons and CO_2 from a rock sample during heating. Important measurements include S_1, S_2, S_3, and calculations are shown for T_{max}, TOC, HI and OI (Hunt, 1996).

APPENDIX F: ORGANIC PETROLOGY DATA

All data determed from organic petrology undertaken at the Organic Petrology Laboratory at the Geological Survey of Canada (Calgary) are provided in this appendix in the form of a spreadsheet. All samples utilized for organic petrology are organized based on well location in ascending order, then by sample depth in descending order (i.e. from deepest to shallowest). The legend is located at the end of the data sheets.

Well Location	Sub-basin	Depth Range of Samples (feet)	Page #'s
00/06-32-107-09W6/0	Rainbow	6798.75 - 6951.9	F2
00/04-16-108-07W6/0	Rainbow	6480 - 6500 and 6566.3 - 6572	F2 - F3
00/04-09-109-08W6/0	Rainbow	6511.5 - 6700.11	F3
00/06-32-109-08W6/0	Rainbow	6448.5 - 6634.73	F3 - F4
00/12-33-109-08W6/0	Rainbow	6487.25 - 6653.25	F4 - F5
00/04-30-110-09W6/0	Rainbow	6391 - 6403	F5
00/07-07-113-21W5/0	Meander	4534 - 4603	F5
00/04-19-116-04W6/0	Zama	5011.5 - 5169	F5 - F6
00/05-36-117-06W6/0	Zama	5512.5 – 5526.5	F6

Well	Depth(feet)	Sample #	Pellet #	Sub-basin	Laminite	Comments	Alginites				Acritarchs	Sporinites
							Prasinophytes		Coccoidal	Filamentous		
							thick walled	thin walled				
6-32-107-9W6	6798.75	116	325/00	Rainbow	URL	above middle						
6-32-107-9W6	6813	111	326/00	Rainbow	MRL							
6-32-107-9W6	6815.5	110	327/00	Rainbow	MRL		none	M	none	none	M	T?
6-32-107-9W6	6837.5	109	328/00	Rainbow	LRL	above lower	none	M	none	none	M	T?
6-32-107-9W6	6843.3	108	329/00	Rainbow	LRL		none	M	T?	none	M	T?
6-32-107-9W6	6849.5	107	330/00	Rainbow	LRL		none	M	none	none	R	R
6-32-107-9W6	6851.5	106	331/00	Rainbow	LRL							
6-32-107-9W6	6853.8	105	332/00	Rainbow	LRL		none	M	none	none	R (*Very.*)	T
6-32-107-9W6	6916	100		Rainbow	LRL	below lower						
6-32-107-9W6	6938.9	0098	333/00	Rainbow	LRL	below lower						
6-32-107-9W6	6951.9	0096	334/00	Rainbow	LRL	below lower	T	D	T	none	R (*Very.*)	T
4-16-108-7W6	6480-6490	184	365/00	Rainbow	URL		T	M	none	none	R	none
4-16-108-7W6	6490-6500	185	366/00	Rainbow	URL		M	M	none	none	M	T?
4-16-108-7W6	6566.3	0054	298/00	Rainbow	MRL		none	D	none	none	R	T
4-16-108-7W6	6566.4	0053	299/00	Rainbow	MRL		T	D	none	none	M	M
4-16-108-7W6	6567	0052	300/00	Rainbow	MRL		none	D	none	none	T	none
4-16-108-7W6	6568.5	0051	301/00	Rainbow	MRL							
4-16-108-7W6	6569.5	0050	302/00	Rainbow	MRL		none	D	T?	none	M	T?
4-16-108-7W6	6570	0049	303/00	Rainbow	MRL		T	D	T?	none	M	none
4-16-108-7W6	6571.75	0048	305/00	Rainbow	MRL							

Well	Depth(feet)	Sample #	Pellet #	Sub-basin	Laminite	Comments	Alginites				Acritarchs	Sporinites
							Prasinophytes		Coccoidal	Filamentous		
							thick walled	thin walled				
4-16-108-7W6	6572	0047	306/00	Rainbow	MRL		T	M	T?	none	R	none
4-9-109-8W6	6511.5	0038	292/00	Rainbow	URL		M	D	none	none	M	T
4-9-109-8W6	6571	0044	304/00	Rainbow	MRL		R	D	none	none	M	R
4-9-109-8W6	6572.3	0045	307/00	Rainbow	MRL		none	D	T?	none	M	R?
4-9-109-8W6	6582.5	0043	308/00	Rainbow	LRL	above lower	R	D	none	none	M	T?
4-9-109-8W6	6591	0023	309/00	Rainbow	LRL	above lower	T	D	T?	none	M	R
4-9-109-8W6	6593.62	0022	310/00	Rainbow	LRL	above lower	T	M	none	none	R	none
4-9-109-8W6	6594	0021	311/00	Rainbow	LRL	above lower	none	R	none	none	none	none
4-9-109-8W6	6601.5	0042	313/00	Rainbow	LRL		M	M	none	none	D	T?
4-9-109-8W6	6700.11	003		Rainbow	LRL	below lower						
4-9-109-8W6	6511.75	0037	293/00	Rainbow	URL		M	M	none	T?	M	T
4-9-109-8W6	6601	0019	312/00	Rainbow	LRL		none	R	none	none	none	none
4-9-109-8W6	6625.5	0014	318/00	Rainbow	LRL	below lower	none	R	none	none	none	none
6-32-109-8W6	6448.5	146	341/00	Rainbow	URL		D	D	none	none	R	none
6-32-109-8W6	6449.25	145	342/00	Rainbow	URL		D	D	none	none	T	none
6-32-109-8W6	6463	143	343/00	Rainbow	URL		D	D	none	none	R	none
6-32-109-8W6	6467.5	142	344/00	Rainbow	URL							
6-32-109-8W6	6518.75	136	345/00	Rainbow	URL		D	D	none	none	T	none
6-32-109-8W6	6537.5	131	346/00	Rainbow	URL		D	D	none	T?	R	none

Well	Depth(feet)	Sample #	Pellet #	Sub-basin	Laminite	Comments	Alginites				Acritarchs	Sporinites
							Prasinophytes		Coccoidal	Filamentous		
							thick walled	thin walled				
6-32-109-8W6	6542	130	347/00	Rainbow	URL		D	D	none	T?	R	none
6-32-109-8W6	6621.8	122	348/00	Rainbow	MRL		T	D	none	none	R	none
6-32-109-8W6	6623.25	121	349/00	Rainbow	MRL							
6-32-109-8W6	6624	120	350/00	Rainbow	MRL		none	M	T?	none	M	T?
6-32-109-8W6	6634.73	117	351/00	Rainbow	LRL	above lower	T	D	none	none	R	T?
12-33-109-8W6	6487.25	0093	288/00	Rainbow	URL		D	M	none	T?	R	none
12-33-109-8W6	6496	0092	289/00	Rainbow	URL		D	M	none	T?	R	none
12-33-109-8W6	6499	0091	290/00	Rainbow	URL		D	M	none	none	R	none
12-33-109-8W6	6507.25	0090	291/00	Rainbow	URL		M	D	none	none	M	none
12-33-109-8W6	6513	0089	294/00	Rainbow	URL		M	M	none	none	R	T?
12-33-109-8W6	6521.75	0086	295/00	Rainbow	URL		D	M	none	none	M	none
12-33-109-8W6	6544	0084	296/00	Rainbow	URL		D	M	none	T?	M	T?
12-33-109-8W6	6557.75	0081	297/00	Rainbow	URL		D	M	none	T?	R	none
12-33-109-8W6	6618.32	0073	314/00	Rainbow	URL	above middle	T	D	none	none	M	none
12-33-109-8W6	6620.25	0072	315/00	Rainbow	MRL		none	M	none	none	D	T?
12-33-109-8W6	6621.5	0071	316/00	Rainbow	MRL							
12-33-109-8W6	6622.25	0070	317/00	Rainbow	MRL		R	M	none	none	R	none
12-33-109-8W6	6631.5	0067	319/00	Rainbow	LRL	above lower	T	D	none	none	M	R?
12-33-109-8W6	6642.5	0066	320/00	Rainbow	LRL	above lower	none	M	none	none	D	R

Well	Depth(feet)	Sample #	Pellet #	Sub-basin	Laminite	Comments	Alginites				Acritarchs	Sporinites
							Prasinophytes		Coccoidal	Filamentous		
							thick walled	thin walled				
12-33-109-8W6	6644.5	0065	321/00	Rainbow	LRL	above lower	none	D	none	none	D	T?
12-33-109-8W6	6647.96	0064	322/00	Rainbow	LRL	above lower	none	M	none	none	D	T?
12-33-109-8W6	6650.2	0063	323/00	Rainbow	LRL	above lower						
12-33-109-8W6	6653.25	0062	324/00	Rainbow	LRL							
4-30-110-9W6	6290-6300	188	367/00	Rainbow	URL		T	M	none	none	R	none
4-30-110-9W6	6310-6320	187	368/00	Rainbow	URL		T	M	none	none	M	none
4-30-110-9W6	6320-6330	186	369/00	Rainbow	URL		R	M	none	none	R	none
4-30-110-9W6	6391	151	336/00	Rainbow	MRL		none	R	T?	none	D	none
4-30-110-9W6	6391.5	150	337/00	Rainbow	MRL							
4-30-110-9W6	6392.5	149	338/00	Rainbow	MRL		none	M	T?	none	M	T?
4-30-110-9W6	6393.5	148	339/00	Rainbow	MRL		none	M	T?	none	M	T?
4-30-110-9W6	6403	147	340/00	Rainbow	LRL	above lower						
7-7-113-21W5	4534	196	354/00	Meander	UML	above upper (MSKG)	T	D	none	none	D	T?
7-7-113-21W5	4581	193	355/00	Meander	LML	above lower						
7-7-113-21W5	4585	192	356/00	Meander	LML	above lower	T	M	none	none	M	none
7-7-113-21W5	4603	191	357/00	Meander	LML		D	D	none	T?	R	T?
4-19-116-4W6	5011.5	178	358/00	Zama	UZL		D	D	none	none	R	none
4-19-116-4W6	5154	169	359/00	Zama	LZL		R	M	none	none	R	T?
4-19-116-4W6	5156	168	360/00	Zama	LZL		none	R	none	none	R	T?

Well	Depth(feet)	Sample #	Pellet #	Sub-basin	Laminite	Comments	Alginites				Acritarchs	Sporinites
							Prasinophytes		Coccoidal	Filamentous		
							thick walled	thin walled				
4-19-116-4W6	5169	167	361/00	Zama	LZL	below lower	T	R	none	none	R	none
5-36-117-6W6	5512.5	162	362/00	Zama	LZL		R	D	T?	none	R	none
5-36-117-6W6	5523	160	363/00	Zama	LZL		T	M	none	none	M	none
5-36-117-6W6	5526.5	159	364/00	Zama	LZL		T	D	T?	none	M	none

KEY:

D	dominant or major maceral
M	minor
R	rare
T	trace
none	absence of maceral
?	questionable data
	sample not analyzed due to low TOC or proximity to other similar samples

APPENDIX G: ROCK-EVAL 6 PYROLYSIS DATA

All data determed from Rock-Eval 6 pyrolysis undertaken at the Organic Geochemistry Laboratory at the Geological Survey of Canada (Calgary) are provided in this appendix in the form of a spreadsheet. All samples utilized for organic geochemistry are organized based on well location in ascending order, then by sample depth in descending order (i.e., from deepest to shallowest). Pellet numbers correspond to the archived sample set at the Geological Survey of Canada (Calgary). Note: Neither Rock-Eval nor Organic Petrology done for samples 003 and 100. Rock Eval and Organic Petrology was completed for all for all samples except pellets 365/00 - 369/00.

Well Location	Sub-basin	Depth Range of Samples (feet)	Page #'s
00/06-32-107-09W6/0	Rainbow	6798.75 – 6587.9	G2-G4
00/04-16-108-07W6/0	Rainbow	6566.3 - 6572	G2-G4
00/04-09-109-08W6/0	Rainbow	6511.5 – 6625.5	G2-G4
00/06-32-109-08W6/0	Rainbow	6448.5 – 6634.73	G2-G7
00/12-33-109-08W6/0	Rainbow	6487.25 – 6653.25	G5-G7
00/04-30-110-09W6/0	Rainbow	6391 - 6403	G5-G7
00/07-07-113-21W5/0	Meander	4534 - 4603	G5-G7
00/04-19-116-04W6/0	Zama	5011.5 - 4603	G5-G7
00/05-36-117-06W6/0	Zama	5512.5 – 5526.5	G5-G7

SAMPLE	LOCATION	DEPTH (feet)	PELLET #	C #	SUB-BASIN	POSITION	LAMINITE	Qty	S1	S2	S'2	PI	S3CO2	Tmax
116	6-32-107-9W6	6798.75	325/00		Rainbow	foreslope	middle	100.4	0.16	0.23	0.01	0.4	0.5	458
111	6-32-107-9W6	6813	326/00		Rainbow	foreslope	middle	100.6	0.2	0.27	0.01	0.41	0.32	449
110	6-32-107-9W6	6815.5	327/00		Rainbow	foreslope	middle	100	0.41	1.16	0.01	0.26	0.96	436
109	6-32-107-9W6	6837.5	328/00		Rainbow	foreslope	lower	100.4	0.58	1.44	0.03	0.28	0.28	465
108	6-32-107-9W6	6843.3	329/00		Rainbow	foreslope	lower	99.9	1.52	5.56	0.09	0.21	0.64	459
107	6-32-107-9W6	6849.5	330/00		Rainbow	foreslope	lower	100.6	0.85	2.74	0.05	0.23	0.37	457
106	6-32-107-9W6	6851.5	331/00		Rainbow	foreslope	lower	100.5	0.05	0.1	0.01	0.31	0.14	447
105	6-32-107-9W6	6853.8	332/00		Rainbow	foreslope	lower	100.7	1.51	4.46	0.06	0.25	0.55	462
98	6-32-107-9W6	6938.9	333/00		Rainbow	foreslope	lower	100	0.17	0.38	0.01	0.31	0.18	461
96	6-32-107-9W6	6951.9	334/00		Rainbow	foreslope	lower	100.8	0.85	2.06	0.04	0.29	0.37	457
54	4-16-108-7W6	6566.3	298/00		Rainbow	distal foreslope	middle	100.5	0.27	0.71	0.01	0.27	0.61	454
53	4-16-108-7W6	6566.4	299/00		Rainbow	distal foreslope	middle	100.7	0.34	0.69	0.01	0.32	0.35	458
52	4-16-108-7W6	6567	300/00		Rainbow	distal foreslope	middle	100.4	0.2	0.58	0.01	0.25	0.23	452
51	4-16-108-7W6	6568.5	301/00		Rainbow	distal foreslope	middle	100.8	0.15	0.25	0.01	0.37	0.14	453
50	4-16-108-7W6	6569.5	302/00		Rainbow	distal foreslope	middle	100	0.31	0.42	0.01	0.42	0.21	458
49	4-16-108-7W6	6570	303/00		Rainbow	distal foreslope	middle	100.7	0.31	0.49	0.01	0.39	0.17	455
48	4-16-108-7W6	6571.75	305/00		Rainbow	distal foreslope	middle	100.2	0.24	0.63	0.01	0.27	0.24	440
47	4-16-108-7W6	6572	306/00		Rainbow	distal foreslope	middle	100.7	0.78	1.07	0.01	0.42	0.48	433
38	4-9-109-8W6	6511.5	292/00		Rainbow	foreslope	upper	100.2	0.47	4.95	0.05	0.09	0.3	442
37	4-9-109-8W6	6511.75	293/00		Rainbow	foreslope	upper	100.7	0.18	1.43	0.02	0.11	0.26	448
44	4-9-109-8W6	6571	304/00		Rainbow	foreslope	middle	99.9	1.47	2.44	0.01	0.37	0.67	426
45	4-9-109-8W6	6572.3	307/00		Rainbow	foreslope	middle	100.1	0.96	2.06	0.01	0.32	0.72	427
43	4-9-109-8W6	6582.5	308/00		Rainbow	foreslope	above lower	100.4	1.16	3.28	0.02	0.26	0.69	447
23	4-9-109-8W6	6591	309/00		Rainbow	foreslope	lower	100.6	1.21	2.42	0.02	0.33	0.35	448
22	4-9-109-8W6	6593.62	310/00		Rainbow	foreslope	lower	99.8	2	10.07	0.09	0.16	0.39	452
21	4-9-109-8W6	6594	311/00		Rainbow	foreslope	lower	100.5	1.72	5.7	0.05	0.23	0.55	450
19	4-9-109-8W6	6601	312/00		Rainbow	foreslope	lower	100.5	0.59	2.47	0.02	0.19	0.74	454
42	4-9-109-8W6	6601.5	313/00		Rainbow	foreslope	lower	100.2	0.38	1.28	0.01	0.23	0.69	441
14	4-9-109-8W6	6625.5	318/00		Rainbow	foreslope	lower	100	0.25	1.5	0.02	0.14	0.56	449
146	6-32-109-8W6	6448.5	341/00	C-405496	Rainbow	foreslope	upper	100.6	0.28	1.41	0.02	0.16	0.18	447
145	6-32-109-8W6	6449.25	342/00	C-405497	Rainbow	foreslope	upper	100.6	0.32	1.69	0.02	0.16	0.15	450
143	6-32-109-8W6	6463	343/00	C-405498	Rainbow	foreslope	upper	100.5	1.59	4.2	0.04	0.27	0.3	445
142	6-32-109-8W6	6467.5	344/00	C-405499	Rainbow	foreslope	upper	10	41.62	113.13	2.28	0.27	1.18	458
136	6-32-109-8W6	6518.75	345/00	C-405500	Rainbow	foreslope	upper	100.3	1.98	3.37	0.04	0.37	0.51	447
131	6-32-109-8W6	6537.5	346/00	C-405501	Rainbow	foreslope	upper	100	0.7	5.13	0.05	0.12	0.3	444
130	6-32-109-8W6	6542	347/00	C-405502	Rainbow	foreslope	upper	99.9	0.4	1.25	0.02	0.24	0.24	448
122	6-32-109-8W6	6621.8	348/00	C-405503	Rainbow	foreslope	middle	100.2	0.78	1.89	0.01	0.29	0.62	434
121	6-32-109-8W6	6623.25	349/00	C-405504	Rainbow	foreslope	middle	100.5	0.79	1.48	0	0.35	0.55	421

SAMPLE	LOCATION	DEPTH (feet)	Tpeak	S3CO	PC(%)	TOC	RC%	HI	OICO	OICO2	OIRE6	MINC%	S4CO	S4CO2	RCCO(%)	S4CO2
116	6-32-107-9W6	6798.75	501	0.06	0.04	0.28	0.24	86	21	179	142	0.4	1	7.3	0.043	7.3
111	6-32-107-9W6	6813	492	0.11	0.04	0.41	0.37	68	27	78	72	0.5	1.5	11.3	0.064	11.3
110	6-32-107-9W6	6815.5	479	0.17	0.14	0.5	0.36	234	34	192	159	1.1	2.4	9.3	0.103	9.3
109	6-32-107-9W6	6837.5	508	0.04	0.17	1.65	1.48	89	2	17	14	0.7	7.3	42.9	0.313	42.9
108	6-32-107-9W6	6843.3	502	0.06	0.6	4.61	4.01	123	1	14	11	1.3	19.5	116.5	0.836	116.5
107	6-32-107-9W6	6849.5	500	0.03	0.3	2.33	2.03	120	1	16	12	0.8	9.3	59.9	0.399	59.9
106	6-32-107-9W6	6851.5	490	0.03	0.01	0.12	0.11	92	25	117	99	0.3	0.2	3.8	0.009	3.8
105	6-32-107-9W6	6853.8	505	0.3	0.51	3.06	2.55	148	10	18	19	1.1	12.7	73.4	0.544	73.4
98	6-32-107-9W6	6938.9	504	0.02	0.05	0.61	0.56	64	3	30	24	0.3	2.9	15.8	0.124	15.8
96	6-32-107-9W6	6951.9	500	0.04	0.25	2.34	2.09	90	2	16	13	0.9	10.8	59.8	0.463	59.8
54	4-16-108-7W6	6566.3	497	0.05	0.08	1	0.92	72	5	61	47	0.8	4	27.5	0.171	27.5
53	4-16-108-7W6	6566.4	501	0.05	0.09	0.83	0.74	84	6	42	34	0.6	3.3	21.9	0.141	21.9
52	4-16-108-7W6	6567	495	0.07	0.07	0.57	0.5	104	12	40	36	0.5	2	15.2	0.086	15.2
51	4-16-108-7W6	6568.5	496	0.02	0.03	0.31	0.28	84	6	45	36	0.3	1	8.7	0.043	8.7
50	4-16-108-7W6	6569.5	501	0.05	0.06	0.56	0.5	77	9	38	33	0.5	2.3	14.8	0.099	14.8
49	4-16-108-7W6	6570	498	0.11	0.07	0.68	0.61	74	16	25	27	0.6	3	17.8	0.129	17.8
48	4-16-108-7W6	6571.75	483	0.05	0.08	0.51	0.43	125	10	47	40	0.7	2	12.8	0.086	12.8
47	4-16-108-7W6	6572	476	0.05	0.16	0.75	0.59	144	7	64	51	1.1	2.5	17.6	0.107	17.6
38	4-9-109-8W6	6511.5	485	0.16	0.46	2.38	1.92	210	7	13	13	0.5	9.1	56.1	0.39	56.1
37	4-9-109-8W6	6511.75	491	0.18	0.14	0.91	0.77	159	20	29	33	0.4	3	23.5	0.129	23.5
44	4-9-109-8W6	6571	469	0.1	0.33	0.9	0.57	272	11	74	60	1.1	2.2	17.5	0.094	17.5
45	4-9-109-8W6	6572.3	470	0.07	0.25	0.74	0.49	280	9	97	76	1.1	1.9	15	0.081	15
43	4-9-109-8W6	6582.5	490	0.1	0.37	1.49	1.12	221	7	46	37	1	4.1	34.7	0.176	34.7
23	4-9-109-8W6	6591	491	0.17	0.31	1.41	1.1	173	12	25	25	0.9	4.5	33.3	0.193	33.3
22	4-9-109-8W6	6593.62	495	0.23	1.02	4.99	3.97	204	5	8	9	1	19.7	114.7	0.844	114.7
21	4-9-109-8W6	6594	493	0.07	0.62	2.94	2.32	196	2	19	15	0.8	11.3	67.2	0.484	67.2
19	4-9-109-8W6	6601	497	0.1	0.26	0.62	0.36	402	16	119	96	0.9	2	10	0.086	10
42	4-9-109-8W6	6601.5	484	0.05	0.14	0.37	0.23	349	14	186	143	0.8	1.3	6.3	0.056	6.3
14	4-9-109-8W6	6625.5	492	0.06	0.15	0.53	0.38	287	11	106	83	1.1	2.6	9.8	0.111	9.8
146	6-32-109-8W6	6448.5	490	0.04	0.14	1.07	0.93	134	4	17	15	0.5	4.1	27.7	0.176	27.7
145	6-32-109-8W6	6449.25	493	0.05	0.17	1.21	1.04	141	4	12	11	0.5	5.2	29.8	0.223	29.8
143	6-32-109-8W6	6463	488	0.24	0.49	3.62	3.13	117	7	8	10	0.5	15.5	90.5	0.664	90.5
142	6-32-109-8W6	6467.5	501	2.17	13.13	44.77	31.64	258	5	3	5	32	548.9	297.7	23.524	297.7
136	6-32-109-8W6	6518.75	490	0.41	0.46	4.25	3.79	80	10	12	14	0.8	18.9	109.2	0.81	109.2
131	6-32-109-8W6	6537.5	487	0.05	0.49	2.73	2.24	190	2	11	9	0.6	10.6	65.3	0.454	65.3
130	6-32-109-8W6	6542	491	0	0.14	1.01	0.87	126	0	24	17	0.5	3.7	26.1	0.159	26.1
122	6-32-109-8W6	6621.8	477	0.24	0.23	1.05	0.82	181	23	59	56	1.5	3.2	25.2	0.137	25.2
121	6-32-109-8W6	6623.25	464	0.19	0.2	0.73	0.53	203	26	75	69	1.4	1.9	16.4	0.081	16.4

SAMPLE	LOCATION	DEPTH (feet)	S5aCO2	S5bCO2	KFID	RCCO2(%)	
116	6-32-107-9W6	6798.75	1.4	6.1	1594.558	0.2	TOC <.5 and S1 < 0.2
111	6-32-107-9W6	6813	2.7	6.5	1594.558	0.31	TOC <.5
110	6-32-107-9W6	6815.5	11.1	10.4	1594.558	0.25	
109	6-32-107-9W6	6837.5	3.8	11.3	1594.558	1.17	
108	6-32-107-9W6	6843.3	0	34.5	1594.558	3.18	
107	6-32-107-9W6	6849.5	0	18	1594.558	1.63	
106	6-32-107-9W6	6851.5	0.8	4.2	1594.558	0.1	TOC <.5 and S1 < 0.2
105	6-32-107-9W6	6853.8	0	26.6	1594.558	2	
98	6-32-107-9W6	6938.9	0.6	4.5	1594.558	0.43	S1 < 0.2
96	6-32-107-9W6	6951.9	1.8	11.5	1594.558	1.63	
54	4-16-108-7W6	6566.3	3.5	10.1	1594.558	0.75	
53	4-16-108-7W6	6566.4	3.2	8.3	1594.558	0.6	
52	4-16-108-7W6	6567	1.9	6.4	1594.558	0.41	
51	4-16-108-7W6	6568.5	1.5	4.5	1594.558	0.24	TOC <.5 and S1 < 0.2
50	4-16-108-7W6	6569.5	2.7	6.2	1594.558	0.4	
49	4-16-108-7W6	6570	3	8.4	1594.558	0.49	
48	4-16-108-7W6	6571.75	3.6	8.5	1594.558	0.35	
47	4-16-108-7W6	6572	6.9	14	1594.558	0.48	Tmax < 435
38	4-9-109-8W6	6511.5	2.9	5.9	1594.558	1.53	PI < 0.1
37	4-9-109-8W6	6511.75	1.7	4.5	1594.558	0.64	S1 < 0.2
44	4-9-109-8W6	6571	7.2	13.3	1594.558	0.48	Tmax < 435
45	4-9-109-8W6	6572.3	6.8	12.6	1594.558	0.41	Tmax < 435
43	4-9-109-8W6	6582.5	4.7	14.7	1594.558	0.95	
23	4-9-109-8W6	6591	4.8	12.5	1594.558	0.91	
22	4-9-109-8W6	6593.62	0	23.6	1594.558	3.13	
21	4-9-109-8W6	6594	2.4	15.5	1594.558	1.83	
19	4-9-109-8W6	6601	11.1	9.3	1594.558	0.27	
42	4-9-109-8W6	6601.5	6.9	7.9	1594.558	0.17	TOC <.5
14	4-9-109-8W6	6625.5	13.3	10.4	1594.558	0.27	
146	6-32-109-8W6	6448.5	2.8	5.8	1594.558	0.76	
145	6-32-109-8W6	6449.25	2.3	6.1	1594.558	0.81	
143	6-32-109-8W6	6463	0	5.9	1594.558	2.47	
142	6-32-109-8W6	6467.5	739.3	401.2	1594.558	8.12	TOC > 10
136	6-32-109-8W6	6518.75	0	6.4	1594.558	2.98	
131	6-32-109-8W6	6537.5	2.3	6.2	1594.558	1.78	
130	6-32-109-8W6	6542	1.9	5.8	1594.558	0.71	
122	6-32-109-8W6	6621.8	8	14.5	1594.558	0.69	Tmax < 435
121	6-32-109-8W6	6623.25	6.8	13.8	1594.558	0.45	Tmax < 435

SAMPLE	LOCATION	DEPTH (feet)	PELLET #	C #	SUB-BASIN	POSITION	LAMINITE	Qty	S1	S2	S'2	PI	S3CO2	Tmax
120	6-32-109-8W6	6624	350/00	C-405505	Rainbow	foreslope	middle	100.8	1.09	2.07	0.01	0.34	0.84	326
117	6-32-109-8W6	6634.73	351/00	C-405506	Rainbow	foreslope	lower	100.5	1.19	2.32	0.02	0.34	0.35	451
93	12-33-109-8W6	6487.25	288/00		Rainbow	foreslope	upper	100.2	3.08	11.49	0.12	0.21	0.82	450
92	12-33-109-8W6	6496	289/00		Rainbow	foreslope	upper	100.1	0.31	4.14	0.04	0.07	0.35	445
91	12-33-109-8W6	6499	290/00		Rainbow	foreslope	upper	100.8	0.48	4.28	0.04	0.1	0.48	443
90	12-33-109-8W6	6507.25	291/00		Rainbow	foreslope	upper	99.7	0.22	1.22	0.02	0.15	0.26	450
89	12-33-109-8W6	6513	294/00		Rainbow	foreslope	upper	99.8	0.72	5.67	0.04	0.11	0.29	442
86	12-33-109-8W6	6521.75	295/00		Rainbow	foreslope	upper	100.6	0.37	3.43	0.03	0.1	0.47	447
84	12-33-109-8W6	6544	296/00		Rainbow	foreslope	upper	100.4	0.78	4.21	0.04	0.15	0.52	449
81	12-33-109-8W6	6557.75	297/00		Rainbow	foreslope	upper	100.5	1.32	2.21	0.03	0.37	0.54	452
73	12-33-109-8W6	6618.32	314/00		Rainbow	foreslope	middle	99.9	0.65	1.77	0.02	0.26	0.38	451
72	12-33-109-8W6	6620.25	315/00		Rainbow	foreslope	middle	100.1	1.31	5.08	0.06	0.2	0.4	451
71	12-33-109-8W6	6621.5	316/00		Rainbow	foreslope	middle	100.3	0.85	1.92	0.01	0.31	0.9	430
70	12-33-109-8W6	6622.25	317/00		Rainbow	foreslope	middle	100.6	1.13	1.65	0.01	0.41	0.81	419
67	12-33-109-8W6	6631.5	319/00		Rainbow	foreslope	lower	99.7	0.9	1.21	0.01	0.42	0.66	444
66	12-33-109-8W6	6642.5	320/00		Rainbow	foreslope	lower	100.3	2.07	4.94	0.05	0.29	0.37	453
65	12-33-109-8W6	6644.5	321/00		Rainbow	foreslope	lower	99.9	2.62	5.8	0.05	0.31	0.43	453
64	12-33-109-8W6	6647.96	322/00		Rainbow	foreslope	lower	100.2	2.8	7.09	0.07	0.28	0.72	452
63	12-33-109-8W6	6650.2	323/00		Rainbow	foreslope	lower	100.5	0.57	0.91	0.01	0.38	0.25	451
62	12-33-109-8W6	6653.25	324/00		Rainbow	foreslope	lower	99.9	0.68	1.71	0.02	0.28	0.79	437
151	4-30-110-9W6	6391	336/00	C-405491	Rainbow	foreslope	middle	100.8	0.54	1.83	0.03	0.22	0.38	461
150	4-30-110-9W6	6391.5	337/00	C-405492	Rainbow	foreslope	middle	100.6	0.46	1.16	0.01	0.28	0.38	446
149	4-30-110-9W6	6392.5	338/00	C-405493	Rainbow	foreslope	middle	100	0.64	1.29	0.01	0.33	0.28	447
148	4-30-110-9W6	6393.5	339/00	C-405494	Rainbow	foreslope	middle	100.5	0.6	1.22	0.02	0.33	0.36	450
147	4-30-110-9W6	6403	340/00	C-405495	Rainbow	foreslope	lower	99.8	0.14	0.21	0	0.39	0.14	445
196	7-7-113-21W5	4534	354/00		Meander	off-reef	upper	100.6	0.22	3.23	0.02	0.06	0.25	440
193	7-7-113-21W5	4581	355/00		Meander	off-reef	lower	100.4	0.2	1.81	0.01	0.1	0.33	441
192	7-7-113-21W5	4585	356/00		Meander	off-reef	lower	100.9	0.26	2.18	0.01	0.11	0.59	431
191	7-7-113-21W5	4603	357/00		Meander	off-reef	lower	100.1	5.38	44.69	0.22	0.11	0.54	441
178	4-19-116-4W6	5011.5	358/00		Zama	foreslope	upper	100.5	0.49	3.95	0.02	0.11	0.35	434
169	4-19-116-4W6	5154	359/00		Zama	foreslope	lower	100.1	1.12	12.43	0.05	0.08	0.34	441
168	4-19-116-4W6	5156	360/00		Zama	foreslope	lower	100.7	1.48	20.62	0.09	0.07	0.38	439
167	4-19-116-4W6	5169	361/00		Zama	foreslope	lower	100.9	1.6	17.62	0.08	0.08	0.41	441
162	5-36-117-6W6	5512.5	362/00		Zama	foreslope	lower	100	3.13	5.87	0.12	0.34	0.34	454
160	5-36-117-6W6	5523	363/00		Zama	foreslope	lower	100.3	1.26	4.54	0.08	0.22	0.33	451
159	5-36-117-6W6	5526.5	364/00		Zama	foreslope	lower	100.4	3.15	16.96	0.21	0.15	0.5	448

SAMPLE	LOCATION	DEPTH (feet)	Tpeak	S3CO	PC(%)	TOC	RC%	HI	OICO	OICO2	OIRE6	MINC%	S4CO	S4CO2	RCCO(%)	S4CO2
120	6-32-109-8W6	6624	369	0.19	0.27	0.91	0.64	229	21	92	79	1.5	2.4	19.7	0.103	19.7
117	6-32-109-8W6	6634.73	494	0.1	0.3	1.38	1.08	170	7	25	22	0.8	4.8	32.1	0.206	32.1
93	12-33-109-8W6	6487.25	493	0.38	1.24	8.57	7.33	135	4	10	10	1.4	34.7	214.3	1.487	214.3
92	12-33-109-8W6	6496	488	0.19	0.38	2.17	1.79	193	9	16	17	0.5	9.2	51.2	0.394	51.2
91	12-33-109-8W6	6499	486	0.07	0.4	2.56	2.16	169	3	19	16	0.4	10.9	62.2	0.467	62.2
90	12-33-109-8W6	6507.25	493	0.11	0.13	1.09	0.96	114	10	24	23	0.3	4.3	28.3	0.184	28.3
89	12-33-109-8W6	6513	485	0.2	0.54	3.61	3.07	158	6	8	9	0.6	15.2	88.6	0.651	88.6
86	12-33-109-8W6	6521.75	490	0.21	0.33	2.16	1.83	160	10	22	22	0.6	8.9	53.2	0.381	53.2
84	12-33-109-8W6	6544	492	0.16	0.42	3.49	3.07	122	5	15	14	1	13.5	91.2	0.579	91.2
81	12-33-109-8W6	6557.75	495	0.13	0.3	2.13	1.83	105	6	25	22	0.9	8.7	53.3	0.373	53.3
73	12-33-109-8W6	6618.32	494	0.11	0.21	1.72	1.51	104	6	22	19	0.7	7.7	43.4	0.33	43.4
72	12-33-109-8W6	6620.25	494	0.2	0.54	3.32	2.78	155	6	12	12	0.9	12.6	82.3	0.54	82.3
71	12-33-109-8W6	6621.5	473	0.16	0.24	0.9	0.66	214	18	100	83	1.4	2.7	20.1	0.116	20.1
70	12-33-109-8W6	6622.25	462	0.02	0.23	1.08	0.85	154	2	75	56	1.7	2.9	26.5	0.124	26.5
67	12-33-109-8W6	6631.5	487	0.02	0.18	1.12	0.94	109	2	59	44	1.2	3.7	28.5	0.159	28.5
66	12-33-109-8W6	6642.5	496	0.01	0.59	2.83	2.24	176	0	13	9	1	10.6	65.4	0.454	65.4
65	12-33-109-8W6	6644.5	496	0.07	0.71	3.38	2.67	173	2	13	11	0.8	13.4	76.8	0.574	76.8
64	12-33-109-8W6	6647.96	495	0.08	0.83	3.97	3.14	180	2	18	14	0.9	14.7	92.2	0.63	92.2
63	12-33-109-8W6	6650.2	494	0.02	0.12	0.67	0.55	137	3	37	29	0.4	2.4	16.3	0.103	16.3
62	12-33-109-8W6	6653.25	480	0.04	0.2	0.5	0.3	346	8	158	119	0.9	1.7	8.2	0.073	8.2
151	4-30-110-9W6	6391	504	0.02	0.2	0.95	0.75	196	2	40	30	1.2	5.1	19.4	0.219	19.4
150	4-30-110-9W6	6391.5	489	0.05	0.14	0.58	0.44	202	9	66	53	0.9	2.8	11.8	0.12	11.8
149	4-30-110-9W6	6392.5	490	0.01	0.16	0.67	0.51	194	1	42	31	1	3	14	0.129	14
148	4-30-110-9W6	6393.5	493	0.02	0.15	0.77	0.62	161	3	47	36	1.1	3.4	17.5	0.146	17.5
147	4-30-110-9W6	6403	488	0.02	0.03	0.3	0.27	70	7	47	38	0.5	0.7	8.7	0.03	8.7
196	7-7-113-21W5	4534	483	0.22	0.3	0.95	0.65	342	23	26	32	0.6	2.9	19.4	0.124	19.4
193	7-7-113-21W5	4581	484	0.06	0.17	0.65	0.48	280	9	51	42	0.6	1.1	15.8	0.047	15.8
192	7-7-113-21W5	4585	474	0.03	0.2	1	0.8	219	3	59	45	1.4	2.7	25.1	0.116	25.1
191	7-7-113-21W5	4603	484	0.29	4.19	13.84	9.65	324	2	4	4	1.3	55.1	267.3	2.361	267.3
178	4-19-116-4W6	5011.5	477	0.2	0.38	1.5	1.12	265	13	23	24	0.4	5.7	31.9	0.244	31.9
169	4-19-116-4W6	5154	484	0.18	1.14	3.58	2.44	349	5	9	9	0.7	12.1	70.5	0.519	70.5
168	4-19-116-4W6	5156	482	0.24	1.85	5.5	3.65	377	4	7	7	0.6	18	105.6	0.771	105.6
167	4-19-116-4W6	5169	484	0.18	1.61	4.73	3.12	374	4	9	9	0.8	14.8	91	0.634	91
162	5-36-117-6W6	5512.5	497	0.31	0.77	4.63	3.86	129	7	7	9	0.8	22.8	105.6	0.977	105.6
160	5-36-117-6W6	5523	494	0.06	0.49	3	2.51	154	2	11	9	0.3	14.4	69.4	0.617	69.4
159	5-36-117-6W6	5526.5	491	0.39	1.7	9.61	7.91	179	4	5	6	0.7	41.7	224.4	1.787	224.4

SAMPLE	LOCATION	DEPTH (feet)	S5aCO2	S5bCO2	KFID	RCCO2(%)	
120	6-32-109-8W6	6624	8.1	15	1594.558	0.54	Tmax < 435
117	6-32-109-8W6	6634.73	4.8	11.9	1594.558	0.88	
93	12-33-109-8W6	6487.25	0	11.4	1594.558	5.84	
92	12-33-109-8W6	6496	3.5	6.8	1594.558	1.4	PI < 0.1
91	12-33-109-8W6	6499	0.2	4.8	1594.558	1.7	
90	12-33-109-8W6	6507.25	0.5	3.9	1594.558	0.77	
89	12-33-109-8W6	6513	0	7.1	1594.558	2.42	
86	12-33-109-8W6	6521.75	2.7	6.9	1594.558	1.45	
84	12-33-109-8W6	6544	0	9.3	1594.558	2.49	
81	12-33-109-8W6	6557.75	3.3	7.5	1594.558	1.45	
73	12-33-109-8W6	6618.32	1.9	8.4	1594.558	1.18	
72	12-33-109-8W6	6620.25	0	16.5	1594.558	2.24	
71	12-33-109-8W6	6621.5	7.8	14.2	1594.558	0.55	Tmax < 435
70	12-33-109-8W6	6622.25	8.4	15.9	1594.558	0.72	Tmax < 435
67	12-33-109-8W6	6631.5	6.3	13.8	1594.558	0.78	
66	12-33-109-8W6	6642.5	5.6	17.8	1594.558	1.78	
65	12-33-109-8W6	6644.5	0	16.1	1594.558	2.09	
64	12-33-109-8W6	6647.96	0	19.8	1594.558	2.51	
63	12-33-109-8W6	6650.2	2.1	5.5	1594.558	0.44	
62	12-33-109-8W6	6653.25	9	8.7	1594.558	0.22	
151	4-30-110-9W6	6391	17.3	14.4	1594.558	0.53	
150	4-30-110-9W6	6391.5	7.7	9.7	1594.558	0.32	
149	4-30-110-9W6	6392.5	8.7	12.5	1594.558	0.38	
148	4-30-110-9W6	6393.5	8.1	13.3	1594.558	0.48	
147	4-30-110-9W6	6403	1.7	5	1594.558	0.24	TOC <.5 and S1 < 0.2
196	7-7-113-21W5	4534	3.5	8.9	1594.558	0.53	PI < 0.1
193	7-7-113-21W5	4581	3.1	7.9	1594.558	0.43	
192	7-7-113-21W5	4585	6.4	11.1	1594.558	0.68	Tmax < 435
191	7-7-113-21W5	4603	0	23.6	1594.558	7.29	TOC > 10
178	4-19-116-4W6	5011.5	1.1	4.9	1594.558	0.87	Tmax < 435
169	4-19-116-4W6	5154	3.5	10.5	1594.558	1.92	PI < 0.1
168	4-19-116-4W6	5156	3.6	10.2	1594.558	2.88	PI < 0.1
167	4-19-116-4W6	5169	5.3	14.2	1594.558	2.48	PI < 0.1
162	5-36-117-6W6	5512.5	2.3	7.3	1594.558	2.88	
160	5-36-117-6W6	5523	1.8	4.7	1594.558	1.89	
159	5-36-117-6W6	5526.5	0	12.9	1594.558	6.12	

00/07-07-113-21W5/0
KB: 398.7 m
TD: 1604.8 m [TVD]
Mode: Abnd
RR: 1968-10-05
FormTD: PCMB
Fluid: N/A
CHEVRON WATT 7-7-113-21
< 89549.9m to previous well

A'

Rainbow, Zama, & Meander Area Cross Section A-A'

Produced by :
AccuLogs Cross Section
version 6.5.3.0

Author: Naomi S. Wiebe
Modified On: Tuesday, December 30, 2003 02:51PM
Printed On: Tuesday, December 30, 2003 05:00PM
Start Formation: 20m. above KEGR
End Formation: 20m. below CNCG
Cross Section Name: RAINBOW SBB

Well Spacing Scale (actual scale 1:500000)

0.0 1.0 2.0 3.0 4.0 5.0 6.0 7.0 8.0 9.0 10. 11. 12. 13. 14. 15. 16. 17. 18. 19. 20. 21. 22. 23. 24. 25. 26. 27. 28. 29. 30. 31. 32. 33. 34. 35. 36. 37. 38. 39. 40. KILOMETERS

0.00.61.21.82.42.83.03.64.04.65.05.66.06.67.07.68.08.69.09.610.010.611.111.712.112.713.114.114.615.116.116.717.118.118.719.120.020.721.222.223.223.824.225. MILES

Depth Scale (actual scale 1: 600)

0 10 20 30 40 50 METRES

0 25 50 75 100 125 150 FEET

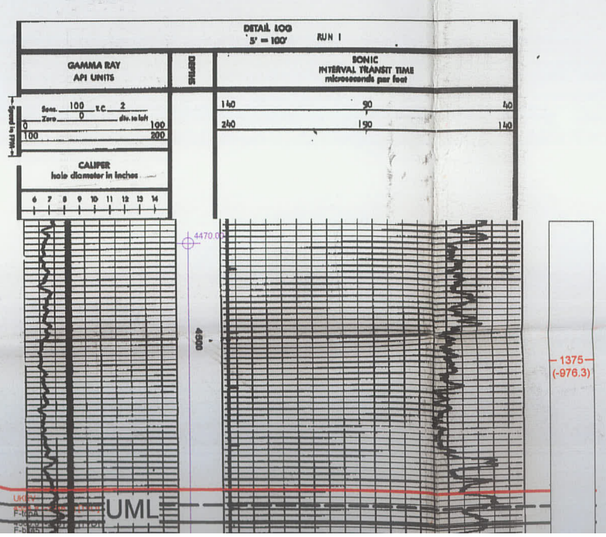

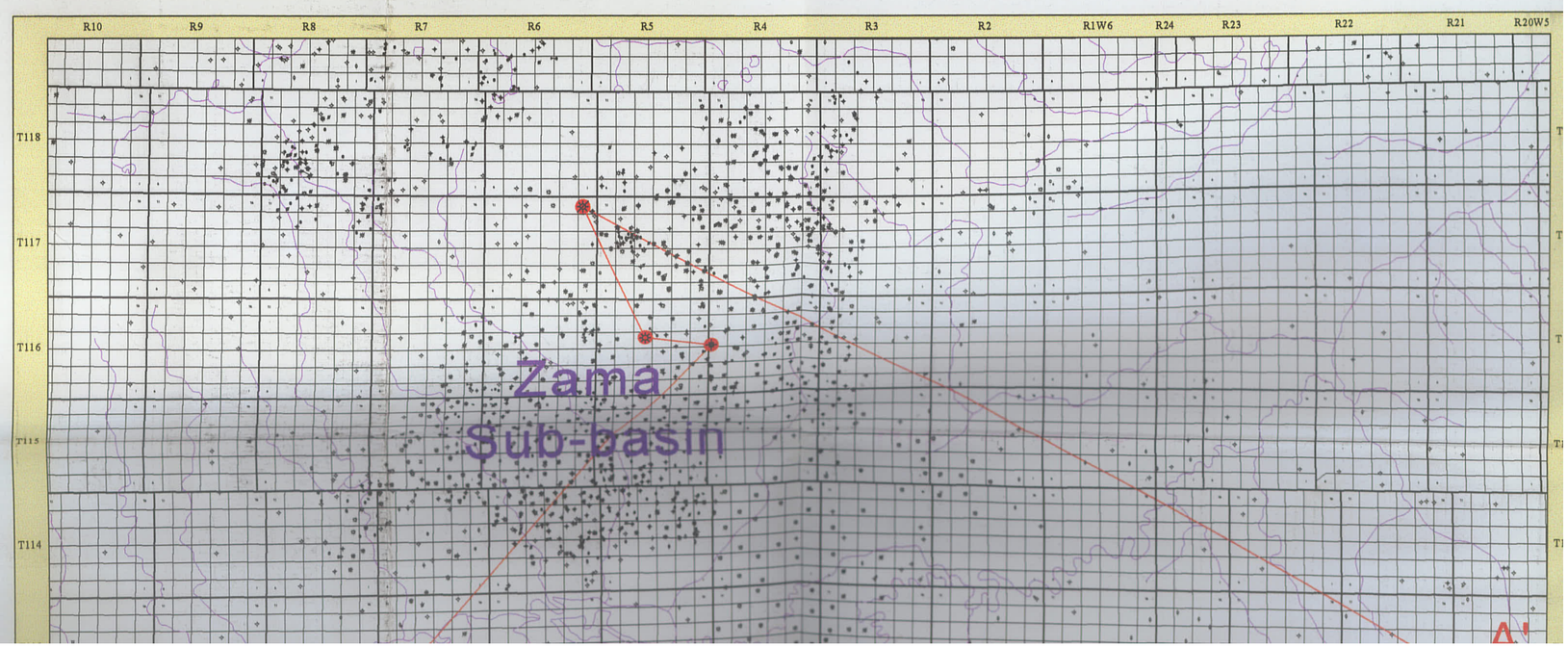

Top of URL

URL

Base of URL

MRL

LRL

Lower Keg River Member

Chinchaga

Top of URL

URL

Base of URL

MRL

LRL

Chinchaga

URL

MRL

LRL

2025 (-1537.9)

2050 (-1562.9)

2075 (-1587.9)

2100 (-1612.9)

2125 (-1637.9)

1950 (-1451.7)

1975 (-1476.7)

2000 (-1501.7)

2025 (-1526.7)

2050 (-1551.7)

1950 (-1481.4)

1975 (-1486.4)

2000 (-1511.4)

2025 (-1536.4)

2050 (-1561.4)

CALIPER
hole diameter in inches

GAMMA RAY
API UNITS

SONIC
INTERVAL TRANSIT TIME
microseconds per foot

<----------Rainbow Sub-ba

00/04-09-109-08W6/0

KB: 48.6 m
TD: 2065.3 m [VD]
Mode: Abnd
Fluid: Oil
RR: 1966-06-26
FormTD: CNCG
HUSKY MOBIL RAINBOW 5-9-1

2672.0m to previous well
7020.2m to next well >

00/06-32-109-08W6/0

KB: 535.5 m
TD: 2074.2 m [TVD]
Mode: Abnd
Fluid: Oil
RR: 1967-11-23
FormTD: CNCG
HUSKY MOBIL HZ RAINBOW 8-

< 7020.2m to previous well
1123.2m to next well >

00/12-33-109-08W6/0

KB: 533.4 m
TD: 2080.4 m
Mode: Inj
Fluid: Water
RR: 1965-08-31
FormTD: CNCG
HUSKY MOBIL RAINBOW 12-33

< 1123.2m to previous well
14802.3m to next well >

00/04-30-110-09W6/0

KB: 438.0 m
TD: 2123.8 m
Mode: Abnd
Fluid: N/A
RR: 1967-10-10
FormTD: PCMB
SCEPTRE ET AL W RAINBOW 4

< 14802.3m to previous well
73953.7m to

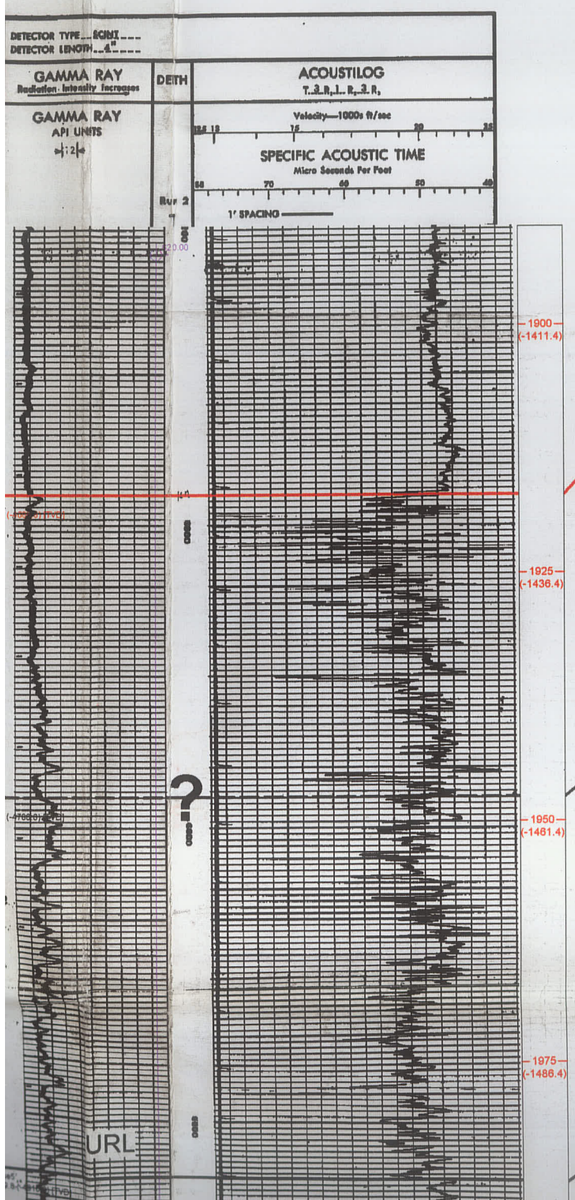

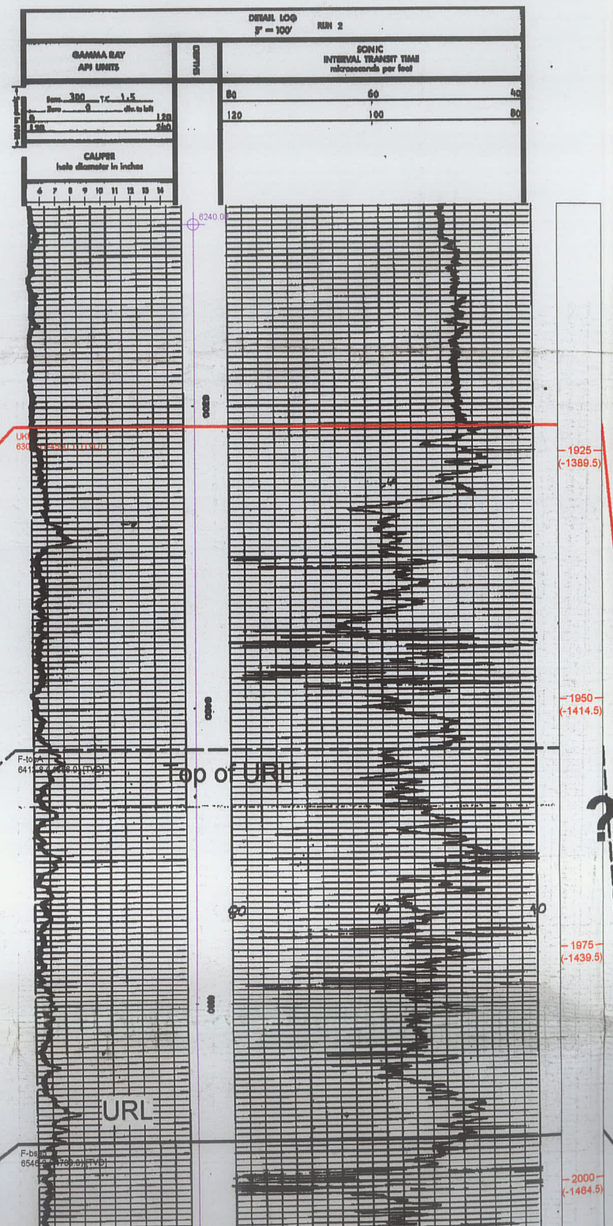

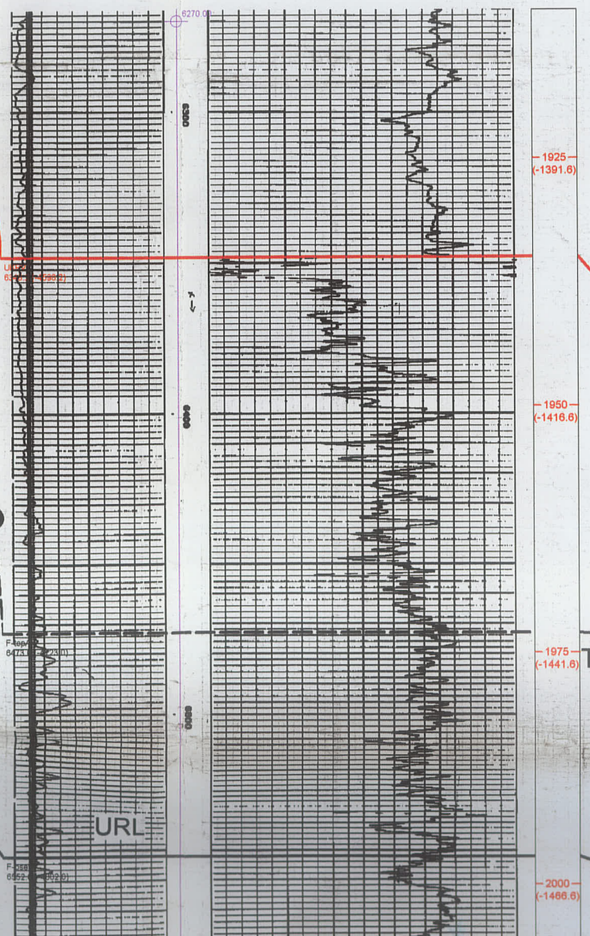

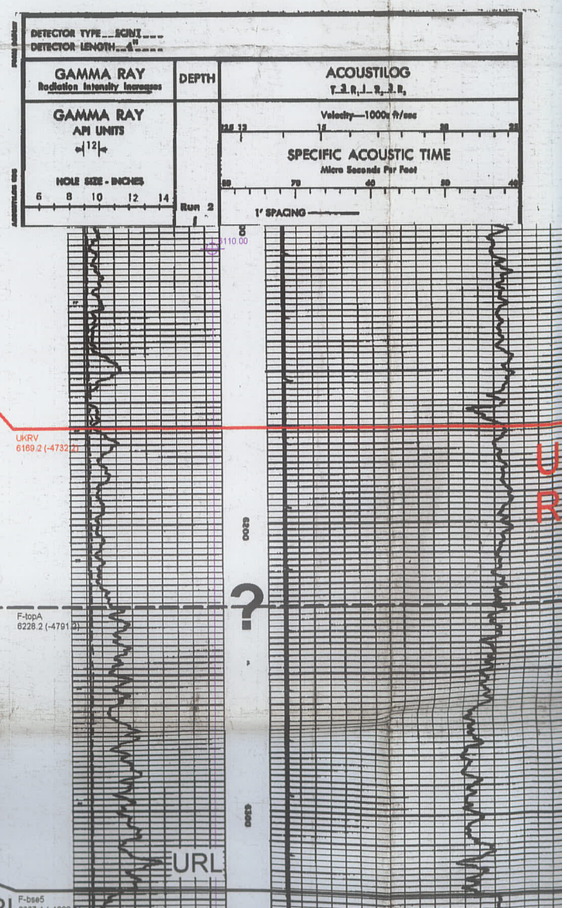

Top of URL

URL

MRL

LRL

Top of URL

URL

Base of URL

MRL

LRL

Chinchaga

CALIPER
hole diameter in inches

GAMMA RAY
API UNITS

SONIC
INTERVAL TRANSIT TIME
microseconds per foot

Rainbow Sub-basin

3m to next well >

00/04-30-110-09W6/0
KB: 438.0 m
TD: 2123.8 m
Mode: Abnd
RR: 1967-10-10
FormTD: PCMB
Fluid: N/A
SCEPTRE ET AL W RAINBOW 4
< 14802.3m to previous well
73953.7m to next well >

00/04-19-116-04W6/3
KB: 377.0 m
TD: 1635.3 m
Mode: Susp
RR: 1966-08-28
FormTD: CNCG
Fluid: Gas
ACL ZAMA 4-19-116-4
< 73953.7m to previous well
5844.0m to next well >

< 5844.0

Hay River Bank

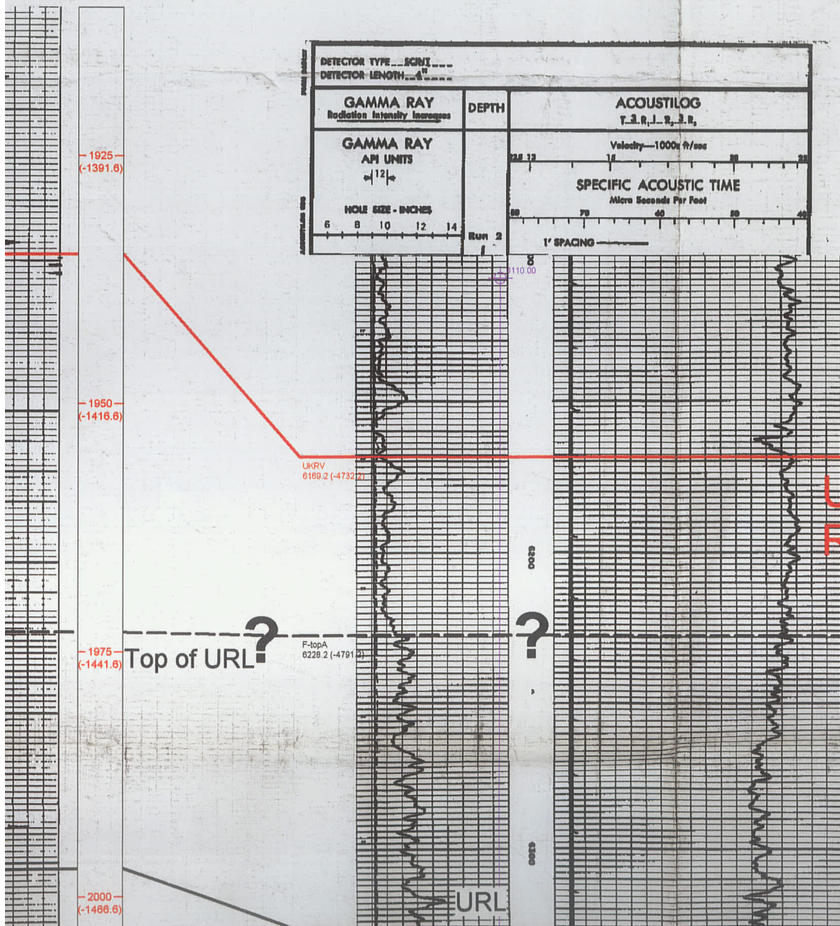

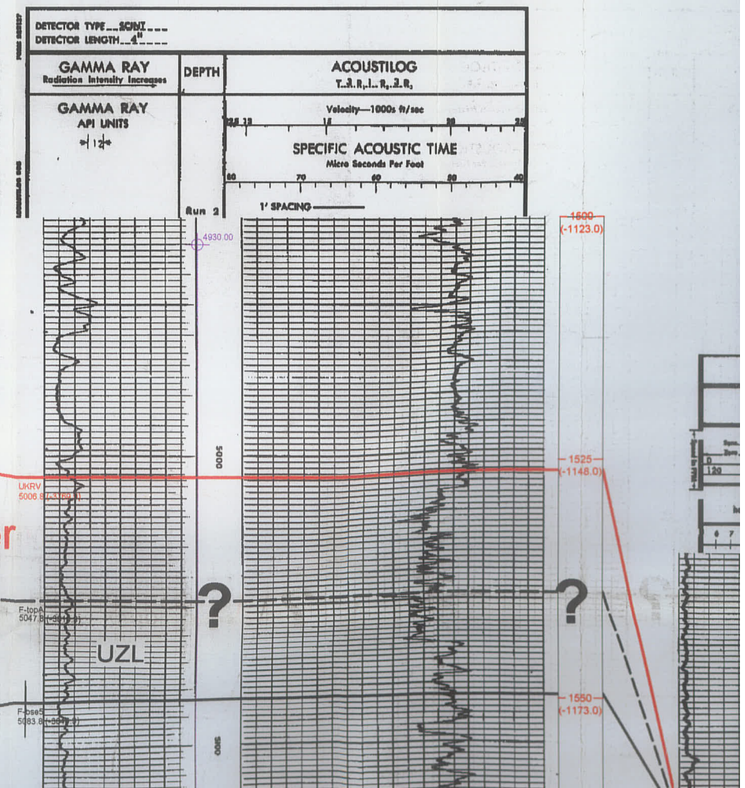

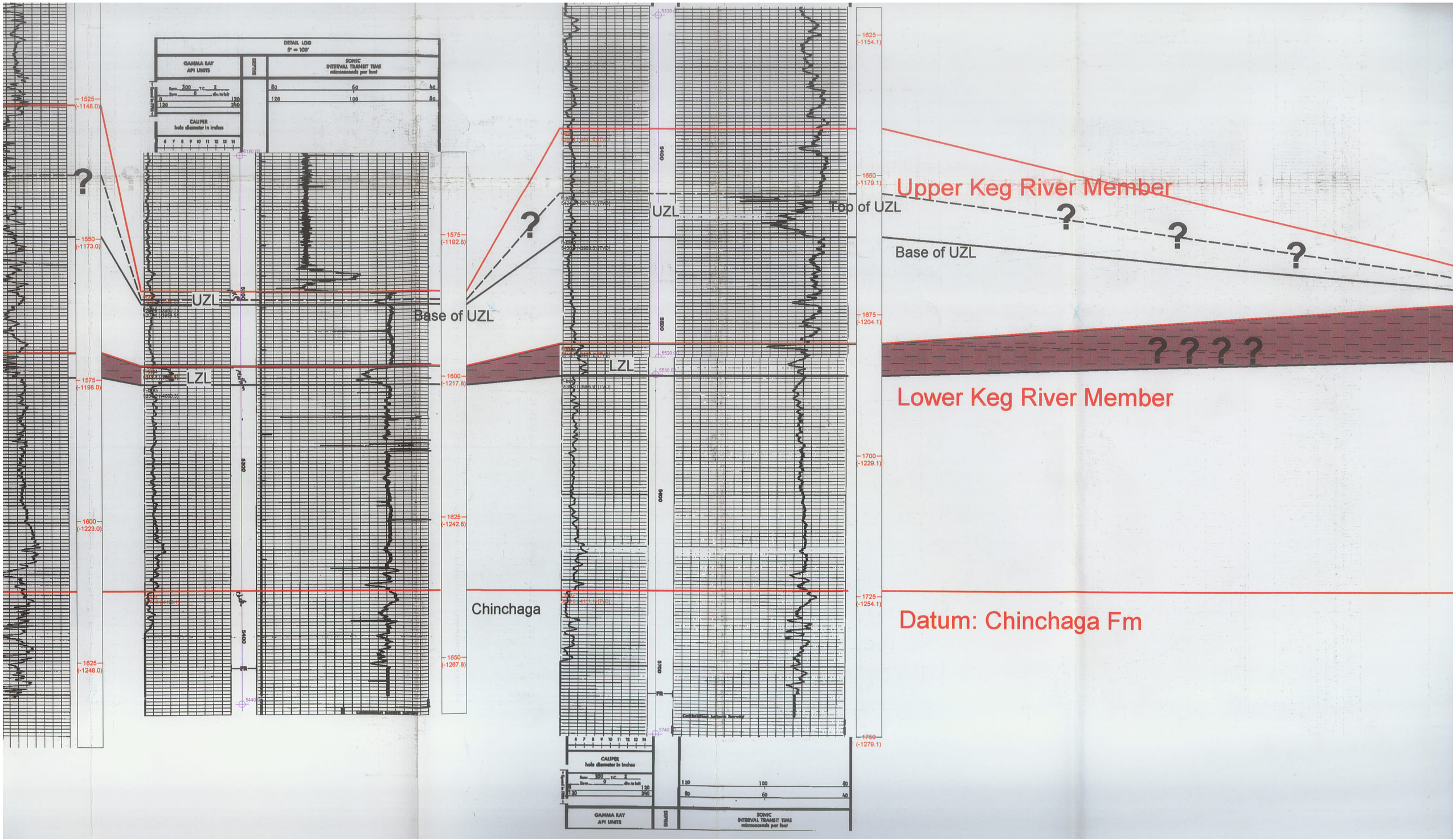
DETAIL LOG
5" = 100'
GAMMA RAY
API UNITS
DEPTHS
SONIC
INTERVAL TRANSIT TIME
microseconds per foot
CALIPER
hole diameter in inches
1525
(-1148.0)
1550
(-1173.0)
1575
(-1198.0)
1600
(-1223.0)
1625
(-1248.0)
UZL
LZL
Base of UZL
1575
(-1192.8)
1600
(-1217.8)
1625
(-1242.8)
1650
(-1267.8)
Chinchaga
1625
(-1154.1)
1650
(-1179.1)
1675
(-1204.1)
1700
(-1229.1)
1725
(-1254.1)
1750
(-1279.1)
Top of UZL
Upper Keg River Member
Base of UZL
Lower Keg River Member
Datum: Chinchaga Fm
Zama Sub-basin

00/10-21-116-05W6/0
KB: 382.2 m
TD: 1654.1 m
Mode: Prod
RR: 1967-07-12
FormTD: CNCG
Fluid: Gas
ACL ZAMA 10-21-116-5
o previous well
13724.3m to next well >

00/05-36-117-06W6/0
KB: 470.9 m
TD: 1745.3 m [TVD]
Mode: Susp
RR: 1967-07-09
FormTD: CNCG
Fluid: Gas
ACL ZAMA 5-36-117-6
< 13724.3m to previous well
89549.9m to next well >

00/07-07-
KB: 398.7 m
TD: 1604.8 m [TVD]
Mode: Abnd
CHEVRON
< 89549.9m to previous well

DETAIL LOG
5" = 100'
RUN 2

GAMMA RAY
API UNITS

DEPTHS

SONIC
INTERVAL TRANSIT TIME
microseconds per foot

CALIPER
hole diameter in inches

5320

1625
(-1154.1)

1650
(-1179.1)

1575
(-1192.8)

UZL

Top of UZL

Base of UZL

Upper Keg River Member

?

?

?

UML

Upper Keg River Member

Top of URL

Base of URL

URL

MRL

LRL

Upper Keg River Member

Top of UZL

Base of UZL

UZL

LZL

Lower Keg River Member

Datum: Chinchaga Fm

Zama

A

00/06-32-107-09W6/0

KB: 487.1 m
TD: 2148.2 m
Mode: Abnd
HUSKY RAINBOW SOUTH 11-32

RR: 1965-07-03
FormTD: CNCG
Fluid: Oil

21416.9m to next well >

00/04-16-108-07W6/0

KB: 498.3 m
TD: 2184.8 m
Mode: Abnd
PAN AM B- 1 RAINBOW 4-16-

RR: 1965-12-05
FormTD: PCMB
Fluid: N/A

< 21416.9m to previous well
12672.0m to next well >

00/04-09-109-08W6/0

KB: 38.6 m
TD: 2065.3 m [VD]
Moe: Abnd
HUSKY MOBIL RAINBOW 5-9-1

RR: 1966-06-26
FormTD: CNCG
Fluid: Oil

< 12672.0m to previous well
7020.2m to next well >

00/0

KB
TD: 2074.2 m
M
H

< 7020.2m to previous well

Upper Keg River Member

Top of URL

URL

Base of URL

?

1950 (-1462.9)
1975 (-1487.9)
2000 (-1512.9)
2025 (-1537.9)
2050 (-1562.9)

1925 (-1426.7)
1950 (-1451.7)
1975 (-1476.7)

1900 (-1411.4)
1925 (-1436.4)
1950 (-1461.4)
1975 (-1486.4)

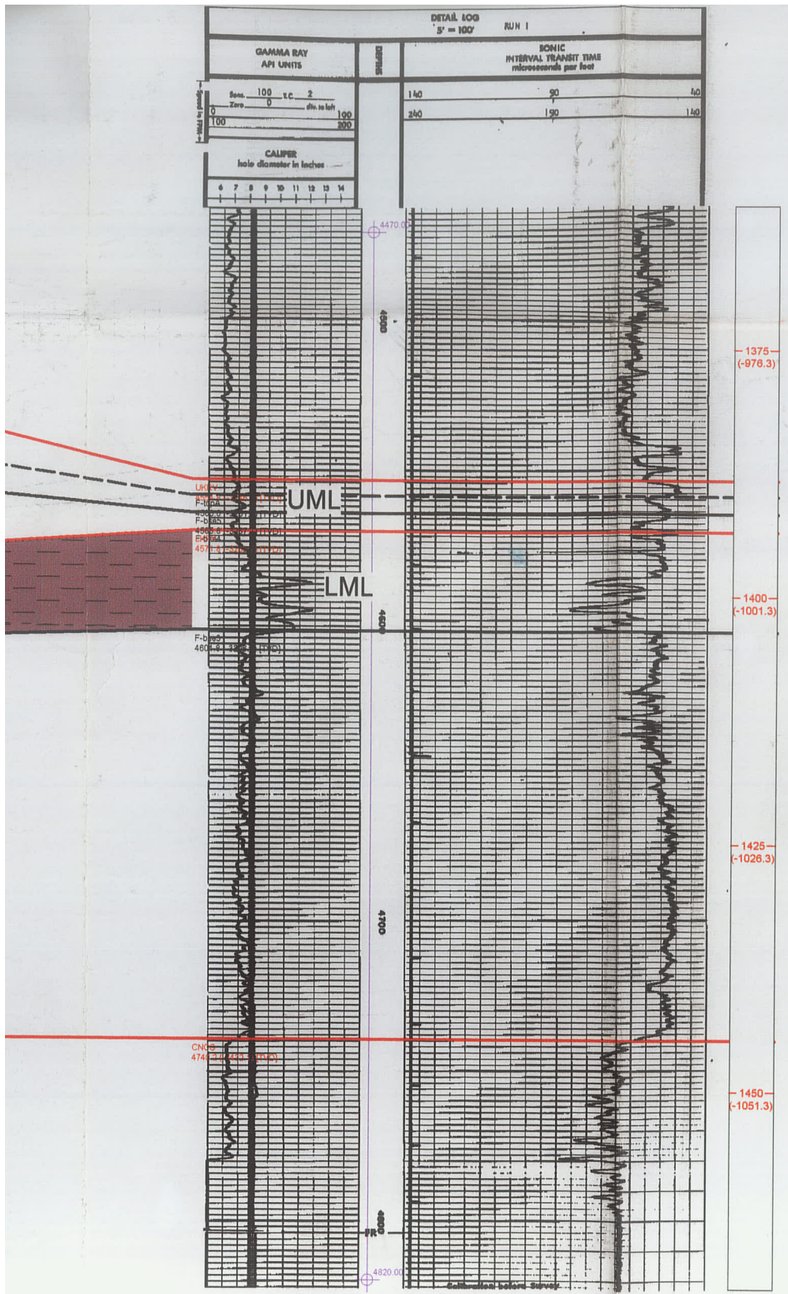

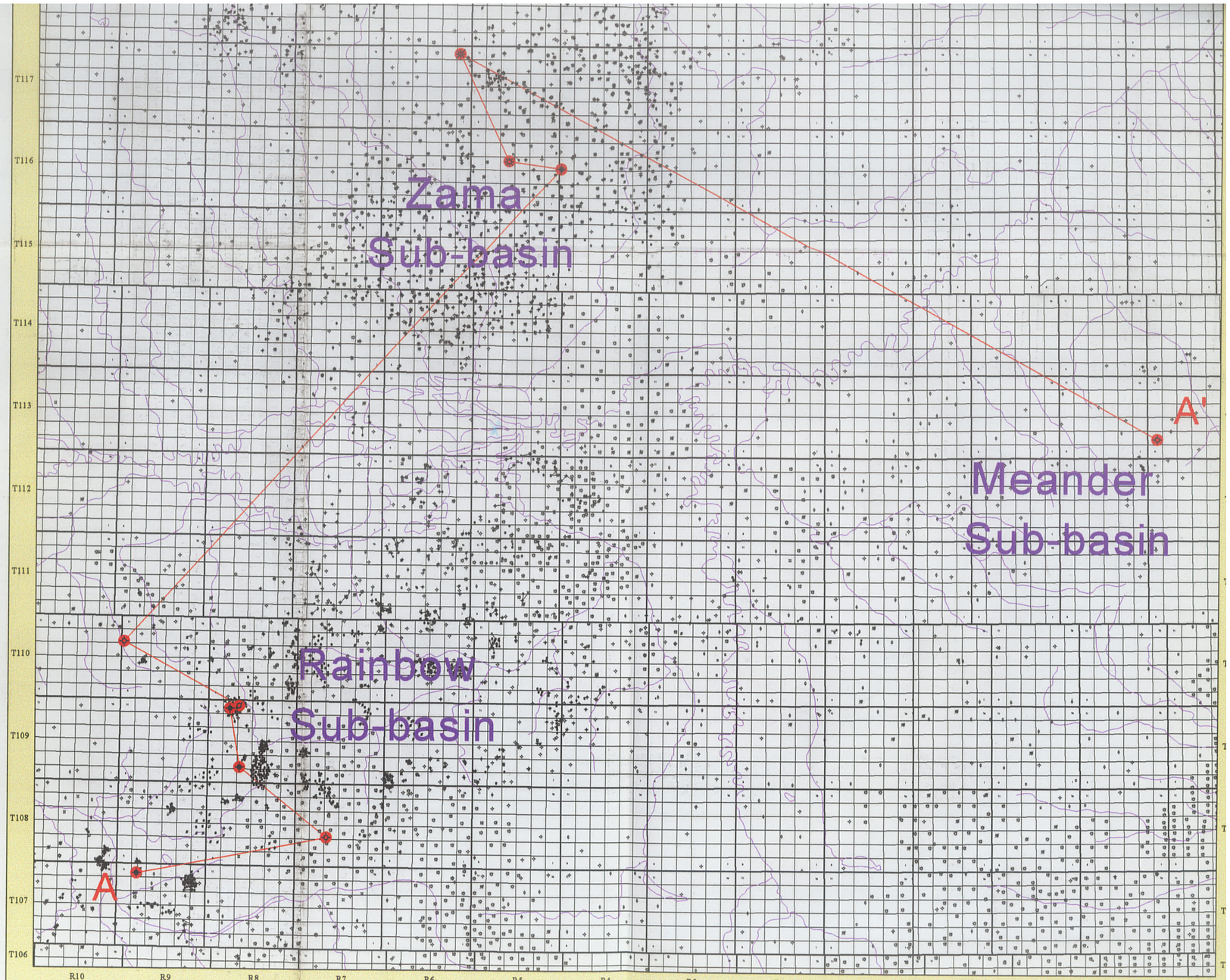

Meander Sub-basin

CROS

RAINBOW SUB-BASIN

S

6-32-107-9W6	2.1 Km	4-16-108-7W6	12.7 Km	4-9-109-8W6	7 Km	6-32-109-8W6	1 Km	12-33-109-8W6
K.B. 1598.1' (487.1 m)		K.B. 1634.8' (498.3 m)		K.B. 1603.0' (488.6 m)		K.B. 1756.9' (535.5 m)		K.B. 1750' (533.4 m)

700'
600'
500'
400'
300'
200'
100'
0'

200 m
150 m
100 m
50 m
0 m

UPPER KEG RIVER MEMBER

LOWER KEG RIVER MEMBER

TOP OF UPPER KEG RIVER MEMBER: 6398.2' (1950.2 m)

TOP OF URL: 6554.1' (1997.7 m)
refer to Encl. 1 for log detail

6384.4' (1946.0 m)

TOP OF URL 6435.6' (1961.6 m)

6289.9' (1917.2 m)

TOP OF URL 6389.7' (1947.6 m)

6307.0' (1922.4 m)

TOP OF URL 6413.6' (1954.9 m)

6348.0' (1934.9 m)

TOP OF URL 6473.0' (1973.0 m)

URL

SCALE CHANGE

BASE OF URL: 6717.8' (2047.6 m)

BASE OF URL 6507.8' (1983.6 m)

BASE OF URL 6519.9' (1987.3 m)

BASE OF URL 6546.2' (1995.3 m)

BASE OF URL 6552.1' (1928.6 m)

MRL

6567.2' (2001.7 m)
6571.8' (2003.1 m)
6594.4' (2010.0 m)
6601.6' (2012.2 m)

6568.8' (2002.2 m)
6573.4' (2003.6 m)
6599.0' (2011.4 m)
6613.8' (2015.9 m)

6620.7' (2018.0 m)
6625.2' (2019.4 m)
6650.2' (2027.0 m)
6670.2' (2033.1 m)

6619.7' (2017.7 m)
6623.6' (2018.9 m)
6651.2' (2027.2 m)
6666.3' (2031.9 m)

LRL

R1
R2
R3

LOWER KEG RIVER MEMBER: 6812.3' (2076.4 m)

BASE OF MRL: 6816.8' (2077.8 m)

TOP OF LRL: 6838.2' (2084.3 m)

BASE OF LRL: 6853.9' (2089.1 m)

CHINCHAGA

TOP OF CHINCHAGA FM.: 6947.8' (2117.7 m)

6717.8' (2047.6 m)

6702.7' (2043.0 m)

6749.9' (2057.4 m)

6749.9' (2057.4 m)

LEGEND

- LITHOFACIES A (bituminous laminite)
- LITHOFACIES B (irregular-bedded lime mudstone)
- LITHOFACIES C (nodular crinoid-brachiopod wackestone)
- LITHOFACIES D (massive crinoid brachiopod wackestone)
- LITHOFACIES E (bioturbated crinoid-brachiopod floatstone)
- LITHOFACIES F (bituminous peloidal laminite)
- LITHOFACIES G (massive peloidal
- LITHOFACIES H (stromatoporoid-c

CROSS SECTION A - A'

RAINBOW SUB-BASIN

Z

108-7W6
4.8' (498.3 m)

12.7 Km

4-9-109-8W6
K.B. 1603.0' (488.6 m)

7 Km

6-32-109-8W6
K.B. 1756.9' (535.5 m)

1 Km

12-33-109-8W6
K.B. 1750' (533.4 m)

14.8 Km

4-30-110-9W6
K.B 1437' (438.0 m)

73.9 Km

4-19-116-4W6
K.B. 1236.9' (377.0 m)

5.8 Km

HAY RIVER BANK

6289.9' 1917.2 m)
6307.0' (1922.4 m)
6348.0' (1934.9 m)
6169.2' (1880.4 m)

TOP OF URL
6389.7' (1947.6 m)
6413.6' (1954.9 m)
6473.0' (1973.0 m)
6228.3' (1898.4 m)
TOP OF URL

URL

BASE OF URL
6519.9' (1987.3 m)
6546.2' (1995.3 m)
6552.1' (1928.6 m)
6327.4' (1928.6 m)

MRL
6568.8' (2002.2 m)
6620.7' (2018.0 m)
6619.7' (2017.7 m)
6389.4' (1947.5 m)

6573.4' (2003.6 m)
6625.2' (2019.4 m)
6623.6' (2018.9 m)
6392.6' (1948.5 m)

6599.0' (2011.4 m)
6650.2' (2027.0 m)
6651.2' (2027.2 m)
6410.4' (1953.9 m)

6613.8' (2015.9 m)
6670.2' (2033.1 m)
6666.3' (2031.9 m)
6420.9' (1957.1 m)

LRL

6702.7' (2043.0 m)
6749.9' (2057.4 m)
6749.9' (2057.4 m)
6503.9' (1982.4 m)

R1
R2
R3

TOP OF URL
6250'

UPPER KEG RIVER MEMBER

TOP OF UPPER KEG RIVER MEMBER:
5006.8' (1526.1 m)

TOP OF UZL
5047.8' (1538.6 m)

UZL

BASE OF UZL
5083.9' (1549.6 m)

TOP OF LOWER KEG RIVER MEMBER:
5151.8' (1570.3 m)

BASE OF LZL:
5165.6' (1574.5 m)

LZL

???
LOWER KEG RIVER MEMBER

TOP OF CHINCHAGA FM.:
5290.0' (1612.4 m)

5204.7' (1586.4 m)
5207.3' (1587.2 m)
5243.4' (1598.2 m)
5254.2' (1601.5 m)
5374.0' (1638 m)

Z1
Z2

rachiopod wackestone)
LITHOFACIES E (bioturbated crinoid-brachiopod floatstone)
LITHOFACIES G (massive peloidal-skeletal dolopackstone to dolograinstone)
LITHOFACIES I (non-fossiliferous dolomudstone)
R1 - cycle R1
R2 - cycle R2
R3 - cycle R3

rachiopod wackestone)
LITHOFACIES F (bituminous peloidal laminite)
LITHOFACIES H (stromatoporoid-coral dolofloatstone to dolorudstone)
ANHYDRITE

ON A - A'

ZAMA SUB-BASIN

N

MEANDER SUB-BASIN

-110-9W6
437' (438.0 m)

73.9 Km

4-19-116-4W6
K.B. 1236.9' (377.0 m)

5.8 Km

10-21-116-5W6
K.B. 1253.9' (382.2 m)

13.7 Km

5-36-117-6W6
K.B. 1544.9' (470.9 m)

89.5 Km

7-7-113-21W5
K.B. 1308.1' (398.7 m)

HAY RIVER BANK

TOP OF URL

UPPER KEG RIVER MEMBER

URL

BASE OF URL

MRL

LRL

LOWER KEG RIVER MEMBER

???

TOP OF UPPER KEG RIVER MEMBER: 5006.8' (1526.1 m)

TOP OF UZL 5047.8' (1538.6 m)

UZL

BASE OF UZL 5083.9' (1549.6 m)

TOP OF LOWER KEG RIVER MEMBER: 5151.8' (1570.3 m)

BASE OF LZL: 5165.6' (1574.5 m)

LZL

TOP OF CHINCHAGA FM.: 5290.0' (1612.4 m)

5204.7' (1585.4 m)

5199.7' (1584.9 m)

BASE OF UZL 5207.3' (1587.2 m)

5243.4' (1598.2 m)

5254.2' (1601.5 m)

LZL

5374.0' (1638 m)

5386.4' (1641.8 m)

TOP OF UZL

BASE OF UZL 5450.4' (1661.3 m)

UZL

5512.1' (1680.1 m)

5530.8' (1685.8 m)

LZL

5655.8' (1723.9 m)

UPPER KEG RIVER MEMBER

TOP OF UZL 5424.1' (1653.3 m)

TOP OF UML 4554.7' (1388.3 m)

BASE OF UML 4565.9' (1391.7 m)

4572.0' (1393.5 m)

BASE OF LML: 4603.3' (1403.1 m)

LZL

LOWER KEG RIVER MEMBER

TOP OF CHINCHAGA FM.: 4740.1' (1444.8 m)

LML

UPPER KEG RIVER MEMBER

TOP OF URL: 5424.1' (1653.3 m)

LOWER KEG RIVER MEMBER

CHINCHAGA

R3 R2 R1 Z2 Z1 M2 M1

6050' 6100' 6150' 6200' 6250' 6300' 6350' 6400' 6450' 6500' 6550'

4750' 4800' 4850' 4900' 4950' 5000' 5050' 5100' 5150' 5200' 5250' 5300' 5350' 5400'

4850' 4900' 4950' 5000' 5050' 5100' 5150' 5200' 5250' 5300' 5350' 5400' 5450'

5150' 5200' 5250' 5300' 5350' 5400' 5450' 5500' 5550' 5600' 5650' 5700' 7050'

4200' 4250' 4300' 4350' 4400' 4450' 4500' 4550' 4600' 4650' 4700' 4750' 4800' 4850'

o dolograinstone)

olorudstone)

LITHOFACIES I (non-fossiliferous dolomudstone)

ANHYDRITE

R1 - cycle R1
R2 - cycle R2
R3 - cycle R3

Z1 - cycle Z1
Z2 - cycle Z2
M1 - cycle M1
M2 - cycle M2

LRL - lower Rainbow laminite
MRL - middle Rainbow laminite
URL - upper Rainbow laminite

LZL - lower Zama laminite
UZL - upper Zama laminite
LML - lower Meander laminite
UML - upper Meander laminite

Abandoned Gas
Abandoned Oil
Water Injection
Suspended Gas
Gas Producer